

FORMABILITY OF SHEET METAL

UNDER

NON-COAXIAL AND ZIGZAG STRAIN PATHS

FORMABILITY OF SHEET METAL  
UNDER  
NON-COAXIAL AND ZIGZAG STRAIN PATHS

A thesis presented for the degree of

DOCTOR OF PHILOSOPHY

of the

UNIVERSITY OF ASTON IN BIRMINGHAM, ENGLAND.

by

Shiun-Yong LEE

621.772 LEE

190410 27 APR 1978

June, 1975.

## Summary

The aim of this thesis is to provide a wider conception of the formability of sheet metal to cover a wider range of sheet metal products.

In circular cup drawing, the deformation in the work-piece is coaxial owing to axial symmetry; in other words, during the forming operation, the principal axes of stress and strain coincide with each other and are fixed with respect to the material. The directions of the principal axes are along the meridional tangential and the circumferential directions all the time during the forming operation. In non-axisymmetrical forming, however, non-coaxial deformation is involved in the forming operation owing to the lack of axial symmetry. The principal axes of stress and strain do not coincide with each other and they both rotate with respect to the material.

To widen the meaning of formability, it is defined on the one hand to mean the forming limits of sheet metal, which is represented by the forming limit curve; on the other hand, to mean the drawability of sheet metal in a drawing process. The forming limits of sheet metal under coaxial simple and coaxial zigzag strain paths as well as the drawability of sheet metal in a circular cup drawing have been investigated by many sheet metal forming research scientists hitherto. There has not been, however, any investigation

Continued.....

on the forming limits of sheet metal under non-coaxial strain paths. This omission is no doubt due to the lack of theoretical analysis of non-coaxial strains, as can be seen in the usual incomplete representation for a state of strain by only the three principal strains.

Although there are some investigations on non-circular cup drawing, they are all empirical studies. The drawability of sheet metal is up to now limited to the circular cup drawing and the definition of drawability is restricted to mean the ratio of the blank diameter to the punch diameter, as defined in the Swift test.

In this thesis, a fundamental analysis of non-coaxial strains is pursued. A state of strain is completely represented by the three principal strains and the directions of the principal axes of strain with respect to the material. With the complete representation of a state of strain, a non-coaxial strain path can be represented graphically and is plotted for the first time in this thesis. The relation between the rotation of the principal axis of stress with respect to the material and that of the principal axis of strain is investigated. The non-coaxiality of the principal axes of stress and strain results in a type of zigzag strain path, and such zigzag strain path is also investigated both theoretically and experimentally. At the same time, the definition of drawability is generalised to be the largest draw-in

Continued.....

at the completion of the drawing operation so that it is applicable to any shape of cup drawing. An index of nonsymmetry is proposed to specify the characteristics of a non-circular forming process. The large volume of useful experimental work which these investigations can lead to is discussed in a separate chapter on suggestions for future work.

The achievements of this project are as follows:

1. The investigation of non-coaxial deformations on both theoretical and experimental bases.
2. The generalisation of the definition of drawability and the drawability test to cover all shapes of cups.
3. The provision of a theoretical link between the partial view of stretchability in the Forming Limit Curve and Swift's Limiting Drawing Ratio to form a more nearly complete view of sheet metal formability.

## C O N T E N T S

Summary

Notation

			<u>Page</u>
Chapter	1	Introduction	1
Chapter	2	Definitions	13
	2.1	Strain	13
	2.2	Coaxial and Non-coaxial Deformations.	15
	2.3	Strain Path	16
	2.4	Forming Process and Forming Conditions.	17
	2.5	Formability	17
Chapter	3	Review of Past Literature	23
	3.1	Forming Limit Curve of Sheet Metal	23
	3.2	Formability of Sheet Metal Under Zigzag Strain Path.	27
	3.3	Sheet Metal Test	29
	3.4	Non-axisymmetrical Formings.	36
Chapter	4	Strain Analysis	41
	4.1	Deformation Represented by an Affine Transformation.	41
	4.2	Matrices Representing Typical Modes of Deformation .	47
	4.3	The Thickness Strain	51
	4.4	Matric Analysis of Deformation	53

Continued.....

		<u>Page</u>
	4.5	The Incapability of Circular Grid for Strain Measurement in Non-coaxial Deformation. 59
	4.6	Strain Measurement by Using Square Grid. 62
	4.7	Invariance of the Transformation Matrix. 65
	4.8	The Detection and the Magnitude of Non-coaxiality. 67
Chapter	5	Graphical Representations of Strain Paths. 69
	5.1	2-D Triangular Co-ordinate. 71
	5.2	3-D Triangular Co-ordinate 73
	5.3	Coaxial Strain Path 74
	5.4	Non-coaxial Strain Path 76
	5.5	Linearity of Non-coaxial Strain Path. 77
	5.6	Simple Shear 78
Chapter	6	Analysis of Non-coaxial Deformation. 81
	6.1	Resultant of Two Deformations. 82
	6.2	The Nonalignment of the Principal Axes of Stress and Strain in Non-Coaxial Deformations. 88
	6.3	Deformations Without Changing the Resultant Strain. 91
Chapter	7	Implications On the Theory of Plasticity. 98
	7.1	Plastic Work Done in Coaxial Deformation. 98
	7.2	Plastic Work Done in Non-coaxial Deformation. 101

Continued.....

			<u>Page</u>
	7.3	Work-hardening	106
	7.4	Validity of Lévy-Mises and Prandtl-Reuses Equations.	107
	7.5	Stress-Strain Relationship	113
	7.6	The Effect of Non-coaxiality on Formability.	117
Chapter	8	The Drawability of Sheet Metal	119
	8.1	Arbitrary Elements in the Swift Test.	123
	8.2	Boundary and the Completion of Drawing Operation.	126
	8.3	The Extent of Drawing	127
	8.4	Generalised Definition of Drawability.	129
Chapter	9	Experimental Technique	136
	9.1	Experimental Equipment	136
	9.2	Data on Work Material	138
	9.3	Experimental Technique	138
	9.4	Experimental Procedure	141
Chapter	10	Non-coaxial and Non-coaxial Zigzag Strain Paths.	149
	10.1	Preliminary Tests	151
	10.2	Non-coaxial Strain Paths	152
	10.3	Forming Limit Curve	155
	10.4	Non-coaxial Zigzag Strain Paths.	156
Chapter	11	Drawability - A Generalised Definition.	161
	11.1	Process Parameters and Forming Conditions	161

Continued.....

		<u>Page</u>
	11.2	Boundary and Blank 162
	11.3	The Orientation of the Blank with Respect to the Rolling Direction. 171
	11.4	The Orientation of the Blank with Respect to the Punch and Die. 173
	11.5	Blank Shape and Size 177
	11.6	The Stretching and the Drawing Actions. 184
Chapter	12	Characteristics of the Forming Process. 190
	12.1	Convergence of Metal Flow 190
	12.2	The Index of Nonsymmetry 194
	12.3	Stresses in a Non-circular Cup Drawing Process. 199
	12.4	The Optimization of the Blank Shape and Size. 205
	12.5	The Involvement of Non-coaxial Deformation in Non-circular Cup Drawing Processes. 207
Chapter	13	Conclusions 210
Chapter	14	Suggestions for Future Work 219
		Acknowledgements 225
		Bibliography 226

## NOTATION

A number in a blanket for example, (5)	the number of reference in <sup>the</sup> Bibliography.
$X_1, X_2; X_1, X_2$	co-ordinates of a point.
$ A_{ij} $	matrix with elements $A_{ij}$ .
$m, M$	uniform dilatation.
$\theta$	the angle specifying the directions of the principal axes of strain with respect to the material.
$\alpha$	an angle, a pure number.
$\epsilon$	natural strain.
$\epsilon_1, \epsilon_2, \epsilon_3$	principal strains.
$A_0, A_1$	areas.
$t_0, t_1$	thicknesses.
$l$	length.
$\phi$	angle, the orientation of the blank with respect to the rolling direction.
$\eta$	characteristic index of deformation, gross surface strain.
$\beta$	magnitude of non-coaxiality, an angle.
$\delta$	a positive number.
$\epsilon_{ij}$	strains.
$\epsilon_{ij}^e, \epsilon_{ij}^p$	elastic and plastic strains respectively.
$\sigma_{ij}$	stress.
$\bar{\sigma}$	equivalent stress.
$d\bar{\epsilon}$	equivalent incremental strain.
$w$	work.
$\lambda, \lambda'$	constants.

Continued.....

R	a ratio.
$\psi$	draw-in.
$A_d$	the area of material being drawn into the boundary.
$A_b$	the area inside the boundary.
$A_c$	the area of material being drawn at the completion of the drawing operation.
$A_s$	the surface area of the cup.
$\xi$	an angle, the inclination of the cuts in coupon form specimen, index of <del>an</del> symmetry.
d	distance between the cuts in coupon form specimen.
$\zeta$	the orientation of the blank with respect to the punch and die.
$\varphi$	average surface strain.

CHAPTER 1

INTRODUCTION

## Introduction

This chapter is devoted to defining the problem for which this thesis provides the answer. That the problem requires definition is due as much to the imprecise use hitherto of such basic terms as "formability" and "drawability" in the research literature on sheet metal forming, as to the need to delineate, for the sake of clarity, the scope and limit of the project. A complete definition of the problem also provides the schema by which the different parts of the research project are related to each other.

Sheet metal is used in many different kinds of manufacturing process involving plastic deformation of metal, such as blanking, coining, shaving, ironing, bending, stamping, folding, stretching and polishing. In this thesis, forming is understood to be the process in which a workpiece of sheet metal is clamped against a die and a punch pushes the sheet through a hole in the die. To confine the project to such a process is a matter of deliberate choice, based on the generally accepted usage of the term "sheet metal forming". It is, of course, understood that the sheet metal is thin enough for the variation of the deformation across the thickness to be negligible, otherwise, the process becomes one of forging.

The need for a test of sheet metal formability is a practical need and ~~the~~ research into sheet metal form-

Continued.....

ability has always been motivated by practical engineering problems. Formability is what formability tests measure. Therefore "formability" has come to mean, not a material property such as hardness and elastic rigidity, but the resistance to failure and the performance of sheet metal in the forming process. Those who wish to determine sheet metal formability do not look for a physical property of the material, rather they wish to know "how well a sheet material will stand up to the forming process". The precision of its meaning lies somewhere between that of forgeability, which has more or less the same meaning as ductility, and that of machinability, which has an even less distinct connotation. Indeed, part of the research and research results reported in this thesis consists of careful analysis and accurate definition of sheet metal formability. Such accurate analysis is necessary in any study in depth of an engineering problem. Without the precision in such a pedagogical study, the measurement of formability can hardly be serviceable in practical processes, quite apart from the elimination of semantic confusion.

The phrase "how well will a material stand up to the forming process" conceals several ambiguities and tacit implications. A precise definition of formability is best found by removing these ambiguities and exploring these implications. A forming process (fig. 1-1)

Continued.....

consists of producing a cup or bulge out of a flat sheet. The phrase "how well a material will stand up to the forming process" implies an extent of forming to a limit which is a failure of material in the forming process. To get a precise meaning of formability, therefore, it is necessary first to confine oneself to a mode of failure. To the practical engineer, a forming process may fail by puckering, fracture or excessive deterioration of the surface finish. In this project, the mode of failure investigated is the mechanical failure of the workpiece, namely, necking leading to fracture, or fracture itself. It is, for obvious reasons, necessary to limit the scope of the research project to a manageable magnitude with a unity of purpose, hence the exclusion of metallurgical study. Such a choice in no way implies, of course, that the other modes of failure in sheet metal forming are unimportant.

In sheet metal forming, stretching is always associated with drawing, and ~~the~~ failure in the workpiece normally occurs in the stretching region. But the severity of stretching is largely determined by the conditions in the drawing region. The success of a sheet metal forming process, therefore, relies on the strength of the material under forming and the resistance of material to *being* drawn in in the forming process. Formability of sheet metal is investigated in these two aspects.

Continued.....

The first aspect of formability is the ductility of the material. This is dependent on the strain path, as will be explained later in this thesis. In the tension test, ductility is measured as the percentage elongation or the percentage reduction in area, both of which <sup>are</sup> taken at the critical section where necking and fracture occur. The material in the tension test is, of course, deformed along a particular strain path. If in another forming process, say, in biaxial stretching, the material at the critical section ~~is~~ deformed under another strain path, then the ductility of material in biaxial stretching is different from that in the tension test. In fact, a tension test is only one of the infinite number of forming processes and ductility is only the formability in a particular forming process. Therefore, the formability of material under forming in all possible forming processes, as usually represented by <sup>the</sup> Forming Limiting Curve (F.L.C.) <sup>which</sup> is a spectrum of ductility but not a single material property. Because formability is strain path dependent, it is significant to study the strain path under which the material at the critical section is deformed.

However, the Forming Limiting Curve hitherto has been investigated either by measuring the strain at the neck without showing the strain path (Keeler's and Goodwins' curves) or by measuring the strain at the neck with strain path leading to the limit in axisymmetrical forming

Continued.....

process so that the strain path is limited to be a coaxial one. A distinction between a coaxial and a non-coaxial deformation is made in the following.

A square (fig.1-2 (a)) is deformed into a rectangle (fig. 1-2 (b)). From the ellipse inside the rectangle (fig.1-2 (b)), it is known that the principal axes of stress are along the fibres AC and BD when the square is deformed. The principal strains are measured from the major and minor axes A'C' and B'D' respectively of the ellipse. The principal axes of strain in fig.1-2 (b) are along the fibres A'C' and B'D' which when referred back to the undeformed state are the fibres AC and BD in the square (fig.1-2 (a)). Suppose the rectangle (fig.1-2 (b)) is further deformed into another rectangle (fig.1-2 (c)). Again, from the ellipse in the further deformed rectangle (fig.1-2 (c)), the principal strains are measured from the fibres A''C'' and B''D''. The principal axes of strain in fig.1-2 (c) are along the fibres A''C'' and B''D'' which, when referred back to the undeformed state, are the fibres AC and BD too. It is understood that the principal axes of stress are fixed and are along the fibres A' C' and B' D' when the rectangle (fig.1-2 (b)) is further deformed. Therefore, from the square (fig.1-2 (a)) to the rectangle (fig.1-2 (b)) and from the rectangle (fig.1-2 (b)) to another rectangle (fig.1-2 (c)), the

Continued.....

principal axes of strain are fixed with respect to the material, and the principal strains at the two states (fig.1-2 (b) and fig.1-2 (c)) are all measured from the deformed states of the fibres AC and BD. The deformations from fig.1-2 (a) to fig.1-2 (b) and from fig.1-2 (b) to fig.1-2 (c) are said to be coaxial because the principal axes of strain are fixed with respect to the material in the deformations. The strain path of the material in fig. 1-2 (a) deformed to fig.1-2 (b) and then to fig.1-2 (c) is a coaxial one.

Figs.1-3 (a) and (b) show the same deformation as that in figs.1-2 (a) and (b). The principal axes of stress and strain are along the fibres AC and BD in the square. If the rectangle (fig.1-3 (b) ) is further deformed into that as shown in fig.1-3 (c), from the ellipse in the parallelogram, the principal strains can still be obtained by measuring the major and minor axes of the ellipse which are E" G" and F" H". The fibres E" G" and F" H" if referred back to the state in fig.1-3 (b) and fig.1-3 (a), <sup>are</sup> E' G', F' H' and EG, FH. (~~fig.1-3 (a), (b)~~) <sup>respectively</sup>. From fig.1-3 (a) to fig. 1-3 (b) the principal axes of stress and strain are along the fibres AC and BD and <sup>the</sup> principal strains are measured from the deformed state of AC and BD. But from fig.1-3 (b) to fig.1-3 (c), the principal axes of stress are not along A' C' and B' D', otherwise, the rectangle in fig. 1-2 (c) should be obtained; and the principal strains

Continued.....

would be measured from the deformed state of AC and BD instead of EG and FH. The principal axes of strain in fig.1-3 (b) and in fig.1-3 (c) with respect to the material are not coincident, those in fig.1-3 (b) are along AC and BD and those in fig.1-3 (c) are along EG and FH. Therefore, the deformation from fig.1-3 (b) to fig.1-3 (c) is said to be non-coaxial. The strain path of the material deformed from fig.1-3 (a) to fig.1-3 (b) and then to fig.1-3 (c) is a non-coaxial one. Further discussion about the difference between a coaxial and a non-coaxial deformation will be made in this thesis.

For the completeness of <sup>the</sup> forming limiting curve of sheet metal, it is necessary to investigate non-coaxial strain paths. There are some more significant reasons than the completeness of <sup>the</sup> forming limiting curve of sheet metal. The non-coaxiality of principal axes of strain will zigzag the strain path even when the stress ratio is kept constant. This zigzagging of <sup>the</sup> strain path may bring another mode of failure. And, in fact, the deformations in which the material is deformed under non-coaxial and zigzag strain paths are very common in practice. Any forming process apart from axisymmetrical ones, for example, an elliptical cup drawing, would involve those kinds of deformation. In axisymmetrical forming like a circular cup drawing, if the blank is not a round one there will be non-coaxial deformations or, even if the blank is a round one, the earring would induce the involvement of non-coaxial deformation. In <sup>the</sup> sheet metal industry, many products are

Continued.....

not formed in one forming process, in particular, redrawing is widely used in deep drawing. Multiple forming processes and redrawing are very likely to bring non-coaxial deformation to the material under forming due to the nonalignment of the principal axes of stress in different parts of the forming processes. The necessity for exploring non-coaxial deformation is quite obvious.

In the second aspect, formability is the performance of sheet metal in a forming process. As said in the second paragraph in this chapter, forming is understood to be the process in which a workpiece of sheet metal is clamped against a die and a punch pushes the sheet through a hole in the die. There are two possible cases in forming. One is pure stretching in which the workpiece is clamped firmly so that no material clamped is drawn in to form the wall of the shell and the punch stretches the material in the unsupported region. The performance of the material in pure stretching is usually called stretchability and can be represented by the maximum punch penetration as in the Erichsen test or by the average surface strain in the shell. The formability of sheet metal in pure stretching can also be represented by the forming limit at the critical section, which lies in the first aspect of formability. The other case in forming is deep drawing in which both stretching and drawing are involved. Drawability is used to represent the formability

Continued.....

in deep drawing.

In deep drawing, the measure of drawability is the largest blank that can be used - hence the Swift's test.

However, the Swift's test has probably encouraged the impression of drawability as a material property. In fact, drawability is the performance of sheet metal in a forming process so it is dependent on the forming process.

As <sup>the</sup> forming limit curve is a spectrum of forming limits of <sup>a</sup> material deformed under different possible strain paths and the ductility of material in <sup>a</sup> tension test is only one of the forming limits in <sup>the</sup> forming limit curve, the drawability should also be a spectrum of the performance of material in different forming processes and the Limiting Drawing Ratio defined in the Swift's test is only <sup>one</sup> of the performances in that spectrum.

The Swift's test is limited to the drawing of circular cups. In fact, this limitation was not set by Professor Swift himself. The investigation of non-circular cups was not done by Professor Swift because he thought the problem of the circular cup should be solved first. To quote Professor Swift:-

"When the intensity of the drawing and blank-holding action vary from one point to another, as for example, in the case of a pressing of square plan with

Continued.....

round corners, local distortion and the possibility of another mode of failure arises which may bring into play another property of the material. But while the simple drawing and stretching problem is still unsolved little purpose would be served by pursuing this more complex effect."

Proceedings, Institute of Automobile Engineers, 1940, vol. 34, page 365.

This quotation shows that the complexity in non-circular cup drawing was ~~observed~~ observed at a very early stage of sheet metal forming research. After three and a half decades of these remarks being made, it is surely not too early to pursue the "more complex effect" which that writer eschewed. In this project, the definition of drawability and the drawability test is generalised to cover all shapes of cup. The quantitative distinction between stretching and drawing is also made in this thesis. The achievements of this project are therefore mainly as follows,

1. The investigation and development of non-coaxial deformation on both theoretical and experimental bases.

Continued.....

2. To define and generalise the definition of drawability and the drawability test to cover all shapes of cup.
3. To link up the drawability with <sup>the</sup> Forming Limit Curve for a complete view of formability, otherwise Swift's Limiting Drawing Ratio and Keeler's Forming Limit Curve remain unrelated.

In this thesis, the research reported is put in its historical perspective in Chapter 3, Review of Past Literature and the theoretical background of the work is outlined in Chapter 4. In Chapter 5 and Chapter 6, strain analysis is presented for both the coaxial and the non-coaxial case. This analysis is necessary because the strains in sheet metal have hitherto been investigated with the two definitions of elastic strain - direct and simple shear strains - and in some literature the engineering rather than the natural strains are used. The slightly more complicated mathematics is therefore merely to meet a realistic need. The implications of the theory of plasticity, including the strain-hardening, Lévy-Mises equations and the stress-strain relationship, in the non-coaxial case are discussed in Chapter 7. In Chapter 8, the performance of sheet metal in a forming process is

Continued.....

defined and the definition of drawability is generalised to be applicable to all shapes of cups. The experimental technique is described in Chapter 9 and the results and discussions are in Chapter 10 and Chapter 11. In Chapter 12, the characteristics of a forming process in terms of the convergence of metal flow and an index of ~~the~~ roundness are defined. The conclusions of this project are presented in Chapter 13 and some suggestions for ~~the~~ future work are made in Chapter 14.

Continued.....

CHAPTER 2

DEFINITIONS

## Definitions

Because of the inconsistency in the use of the terms in sheet metal forming literature, it is necessary, for the clarity of later discussion, to define the basic terms clearly first.

### 2.1 Strain

Strain is the quantitative measurement of the displacement of points in a material relative to one another when the material is deformed. There are two strain measures, engineering strain and natural strain. For instance when a bar of material with gauge length  $l_0$  is strained under a uniaxial tension to a length  $l_1$ , the engineering strain is  $(l_1 - l_0)/l_0$  and the natural strain,  $\ln (l_1/l_0)$ .

In fact, the term "strain" is very often used as the abbreviation of "state of strain". In a real material, deformation is always three-dimensional and is represented quantitatively by three direct strains which are the relative displacement along the co-ordinate axes, and six shear strains which are the transverse displacement gradients. These nine components representing a state of strain could be reduced to three by choosing suitable co-ordinate axes. It is always possible to find three orthogonal axes passing through the material before the deformation, which remain orthogonal after the deformation. In other words, there are always three and

Continued.....

in general only three fibres in the material which are orthogonal to one another both before and after the deformation. No relative rotation occurs among these three fibres in the deformation, therefore no <sup>transverse</sup> displacement gradient or shear strain occurs along these fibres. These orthogonal directions are called principal directions or principal axes. The strain along the principal axes are called principal strains. Thus, a state of strain is normally represented by the three principal strains instead of three direct strains and six shear strains.

Strictly speaking, three more factors specifying the principal directions with respect to the material are necessary for completely representing a state of strain. The principal directions with respect to the material are very often neglected when only a state of strain is discussed or when the principal axes of all the states of strain discussed are fixed with respect to the material. *This* does not mean that specifying the principal axes with respect to the material is not necessary, it only means that in some special cases, the principal axes with respect to the material is less interesting. In fact, the principal directions with respect to the material are very important when two or more states of strain discussed have their principal directions different from one another. Therefore, generally speaking, there are six values needed for specifying a state of strain.

Continued.....

In sheet metal forming, one of the principal axes is always normal to the sheet surface no matter how the material is deformed. This fixture of one principal axis cuts down the three factors necessary for specifying the principal axes with respect to the material to one only. Therefore, in sheet metal forming, a state of strain is completely represented by four parameters, three principal strains and one to specify the principal directions with respect to the material.

In this thesis, natural strain is always used because it is more convenient for large strains like those in plastic deformation. Also, due to <sup>the</sup> incompressibility of metal, the sum of the principal strains is equal to zero when natural strains are used.

## 2.2 Coaxial and Non-coaxial Deformations

In sheet metal a state of strain is completely represented by the three principal strains and an angle specifying the directions of the principal axes of strain with respect to the material, but not the three principal strains only. Deformation is changing the state of strain. As long as deformation occurs, the state of strain of the material changes. The state of strain may be changed by changing the principal strains and keeping the directions of principal axes of strain fixed with respect to the material, or by changing the directions of the principal axes of strain with respect to the material.

Continued.....

and keeping the principal strains unchanged or by changing both.

A deformation which changes a state of strain by changing only the principal strains but not the directions of the principal axes of strain with respect to the material, is a coaxial deformation such as that from fig.1-2 (b) to fig.1-2 (c) described in the last Chapter. A deformation which changes a state of strain by changing the directions of the principal axes of strain with respect to the material no matter whether the principal strains are changed or not, is a non-coaxial one such as that from fig.1-3 (b) to fig.1-3 (c).

A deformation which changes the state of strain of the material from an undeformed state to a state of strain without showing the intermediate state can always be reckoned as a coaxial one such as that from fig.1-2 (a) to fig.1-2 (b) and that from fig.1-3 (a) to fig.1-3 (b),

### 2.3 Strain Path

A deformation is a change of state of strain. The changing from an initial to a final strain can not, of course, be instantaneous, nor can a material change from an initial to a final strain without passing through the intermediate stages.

A strain path is the trace, or locus, of all the intermediate states of strain between the initial and the

Continued.....

final states of strain. Strain can always be plotted in a co-ordinate system and so can a strain path. A strain path plotted in a co-ordinate system will be a line passing <sup>through</sup> the initial, all intermediate and the final strains.

#### 2.4 Forming Process and Forming Conditions

A forming process is a forming operation which is specified by the forming tools, such as deep drawing and hydrostatic bulging. Forming conditions are conditions of forming in a forming process, such as condition of lubrication, size and shape of the blank, holding pressure and location of the blank and so on.

A forming process can be operated under different forming conditions. Changing the lubrication condition, for instance, may involve a change in the behaviour of material under forming. This is a change of forming condition but not of the forming process.

#### 2.5 Formability

The term "formability" is usually loosely understood to mean on the one hand, the resistance of material under forming to failure, <sup>and</sup> on the other hand, the performance of material in a particular forming process. There has not yet been a clear definition for it. The large number of different sheet metal tests in current use, and the even larger number of those being proposed, are symptoms showing that the term "formability" has not been defined

Continued.....

with scientific precision. The question "what is the formability of the material?" would not make much sense before the question "what does formability mean?" is answered.

To obtain logical precision, it is necessary first to distinguish between, and separate, the two aspects of formability, the resistance of sheet metal under forming to failure and the performance of sheet metal in a particular forming process. Unless they are clearly distinguished, the formability of sheet metal can not be sensibly discussed.

A. Forming Limit at the Critical Section

There are usually three types of failure in sheet metal forming. They are: deterioration of surface finish, puckering and excessive thinning leading to fracture. The deterioration of surface finish when a material is deformed is a metallurgical rather than a mechanical problem, and puckering is a problem of instability of plastic deformation which is outside the scope of this thesis. In the following, the failure of sheet metal is confined in this thesis to the excessive thinning and fracture only.

In sheet metal forming, the material generally fails

Continued.....

locally. The position in the material where excessive thinning or fracture eventually occurs is called the critical section. The behaviour of the material at the critical section decides how far the material can be deformed in that forming process under certain forming conditions. The material at the critical section is deformed under a certain strain path to a state of strain at which the excessive thinning or fracture occurs. That state of strain is the limit the material can be deformed under that strain path and is the forming limit at that critical section.

The material at the critical section is deformed under different strain paths depending on the forming process and forming conditions. Therefore, the forming limit at the critical section of a material is dependent on the strain path and if it is discussed, the strain path must be specified at the same time.

#### B. Forming Limit Curve

One of the two aspects of formability, namely, the resistance of sheet metal under forming to failure, is defined by the forming limit curve.

Sheet metal can be deformed under various forming conditions in various forming processes, and under each set of forming conditions in each forming process, the

Continued.....

material at the critical section is deformed under a particular strain path which has an end point at which the local thinning or fracture occurs. If all the possible strain paths under which the material at the critical section is deformed are provided, the end points of the strain paths are the limits the material can be deformed, and the curve passing <sup>through</sup> these end points is the forming limit curve.

Strain paths can always be plotted in a co-ordinate system. Then the forming limit curve of a material is the curve in a co-ordinate system which covers all the end points of strain paths. A material under forming would fail when its strain path reached the forming limit curve.

The forming limit curve of a material is not a simple material property which can be represented by a single index, but is a spectrum of properties which can only be represented by a curve. It is the limit that a material can be deformed without the occurrence of local thinning or fracture.

### C. Performance in a Forming Process

The other aspect of formability of sheet metal is the performance of the material in a forming process. Many

Continued.....

sheet metal tests are proposed to rate the formability of sheet metal and every test has its own index to specify the performance of the material in the test, such as the maximum punch penetration, used as an index in <sup>the</sup> Erichsen test; the polar height at the maximum pressure used in the hydrostatic bulge test; and the limiting drawing ratio used in Swift's test. It is understood that the test itself is a forming process. Therefore, formability in this aspect is the performance in a forming process and is dependent on the forming process.

In <sup>the</sup> actual sheet metal forming, there is no process in which the material everywhere in the workpiece is deformed under the same strain path as that at the critical section. The material outside the critical section is not deformed to the strain limit but the strains are related to that at the critical section. By changing the forming conditions the location of the critical section in the workpiece as well as the strain path of the critical section may be moved so that the performance of the material in that forming process is changed.

The forming limit curve of a material is a spectrum of innate material properties and can only be changed or improved by changing its chemical composition, grain size or heat treatment condition which are all in the metallurgical field. The performance of a material in

Continued.....

forming processes can be improved by choosing the suitable forming conditions like blank shape, size and lubrication and so on.

Now it is possible to discuss the formability of a sheet metal by specifying the forming limit of a certain strain path or the performance in a particular forming process.

Continued.....

CHAPTER 3

REVIEW OF PAST LITERATURE

### Review of Past Literature

As mentioned in <sup>the</sup> last Chapter, the term "formability" has been loosely and inconsistently used in the sheet metal forming literature. After clearly describing the two aspects of formability, namely the forming limits of sheet metal and the performance of sheet metal in a particular forming process, it is possible and easy to review the past literature concerning formability of sheet metal from the point of view of these two aspects.

In this review, due to the huge quantity of past literature in sheet metal forming, it is not possible to mention the papers one by one but only the parts which are significant to this thesis will be discussed.

#### 3.1 Forming Limit ~~and~~ Curve of Sheet Metal

Sheet metal tests, such as <sup>the</sup> Erichsen, Olsen, Fukni and Swift's tests, were originally proposed for testing the quality of sheet metal under forming. But, for a single test, for instance, the Erichsen test, some-times, inconsistent results are obtained when a high Erichsen value material fails in a forming process but a low Erichsen value material succeeds. Now it is understood that no single ~~one~~ sheet metal test can ~~be~~ rate the quality of material under all forming operations. Sheet metal tests may not duplicate the process involved in an actual sheet metal forming operation so that the test results are npt adequate for predicting precisely the performance of

Continued.....

the material in the forming process. Therefore, another approach has<sup>been</sup> used in pursuing the limiting strains a material sustains before excessive thinning and fracture occur, for all possible forming operations. Formability curves for mild steel have been investigated by Keeler<sup>(1)</sup> Goodwin<sup>(4)</sup> and, Lee and Hsü<sup>(5)</sup> and some others.

#### A. Keeler's Curve

In Keeler's forming limiting curve (1) the two principal strains on the sheet surface were measured at the onset of fracture in a number of biaxial stretching experiments (2) in which eight-inch diameter steel blanks were securely clamped between a die ring and blank holder, and stretched by various shapes of punches under different lubrication conditions.

The formability curve, or by the name Keeler called it, the critical strain level, was plotted in a co-ordinate system with the large strain on the sheet surface as ordinate and the smaller one as abscissa, and both strains were presented in the engineering strain measure. The curve separated the failure and non-failure of states of strain that mild steel could be deformed to. In fact, it was shown as a band (3) covering the scattering of failure and non-failure states of strain. The scatter could be due to many causes such as inhomogeneity of the material, the difficulty in the determination of end points, variable draw-in, and errors arising from<sup>not</sup> using a fine enough

Continued.....

grid or even the involvement of non-coaxial deformation. Keeler's formability curve was redrawn by Goodwin (4) as shown in fig.3-1. The curve was obtained by biaxial stretching, therefore it only covered the region in which both the major and minor strains on the sheet surface were positive.

#### B. Goodwin's Curve

Goodwin (4) expanded Keeler's formability curve to the tension-compression quadrant by means of various cup and tension tests to obtain the failure strains in that region. The cup tests were made by using flat and round nosed circular punches to draw various shaped blanks into a two-inch diameter die. The shape of the blank and the clamping pressure controlled the location of failure and the degree of <sup>the</sup> minor strain. By varying the clamping pressure from a minimum which was just large enough to prevent the buckling of the blank when it was drawn into the die, to a maximum where the minor failure strain was positive, the formability curve (fig.3-1) in both <sup>the</sup> tension-tension and tension-compression regions, was obtained.

It is interesting to note that Goodwin used a different shapes of blank in his experiment and found that an elliptical blank in combination with the round nosed punch produced the greatest variety of failure strains. An elliptical blank drawn by a circular punch is no longer an axisymmetrical forming and it would involve non-coaxial

Continued.....

deformation somewhere in the workpiece.

C. Lee and Hsü's Formability Curve

In Lee and Hsü's formability curve, (5) <sup>the</sup> strain path under which the material at the critical section is deformed is plotted in a triangular co-ordinate <sup>system</sup>, (which will be discussed in Chapter 4.). A series of symmetrical forming processes (fig. 3-2) with different punch nose profiles - from semi-spherical to very small radius nose - different lubrication conditions including <sup>separated</sup> die face and blank holder, and different holding pressures were used to get the material at the critical section deformed under strain paths with different strain ratios. The formability curve which passes all the end points of the strain paths is drawn in the regions of tension-tension and tension-compression <sup>strains</sup>. Two branches of the formability curve meet at a cusp which suggests that there are two mechanisms of neck formation, one in the tension-tension region and one in <sup>the</sup> tension-compression region.

Lee and Hsü's curve is a curve instead of a band like Keeler's and Goodwin's curve. In Lee and Hsü's work, it is significant that the strain paths are shown together with the formability curve, because ~~the~~ formability curve is dependent on the strain path.

Although there are still many papers <sup>e.g.</sup> (6)-(9) concerning the forming limits of sheet metal, they are almost the

Continued.....

same as those having been reviewed. Differences lie in the determination of <sup>the</sup> end point which is a problem of instability and is outside the scope of this project.

### 3.2 Formability of Sheet Metal under Zigzag Strain Paths

It is well known that a flat blank can be drawn into a deeper cup without fracture by redrawing in two or more stages. The strain path of the critical section in the redrawing operation may be zigzagged because the straining varies from one stage to another.

The formability of sheet metal is path dependent, surely, it would be affected by the zigzagging of the strain path. This is the reason why many efforts <sup>e.g.</sup> (10)-(12) were made to investigate the effect of <sup>a</sup> zigzag strain path on <sup>the</sup> formability of sheet metal.

Due to the similarity of the experimental results in past literature on the effect of zigzag strain paths on formability, a typical one (10) is reviewed. The effect of the strain path on the fracture strain of steel sheet was investigated in two stages of forming, combining uniaxial tension, biaxial and equi-biaxial tension and tension-compression, with the principal axes of stress and strain fixed with respect to the material. The fracture strain is plotted in Cartesian co-ordinates with  $\epsilon_x$  and  $\epsilon_y$  which are the two principal strains on the sheet surface, as axes. Between the lines with strain ratio  $\epsilon_x/\epsilon_y$  from +1

Continued.....

to -1, it is divided into three regions, the region I (fig.3-3) in which fracture never occurs no matter what the combination of the two stages of deformation, the region II, <sup>where</sup> fracture always occurs and the region III, <sup>where</sup> fracture occurs depending on the strain path or the combination of the deformations. The diagram (fig.3-3), clearly shows that the region III in which the occurrence of fracture is uncertain, spreads over a very large area compared with the region I in which fracture never occurs. In other words, the formability of sheet metal under zigzag strain paths can not be represented by a curve or a narrow band as that under linear or nearly linear strain paths. The reason is due to the large number of possible variety of stress combinations which produce a large number of different strain paths. The zigzag strain paths investigated are all obtained by two or more stages of deformation with the principal axes of stress and strain fixed with respect to the material. In other words, the strain paths are zigzagged by changing the strain ratios with the principal axes of stress and strain fixed with respect to the material.

When the principal axes of stress are fixed with respect to the material, the strain ratios can only be changed by changing the ratios between the principal stresses. But changing the ratios between the principal stresses is not the only way to change the strain ratios. Strain ratios

Continued.....

can also be changed by keeping the ratios between the principal stresses constant but rotating the directions of principal axes of stress with respect to the material in which non-coaxial deformation is involved.

However, quite a large number of industrial sheet metal products are not circular and are manufactured by re-drawing operations. In these products the strain path of the critical section in the product will be both non-coaxial and zigzag ones. Hitherto, no non-coaxial zigzag strain path has been investigated. In this thesis, non-coaxial zigzag strain path will be investigated both theoretically and experimentally.

### 3.3 Sheet Metal Test

The other aspect of formability is the performance of sheet metal in a particular forming process or a sheet metal test. For convenience, cost and co-ordination between producer and user, a flexible system of testing based on the principle of reproducing the essential material behaviour under forming in a simplified form is needed. For an engineer or a process designer in <sup>the</sup> sheet metal industry, although a test does not provide the exact information needed, if a reasonable guidance could be obtained, it is very helpful. Empirical tests can be extremely useful in practice, even though they may not be the same as the actual forming process or processes, the behaviour of the material in the tests may happen to be very similar to

Continued.....

that in<sup>an</sup> actual forming operation to which the test results are to be applied. This is the reason why sheet metal tests are still widely used even though it is known that the results of a single test are not adequate to rate the forming quality of sheet metal for general validity.

According to Shawki (13), ~~there are~~ at least nineteen sheet metal tests have<sup>are</sup> been proposed and<sup>are</sup> in current use. In this review, only typical tests and those significantly related to the project in this thesis will be reviewed.

#### A. The Erichsen Test

The test was proposed by Erichsen (14) in 1914. The general configuration of the test and its principal dimensions are specified in British Standard No. 3855, 1965. This is the only sheet metal test in the B.S.S.. In the test, the blank is held against a holder, and is deformed by a cylindrical punch with<sup>a</sup> spherical nose of standard diameter 20mm. The maximum punch penetration attained before fracture occurs is taken as the Erichsen value.

In<sup>the</sup> Erichsen test, the blank holding load is set to be 1000 ( $\pm 100$ ) kgf. It is doubtful if the material in the flange could be prevented from being drawn into the curved part. The amount of draw-in and its influence on the Erichsen value under a variety of testing conditions were

Continued.....

measured by Kaftanoglu and Alexander (15).

If the draw-in is prevented completely, <sup>the</sup> Erichsen test is a purely stretching test.

B. The Hydrostatic Bulge Test

Although no standard form is suggested, the blank is held with <sup>a</sup> special clamping device (16)-(17) against a die and is deformed by hydraulic pressure instead of a solid punch. The polar height at the maximum pressure is used as the index for the test.

Because there is no friction between the blank and the punch, the stresses and strains can be calculated by assuming the bulged shape as part of a sphere (17)-(20).

The real shape or its deviation from the sphere <sup>has</sup> <sup>been measured</sup> recently ~~measured~~ (21) and the stress distributions in the shell are determined.

The hydrostatic bulge test is a stretching test too.

C. The Swift's Test

The Swift's test (22)-(24) is one of the deep drawing tests. There are several proposals of the deep drawing test (25)-(27) and the Swift's test is the best known and is well established. In the early standard Swift's test, a flat nosed punch of 2.000 in. diameter with a profile radius of 0.25 in. was used (25). Recently, the International Deep Drawing Research Group on Swift's Cup-Drawing Test (28)

Continued.....

proposed standard test conditions for the test. They are as follows:-

Punch diameter	50mm
Punch radius	4.5 mm
Die opening diameter	53.65 mm
Die radius	13.0 mm
Die surface roughness	CLA 0.04-0.15 $\mu\text{m}$
Punch speed	1.7 mm/sec.

Clamping load: it is set to be just large enough to prevent wrinkling of the blank.

Lubrication conditions:

the die and the holding plate are lubricated with polythene film on grease, and the punch is unlubricated.

In the test, a circular blank located symmetrically with respect to the punch is drawn through the die hole. The diameter of the blank drawn is progressively increased until fracture occurs in the cup. The maximum diameter of the blank which can be drawn successfully, divided by the punch diameter is known as the Limiting Drawing Ratio and serves as a criterion of drawability.

The Swift's test has several attractive features, it is so closely simulative of many common forms of pressing, the

Continued.....

specimen is inexpensive, the testing technique is simple and it reveals any directional properties of the material by the formation of ears. But it has also its disadvantages and in its simplicity lies the limitation for the extension and generalisation of the definition of drawability and of the drawability test which will be done in this project.

In order to find the Limiting Drawing Ratio in the Swift test, blanks of progressively increased diameter are drawn until fracture occurs in the cup. In fact, this is a trial-and-error approach. It was found (29) that the relationship between the maximum drawing load and blank diameter was nearly linear, and the maximum diameter of the blank which could be drawn successfully was that when the maximum drawing load was near the fracture load of the cup. Also, the fracture load of the cup depended on the strength of the material at the punch profile region which was nearly constant and independent of the blank size. Therefore, a single-blank test was suggested (29).

Usually, at the stage where the maximum drawing load is reached, only  $\frac{1}{3}$  or  $\frac{1}{2}$  of the drawing operation has been completed. Thus the maximum drawing load can be measured without completing the whole drawing operation. A blank of diameter  $D_s$  which can be drawn successfully is drawn until the maximum drawing load  $L_s$  is reached and recorded. Then the flange of the uncompleted cup is clamped firmly

Continued.....

and <sup>the</sup> punch travel continues. Because the flange of the cup is clamped firmly, the drawing load goes up with the punch travel and reaches the fracture load  $L_f$  of the cup when fracture occurs in the cup. Because the relationship between the maximum drawing load and the diameter of blank is nearly linear.

$$\frac{\Delta D}{\Delta L} = \frac{D_c - D_s}{L_f - L_s} = K$$

where  $D_c$  is the maximum diameter of blank which can be drawn successfully and  $K$  is the slope of the maximum drawing load and blank diameter relationship. In order to find  $K$ , another blank of diameter  $D_t$  other than  $D_s$  should be drawn and the maximum drawing load is  $L_t$ . Thus

$$K = \frac{D_t - D_s}{L_t - L_s}$$

and

$$D_c = \frac{D_t - D_s}{L_t - L_s} (L_f - L_s) + D_s$$

In fact in the single-blank test at least two blanks must be used. Even so, it is a good approach and this approach is used in this project.

The anisotropy of sheet metal is usually represented by the  $r$  - value which is <sup>the</sup> ratio between the strains in <sub>A</sub> width and the thickness directions in a rectangular tensile test

Continued.....

piece. It is well known that the anisotropy of sheet metal produces earring in deep drawing and there are many research papers <sup>e.g.</sup> (30)-(33) concerning the anisotropy of sheet metal and its effects in forming operations. But those papers are not significantly related to this project. The effect of the anisotropy of sheet metal on formability in the forming operation investigated in this project is classified as the orientation of <sup>the</sup> blank with respect to the rolling direction of the sheet and will be discussed in Chapter 11.

Among the papers so far reviewed, those concerning the forming limiting curve are either limited to the coaxial case or <sup>have</sup> paid no attention at all to the coaxiality of the principal axes of stress and strain, and those concerning the performance of sheet metal in a forming process are limited to the performance in an axisymmetrical forming operation. Hitherto there has been no literature reporting the investigation of non-coaxial deformation in sheet metal forming and there has been no general assessment of the performance of sheet metal in all forming processes, including both axisymmetrical and non-axisymmetrical forming operations. The incompleteness of the forming limiting curve requires naturally the development and investigation of non-coaxial deformation, and as many sheet metal products are not axisymmetrical, it is necessary and significant to develop and investigate the

Continued.....

more complex cases in non-axisymmetrical forming. These are the main purposes of this project.

#### 3.4 Non-axisymmetrical Formings

Many investigations have been done both theoretically and experimentally on ~~the~~ axisymmetrical forming, like cylindrical cup drawing, hydrostatic bulging and so on. The behaviour of material under axisymmetrical forming is well understood and many sheet metal tests based on it are in current use. It is well known that the behaviour of material in a non-axisymmetrical forming process is much more complex than that in an axisymmetrical one. Test results in general are reliable only when the actual forming process and forming conditions are the same as those in the test. The more they deviate from those in the test, the less reliable the test results are for predicting the performance in the actual forming process. However, there has not been either a test or even a definition of measurement for specifying the performance of sheet metal in non-axisymmetrical forming processes. Although non-axisymmetrical sheet metal products have been produced for many decades in industry and non-axisymmetrical forming has been investigated by many sheet metal forming research scientists, the achievement is mainly on the purely empirical aspect, perhaps due to the lack of theoretical development.

Car body and automobile panel making is one of the most

Continued.....

popular non-axisymmetrical forming <sup>processes</sup> in industry. The study of formability in car body and automotive panel making is still limited to the measurement of <sup>the</sup> limiting strain at the critical section (1),(4),(34),(35) and mostly by using <sup>a</sup>circular grid which fails to distinguish between coaxial and non-coaxial deformations.

Square, rectangular and elliptical cup drawing have been investigated by many sheet metal research scientists (36)-(46). The blank shape for a rectangular shell was sketched out, by assuming that the material in the shell walls did not thicken or elongate during the drawing operation and that the amount of material for forming the four corners was equal to that required for drawing a cylindrical shell of a diameter double the corner radius of the rectangular shell, having the same height and bottom radius as in the rectangular shell, and then modification was done on smoothing the blank corners (36)-(38). No significant conclusion about the formability was made.

The strain distribution along the meridian of a square shell was measured and investigated in different shapes of blank (37)-(40). Only purely empirical but no significant conclusions for the formability of sheet metal in non-axisymmetrical forming, were suggested.

The effect of anisotropy of sheet metal on the depth in a rectangular cup drawing was investigated by Lilet (41).

Continued.....

The cup could be drawn deeper if the rolling direction of the sheet was  $45^\circ$  to the flat side of the rectangular cross-section. This effect was also investigated by Wilson (42) in square cup drawing. A circular blank was drawn and the largest diameter of the blank which could be drawn successfully, namely, the critical blank diameter, was used to represent the formability in the square cup drawing. He found that the critical blank diameter was larger when the rolling direction of the sheet was parallel to the diagonal of the square section than that when it was  $45^\circ$  to the diagonal. Even so, the extent of forming in <sup>the</sup> non-axisymmetrical case was limited to the circular blank drawing.

The "draw-in" in a non-axisymmetrical <sup>draw</sup> was defined by Miyauchi et al (43) as

$$c = \frac{\Delta l_f}{\Delta l_s}$$

where  $\Delta l_s = l_s - l_{s0}$   $\Delta l = l - l_0$  and

$$\Delta l_f = \Delta l - \Delta l_s \quad (\text{fig.3-4})$$

From fig 3-4, it is understood that  $\Delta l_s$  is the elongation of  $l_{s0}$ , but what  $\Delta l$  represents is difficult to visualise because  $c'$  is not the current position of the point b in the blank. This vagueness makes the definition difficult to understand. A more general and logical definition of "draw-in" will be defined in this thesis.

Continued.....

A square grid was used for strain measurement in a square cup drawing by Masuda and Mishiro (40). Not only the strain distribution along the meridian and at the flange of a square cup at different stages of <sup>the</sup> drawing operation was measured, but also the directions of the principal strains were pointed out. Unfortunately, they did not pay attention to the change in direction of the principal axes of ~~the~~ strain and thereby missed the discovery of non-coaxial deformation.

In the deep drawing of elliptical shells, Yoshida et al (45) found that a rectangular blank of certain dimensions can be successfully drawn while another rectangular blank of the same length in the major axis direction but smaller width in the minor axis direction, can not be drawn successfully. The metal flow in the blanks was investigated for understanding this phenomenon. But the effort was put onto purely empirical grounds relating the blank size to the  $r$ -value and the  $n$ -value without any theoretical analysis. The metal flow in deep drawing of some other irregular-shaped shells was also investigated by Yoshida et al (46). It is hard to expect a sound conclusion based on <sup>a</sup> purely empirical approach unless a huge amount of experimental data is provided.

It is believed that for investigating the deep drawing of non-circular shapes, careful study of the metal flow in the

Continued.....

blank provides a good approach. But before the <sup>present</sup> experiments  
<sup>are discussed</sup> some theoretical analysis is necessary, otherwise the work  
may be self-defeating due to the infinite number of  
irregular shapes.

Continued.....

CHAPTER 4

STRAIN ANALYSIS

## Strain Analysis

The typical sheet metal forming process considered in this thesis is illustrated in fig.4-1. A piece of sheet metal, flat and of uniform thickness, is clamped at its edge (between the edge B and the closed curve B<sub>0</sub>) and formed by a rigid or liquid punch so that the material inside the curve C becomes a curved surface. Such a process may be idealized mathematically as a transformation of a plane into a curved surface.

A co-ordinate<sup>system</sup> fixed with respect to the material, has an axis always normal to the sheet surface no matter how the flat plane is deformed, and that axis is always one of the principal axes in sheet metal forming. Also, due to the incompressibility of metal in plastic deformations the sum of the three principal strains is zero and there are only two degrees of freedom for the three principal strains. Therefore, it is sufficient and convenient to analyse the strain in two-dimensions in sheet metal forming.

### 4.1 Deformation Represented by an Affine Transformation.

A typical point  $(X_1, X_2)$  in the blank is deformed or (47) transformed to a new position  $(X_1', X_2')$  in a co-ordinate system which is fixed with respect to the material. The equations for this transformation are as follows,

$$\begin{aligned} X_1' &= X_1' (X_1, X_2) \\ X_2' &= X_2' (X_1, X_2) \end{aligned} \quad 4-1$$

In general, Eqs. 4-1 are nonlinear functions and <sup>they</sup> may be

Continued.....

expanded in Taylor's series at the vicinity of the point under consideration provided that the transformation in the region around the point is continuous.

Eqs. 4-1 are expanded in Taylor's series at the point whose initial co-ordinates are (a,b), and become:

$$\begin{aligned}
 X'_1(X_1, X_2) &= X'_1(a, b) + \frac{\partial X'_1}{\partial X_1} (X_1 - a) + \frac{\partial X'_1}{\partial X_2} (X_2 - b) \\
 &+ \frac{1}{2!} \frac{\partial^2 X'_1}{\partial X_1^2} (X_1 - a)^2 + \frac{\partial^2 X'_1}{\partial X_1 \partial X_2} (X_1 - a)(X_2 - b) \\
 &+ \frac{1}{2!} \frac{\partial^2 X'_1}{\partial X_2^2} (X_2 - b)^2 + \dots
 \end{aligned}$$

$$X'_2(X_1, X_2) = X'_2(a, b) + \frac{\partial X'_2}{\partial X_1} (X_1 - a) + \frac{\partial X'_2}{\partial X_2} (X_2 - b)$$

4-2

$$\begin{aligned}
 &+ \frac{1}{2!} \frac{\partial^2 X'_2}{\partial X_1^2} (X_1 - a)^2 + \frac{\partial^2 X'_2}{\partial X_1 \partial X_2} (X_1 - a)(X_2 - b) \\
 &+ \frac{1}{2!} \frac{\partial^2 X'_2}{\partial X_2^2} (X_2 - b)^2 + \dots
 \end{aligned}$$

They may also be written as:

$$X'_1(X_1, X_2) - X'_1(a, b) = \frac{\partial X'_1}{\partial X_1} (X_1 - a) + \frac{\partial X'_1}{\partial X_2} (X_2 - b)$$

+ terms of higher orders in (X<sub>1</sub>-a) and (X<sub>2</sub>-b)

Continued.....

$$X_2' (X_1, X_2) - X_2' (a, b) = \frac{\partial X_2'}{\partial X_1} (X_1 - a) + \frac{\partial X_2'}{\partial X_2} (X_2 - b)$$

4-3

+ terms of higher orders in  $(X_1 - a)$  and  $(X_2 - b)$

If the deformation around the point  $(a, b)$  which is considered to be homogeneous, or the region being considered is small enough so that the higher orders of  $(X_1 - a)$  and  $(X_2 - b)$  can be neglected, in other words, straight lines remain straight and parallel lines remain parallel after the deformation, then  $\frac{\partial X_1'}{\partial X_1}$ ,  $\frac{\partial X_1'}{\partial X_2}$ ,  $\frac{\partial X_2'}{\partial X_1}$  and  $\frac{\partial X_2'}{\partial X_2}$  are all constant and terms of higher orders in  $(X_1 - a)$  and  $(X_2 - b)$  vanish. Equations 4-3 become

$$X_1' (X_1, X_2) - X_1' (a, b) = A_{11} (X_1 - a) + A_{12} (X_2 - b)$$

4-4

$$X_2' (X_1, X_2) - X_2' (a, b) = A_{21} (X_1 - a) + A_{22} (X_2 - b)$$

where

$A_{11}$ ,  $A_{12}$ ,  $A_{21}$  and  $A_{22}$  are  $\frac{\partial X_1'}{\partial X_1}$ ,  $\frac{\partial X_1'}{\partial X_2}$ ,  $\frac{\partial X_2'}{\partial X_1}$  and  $\frac{\partial X_2'}{\partial X_2}$  respectively.

If the point being considered is taken as the origin of the co-ordinates before and after the transformation, or

$a = 0$ ,  $b = 0$  and  $X_1'(a, b) = 0$ ,  $X_2'(a, b) = 0$ , then

Continued.....

Eq. 4-4 becomes,

$$X_1' = \frac{\partial X_1'}{\partial X_1} X_1 + \frac{\partial X_1'}{\partial X_2} X_2 = A_{11} X_1 + A_{12} X_2 \quad 4-5$$

$$X_2' = \frac{\partial X_2'}{\partial X_1} X_1 + \frac{\partial X_2'}{\partial X_2} X_2 = A_{21} X_1 + A_{22} X_2$$

It may also be written in matrix form as

$$\begin{pmatrix} X_1' \\ X_2' \end{pmatrix} = \begin{pmatrix} \frac{\partial X_1'}{\partial X_1} & \frac{\partial X_1'}{\partial X_2} \\ \frac{\partial X_2'}{\partial X_1} & \frac{\partial X_2'}{\partial X_2} \end{pmatrix} \begin{pmatrix} X_1 \\ X_2 \end{pmatrix} = \begin{pmatrix} A_{11} & A_{12} \\ A_{21} & A_{22} \end{pmatrix} \begin{pmatrix} X_1 \\ X_2 \end{pmatrix} \quad 4-6$$

where  $X_1$  and  $X_2$ ,  $X_1'$  and  $X_2'$  are the Cartesian co-ordinates of a point near the point being considered, before and after the deformation respectively, and

$$A_{ij} = \frac{\partial X_i}{\partial X_j} \quad 4-7$$

The co-ordinates  $X_1$  and  $X_2$  may also be considered as the two components of the vector  $\vec{X}$  drawn from the origin to the point  $(X_1, X_2)$  in a Cartesian co-ordinate<sub>system</sub>, and, similarly,  $X_1'$  and  $X_2'$  as the components of the vector  $\vec{X}'$  in the same Cartesian co-ordinate<sub>system</sub> (fig.4-2). The matrix  $|A_{ij}|$  changes the vector  $\vec{X}$  into a different vector  $\vec{X}'$ . Eq. 4-6 represents a transformation and this linear function in fact, is also called affine transformation. Let

Continued.....

$$\vec{U} = \vec{X'} - \vec{X}$$

or

$$U_1 = X_1' - X_1 \quad 4-8$$

$$U_2 = X_2' - X_2$$

Eq. 4-6 becomes:

$$\begin{aligned} \begin{vmatrix} X_1' \\ X_2' \end{vmatrix} &= \begin{vmatrix} \frac{\partial X_1'}{\partial X_1} & \frac{\partial X_1'}{\partial X_2} \\ \frac{\partial X_2'}{\partial X_1} & \frac{\partial X_2'}{\partial X_2} \end{vmatrix} \cdot \begin{vmatrix} X_1 \\ X_2 \end{vmatrix} \\ &= \begin{vmatrix} 1 + \frac{\partial U_1}{\partial X_1} & \frac{\partial U_1}{\partial X_2} \\ \frac{\partial U_2}{\partial X_1} & 1 + \frac{\partial U_2}{\partial X_2} \end{vmatrix} \begin{vmatrix} X_1 \\ X_2 \end{vmatrix} \quad 4-9 \\ &= \begin{vmatrix} A_{11} & A_{12} \\ A_{21} & A_{22} \end{vmatrix} \cdot \begin{vmatrix} X_1 \\ X_2 \end{vmatrix} \end{aligned}$$

Thus:

$$\begin{aligned} A_{11} &= 1 + \frac{\partial U_1}{\partial X_1} \\ A_{12} &= \frac{\partial U_1}{\partial X_2} \\ A_{21} &= \frac{\partial U_2}{\partial X_1} \\ A_{22} &= 1 + \frac{\partial U_2}{\partial X_2} \end{aligned} \quad 4-10$$

Continued.....

Where  $\frac{\partial U_1}{\partial X_1}$  and  $\frac{\partial U_2}{\partial X_2}$  are longitudinal displacement gradients in  $X_1$  and  $X_2$  directions respectively, and,  $\frac{\partial U_2}{\partial X_1}$  and  $\frac{\partial U_1}{\partial X_2}$  are the transverse ones.

In a transformation, in order to find  $A_{ij}$  in Eq. 4-10, at least two points near the point being considered in the directions of  $X_1$ - and  $X_2$ - axes have to be considered too. As shown in fig.4-3, the origin  $O$  of the co-ordinate is the point being considered;  $\overline{OA}$  and  $\overline{OB}$  are the vectors before the transformation; and,  $\overline{OA'}$  and  $\overline{OB'}$  are the vectors after the transformation. The co-ordinates of the point  $A'$  are  $(1 + \frac{\partial U_1}{\partial X_1}) \cdot X_1$  and  $\frac{\partial U_2}{\partial X_1} X_1$  and those of  $B'$  are  $\frac{\partial U_1}{\partial X_2} X_2$  and  $(1 + \frac{\partial U_2}{\partial X_2}) \cdot X_2$ .

Therefore, when the deformation at a point is investigated, a small square grid with the point at one of the corners, which is so small that the deformation in it is uniform and the same as that at the point being investigated, is printed or scribed on the material. After the deformation, by measuring the co-ordinates of the two corners adjacent to the point in the deformed grid,  $A_{ij}$ , which represents the transformation or deformation, can be obtained. It will be proved later that the position of the co-ordinate axes for measuring the deformed grid can be arbitrarily chosen without affecting the transformation or deformation.

Continued.....

#### 4.2 Matrices Representing Typical Modes of Deformation.

As shown in Eq. 4-6, the matrix  $|A_{ij}|$  represents the transformation of co-ordinates, or deformation in metal forming. In <sup>the</sup> last section it has been said that by measuring the deformed square grid,  $A_{ij}$  can be found. Now some matrices obtained from some deformed grids representing a few typical modes of deformation are illustrated in the following.

$$\begin{vmatrix} 1 & 0 \\ 0 & 1 \end{vmatrix} \text{ is a unit matrix and from Eq. 4-6}$$

$$\begin{aligned} X_1' &= 1 \cdot X_1 + 0 \cdot X_2 = X_1 \\ X_2' &= 0 \cdot X_1 + 1 \cdot X_2 = X_2 \end{aligned}$$

it represents a null deformation.

$$\begin{vmatrix} m & 0 \\ 0 & m \end{vmatrix} \text{ represents the transformation}$$

$$\begin{aligned} X_1' &= m \cdot X_1 + 0 \cdot X_2 = mX_1 \\ X_2' &= 0 \cdot X_1 + m \cdot X_2 = mX_2 \end{aligned}$$

It is a uniform dilatation if  $m > 1$  (fig. 4-4a) and is a uniform contraction if  $m < 1$  (fig. 4-4 b). All the fibres elongate or contract to a ratio  $m$ .

Continued.....

$$\begin{vmatrix} \cos\theta & \sin\theta \\ -\sin\theta & \cos\theta \end{vmatrix} \text{ and } \begin{vmatrix} \cos\theta & -\sin\theta \\ \sin\theta & \cos\theta \end{vmatrix} \text{ represent the transformation.}$$

$$X_1' = \cos\theta X_1 + \sin\theta X_2$$

$$X_2' = -\sin\theta X_1 + \cos\theta X_2$$

and

$$X_1' = \cos\theta X_1 - \sin\theta X_2$$

$$X_2' = \sin\theta X_1 + \cos\theta X_2$$

which are clockwise and anti-clockwise rigid body rotations, respectively, (fig.4-4c and fig.4-4 d), where  $\theta$  is the angle the body rotates through. No change of shape or size occurs in these transformations.

$$\begin{vmatrix} 1 & r \\ 0 & 1 \end{vmatrix} \text{ represents the transformation}$$

$$X_1' = 1 \cdot X_1 + r \cdot X_2$$

$$X_2' = 0 \cdot X_1 + 1 \cdot X_2 = X_2$$

which is a transformation of simple shear (fig.4-4c) and  $r$  is the shear strain.

Continued.....

$$\begin{vmatrix} e^{\epsilon} & 0 \\ 0 & e^{-\epsilon} \end{vmatrix} \quad \text{represents the transformation}$$

$$X_1' = e^{\epsilon} \cdot X_1 + 0 \cdot X_2 = e^{\epsilon} X_1$$

$$X_2' = 0 \cdot X_1 + e^{-\epsilon} \cdot X_2 = e^{-\epsilon} X_2$$

which is a transformation of pure shear (fig.4-4f), and  $e$  is the natural base and  $\epsilon$ , <sup>the</sup> natural strain. This pure shear is also called aligned pure shear because in it the maximum extension and contraction of radial lines in the square are aligned with the co-ordinate axes (fig.4-4f).

An aligned pure shear may be visualised as a deformation of stretching and compressing to the same strain along the directions of <sup>the</sup> co-ordinate axes.

An unaligned pure shear is a pure shear with its maximum extension and contraction of radial lines not along the co-ordinate axes but at an angle to them. As shown in fig.4-5a, a square OABC is stretched along the direction with an angle  $\theta$  to  $X_1$ -axis, or along the fibre OP, and compressed in the perpendicular direction to the same amount of strain  $\epsilon$ . It is a pure shear and OA'B'C' is the deformed figure. Because OP is in the direction of stretching and perpendicular to that of compressing, it will not rotate in the deformation, thus the final position of

Continued.....

OP' after the deformation should still be in the direction making an angle  $\theta$  to  $X_1$ -axis.

This deformation, an unaligned pure shear, may now be analysed and can be shown to be equivalent to the resultant of three operations: first, a clockwise rigid body rotation through an angle  $\theta$ , (fig.4-5b) so that the fibre OP is aligned with <sup>the</sup> $X_1$ -axis; second, an aligned pure shear by stretching along <sup>the</sup> $X_1$ -axis and compressing along <sup>the</sup> $X_2$ -axis, (fig.4-5c), the fibre OP which becomes OP' is still aligned with <sup>the</sup> $X_1$ -axis; <sup>and</sup> third, an anti-clockwise rigid body rotation through an angle  $\theta$ , (fig.4-5d), so that the final position is exactly the same as that in fig.4-5a. Thus, an unaligned pure shear (48) may be represented by a product of the three matrices as follows;

$$\begin{aligned}
 & \begin{vmatrix} \cos\theta & -\sin\theta \\ \sin\theta & \cos\theta \end{vmatrix} \begin{vmatrix} e^\epsilon & 0 \\ 0 & e^{-\epsilon} \end{vmatrix} \begin{vmatrix} \cos\theta & \sin\theta \\ -\sin\theta & \cos\theta \end{vmatrix} \\
 = & \begin{vmatrix} \cosh\epsilon + \sinh\epsilon \cos 2\theta & \sinh\epsilon \sin 2\theta \\ \sinh\epsilon \sin 2\theta & \cosh\epsilon - \sinh\epsilon \cos 2\theta \end{vmatrix} \quad 4-11
 \end{aligned}$$

In other words, the matrix at the right hand side in Eq. 4-11, represents an unaligned pure shear having the principal strain  $\epsilon$  and  $-\epsilon$  in the directions making an angle  $\theta$  to the co-ordinate axes. It can be seen that the matrix is symmetrical.

Continued.....

### 4.3 The Thickness Strain

In sheet metal forming, the material often fails due to excessive thinning which leads to fracture, therefore, it is important and desirable to know whether the material becomes thinner after the deformation, and if so, by how much.

Due to the incompressibility of metal, the volume of the material does not change in any plastic deformation and is equal to the product of surface area and the thickness. In mathematical language, it is as follows:

$$A_i \times t_i = V = A_o \times t_o$$

or

4-12

$$\frac{A_i}{A_o} \times \frac{t_i}{t_o} = 1$$

Where  $A_o$ ,  $t_o$  and  $A_i$ ,  $t_i$  are the surface area and thickness of the material before and after the deformation, respectively. It may also be written as:

$$\ln \frac{A_i}{A_o} + \ln \frac{t_i}{t_o} = 0 \quad 4-13$$

and

$$\epsilon_t = \ln \frac{t_i}{t_o} = -\ln \frac{A_i}{A_o} \quad 4-14$$

The thickness strain is equal to the negative of the surface strain.

Continued.....

A unit square OABC having its sides aligned with the co-ordinate axes is deformed or transformed by Eq. 4-1 to a parallelogram OA'B'C' (fig.4-6). By substituting the co-ordinates of the corners A (1,0) and C(0,1) into Eq. 4-1, the co-ordinates of A' and C' can be obtained and are  $(A_{11}, A_{21})$ ,  $(A_{12}, A_{22})$  respectively. In other words, when a deformation or transformation represented by Eq. 4-6, transforming a unit square having its sides aligned with the co-ordinate axes to a parallelogram, the elements of the matrix  $|A_{ij}|$  in Eq. 4-6, are just the co-ordinates of the two corners of the deformed parallelogram.

The surface area of a unit square is unity and it can be proved that the area of a parallelogram with its four corners at  $(0,0)$ ,  $(A_{11}, A_{21})$ ,  $(A_{12}, A_{22})$  and  $(A_{11}+A_{12}, A_{21} + A_{22})$  (fig.4-6) is just the determinant of the matrix  $|A_{ij}|$  or

$$\begin{vmatrix} A_{11} & A_{12} \\ A_{21} & A_{22} \end{vmatrix} = A_{11} A_{22} - A_{12} A_{21} \equiv M^2 \quad 4-15$$

Then, the surface strain

$$\ln \frac{A_t}{A_0} = \ln \frac{A_{11} A_{22} - A_{12} A_{21}}{1} = \ln M^2 \quad 4-16$$

and

$$\epsilon_t = -\ln \frac{A_t}{A_0} = -\ln M^2 \quad 4-17$$

Continued.....

4.4 Matrix Analysis of Deformation (48)

A unit square is deformed or transformed into a parallelogram by the matrix  $|A_{ij}|$  in Eq. 4-6. Because the surface strain is just the determinant of the matrix  $|A_{ij}|$ , it is possible to factorise the deformation into two parts, one in balanced biaxial tension which produces only surface strain without changing the shape, namely, uniform dilatation or contraction, and the other, in changing the shape without thinning or thickening. Thus:

$$\begin{aligned}
 \begin{vmatrix} A_{11} & A_{12} \\ A_{21} & A_{22} \end{vmatrix} &= \begin{vmatrix} \sqrt{A_{11}A_{22} - A_{12}A_{21}} & 0 \\ 0 & \sqrt{A_{11}A_{22} - A_{12}A_{21}} \end{vmatrix} \begin{vmatrix} \frac{A_{11}}{\sqrt{A_{11}A_{22} - A_{12}A_{21}}} & \frac{A_{12}}{\sqrt{A_{11}A_{22} - A_{12}A_{21}}} \\ \frac{A_{21}}{\sqrt{A_{11}A_{22} - A_{12}A_{21}}} & \frac{A_{22}}{\sqrt{A_{11}A_{22} - A_{12}A_{21}}} \end{vmatrix} \\
 &\equiv \begin{vmatrix} M & 0 \\ 0 & M \end{vmatrix} \begin{vmatrix} \frac{A_{11}}{M} & \frac{A_{12}}{M} \\ \frac{A_{21}}{M} & \frac{A_{22}}{M} \end{vmatrix} \\
 &\equiv \begin{vmatrix} M & 0 \\ 0 & M \end{vmatrix} \begin{vmatrix} B_{11} & B_{12} \\ B_{21} & B_{22} \end{vmatrix} \qquad \qquad \qquad 4-18
 \end{aligned}$$

where  $M = \sqrt{A_{11}A_{22} - A_{12}A_{21}}$  and  $B_{ij} = \frac{A_{ij}}{M}$

The first matrix, reading from the left, in the right hand side in Eq. 4-18 is a uniform dilatation or contraction depending on the value of M, and the second one is a matrix with its determinant equal to unity, or

$$\begin{vmatrix} B_{11} & B_{12} \\ B_{21} & B_{22} \end{vmatrix} = 1 \qquad \qquad \qquad 4-19$$

Continued.....

Any affine transformation can always be changed into a symmetrical one by multiplying it with a rotation matrix.

$$\begin{vmatrix} \cos\alpha & \sin\alpha \\ -\sin\alpha & \cos\alpha \end{vmatrix} \begin{vmatrix} B_{11} & B_{12} \\ B_{21} & B_{22} \end{vmatrix} = \begin{vmatrix} B_{11} \cos\alpha - B_{21} \sin\alpha & B_{12} \cos\alpha + B_{22} \sin\alpha \\ -B_{11} \sin\alpha + B_{21} \cos\alpha & -B_{12} \sin\alpha + B_{22} \cos\alpha \end{vmatrix} \quad 4-20$$

If the matrix at the right hand side in Eq. 4-20 is symmetrical then  $B_{11} \cos\alpha + B_{22} \sin\alpha = -B_{11} \sin\alpha + B_{21} \cos\alpha$

$$\tan \alpha = \frac{B_{21} - B_{12}}{B_{11} + B_{22}} \quad (\equiv \lambda) \quad 4-21$$

and

$$\sin \alpha = \frac{\lambda}{(1+\lambda^2)^{1/2}} \quad \cos \alpha = \frac{1}{(1+\lambda^2)^{1/2}} \quad 4-22$$

(positive value of square roots is taken)

$$\text{Let } \begin{vmatrix} \cos\alpha & \sin\alpha \\ -\sin\alpha & \cos\alpha \end{vmatrix} \begin{vmatrix} B_{11} & B_{12} \\ B_{21} & B_{22} \end{vmatrix} \equiv \begin{vmatrix} C_{11} & C_{12} \\ C_{12} & C_{22} \end{vmatrix}$$

$$\text{then } \begin{vmatrix} B_{11} & B_{12} \\ B_{21} & B_{22} \end{vmatrix} = \begin{vmatrix} \cos\alpha & -\sin\alpha \\ \sin\alpha & \cos\alpha \end{vmatrix} \begin{vmatrix} C_{11} & C_{12} \\ C_{12} & C_{22} \end{vmatrix}$$

$$= \begin{vmatrix} \frac{1}{(1+\lambda^2)^{1/2}} & \frac{-\lambda}{(1+\lambda^2)^{1/2}} \\ \frac{\lambda}{(1+\lambda^2)^{1/2}} & \frac{1}{(1+\lambda^2)^{1/2}} \end{vmatrix} \begin{vmatrix} C_{11} & C_{12} \\ C_{12} & C_{22} \end{vmatrix} \quad 4-23$$

$$\text{where } \begin{vmatrix} C_{11} & C_{12} \\ C_{12} & C_{22} \end{vmatrix} \equiv \begin{vmatrix} \frac{B_{11} + B_{21}\lambda}{(1+\lambda^2)^{1/2}} & \frac{B_{12} + B_{22}\lambda}{(1+\lambda^2)^{1/2}} \\ \frac{B_{21} - B_{11}\lambda}{(1+\lambda^2)^{1/2}} & \frac{B_{22} - \lambda B_{12}}{(1+\lambda^2)^{1/2}} \end{vmatrix} \quad 4-24$$

Continued.....

and 
$$\begin{vmatrix} C_{11} & C_{12} \\ C_{12} & C_{22} \end{vmatrix} = 1 \quad 4-25$$

In order to describe the deformation<sup>*in general*</sup>, a typical deformation without changing the surface area, such as pure shear or simple shear, has to be chosen as a standard type of deformation for easy reckoning. Strictly speaking, any deformation may be considered as a standard type, but in this thesis, pure shear is chosen as a standard type of deformation due to the following advantages:

1. It satisfies the condition of no changing of surface area.
2. It is easy to visualise; stretching in one direction and compressing in the perpendicular direction to the same amount of strain.
3. Pure shear, no matter how large the strain is, is a coaxial deformation, but not, for example, simple shear, (will be discussed in Chapter 5).

Any symmetrical matrix having its determinant equal to unity as that in Eq. 4-24, may be analysed into three matrices as those at the left hand side in Eq. 4-11.

Thus:

$$\begin{vmatrix} C_{11} & C_{12} \\ C_{12} & C_{22} \end{vmatrix} = \begin{vmatrix} \cos\theta & -\sin\theta \\ \sin\theta & \cos\theta \end{vmatrix} \begin{vmatrix} e^\epsilon & 0 \\ 0 & e^{-\epsilon} \end{vmatrix} \begin{vmatrix} \cos\theta & \sin\theta \\ -\sin\theta & \cos\theta \end{vmatrix} \quad 4-26$$

Continued.....

Therefore, from Eqs, 4-18, 4-23, and 4-26

$$\begin{vmatrix} A_{11} & A_{12} \\ A_{21} & A_{22} \end{vmatrix} = \begin{vmatrix} M & 0 \\ 0 & M \end{vmatrix} \begin{vmatrix} \cos\alpha & -\sin\alpha \\ \sin\alpha & \cos\alpha \end{vmatrix} \begin{vmatrix} \cos\theta & -\sin\theta \\ \sin\theta & \cos\theta \end{vmatrix} \begin{vmatrix} e^\epsilon & 0 \\ 0 & e^{-\epsilon} \end{vmatrix} \begin{vmatrix} \cos\theta & \sin\theta \\ -\sin\theta & \cos\theta \end{vmatrix}$$

And by solving Eqs, 4-18, 4-23, 4-26 we find,

$$M = (A_{11} A_{22} - A_{12} A_{21}) \quad 4-28$$

$$\tan \alpha = \frac{A_{21} - A_{12}}{A_{11} + A_{22}} \quad 4-29$$

$$\tan 2\theta = \frac{2(A_{11} A_{12} + A_{21} A_{22})}{A_{11}^2 + A_{21}^2 - A_{12}^2 - A_{22}^2} \quad 4-30$$

$$\epsilon = \ln \left( \sqrt{C_{12}^2 + \left( \frac{C_{11} - C_{22}}{2} \right)^2} + \frac{C_{11} + C_{22}}{2} \right) \quad 4-31$$

where

$$C_{11} = \frac{A_{11} (A_{11} + A_{22}) + A_{21} (A_{21} - A_{12})}{[(A_{11} A_{22} - A_{12} A_{21}) \{(A_{11} + A_{22})^2 + (A_{21} - A_{12})^2\}]^{1/2}}$$

$$C_{12} = \frac{A_{11} A_{12} + A_{21} A_{22}}{[(A_{11} A_{22} - A_{12} A_{21}) \{(A_{11} + A_{22})^2 + (A_{21} - A_{12})^2\}]^{1/2}} \quad 4-32$$

$$C_{22} = \frac{A_{22} (A_{11} + A_{22}) - A_{12} (A_{21} - A_{12})}{[(A_{11} A_{22} - A_{12} A_{21}) \{(A_{11} + A_{22})^2 + (A_{21} - A_{12})^2\}]^{1/2}}$$

In other words, any deformation represented by the matrix  $|A_{ij}|$  which is obtained from measuring the co-ordinates of the corners of the deformed parallelogram, may be analysed into the combination of, an unaligned pure shear (the

Continued.....

first three matrices reading from the right), a rigid body rotation (the fourth matrix) and a uniform dilatation (the fifth matrix), as shown in Eq. 4-27.

In fact, the operation of rigid body rotation does nothing to the shape or the size. It is only due to the choice of the position of the co-ordinate axes with respect to the deformed parallelogram. A set of co-ordinate axes printed or scribed on the metal surface, in general, will be changed after the deformation. When the deformed parallelogram is measured, the original co-ordinate axes have disappeared and another set of co-ordinate axes is drawn arbitrarily for the measurement. This is the reason why a rigid body rotation which is not concerned with deformation appears in Eq. 4-27. With the suitable choice of the position of the co-ordinate axes so that  $A_{12} = A_{21}$ , the rigid body rotation will disappear.

The elements of the matrix  $|A_{ij}|$  are obtained by measuring the co-ordinates of two corners of the deformed parallelogram in an arbitrarily chosen co-ordinate<sup>system</sup>. Changing the relative position of the co-ordinate axes with respect to the deformed parallelogram, surely, will change the magnitudes of  $A_{ij}$ . But it can be easily proved that these changes in the magnitudes of  $A_{ij}$  will only affect the magnitude of  $\alpha$  but not the strain  $\epsilon$  and the angle  $\theta$ .

Continued.....

The uniform dilatation or contraction is non-directional and its effect on the deformation can be considered by adding a strain  $\ln(M)$  to both the two principal strains no matter where the principal directions are. Then our attention should be concentrated on the pure shear which is the most significant one in a deformation analysis. The shape of a deformed parallelogram is unique by deforming a unit square under pure shear. A deformed parallelogram can have many different  $|A_{ij}|$  matrices to describe it, but the shape can only be obtained by deforming a unit square under a pure shear having its principal axes in the directions making an angle  $\theta$  to the sides of the unit square until a pure shear strain  $\epsilon$  is produced. In other words, for a deformed parallelogram, no matter how many  $|A_{ij}|$  matrices are obtained from different choices of co-ordinate axes, the magnitudes of  $\theta$  and  $\epsilon$  in Eqs. 4-30, 4-31 are all unique.

By considering the uniform dilatation or contraction together with the pure shear, the principal strains of a deformation should be as follows:

$$\begin{aligned} \epsilon_1 &= \ln M + \epsilon \\ \epsilon_2 &= \ln M - \epsilon \end{aligned} \qquad 4-33$$

and the thickness strain

$$\epsilon_3 = -(\epsilon_1 + \epsilon_2) = -2 \ln M = -\ln M^2 \qquad 4-34$$

Eq. 4-34 is exactly the same as Eq. 4-17.

Continued.....

4.5 The Incapability of A Circular Grid for Strain Measurement in Non-coaxial Deformation.

A circular grid is widely printed, scribed or etched on a metal surface for strain measurement due to the following advantages.

1. It is easy and quick to produce the grids, especially photoprinting has been well developed.
2. A circle is non-directional, therefore alignment is not necessary when producing the grid.
3. When the material is deformed, the circles become ellipses, and the principal strains can be readily measured from the major and minor axes of the deformed ellipse.
4. The major and minor axes of the ellipse are also the principal axes of strain.

In fact, the advantage that a circle is non-directional is a disadvantage because it involves the incapability of a circle to detect the rotation of the major and minor axes of the ellipse when it is deformed in a non-coaxial deformation. This will be discussed in the following section.

A circle is deformed into an ellipse in a finite deformation (fig.4-7a), the major and minor axes of the ellipse

Continued.....

are the principal axes of strain and <sup>the</sup> principal strains can be obtained by measuring the major and minor axes of the ellipse, thus

$$\epsilon_1' = \ln \frac{b_1}{a}$$

$$\epsilon_2' = \ln \frac{c_1}{a}$$

4-35

If the ellipse is further deformed with the principal axes of stress along <sup>the</sup>  $X_1$ - and  $X_2$ -axes or the major and minor axes of the ellipse, the ellipse will become another ellipse, as shown in fig.4-7b. The ellipse of the dotted line is the deformed ellipse and of the solid line is the further deformed one. This deformation is a coaxial one, and the principal axes of strain are still aligned with the major and minor axes of the further deformed ellipse. The strain increments or the principal strains in the further deformation are:

$$\epsilon_1'' = \ln \frac{b_2}{b_1}$$

$$\epsilon_2'' = \ln \frac{c_2}{c_1}$$

4-36

The resultant strains are :

$$\epsilon_{1c} = \ln \frac{b_2}{a} = \ln \frac{b_1}{a} + \ln \frac{b_2}{b_1}$$

Continued.....

$$= \epsilon_1' + \epsilon_2''$$

$$\epsilon_{2c} = \ln \frac{c_2}{a} = \ln \frac{c_1}{a} + \ln \frac{c_2}{c_1} \quad 4-37$$

$$= \epsilon_2' + \epsilon_2''$$

and are just the sum of the two deformations.

If the further deformation which has the same amount of work done as that in <sup>the</sup> last paragraph is achieved with its principal axes of stress not along <sup>the</sup>  $X_1$ - and  $X_2$ -axes, but along the directions with an angle  $\psi$  to them, as shown in fig.4-7c, the dotted ellipse which is the same as that in fig.4-7b is deformed into the solid one. This deformation, obviously is non-coaxial. The total amount of work done to the material in fig.4-7c is exactly the same as that in fig.4-7b.

The material is supposed to be isotropic throughout the deformation, thus, the resultant strains should be the same. But if the resultant strains are measured from the further deformed ellipse in fig.4-7c, they are as follows:

$$\epsilon_{1n} = \ln \frac{b_2'}{a}$$

4-38

$$\epsilon_{2n} = \ln \frac{c_2'}{a}$$

and

$$\epsilon_{1n} \neq \epsilon_{1c}, \quad \epsilon_{2n} \neq \epsilon_{2c}$$

This shows the incapability of using <sup>a</sup>circular grid <sup>for</sup> truthful strain measuring in non-coaxial deformations.

#### 4.6 Strain Measurement by Using <sup>A</sup>Square Grid

It may be convenient to use <sup>A</sup>circular grid if it is known that the deformation is coaxial, otherwise that grid system may induce errors as described in <sup>the</sup>last section. In fact, as said before, even in a circular cup drawing operation, earing would bring the involvement of non-coaxial deformation to the workpiece. It is better to use <sup>A</sup>square grid in cases when non-coaxial deformation is involved, especially when the forming operation is unsymmetrical.

When a square grid is used for strain measurement in a forming operation, it is printed or scribed on the metal surface, (fig.4-8a). The square grid should be so fine that the deformation inside the grid is uniform, and therefore, when the material is deformed, the square grid is distorted into a parallelogram (fig.4-8b). From the deformed parallelogram, three principal strains and the directions of the principal axes of strain with respect to the material are obtained. As discussed in section 4.1, the transformation matrix  $|A_{ij}|$  can be obtained from the co-ordinates of the corners of the parallelogram. But because of the deformation, the original co-ordinate axes

Continued.....

along which the sides of the square grid are aligned has disappeared. Now, where are we <sup>going</sup> to set the co-ordinate axes with respect to the parallelogram for measuring the co-ordinates of the corners of the parallelogram?

The answer is "anywhere". It will be proved that the arbitrary setting of <sup>the</sup> co-ordinate axes does not affect the strain measurement. The deformed grid is put without any alignment under a travelling microscope, and a corner of the parallelogram (the point O in fig.4-9) is chosen as the origin of the co-ordinate <sup>system</sup> and the axes in <sup>the</sup> microscope are the co-ordinate axes, ( $X_1$ -and  $X_2$ -axes in fig. 4-9). Therefore the co-ordinates of the points A' and B' (fig.4-9) which <sup>are</sup>  $(a_1, a_2)$  and  $(b_1, b_2)$  respectively, can be measured. Now, the deformation may be explained as a co-ordinate transformation as shown in fig.4-3, OACB is the undeformed grid and, OA and OB are transformed into OA' and OB'. If the square grid size is  $1 \times 1$ , then, according to Eq. 4-10 and fig.4-3,

$$a_1 = \left(1 + \frac{\partial U_1}{\partial X_1}\right) \cdot 1 = A_{11} \cdot 1$$

$$a_2 = \left(\frac{\partial U_2}{\partial X_1}\right) \cdot 1 = A_{21} \cdot 1$$

$$b_1 = \left(\frac{\partial U_1}{\partial X_2}\right) \cdot 1 = A_{12} \cdot 1$$

$$b_2 = \left(1 + \frac{\partial U_2}{\partial X_2}\right) \cdot 1 = A_{22} \cdot 1$$

Continued.....

Thus,

$$A_{11} = \frac{a_1}{1}$$

$$A_{21} = \frac{a_2}{1}$$

$$A_{12} = \frac{b_1}{1}$$

4-39

$$A_{22} = \frac{b_2}{1}$$

By substituting  $A_{ij}$  into Eqs. 4-28, 4-30, 4-31, and 4-32, the uniform dilatation  $M$ , the angle  $\theta$  and the pure shear strain can be found as follows:-

$$M = (A_{11}A_{22} - A_{12}A_{21}) \quad 4-39$$

$$\tan 2\theta = \frac{2(A_{11}A_{12} + A_{21}A_{22})}{A_{11}^2 + A_{21}^2 - A_{12}^2 - A_{22}^2} \quad 4-40$$

$$\epsilon = \ln \left( \sqrt{C_{12}^2 + \left(\frac{C_{11} - C_{22}}{2}\right)^2} + \frac{C_{11} + C_{22}}{2} \right) \quad 4-41$$

where  $C_{ij}$  are those in Eq. 4-32.

The principal strains, therefore, are

$$\epsilon_1 = \ln M + \epsilon$$

$$\epsilon_2 = \ln M - \epsilon \quad 4-42$$

$$\epsilon_3 = -\ln M^2 \quad 4-43$$

Continued.....

The angle  $\theta_1$ , obtained from Eq. 4-40 is the angle in the undeformed grid (OACB in fig.4-10) between the fibre OA and the fibre OS which in the deformed state (OS' in fig.4-10) is parallel with the principal axis of the major strain (SS in fig.4-10.).

#### 4.7 Invariance of the Transformation Matrix

As illustrated in the last section, after  $A_{ij}$  are found, the principal strains and the directions of the principal axes of strain with respect to the material can be easily obtained. But there is an ambiguity<sup>in</sup> that the co-ordinate system axes for measuring the co-ordinates of the points A' and B' (fig.4-9) are set arbitrarily without explanation. In this section, it will be proved that the transformation matrix is invariant with respect to the choice of the co-ordinate axes.

In the last section, the points A' and B' were measured with respect to <sup>the</sup>  $X_1$ - and  $X_2$ - axes. Now if another set of co-ordinate axes, say  $Y_1$ - and  $Y_2$ - axes, are set for the measurement, the co-ordinates of the points A' and B' would be  $(b_{11} \cdot l, b_{21} \cdot l)$  and  $(b_{12} \cdot l, b_{22} \cdot l)$  respectively, and

$$b_{11} = \cos \alpha A_{11} - \sin \alpha A_{21}$$

$$b_{21} = \sin \alpha A_{11} + \cos \alpha A_{21}$$

$$b_{12} = \cos \alpha A_{12} - \sin \alpha A_{22}$$

$$b_{22} = \sin \alpha A_{12} + \cos \alpha A_{22}$$

4-44

Continued.....

For calculating the principal strains and the angle specifying the directions of the principal strains with respect to the material,  $b_{ij}$  are substituted into Eqs. 4-28, 4-30, 4-31 and 4-32, and

$$\begin{aligned} M &= (b_{11} b_{22} - b_{12} b_{21}) \\ &= (\cos\alpha A_{11} - \sin\alpha A_{21}) (\sin\alpha A_{12} + \cos\alpha A_{22}) \\ &\quad - (\sin\alpha A_{11} + \cos\alpha A_{21}) (\cos\alpha A_{12} - \sin\alpha A_{22}) \\ &= (A_{11} A_{22} - A_{12} A_{21}) \end{aligned} \tag{4-45}$$

$$\begin{aligned} \tan 2\theta_1 &= \frac{2 (b_{11} b_{12} + b_{21} b_{22})}{b_{11}^2 + b_{21}^2 - b_{12}^2 - b_{22}^2} \\ &= \frac{2 (A_{11} A_{12} + A_{21} A_{22})}{A_{11}^2 + A_{21}^2 - A_{12}^2 - A_{22}^2} \end{aligned} \tag{4-46}$$

Similarly, the pure shear strain  $\epsilon$  is the same as that obtained in <sup>the</sup> last section, and so are the principal strains and the angle  $\theta_1$ .

Thus it is proved that a transformation or a deformation is determined by the shape of the deformed grid and is not dependent on the relative position of the co-ordinate axes for the measurement. When the shape of the deformed grid is determined, the principal strains and the directions of the principal axes of strain with respect to the material can all be found.

Continued.....

4.8 The Detection and the Magnitude of Non-coaxiality.

When the material is deformed, the principal strains and the directions of the principal axes of strain can be found by measuring the deformed grid as described in the last two sections. Now if the material in fig.4-8b is further deformed, the parallelogram in fig.4-9 will be distorted into another parallelogram(OA"B"C" in fig.4-11). From the parallelogram OA"B"C", the principal strains and the directions of the principal axes of strain with respect to the material can be found. If the angle specifying the directions of the principal axes of strain with respect to the material is found to be  $\theta_2$  which is different from  $\theta_1$ , as in Eq. 4-40, it means that before this subsequent deformation, the principal axis of the major strain is along the fibre OS (fig.4-12) which lies in the direction with an angle  $\theta_1$  to the fibre OA, and after the subsequent deformation, the principal axis of the major strain is along the fibre OT (fig.4-12) which lies in the direction making angle  $\theta_2$  with the fibre OA in the undeformed state of the material. In this subsequent deformation, the principal axis of the major strain with respect to the material rotates from OS to OT. Therefore, this subsequent deformation is non-coaxial. The magnitude of the non-coaxiality of the principal axis of strain in this non-coaxial deformation is, therefore, represented by the angle between the fibres OS and OT or by the angle  $\theta_2 - \theta_1$ .

Continued.....

In other words, the detection of the coaxiality of a deformation depends on the equality of the value of  $\theta$  measured and calculated from the deformed grids before and after the deformation, and the magnitude of the non-coaxiality of the deformation is the difference between the values of the angle  $\theta$  before and after the deformation.

Hitherto, the full analysis of finite strains has <sup>not</sup> been possible by ~~the~~ sheet metal forming research scientists due to the use of <sup>a</sup> circular grid, which fails to specify the directions of the principal axes of strain with respect to the material. Only the principal strains were used to represent a state of strain, even in unsymmetrical cases in which non-coaxial deformation was involved. Here, with the complete representation of a state of strain including the directions of the principal axes of strain with respect to the material, and the mathematical analysis, non-coaxial deformation can be handled. More complicated analysis will follow in the next few chapters.

Continued.....

CHAPTER 5

GRAPHICAL REPRESENTATIONS  
OF STRAIN PATHS

### Graphical Representations of Strain Paths

A strain path is a series of states of strain and a state of strain is represented by quantitative numbers, hence it should be possible to represent<sup>a</sup> strain path in a co-ordinate system. The more suitable the co-ordinate system is, the better the representation will be. Therefore, it is worth considering the most suitable co-ordinate system for the best representation of<sup>a</sup> strain path.

Metal deformation is always three-dimensional, even in the tension or the compression test. Although only the strain in the loading direction is considered, the deformation is still three-dimensional. The other two strains are numerically equal to half of the strain being considered and are both compressive (in<sup>the</sup> tension test) or tensile (in<sup>the</sup> compression test) for large deformations. As defined in Chapter 2, in sheet metal forming, a state of strain is completely represented by three principal strains and a factor specifying the principal axes of strain with respect to the material. There are four variables. Due to the incompressibility of metal, the sum of the three principal strains is zero and there are only two degrees of freedom among these three principal strains. Even so, it is still desirable to show the thickness strain as well as the two principal strains on the sheet surface because the failure of material in sheet metal forming is mostly due to excessive thinning. Therefore, the most suitable co-ordinate system is that which is capable of showing the three

Continued.....

principal strains and the factor specifying the principal axes of strain with respect to the material.

In the coaxial case, because the principal axes of strain are fixed with respect to the material ~~is the same~~ throughout the deformation, the factor specifying the principal axes of strain with respect to the material becomes less interesting and is normally ignored. Then there are only two degrees of freedom left although there are three variables. Many co-ordinate systems are capable of showing two-dimensional graphs. The Cartesian co-ordinate system is the most popular one. The two principal strains on the sheet surface are used as <sup>the</sup> co-ordinates (fig. 5-1). But as stated in the last paragraph, it is desirable to read the thickness strain immediately when the graph is shown. The Cartesian co-ordinate system fails to achieve that. Apart from that, the lines representing typical modes of deformation such as uniaxial tension, uniaxial compression and pure shear, are not evenly distributed (fig. 5-1). Another limitation of <sup>the</sup> Cartesian co-ordinate system is its inability to show four variables with three degrees of freedom as in <sup>the</sup> non-coaxial case. Therefore, one particular co-ordinate system, namely, <sup>the</sup> triangular co-ordinate system first proposed by Professor Hsü (49)-(51) is introduced and used in this thesis.

Continued.....

5.1 2-D Triangular Co-ordinate System

The co-ordinate<sup>system</sup> is shown with its co-ordinate lines in fig.5-2. The origin represents the undeformed state. Three axes spaced 120° to one another in a plane are the co-ordinate axes for the three principal strains. Every point in this co-ordinate<sup>system</sup> represents a state of strain with a set of values for the three principal strains. For instance, a typical point P (fig.5-2) such that the line OP make an angle φ with the  $\epsilon_I$  - axis represents a state of strain with

$$\begin{aligned} \epsilon_I &= \overline{OP} \cos \phi \\ \epsilon_{II} &= \overline{OP} \cos \left( \frac{2\pi}{3} - \phi \right) \\ \epsilon_{III} &= \overline{OP} \cos \left( \frac{4\pi}{3} - \phi \right) \end{aligned} \tag{5-1}$$

and

$$\epsilon_I + \epsilon_{II} + \epsilon_{III} = \overline{OP} \left( \cos \phi + \cos \left( \frac{2\pi}{3} - \phi \right) + \cos \left( \frac{4\pi}{3} - \phi \right) \right) = 0$$

which satisfies the incompressibility of metal.

As can be seen in Eq. 5-1, the ratios between the principal strains are dependent on the angle φ only. and it should be possible to represent the ratio by a number from 0 to 2π or 0° to 360°. But it is more convenient to use a number from 1 to 12 because the radial lines shown in fig. 5-3 are so similar to those on a clock face that it is easy to visualise the direction of the lines by analogy

Continued.....

to the clock face. The number is called the characteristic index for strain because it represents the characteristics or type of deformation and is to be represented by  $\eta$  so that

$$\eta = \frac{6}{\pi} \phi .$$

The diagram with twelve radial lines on it may be called the "clock diagram".

In the strain path along the  $\epsilon_I$ -axis ( $\eta = 12$ ),  $\epsilon_1$  is positive and  $\epsilon_2$  and  $\epsilon_3$  are both negative and numerically equal to  $\epsilon_1/2$ . The deformation is the same as in a tension test, pulling in only one direction to produce a tensile strain  $\epsilon_1$  and compressive strains ( $-\epsilon_1/2$ ) in both the other two principal directions. This type of deformation is called pure tension. The deformation having strain paths along  $\epsilon_{II}$  ( $\eta = 4$ ) or  $\epsilon_{III}$  ( $\eta = 8$ ) is also pure tension. In the strain path along the negative branch of the axis, or along  $\eta = 2$ , or 6, or 10, the deformation is the reverse of pure tension and is called pure compression.

In the strain paths with an odd number of the characteristic index, one of the principal strains is zero and the other two are equal in magnitude but opposite in sign. For example, along  $\eta = 3$ ,  $\epsilon_1$  is zero and  $\epsilon_2 = -\epsilon_3$ , so it is a pure shear or plane strain. In other words, the deformation along a strain path of even characteristic index is either a pure tension ( $\eta = 12, 4, 8$ ) or a pure

Continued.....

compression ( $\eta = 6, 10, 2$ ) and that along odd numbers of  $\eta$  is a pure shear. When  $\eta$  is not an integer, the deformation is neither a pure tension or compression nor a pure shear but is something in between.

### 5.2 3-D Triangular Co-ordinate System

In order to represent the state of strain in sheet metal forming completely, including not only the three principal strains but also the directions of <sup>the</sup> principal axes of strain with respect to the material, another co-ordinate axis is needed. The additional co-ordinate axis,  $\beta$ -axis, is set perpendicular to the clock diagram (fig. 5-4). A point in <sup>the</sup> 3-D triangular co-ordinate <sup>system</sup> represents a state of strain with three principal strains which are obtained by projecting the point on to the clock diagram, and the value of  $\beta$  represents the magnitude of the non-coaxiality of the principal axes of strain with respect to the material.

Of course, for only a single state of strain, it is not necessary to use 3-D triangular co-ordinates, but when non-coaxial deformation occurs, the strains have different directions for the principal axes of strain with respect to the material, ~~then~~. It is <sup>then</sup> necessary to represent this difference in <sup>the</sup> principal <sup>strain</sup> direction and <sup>the</sup> 3-D triangular co-ordinate <sup>system</sup> is used.

Continued.....

### 5.3 Coaxial Strain Path

A strain path is the locus of all the states of strain when the material is being deformed from the initial state to the final state of strain. Material is normally deformed from the undeformed state, therefore, the strain path plotted in a co-ordinate <sup>system</sup> goes out from the origin of the co-ordinate system.

A coaxial strain path is a trace of states of strain which all have their principal axes of strain in the same directions with respect to the material so that it can be plotted in a 2-D triangular co-ordinates. In fig.5-5 a coaxial strain path OCD is shown.

In the coaxial strain path, all the states of strain are measured along the same directions, in other words, all the states of strain are measured from <sup>the</sup> two fibres which are deformed but remain perpendicular to each other all the time. It is important to distinguish between finite and incremental strains. For a state of strain C on the strain path OCD in fig.5-5, the finite strain is represented by the vector  $\vec{OC}$  drawn from the origin to the point C, and the magnitude of the vector  $\vec{OC}$  represents the intensity of strain. The vector  $\vec{OC}$  or  $\vec{\epsilon}$  may be written as

$$\vec{\epsilon} = \vec{OC} = \epsilon_1 \vec{i} + \epsilon_2 \vec{j} \quad 5-2$$

Continued.....

where  $\vec{i}$  and  $\vec{j}$  are unit vectors along the co-ordinate axes. The incremental strain at C is represented by a vanishingly small segment of the strain path in the vicinity of C. It is represented by a vector  $\vec{CT}$  (fig.5-5) which is in the tangent direction of the strain path at C, and

$$d\vec{\epsilon} = \vec{CT} = d\epsilon_1 \vec{i} + d\epsilon_2 \vec{j} \quad 5-3$$

Strain rate is the time rate of strain increment and is a vector too. It may be written as

$$\dot{\vec{\epsilon}} = \frac{d\vec{\epsilon}}{dt} = \frac{d\epsilon_1}{dt} \vec{i} + \frac{d\epsilon_2}{dt} \vec{j} \quad 5-4$$

A strain path normally goes out from the origin of the co-ordinate, so, a straight or linear strain path is also a radial one. There are two ways of checking the linearity of a coaxial strain path. ~~The~~ Firstly, if a coaxial strain path is radial, all the states of strain on the strain path should have the same ratio between the strain components, or,  $\epsilon_1/\epsilon_2$  is constant everywhere. ~~The~~ Secondly, the finite strain vector  $\vec{\epsilon}$  at any point on the strain path should align with the incremental strain vector at that point, or,

$$\vec{\epsilon} \times d\vec{\epsilon} = 0 \quad 5-5$$

A radial coaxial strain path is also a strain path with constant characteristic index  $\eta$ .

Continued.....

#### 5.4 Non-coaxial Strain Path

A non-coaxial strain path is the locus of states of strain, as <sup>a</sup> coaxial strain path is, <sup>between these two strain paths</sup> But the difference <sub>A</sub> is that in a non-coaxial strain path, the states of strain are not those <sup>with</sup> the same directions of the principal axes of strain with respect to the material. There is <sup>thus</sup> <sub>A</sub> one more degree of freedom in the representation of a non-coaxial strain path than that in a coaxial one. ~~Therefore~~, A non-coaxial strain path <sub>A</sub> <sup>may</sup> be presented in a 3-D triangular co-ordinates in which not only the three principal strains but also the magnitude of the non-coaxiality of the principal axes of strain with respect to the material can be presented.

A non-coaxial strain path is a space curve in 3-D triangular co-ordinate <sup>system</sup> <sub>A</sub>. The vertical axis perpendicular to the clock diagram in a 2-D triangular co-ordinate is the axis for the magnitude of non-coaxiality of the principal axes of strain with respect to the material.

In a non-coaxial strain path, the magnitude of non-coaxiality at a state of strain should be the difference between the values of the angle  $\theta$  at that state of strain and at the beginning of the forming operation. In practice, it may be difficult to find the directions of the principal axes of strain with respect to the material at the beginning of the deformation, but this difficulty can always be overcome by extrapolation.

Continued.....

A non-coaxial strain path OCN which is a space curve in a 3-D triangular co-ordinate<sup>system</sup> is shown in fig.5-6. The projection of the strain path on the clock diagram, called projected strain path, is OC'N'. From the projected strain path, the principal strains,  $\epsilon_1$ ,  $\epsilon_2$  and  $\epsilon_3$  are found and the vertical distance between the projected strain path and the non-coaxial strain path represents the magnitude of the non-coaxiality of the principal axes of strain with respect to the material.

The strain path of a simple shear which is non-coaxial will be shown later in this Chapter and some other non-coaxial strain paths are shown in Chapter 10.

### 5.5 Linearity of Non-coaxial Strain Path

Like<sup>a</sup> coaxial strain path, it should be possible to define a linear non-coaxial strain path. Because<sup>a</sup> non-coaxial strain path involves rotation of the principal axes of strain, a linear non-coaxial strain path has not only constant ratios between the principal strains but also a constant rate of rotation of the principal axes of strain. Therefore, a linear non-coaxial strain path is a straight line in the 3-D triangular co-ordinates and

$$\frac{(\epsilon_1)_a}{\beta_a} : \frac{(\epsilon_2)_a}{\beta_a} : \frac{(\epsilon_3)_a}{\beta_a} = \frac{(\epsilon_1)_b}{\beta_b} : \frac{(\epsilon_2)_b}{\beta_b} : \frac{(\epsilon_3)_b}{\beta_b} = \dots$$

Continued.....

or  $d\epsilon_1 : d\epsilon_2 : d\epsilon_3 : d\beta = \text{constant}$ .

It is easy to visualise the stress states or stress path for producing a linear coaxial strain path. If the ratios between the principal stresses are kept constant and the principal axes are fixed with respect to the material, a linear coaxial strain path is produced. When the principal axes of stress rotate with respect to the material, the stress state producing a linear non-coaxial strain path is complicated and is not easy to visualise. It will be shown in the next section that within certain limits, the strain path of a simple shear is nearly a linear non-coaxial one.

#### 5.6 Simple Shear

Simple shear is a very common deformation. Perhaps, because it is so popular and so often mentioned, people tend to discuss it without any doubt and thorough understanding. Simple shear means a square being deformed by a shear force into a parallelogram as shown in fig.5-7. In fact, without a compressive force on the side BC or a clockwise rigid body rotation, the square OABC can not be deformed into OA'B'C' in that position shown in fig.5-7. In small deformations like an elastic deformation, simple shear is assumed as pulling and compressing in the diagonal directions. This is accepted not because it is correct

Continued.....

but due to ~~that~~ the induced error ~~is~~ <sup>being</sup> so small that it can be neglected. But in a large deformation like plastic deformation, the error increases with the severity of the deformation and ~~is~~ <sup>is</sup> no longer negligible. The state of stress in a large simple shear is rather complicated and is outside the scope of this thesis. Only the states of strain including the principal axes of strain with respect to the material will be discussed here.

A unit square like OABC in fig.5-7 is deformed under a simple shear, <sup>which</sup> <sub>A</sub> it becomes OAB'C' and then OAB''C'' and so on. The strain analysis of this deformation can be done by measuring the deformed parallelograms and using Eqs. 4-27, 4-28, 4-29, 4-30, <sup>that</sup> <sub>A</sub> the principal strains and the directions of principal axes with respect to the material can all be obtained.

Fig.5-8 shows the strain path of a simple shear, plotted in 3-D triangular co-ordinates. The curve OPS is a space curve and OP'S' which lies on the clock diagram is the projection of OPS. From a point P' on the projected curve, lines perpendicular to the three axes on the clock diagram can be drawn and three principal strains are obtained. PP' is the amount of non-coaxiality. The non-coaxiality shows that in a material under simple shear deformation, the most stretched and ~~compressed~~ fibres are not the same ones but are changing all the time during the

Continued.....

deformation. The strain path OPS or <sup>the</sup> projected one OP'S' is not, a strain path of certain fibres which lie in the same directions as the principal axes of stress and strain, as in a coaxial strain path, rather, it is only a series of states of resultant strain of the material under forming.

In fig. 5-8, it is shown that the strain path OPS is nearly linear at <sup>the</sup> beginning. In other words, if the strain is not too large, or smaller than 0.3, the strain path is a non-coaxial linear strain path.

Continued.....

CHAPTER 6

ANALYSIS OF NON-COAXIAL DEFORMATION

Analysis of Non-coaxial Deformation

Non-coaxial deformation has been defined as a deformation in which the principal axes of strain rotate with respect to the material. This rotation of the principal axes of strain with respect to the material is induced by the nonalignment of the principal axes of stress and of strain during the deformation.

A deformation in a material from the undeformed state to a state of strain without any knowledge of the intermediate state, can always be reckoned as coaxial, and in that deformation, the principal axes of stress coincide with the principal axes of strain. If a subsequent deformation follows, the coincidence of the principal axes of stress with the principal axes of strain at the state before the subsequent deformation is the key factor for deciding whether the subsequent deformation is coaxial or non-coaxial. If they are coincident, then the subsequent deformation will be coaxial, otherwise, it will be non-coaxial. When it is non-coaxial, what will be the result of the successive deformations? How will the result be different from that of a coaxial one? How will the principal axes of strain rotate and what is the relation between the directions of the principal axes of stress and those of strain with respect to the material if they are not coincident? All these questions are discussed and answered in this Chapter.

Continued.....

6.1 Resultant of Two Deformations.

A. Resultant of Two Coaxial Deformations

As mentioned before, a deformation is a transformation of co-ordinate and can be represented in matrix form, for example, as follows:

$$\begin{vmatrix} X_1' \\ X_2' \end{vmatrix} = \begin{vmatrix} e^{\epsilon_1} & 0 \\ 0 & e^{\epsilon_2} \end{vmatrix} \begin{vmatrix} X_1 \\ X_2 \end{vmatrix} \tag{6-1}$$

where  $X_1, X_2$ ; and  $X_1', X_2'$  are <sup>the</sup> co-ordinates of a typical point in the material before and after the deformation respectively, and,  $\epsilon_1$  and  $\epsilon_2$  are the principal strains produced by the deformation. The principal axes of strain, or the directions of the most stretched and ~~compressed~~ fibres referred back to the undeformed state of the material, in the finite deformation represented as in Eq. 6-1, are along <sup>the</sup>  $X_1$ - and  $X_2$ - axes (fig. 6-1) because the non-diagonal elements of the matrix in Eq. 6-1 are zero. It is also obvious that the principal axes of stress in this deformation are along <sup>the</sup>  $X_1$ - and  $X_2$ - axes too.

If another finite deformation takes place in the material with principal axes of stress along <sup>the</sup>  $X_1$ - and  $X_2$ - axes ~~and~~

$$\begin{vmatrix} X_1'' \\ X_2'' \end{vmatrix} = \begin{vmatrix} e^{\epsilon_1''} & 0 \\ 0 & e^{\epsilon_2''} \end{vmatrix} \begin{vmatrix} X_1' \\ X_2' \end{vmatrix} \tag{6-2}$$

Continued.....

where  $X_1'$ ,  $X_2'$  and  $X_1''$ ,  $X_2''$  are co-ordinates of a typical point in the material before and after the second deformation respectively, and  $\epsilon_1'$  and  $\epsilon_2'$  are principal strains produced in the second deformation. Then the resultant of the two finite deformations is as follows:

$$\begin{aligned}
 \begin{vmatrix} X_1'' \\ X_2'' \end{vmatrix} &= \begin{vmatrix} e^{\epsilon_1'} & 0 \\ 0 & e^{\epsilon_2'} \end{vmatrix} \begin{vmatrix} X_1' \\ X_2' \end{vmatrix} \\
 &= \begin{vmatrix} e^{\epsilon_1'} & 0 \\ 0 & e^{\epsilon_2'} \end{vmatrix} \begin{vmatrix} e^{\epsilon_1} & 0 \\ 0 & e^{\epsilon_2} \end{vmatrix} \begin{vmatrix} X_1 \\ X_2 \end{vmatrix} \\
 &= \begin{vmatrix} e^{\epsilon_1 + \epsilon_1'} & 0 \\ 0 & e^{\epsilon_2 + \epsilon_2'} \end{vmatrix} \begin{vmatrix} X_1 \\ X_2 \end{vmatrix}
 \end{aligned} \tag{6-3}$$

The resultant principal strains are:

$$\begin{aligned}
 (\epsilon_1)_c &= \epsilon_1 + \epsilon_1' \\
 (\epsilon_2)_c &= \epsilon_2 + \epsilon_2' \\
 (\epsilon_3)_c &= -((\epsilon_1 + \epsilon_1') + (\epsilon_2 + \epsilon_2'))
 \end{aligned} \tag{6-4}$$

and the principal axes of strain as well as of stress with respect to the undeformed material are along the fibres DA and OC (fig. 6-1).

Continued.....

Because the principal axes of stress and strain coincide with each other in both the two finite deformations, the principal strains are obtained by measuring along the same fibres in the material so that the resultant strain is only the sum of the strain in each deformation.

B. Resultant of Two Finite Non-coaxial Deformations (47)

If the deformation as in Eq. 6-1 is followed by another deformation with the principal axes of stress not along the  $X_1$ - and  $X_2$ - axes but along the direction in which the fibre  $OP'$  lies and its perpendicular direction (fig.6-1), then these two deformations are non-coaxial and the second deformation can be represented as

$$\begin{pmatrix} X_1'' \\ X_2'' \end{pmatrix} = \begin{pmatrix} \cos\phi & -\sin\phi \\ \sin\phi & \cos\phi \end{pmatrix} \begin{pmatrix} e^{\epsilon_1'} & 0 \\ 0 & e^{\epsilon_2'} \end{pmatrix} \begin{pmatrix} \cos\phi & \sin\phi \\ -\sin\phi & \cos\phi \end{pmatrix} \begin{pmatrix} X_1' \\ X_2' \end{pmatrix} \quad 6-5$$

where  $\phi$  is  $\angle A'OP'$  (fig.6-1) or the angle between the principal axes of stress in the first and the second deformations, instead of that in Eq. 6-2.

The resultant of these two deformations then is

$$\begin{pmatrix} X_1'' \\ X_2'' \end{pmatrix} = \begin{pmatrix} \cos\phi & -\sin\phi \\ \sin\phi & \cos\phi \end{pmatrix} \begin{pmatrix} e^{\epsilon_1'} & 0 \\ 0 & e^{\epsilon_2'} \end{pmatrix} \begin{pmatrix} \cos\phi & \sin\phi \\ -\sin\phi & \cos\phi \end{pmatrix} \begin{pmatrix} X_1' \\ X_2' \end{pmatrix}$$

Continued.....

$$= \begin{vmatrix} \cos \phi & -\sin \phi \\ \sin \phi & \cos \phi \end{vmatrix} \begin{vmatrix} e^{\epsilon_1'} & 0 \\ 0 & e^{\epsilon_2'} \end{vmatrix} \begin{vmatrix} \cos \phi & \sin \phi \\ -\sin \phi & \cos \phi \end{vmatrix} \begin{vmatrix} e^{\epsilon_1} & 0 \\ 0 & e^{\epsilon_2} \end{vmatrix} \begin{vmatrix} X_1 \\ X_2 \end{vmatrix} \quad 6-6$$

$$= \begin{vmatrix} \cos \phi & -\sin \phi \\ \sin \phi & \cos \phi \end{vmatrix} \begin{vmatrix} M' & 0 \\ 0 & M' \end{vmatrix} \begin{vmatrix} e^{\epsilon_0'} & 0 \\ 0 & e^{-\epsilon_0'} \end{vmatrix} \begin{vmatrix} \cos \phi & \sin \phi \\ -\sin \phi & \cos \phi \end{vmatrix} \begin{vmatrix} M & 0 \\ 0 & M \end{vmatrix} \begin{vmatrix} e^{\epsilon_0} & 0 \\ 0 & e^{-\epsilon_0} \end{vmatrix} \begin{vmatrix} X_1 \\ X_2 \end{vmatrix} \quad 6-7$$

where

$$\begin{vmatrix} e^{\epsilon_1'} & 0 \\ 0 & e^{\epsilon_2'} \end{vmatrix} = \begin{vmatrix} M' & 0 \\ 0 & M' \end{vmatrix} \begin{vmatrix} e^{\epsilon_0'} & 0 \\ 0 & e^{-\epsilon_0'} \end{vmatrix}$$

$$\begin{vmatrix} e^{\epsilon_1} & 0 \\ 0 & e^{\epsilon_2} \end{vmatrix} = \begin{vmatrix} M & 0 \\ 0 & M \end{vmatrix} \begin{vmatrix} e^{\epsilon_0} & 0 \\ 0 & e^{-\epsilon_0} \end{vmatrix}$$

and

$$M' = \frac{\epsilon_1' + \epsilon_2'}{2} \quad \epsilon_0' = \frac{\epsilon_1' - \epsilon_2'}{2} \quad 6-8$$

$$M = \frac{\epsilon_1 + \epsilon_2}{2} \quad \epsilon_0 = \frac{\epsilon_1 - \epsilon_2}{2}$$

Eq. 6-6 may also be written as

$$\begin{vmatrix} X_1'' \\ X_2'' \end{vmatrix} = \begin{vmatrix} MM' & 0 \\ 0 & MM' \end{vmatrix} \begin{vmatrix} \cos \phi & -\sin \phi \\ \sin \phi & \cos \phi \end{vmatrix} \begin{vmatrix} e^{\epsilon_0 + \epsilon_0'} \cos \phi & e^{\epsilon_0' - \epsilon_0} \sin \phi \\ -e^{\epsilon_0 - \epsilon_0'} \sin \phi & e^{-(\epsilon_0 + \epsilon_0')} \cos \phi \end{vmatrix} \quad 6-9$$

Continued.....

The first matrix reading from right to left on the right hand side' of Eq. 6-9 can be factorised into the product of four matrices as those in Eq. 4-24 with  $M = 1$ . Thus:

$$\begin{vmatrix} e^{\epsilon_0 + \epsilon'_0} \cos \phi & e^{\epsilon'_0 - \epsilon_0} \sin \phi \\ e^{\epsilon_0 - \epsilon'_0} \sin \phi & e^{-(\epsilon_0 + \epsilon'_0)} \cos \phi \end{vmatrix} = \begin{vmatrix} \cos \alpha & -\sin \alpha \\ \sin \alpha & \cos \alpha \end{vmatrix} \cdot \begin{vmatrix} \cos \theta' & -\sin \theta' \\ \sin \theta' & \cos \theta' \end{vmatrix} \cdot \begin{vmatrix} e^\epsilon & 0 \\ 0 & e^{-\epsilon} \end{vmatrix} \cdot \begin{vmatrix} \cos \theta' & \sin \theta' \\ -\sin \theta' & \cos \theta' \end{vmatrix} \quad 6-10$$

according to Eqs. 4-26, 4-27, 4-28 and 4-29

$$\begin{aligned} \tan \alpha &= \frac{(-e^{\epsilon_0 - \epsilon'_0} - e^{\epsilon'_0 - \epsilon_0}) \sin \phi}{(e^{\epsilon_0 + \epsilon'_0} + e^{-(\epsilon_0 + \epsilon'_0)}) \cos \phi} \\ &= - \frac{\cosh (\epsilon_0 - \epsilon'_0)}{\cosh (\epsilon_0 + \epsilon'_0)} \tan \phi \end{aligned} \quad 6-11$$

$$\tan 2\theta' = \frac{\sin 2\phi}{\left(\frac{\sinh 2\epsilon_0}{\tanh 2\epsilon'_0}\right) + \cosh 2\epsilon_0 \cos 2\phi} \quad 6-12$$

and

$$\begin{aligned} \cosh^2 \epsilon &= \cosh^2 (\epsilon_0 - \epsilon'_0) + (\cosh^2 (\epsilon_0 + \epsilon'_0) - \cosh^2 (\epsilon_0 - \epsilon'_0)) \cos^2 \phi \\ &= \cosh^2 (\epsilon_0 + \epsilon'_0) - (\cosh^2 (\epsilon_0 + \epsilon'_0) - \cosh^2 (\epsilon_0 - \epsilon'_0)) \sin^2 \phi \end{aligned} \quad 6-13$$

Therefore Eq. 6-9 may be written as

$$\begin{vmatrix} X_1'' \\ X_2'' \end{vmatrix} = \begin{vmatrix} MM' & 0 \\ 0 & MM' \end{vmatrix} \begin{vmatrix} \cos \phi & -\sin \phi \\ \sin \phi & \cos \phi \end{vmatrix} \begin{vmatrix} \cos \alpha & -\sin \alpha \\ \sin \alpha & \cos \alpha \end{vmatrix} \begin{vmatrix} \cos \theta' & -\sin \theta' \\ \sin \theta' & \cos \theta' \end{vmatrix} \begin{vmatrix} e^\epsilon & 0 \\ 0 & e^{-\epsilon} \end{vmatrix} \begin{vmatrix} \cos \theta' & \sin \theta' \\ -\sin \theta' & \cos \theta' \end{vmatrix}$$

Continued.....

$$= \begin{vmatrix} MM' & 0 \\ 0 & MM' \end{vmatrix} \begin{vmatrix} \cos(\phi+\alpha) & -\sin(\phi+\alpha) \\ \sin(\phi+\alpha) & \cos(\phi+\alpha) \end{vmatrix} \begin{vmatrix} \cos\theta' & -\sin\theta' \\ \sin\theta' & \cos\theta' \end{vmatrix} \begin{vmatrix} e^\epsilon & 0 \\ 0 & e^{-\epsilon} \end{vmatrix} \begin{vmatrix} \cos\theta' & \sin\theta' \\ -\sin\theta' & \cos\theta' \end{vmatrix} \quad 6-14$$

The matrices on the right hand side of Eq. 6-14 are similar to those in Eq. 4-24. In other words, the resultant of those two non-coaxial deformations is like a deformation with its principal axes of strain in the directions as the fibres making an angle  $\theta'$ . (Eq. 6-12) with the sides of the undeformed unit square (dotted line in fig. 6-1) and the three principal strains are as follows:-

$$\begin{aligned} (\epsilon_1)_{\text{non}} &= \ln (MM') + \epsilon \\ (\epsilon_2)_{\text{non}} &= \ln (MM') - \epsilon \\ (\epsilon_3)_{\text{non}} &= -2 \ln (MM') \end{aligned} \quad 6-15$$

The amount of non-coaxiality in these two deformations is

$$\beta = \theta' - 0^\circ = \theta' = \frac{1}{2} \tan^{-1} \left( \frac{\sin 2\phi}{\frac{\sinh 2\epsilon_e}{\tanh 2\epsilon'_e} + \cosh 2\epsilon_e \cos 2\phi} \right) \quad 6-16$$

If  $\phi \neq 0$ , from Eq. 6-13,  $\epsilon$  is always smaller than  $(\epsilon_e + \epsilon'_e)$ .

If  $\epsilon = (\epsilon_e + \epsilon'_e) - \delta$  and  $\delta > 0$ , then

$$\begin{aligned} (\epsilon_1)_{\text{non}} &= \ln(MM') + \epsilon \\ &= \ln M + \ln M' + (\epsilon_e + \epsilon'_e) - \delta \\ &= (\epsilon'_e + \epsilon_e) - \delta \end{aligned}$$

Continued.....

$$\begin{aligned}
(\epsilon_2)_{\text{non}} &= \ln(MM') - \epsilon \\
&= \ln M + \ln M' - (\epsilon_0 + \epsilon'_0) + \delta \\
&= (\epsilon_2 + \epsilon'_2) + \delta
\end{aligned}$$

6-17

$$\begin{aligned}
(\epsilon_3)_{\text{non}} &= -((\epsilon_1)_{\text{non}} + (\epsilon_2)_{\text{non}}) \\
&= -((\epsilon_1 + \epsilon'_1) + (\epsilon_2 + \epsilon'_2))
\end{aligned}$$

6.2 The Nonalignment of the Principal Axes of Stress and Strain in Non-coaxial Deformations.

The principal axes of stress and strain always coincide in coaxial deformations. When the principal axes of stress rotate, so will the principal axes of strain, and non-coaxial deformation takes place. The relationship between  $\phi$  which is the angle the principal axes of stress rotate and  $\theta'$  which is the angle the principal axes of strain rotate, is shown in Eq. 6-12. From Eq. 6-12, it is clearly shown that the relation between  $\phi$  and  $\theta'$  is not only dependent on  $\epsilon_0$ , the prestrain, but also on  $\epsilon'_0$ , the amount of straining in the second deformation. If the strain in the second deformation continues, will the principal axes of strain coincide with the principal axes of stress again?

The principal axes of stress in the second deformation are parallel and perpendicular to OT (fig. 6-1), and stay fixed there throughout the deformation. Therefore, if the principal axes of strain do coincide with the principal axes of stress again, it means that

Continued.....

the most stretched fibre must be the fibre  $OP'$  in  $OA'B'C'$  (fig. 6-1). Because the directions of <sup>the</sup> principal axes of strain, or the angle  $\theta'$  in Eq. 6-12, is always referred back to that in the undeformed unit square  $OABC$ , when the principal axes of strain and stress coincide again, the angle  $\theta'$  should be  $\angle AOP$  instead of  $\angle AOP'$ .

According to Eq. 6-1 and Eq. 6-8,

$$(X_1')_{P'} = e^{\epsilon_1} (X_1)_P \quad 6-18$$

$$(X_2')_{P'} = e^{\epsilon_2} (X_2)_P$$

and  $\epsilon_1 = M + \epsilon_0$  6-19

$$\epsilon_2 = M - \epsilon_0$$

$$\begin{aligned} \angle A'OP' &= \phi \\ &= \tan^{-1} \frac{(X_2')_{P'}}{(X_1')_{P'}} = \tan^{-1} \left( \frac{e^{M-\epsilon_0} (X_2)_P}{e^{M+\epsilon_0} (X_1)_P} \right) \\ &= \tan^{-1} (e^{-2\epsilon_0} \tan(\angle AOP)) \end{aligned} \quad 6-20$$

Thus  $\tan \phi = e^{-2\epsilon_0} \tan \theta'$   
 or  $\tan \theta' = e^{2\epsilon_0} \tan \phi$  6-21

Substituting  $\theta'$  in Eq. 6-21 into Eq. 6-12,

$$\tan 2\theta' = \frac{2 \tan \theta'}{1 - \tan^2 \theta'} = \frac{2 e^{2\epsilon_0} \tan \phi}{1 - e^{4\epsilon_0} \tan^2 \phi}$$

Continued.....

$$= \frac{\sin 2\phi}{\frac{\sinh 2\epsilon_0}{\tanh 2\epsilon_0'} + \cosh 2\epsilon_0 \cos 2\phi} \quad 6-22$$

$$\begin{aligned} \tanh 2\epsilon_0' &= \frac{\sinh 2\epsilon_0 \cdot 2e^{2\epsilon_0} \tan\phi}{\sin 2\phi (1 - e^{4\epsilon_0} \tan^2\phi) - 2e^{2\epsilon_0} \tan\phi \cosh 2\epsilon_0 \cos 2\phi} \\ &= -1 \end{aligned} \quad 6-23$$

In Eq. 6-23,  $\tanh 2\epsilon_0' = -1$ . There is no value of  $\epsilon_0'$  which should be positive to satisfy Eq. 6-23. In other words, if  $\phi$  and  $\epsilon_0$  are not zero, it is impossible for the principal axes of stress and strain to coincide again after they have shifted from each other.

It is proved that the principal axes of stress and strain will not coincide again after they have shifted from each other. Then, how close could the two axes be? It is easily seen that the two axes are closest when the second deformation becomes infinite or  $\epsilon_0'$  is infinitely large. Because  $\tanh \infty = 1$ , Eq. 6-12 becomes

$$\begin{aligned} \tan 2\theta' &= \frac{\sin 2\phi}{\sinh 2\epsilon_0 + \cosh 2\epsilon_0 \cos 2\phi} \\ &= \frac{\sin 2\phi}{\sinh 2\epsilon_0 + \cosh 2\epsilon_0 (1 - 2 \sin^2\phi)} \\ &= \frac{\sin 2\phi}{e^{2\epsilon_0} - (e^{2\epsilon_0} + e^{-2\epsilon_0}) \sin^2\phi} \\ &= \frac{\sin 2\phi}{e^{2\epsilon_0} \cos^2\phi - e^{-2\epsilon_0} \sin^2\phi} \end{aligned}$$

Continued.....

$$\begin{aligned} &= \frac{2e^{-2\epsilon_0} \tan \phi}{1 - e^{-4\epsilon_0} \tan^2 \phi} \\ &= \frac{2 (e^{-2\epsilon_0} \tan \phi)}{1 - (e^{-2\epsilon_0} \tan \phi)^2} \end{aligned} \quad 6-24$$

Therefore,  $\tan \theta' = e^{-2\epsilon_0} \tan \phi$  6-25

Fig. 6-2 shows the relationship between  $\phi$  and  $\theta'$  at the extreme conditions. The curves under the line  $\phi = \theta'$  are curves showing the relationship between  $\phi$  and  $\theta'$  as in Eq. 6-25 at different degrees of prestrain  $\epsilon_0$ , and the second deformation becomes infinitely large. The curves above the line  $\phi = \theta'$  are curves showing the relationship between  $\phi$  and  $\theta'$  as in Eq. 6-21 if the principal axes of strain coincided with the principal axes of stress. At a certain degree of prestrain  $\epsilon_0$ , the difference between the two curves, one under and one above the line  $\phi = \theta'$ , at fixed value of  $\phi$  represents the minimum angle between the final position of the principal axes of stress and strain with respect to the undeformed material in non-coaxial deformation.

### 6.3 Deformations without Changing the Resultant Strain

As said before, deformation is a change of state of strain and a state of strain may be changed by changing the principal strains and keeping the principal axes of strain fixed with respect to the material, or by changing the directions of the principal axes of strain with respect to

Continued.....

to the material and keeping the principal strains unchanged, or by changing both. The first case is the result of a coaxial deformation and the second and the third are results of non-coaxial deformations. Generally speaking, in a non-coaxial deformation, both the principal strains and the directions of the principal axes of strain with respect to the material are changed. But it is still possible that the non-coaxial deformation only changes the directions of the principal axes of strain with respect to the material and keeps the principal strains unchanged. In this case, the strain path in a 3-D triangular co-ordinates is a vertical line coming out from somewhere other than the origin of the co-ordinate on the clock diagram. It is not only interesting but significant to investigate this special case, especially when a circular grid is widely used for strain measurement in sheet metal forming. When a circular grid is used for strain measurement the principal strains are measured from the deformed grid, namely, the ellipse. It is quite possible, as will be discussed in the following, that the shape of the ellipse hence the principal strains is not changed in a subsequent deformation. This is the danger of using circular grid for strain measurement, especially in a non-axisymmetrical forming.

A simple case is taken as an example to explain the complex implication in the deformation without changing the resultant strain, then a theoretical analysis follows for the

Continued.....

more complicated cases. A circle (A in fig.6-3a) becomes an ellipse (B in fig.6-3a) after a deformation and the principal strains are obtained by measuring the major and minor axes of the ellipse. If another deformation reverses the previous one with compressing instead of pulling and pulling instead of compressing along the major and minor axes respectively of the ellipse, the ellipse B will recover to a circle (C in fig.6-3b) and the strains measured from the deformed shape are zero. If the deformation continues, the recovered circle C will be deformed again to another ellipse (D in fig.6-3c) but with the major and minor axes interchanged with each other. In the deformation from B to C then to shape D, the strains obtained only by measuring the major and minor axes of the deformed ellipse, do not change at all. This is a deformation without changing the resultant strain and it is well known but not much development has been done in this approach. In fact, although the principal axes of stress and strain are coincident, all the time during the deformation, strictly speaking, it is a non-coaxial deformation. The major axis of the ellipse has been turned  $90^{\circ}$ . Fig. 6-4 shows the strain paths of the deformations. A is the undeformed state and from A to B (fig.6-3a) the strain path is AB along 3 - o'clock on the clock diagram. From B to C (fig.6-3b), the strain path is BC which coincides with AB. If these are all deformations, then they are coaxial. But if the deformation continues, there is a

Continued.....

sudden jump of non-coaxiality. The major axis is turned through  $90^\circ$  and from C to D (fig.6-3c) the strain path is C'D which is a space line in 3-D triangular co-ordinate and its projection on the clock diagram coincides with AB. If the non-coaxiality is neglected, the strain paths AB, BC and C'D all coincide, . This is an error impossible to <sup>be</sup> detected and explained by using <sup>a</sup> circular grid. If <sup>a</sup> square grid is used, or points are marked on the circular grid, the error would be noticed and avoided.

The above-mentioned deformation is only one of the deformations which take place without changing the resultant strain. In the non-coaxial case, those deformations can occur very often, Eq. 6-13 is copied here for further discussion.

$$\cosh^2 \epsilon = \cosh^2 (\epsilon_0 + \epsilon_1) - (\cosh^2 (\epsilon_0 + \epsilon_1) - \cosh^2 (\epsilon_0 - \epsilon_1)) \sin^2 \phi$$

6-13

where referring to the deformations mentioned in fig.6-3  $\epsilon_0$  is the pure shear strain from A to B,  $\epsilon_1$ , from B to C to D,  $\epsilon$ , the resultant strain in D and  $\phi$ , rotation of the major axis of stress. Eq. 6-13 may also be written as

$$\cosh 2\epsilon = \cosh 2(\epsilon_0 + \epsilon_1) - (\cosh 2(\epsilon_0 + \epsilon_1) - \cosh 2(\epsilon_0 - \epsilon_1)) \sin^2 \phi$$

because 6-26

$$\cosh^2 \epsilon = \frac{1}{2}(\cosh 2\epsilon + 1)$$

Now, if there is no change in <sup>the</sup> resultant strain, that is  $\epsilon = \epsilon_0$ . Therefore:

Continued.....

$$\cosh 2 \epsilon_0 = \cosh 2(\epsilon_0 + \epsilon'_0) - (\cosh 2(\epsilon_0 + \epsilon'_0) - \cosh 2(\epsilon_0 - \epsilon'_0)) \sin^2 \phi$$

$$\cosh 2(\epsilon_0 + \epsilon'_0) - \cosh 2 \epsilon_0 = (\cosh 2(\epsilon_0 + \epsilon'_0) - \cosh 2(\epsilon_0 - \epsilon'_0)) \sin^2 \phi$$

$$2 \sinh (2 \epsilon_0 + \epsilon'_0) \sinh \epsilon'_0 = 2 \sinh 2 \epsilon_0 \sinh 2 \epsilon'_0 \sin^2 \phi$$

$$= 2 \sinh 2 \epsilon_0 (2 \sinh \epsilon'_0 \cosh \epsilon'_0) \sin^2 \phi$$

$$\sinh 2 \epsilon_0 \cosh \epsilon'_0 + \sinh \epsilon'_0 \cosh 2 \epsilon_0 = 2 \sinh 2 \epsilon_0 \cosh \epsilon'_0 \sin^2 \phi$$

$$(\sinh 2 \epsilon_0 - 2 \sinh 2 \epsilon_0 \sin^2 \phi) \cosh \epsilon'_0 + \sinh \epsilon'_0 \cosh 2 \epsilon_0 = 0$$

$$\sinh 2 \epsilon_0 \cos 2 \phi \cosh \epsilon'_0 + \sinh \epsilon'_0 \cosh 2 \epsilon_0 = 0$$

$$\tanh 2 \epsilon_0 \cos 2 \phi + \tanh \epsilon'_0 = 0$$

$$\therefore \tanh \epsilon'_0 = - \tanh 2 \epsilon_0 \cos 2 \phi \qquad 6-27$$

Continued.....

Because

$$0 < \tanh \epsilon_0' < 1,$$

$$\text{so, } -1 < \tanh (2 \epsilon_0) \cos 2\phi < 0$$

and because

$$0 < \tanh (2 \epsilon_0) < 1$$

$$\text{so, } -1 < \cos 2\phi < 0$$

$$-\frac{\pi}{4} < \phi < \frac{\pi}{2} .$$

Continued.....

In other words, no matter what the prestrain is (other than nothing) there is always the possibility of another deformation which will produce no change in <sup>the</sup> resultant strain. Fig.6-5 shows the relationships between  $\epsilon_0$ ,  $\epsilon_0'$  and  $\phi$  for those deformations.

Continued.....

CHAPTER 7

IMPLICATIONS ON THE THEORY OF PLASTICITY

### Implications On the Theory of Plasticity

Formability as defined in Chapter 2 has two aspects, one is the forming limits of the material and the other, the performance of the material in a forming process. As reviewed in Chapter 3, the forming limiting curve of sheet metal that has been investigated <sup>previously</sup> is the formability curve covering the end points of only coaxial strain paths. In other words, the formability curve, in fact, does not represent completely the forming limits of sheet steel but is only a partial view of them. A complete representation should cover the end points of both coaxial and non-coaxial strain paths.

A theoretical analysis of non-coaxial deformation was firstly done by Professor Hsü (48)-(50) in 1965 and 1966. But hitherto no further investigation and no actual non-coaxial strain path has been pursued and plotted. In this thesis, non-coaxial strain paths will be plotted in Chapter 10. In this Chapter, the effect of non-coaxiality on the formability of sheet metal from the point of view of plastic work of deformation and the implication on the theory of plasticity will be discussed.

#### 7.1 Plastic Work Done (52)-(54) in Coaxial Deformation

When a material is deformed, it is firstly deformed elastically, and elastic work is needed to produce elastic strains. After removing the load, the material recovers to

Continued.....

its original form and elastic energy is released during the recovery. For a plastic deformation, after removing the load, a permanent strain exists. It needs plastic work done on the material.

The external work per unit volume done on the material during the strain  $d\epsilon_{ij}$  is  $\sigma_{ij} \cdot d\epsilon_{ij}$  or  $dw = \sigma_{ij} d\epsilon_{ij}$  7-1

where  $\sigma_{ij}$  is the stress tensor. The work includes elastic and plastic work and the strain includes elastic and plastic strain too. Thus:

$$\begin{aligned} dw_p &= dw - dw_e = \sigma_{ij} (d\epsilon_{ij} - d\epsilon_{ij}^e) \\ &= \sigma_{ij} d\epsilon_{ij}^p \end{aligned} \quad 7-2$$

where  $dw_e$  and  $dw_p$  are elastic and plastic work respectively and,  $d\epsilon_{ij}^e$  and  $d\epsilon_{ij}^p$  are elastic and plastic strain-increments.

Due to the incompressibility of metal, plastic deformation always takes place at constant volume and hydrostatic pressure or tension only produces elastic strains. Therefore no plastic work is done by <sup>the</sup> hydrostatic component of the applied stress and the plastic work is done only by the deviatoric or reduced stress

$$\sigma'_{ij} = \sigma_{ij} - \sigma \delta_{ij} \quad 7-3$$

where  $\sigma (= \frac{1}{3} \sigma_{ii})$  is the hydrostatic component of the stress.

Eq. 7-2 can also be written as:

Continued.....

$$dw_p = \sigma_{ij} d\epsilon_{ij}^P = \sigma'_{ij} d\epsilon_{ij}^P \quad 7-3$$

In coaxial deformation, the state of strain is represented by three principal strains measured from three orthogonal fibres which remain orthogonal to each other in the deformation, and the principal axes of strain with respect to the material are usually ignored because they are fixed. The strain-increment is represented by three principal strain-increments which are also the strain-increments of those three orthogonal fibres, so that the strain-increment is additive and integrable. Therefore the total plastic work done on the material from the initial to the final state of the deformation is

$$w_p = \int dw_p = \int \sigma_{ij} d\epsilon_{ij}^P = \int \sigma'_{ij} d\epsilon_{ij}^P \quad 7-4$$

where the integral is taken over the actual strain path.

Eqs. 7-2 and 7-4 imply ((repeated suffixes i and j)) that the total plastic work is the sum of the work done by each component of stress. For simplicity, a generalised or equivalent stress  $\bar{\sigma}$  and equivalent incremental plastic strain  $d\bar{\epsilon}$  are introduced and defined as follows:

$$\bar{\sigma} = \left[ \frac{1}{2} \{ (\sigma_1 - \sigma_2)^2 + (\sigma_2 - \sigma_3)^2 + (\sigma_3 - \sigma_1)^2 \} \right]^{1/2} \quad 7-5$$

Continued.....

$$= \left[ \frac{3}{2} \{ \sigma_{ij}' \sigma_{ij}' \} \right]^{\frac{1}{2}} \quad 7-6$$

where  $\sigma_1, \sigma_2, \sigma_3$ , are the principal stresses, and

$$d\bar{\epsilon}^P = (2/9 ((d\epsilon_1^P - d\epsilon_2^P)^2 + (d\epsilon_2^P - d\epsilon_3^P)^2 + (d\epsilon_3^P - d\epsilon_1^P)^2)^{\frac{1}{2}} \quad 7-7$$

$$= \left( \frac{2}{3} (d\epsilon_{ij}^P d\epsilon_{ij}^P) \right)^{\frac{1}{2}} \quad 7-8$$

Therefore:

$$\begin{aligned} dw_p &= \sigma_{ij} d\epsilon_{ij}^P \\ &= \bar{\sigma} d\bar{\epsilon} \end{aligned} \quad 7-9$$

and

$$w_p = \int dw_p = \int \bar{\sigma} d\bar{\epsilon} \quad 7-10$$

## 7.2 Plastic Work Done in Non-coaxial Deformation

In a non-coaxial strain path, the incremental strain, in fact, does not mean the same thing as the incremental strain in a coaxial strain path. In a non-coaxial deformation, a state of strain is determined not only by the three principal strains but also by the directions of the principal axes of strain with respect to the material. The principal strains are determined by <sup>the</sup> most severely deformed fibres in the grid. Because of the non-coaxiality, the fibres measured for obtaining the principal strains at

Continued.....

one state are different from those measured at another state of strain. For instance, at stage A, fibres a and b are the most severely deformed fibres and are measured for principal strains  $\epsilon_a$  and  $\epsilon_b$ . At stage B, fibres c and d instead of a and b are the most severely deformed and are measured for principal strains  $\epsilon_c$  and  $\epsilon_d$ . From stage A to stage B, the resultant principal strains are from  $\epsilon_a$  and  $\epsilon_b$  to  $\epsilon_c$  and  $\epsilon_d$ , but the strain differences  $(\epsilon_c - \epsilon_a)$  and  $(\epsilon_d - \epsilon_b)$  are not the strain increments of either fibres a and b or fibres c and d. The strain-increment between stage A and stage B is not measured from the same fibres in the material. This is one of the reasons why Eq. 7-3 can not be integrated over the strain path. The other reason that Eq. 7-3 can not be integrated is that in the non-coaxial case, the direction of  $\sigma_{ij}$  is no longer coincident with that of  $d\epsilon_{ij}^p$ , and Eq. 7-3 can be true only when the direction of  $\sigma_{ij}$  is coincident with that of  $d\epsilon_{ij}^p$ .

Eq. 7-3 is not integrable, then what is the plastic work done in non-coaxial deformations? The plastic work done in a deformation under <sup>a</sup> non-coaxial strain path can be found if the angle between the principal axes of stress and principal axes of strain with respect to the material at every stage of <sup>the</sup> deformation is known. The non-coaxial strain path is divided into several parts and each part in which it is assumed that the principal axes of stress

Continued.....

are fixed with respect to the material represents a stage of deformation. The first and the second parts are handled first. The first one starts from the undeformed state, and the plastic work done is <sup>the same as</sup> that in the coaxial case. For the second stage, the angle ( $\phi$ ) between the principal axes of stress and those of strain with respect to the material after the first stage of deformation, is known. Also the resultant strain  $\epsilon$  and the amount of non-coaxiality after the second stage of deformation are known from the non-coaxial strain path. By substituting  $\phi$ ,  $\epsilon$ , and  $\epsilon_0$  which is the resultant strain after the first stage of deformation, into Eq. 6-12 or 6-13,  $\epsilon'_0$ , the amount of straining in the second stage of deformation can be obtained. In other words, if a square or a circular grid is printed or scribed on the metal surface before the second stage of deformation, a strain  $\epsilon'_0$  will be obtained at the end of the second stage of deformation. Therefore, the plastic work done in the second stage of deformation is:

$$(w_p)_2 = \int_0^{\epsilon'_0} \sigma'_{ij} \cdot d\epsilon_{ij} \quad 7-11$$

Eq. 7-11 is integrable because the strain measured is along the same direction as that of  $\sigma'_{ij}$ .

The plastic work done in the first stage of deformation is:

$$(w_p)_1 = \int_0^{\epsilon_0} \sigma'_{ij} \cdot d\epsilon_{ij} \quad 7-12$$

which is also integrable.

Continued.....

So, the plastic work done in the first two stages of deformation is

$$(w_p)_{n2} = (w_p)_1 + (w_p)_2 = \int_0^{\epsilon_0} \sigma'_{ij} d\epsilon_{ij}^p + \int_0^{\epsilon'_0} \sigma'_{ij} d\epsilon_{ij}^p \quad 7-13$$

$$= \int_0^{\epsilon_0 + \epsilon'_0} \sigma'_{ij} d\epsilon_{ij}^p \quad 7-14$$

If the non-coaxiality is neglected, or the non-coaxial strain path is treated as<sup>a</sup> coaxial one, the plastic work done in the first two stages of deformation would be as follows:

$$(w_p)_{c2} = \int_0^{\epsilon} \sigma'_{ij} d\epsilon_{ij}^p \quad 7-15$$

From Eq. 6-13, if  $\phi \neq 0$ ,  $\epsilon$  is always smaller than  $(\epsilon_0 + \epsilon'_0)$ . Therefore in the first two stages of deformation, there is a plastic work difference between<sup>the</sup> coaxial and non-coaxial cases,<sup>and</sup> it is

$$\begin{aligned} (\Delta w_p) &= (w_p)_{n2} - (w_p)_{c2} \\ &= \int_0^{\epsilon_0 + \epsilon'_0} \sigma'_{ij} d\epsilon_{ij}^p - \int_0^{\epsilon} \sigma'_{ij} d\epsilon_{ij}^p \quad 7-16 \end{aligned}$$

In other words, for two deformations both with the same amount of principal strains but one under coaxial and the

Continued.....

other under non-coaxial strain path, the one under non-coaxial strain path will need more plastic work done for getting the same amount of resultant strain.

Now suppose the first two stages of deformation are treated as the first stage, and the third stage is treated as the second stage. Then,

$$\Delta w_2 = \int_0^{\epsilon + \epsilon_0''} \sigma'_{ij} d\epsilon_{ij}^P - \int_0^{\epsilon'} \sigma'_{ij} d\epsilon_{ij}^P \quad 7-17$$

where  $\epsilon$  is as  $\epsilon_0$ ,  $\epsilon_0''$  as  $\epsilon_0'$  and  $\epsilon'$  as  $\epsilon$  in Eq. 7-16. So the plastic work done in the first three stages of deformation is:

$$(w_p)_{n3} = \int_0^{\epsilon'} \sigma'_{ij} d\epsilon_{ij}^P + \Delta w_1 + \Delta w_2 \quad 7-18$$

where the first term reading from left to right in the right hand side of Eq. 7-18 is the plastic work done under a coaxial strain path and the last two terms are the plastic work differences between <sup>the</sup> coaxial and non-coaxial cases.

Repeating the procedures as for Eqs. 7-16, 7-17 and 7-18, a series of differences in plastic work between the coaxial and non-coaxial <sup>components</sup> in each stage of deformation,  $\Delta w_3$ ,  $\Delta w_4$  ..... and  $\Delta w_{n-1}$  can be obtained. Then, the total plastic work done in a non-coaxial deformation is the

Continued.....

sum of the total plastic work done in a coaxial deformation with the same amount of strain as that in a non-coaxial one, plus those plastic work differences between coaxial and non-coaxial deformations in the small stages of deformation. It is:

$$(w_p)_n = \int \sigma'_{ij} d\epsilon_{ij}^P + \sum_i^{n-1} \Delta w_i \quad 7-19$$

where the integral is taken over the projected strain path of the non-coaxial one on the clock diagram.

### 7.3 Work-hardening

When a material is deformed plastically, its resistance to further deformation increases. Such a material is called a work-hardening material.

The hypothesis of work-hardening is that the degree of hardening is a function of the total plastic work done only and is otherwise independent of the strain path (52). The degree of hardening is measured by the yield criterion which is represented by the equivalent stress  $\bar{\sigma}$  as defined in Eq. 7-5. In mathematical language, it may be written as:

$$\bar{\sigma} = F(w_p) \quad 7-20$$

The total plastic work done is dependent on the strain path. This is well known and the literature concerning the

Continued.....

hypothesis of work-hardening states this dependence. But it is not usually pointed out that Eq. 7-3 can not be integrated for obtaining the total plastic work if the strain path is non-coaxial. As shown in Eq. 7-19, there is a difference  $\sum_i^{n-1} \Delta w_i$  between the total plastic work done in coaxial and non-coaxial deformations. Surely, the degree of work-hardening will be different due to that difference.

Therefore, for a material deformed under a coaxial strain path, the degree of work-hardening is:

$$\begin{aligned} \bar{\sigma} &= F(w_p) = F\left(\int \sigma'_{ij} d\epsilon_{ij}^P\right) \\ &= F\left(\int \bar{\sigma} d\bar{\epsilon}\right) \end{aligned} \quad 7-21$$

and for the material deformed under a non-coaxial strain path, the degree of work-hardening should be as follows:

$$\bar{\sigma} = F(w_p) = F\left(\int \sigma'_{ij} d\epsilon_{ij}^P + \sum_i^{n-1} \Delta w_i\right) \quad 7-22$$

For the same amount of resultant strain, the material deformed under a non-coaxial strain path is harder than under a coaxial strain path.

#### 7.4 Validity of Lévy-Mises and Prandtl-Reuss Equations.

The stress-strain relations <sup>of plasticity theory</sup> were originally proposed by Saint-Venant in 1870 (55). <sup>He assumed</sup> that the principal axes of the strain-

Continued.....

-increment coincided with the principal axes of stress. Then a general relationship between strain-increment and the reduced stress was introduced by Lévy (56) in 1871 and independently by von Mises (57) in 1913. The relations were expressed in equations as the following.

$$\frac{d\epsilon_x}{\sigma'_x} = \frac{d\epsilon_y}{\sigma'_y} = \frac{d\epsilon_z}{\sigma'_z} = \frac{d\gamma_{xy}}{\tau_{xy}} = \frac{d\gamma_{yz}}{\tau_{yz}} = \frac{d\gamma_{zx}}{\tau_{zx}} = d\lambda \quad 7-23$$

or more compactly, as

$$d\epsilon_{ij} = \sigma'_{ij} d\lambda \quad 7-24$$

where  $d\lambda$  is a constant of proportionality, and the equations were called <sup>the</sup> Lévy-Mises equations.

In <sup>the</sup> Lévy-Mises equations, total strain-increment was used so that they could only be applied to ~~the~~ materials which are rigid before plastic strain took place. The extension of the Lévy-Mises equations ~~for~~ to materials which ~~are~~ not plastic-rigid was done by Prandtl (58) in 1924 for the plane-strain problem, and in complete generality by Reuss (59) in 1930. The equations were expressed as

$$\frac{d\epsilon_x^P}{\sigma'_x} = \frac{d\epsilon_y^P}{\sigma'_y} = \frac{d\epsilon_z^P}{\sigma'_z} = \frac{d\gamma_{xy}^P}{\tau_{xy}} = \frac{d\gamma_{yz}^P}{\tau_{yz}} = \frac{d\gamma_{zx}^P}{\tau_{zx}} = d\lambda' \quad 7-24$$

or

$$d\epsilon_{ij}^P = \sigma'_{ij} d\lambda' \quad 7-25$$

Continued.....

and were called Prandtl — Reuss equations. If principal stresses and principal strain-increment are chosen, <sup>the</sup> Lévy-Mises equations may be written as

$$\frac{d\epsilon_1}{\sigma_1'} = \frac{d\epsilon_2}{\sigma_2'} = \frac{d\epsilon_3}{\sigma_3'} = d\lambda \quad 7-26$$

and <sup>the</sup> Prandtl - Reuss equations as

$$\frac{d\epsilon_1^P}{\sigma_1'} = \frac{d\epsilon_2^P}{\sigma_2'} = \frac{d\epsilon_3^P}{\sigma_3'} = d\lambda' \quad 7-27$$

It is significant to note that the strain-increments used ~~to be obtained~~ as the strain differences between one state of strain and its adjacent state of strain. In <sup>the</sup> coaxial case, because all the states of strain are obtained by measuring certain fibres all the time during the deformation, the strain difference between a state of strain and its adjacent state is a strain-increment of the same fibre at different stages of forming. This is a very important condition under which <sup>the</sup> Lévy-Mises and Prandtl-Reuss equations are valid. In the non-coaxial case, owing to the rotation of <sup>the</sup> principal axes of stress, the principal axes of strain are rotating with respect to the material all the time during the deformation. The strain-increment, which means the strain difference between a state of strain and its adjacent state, is a strain difference of different fibres at different stages of forming. Although <sup>the</sup> Lévy-Mises and Prandtl-Reuss equations are valid in the coaxial case, they are not

Continued.....

valid in the non-coaxial case unless the strain-increment in <sup>the</sup> non-coaxial case is re-defined as the strain-increment of a certain fibre and not the principal strain-increment.

If principal stresses and principal strain-increments are chosen, then <sup>the</sup> Lévy-Mises equation may be written as:

$$\frac{\sigma_1'}{\sigma_2'} = \frac{\Delta \epsilon_1}{\Delta \epsilon_2} \quad 7-28$$

where  $\Delta \epsilon_1$  and  $\Delta \epsilon_2$  are infinitesimal principal strain-increments. Suppose a material is deformed under stresses with constant ratio  $\lambda (= \frac{\sigma_1'}{\sigma_2'})$  to a state of strain which

is represented by the three principal strains  $(\epsilon_1)_0, (\epsilon_2)_0$  and  $(\epsilon_3)_0$ , and because of the constant stress ratios, the strain ratio  $(\epsilon_1)_0 / (\epsilon_2)_0$  is equal to  $\lambda$ . If the stressing continues with the same stress ratio and the principal axes of stress remain fixed with respect to the material, the material will be further deformed to a new state of

$$\begin{aligned} \text{strain, } \epsilon_1, \epsilon_2 \text{ and } \epsilon_3, \text{ and because } \frac{\Delta \epsilon_1}{\Delta \epsilon_2} &= \frac{\sigma_1'}{\sigma_2'} = \lambda \\ &= \frac{(\epsilon_1)_0}{(\epsilon_2)_0}. \end{aligned}$$

$$\text{Therefore: } \frac{\epsilon_1}{\epsilon_2} = \frac{(\epsilon_1)_0 + \Delta \epsilon_1}{(\epsilon_2)_0 + \Delta \epsilon_2} = \frac{\lambda(\epsilon_2)_0 + \lambda \Delta \epsilon_2}{(\epsilon_2)_0 + \Delta \epsilon_2} = \lambda$$

Continued.....

A state of strain can also be represented by a uniform dilatation and a pure shear strain as shown in the analysis in Chapter 4. Therefore, the strains in the first deformation may also be represented as follows:

$$\ln Mo = \frac{(\epsilon_1)_0 + (\epsilon_2)_0}{2} \quad 7-29$$

$$\epsilon_0 = \frac{(\epsilon_1)_0 - (\epsilon_2)_0}{2} \quad 7-30$$

where  $\ln Mo$  is the amount of uniform dilatation and  $\epsilon_0$ , the pure shear strain. It is understood that  $(\epsilon_3)_0 = -2 \ln Mo$ . Because  $\epsilon_1$ ,  $\epsilon_2$  and  $\epsilon_3$  are the resultant strains of the two deformations, the strains in the second deformation are

$$\ln Mo' = \frac{\epsilon_1 + \epsilon_2}{2} = \ln Mo \quad 7-31$$

$$\epsilon_0' = \frac{\epsilon_1 - \epsilon_2}{2} = \epsilon_0 \quad 7-32$$

If the stressing in the second deformation is such that the stress ratio is unchanged but the principal axes of stress rotate through an angle  $\phi$  with respect to the material it is a non-coaxial case and the resultant strains will be as follows. According to Eq. 6-13

$$\cosh^2 \epsilon = \cosh^2(\epsilon_0 - \epsilon_0') - (\cosh^2(\epsilon_0 + \epsilon_0') - \cosh^2(\epsilon_0 - \epsilon_0')) \sin^2 \phi$$

Continued.....

and

$$\ln M = \ln M_0 + \ln M_0'$$

because uniform dilatation is non-directional. If  $\phi \neq 0$ ,  $\epsilon$  is always smaller than  $(\epsilon_0 + \epsilon_0')$ , so, let

$$\epsilon = (\epsilon_0 + \epsilon_0') - \delta \quad 7-33$$

where  $\delta$  has a positive value. Then the resultant principal strains are:

$$\begin{aligned} \epsilon_1' &= \ln M + \epsilon \\ &= \ln M_0 + \ln M_0' + (\epsilon_0 + \epsilon_0') - \delta \\ &= \frac{\epsilon_1 + \epsilon_2}{2} + \frac{\epsilon_1 - \epsilon_2}{2} - \delta \\ &= \epsilon_1 - \delta \end{aligned} \quad 7-34$$

$$\begin{aligned} \epsilon_2' &= \ln M - \epsilon \\ &= \epsilon_2 + \delta \end{aligned} \quad 7-35$$

$$\text{and } \epsilon_3' = -2 \ln M = -(\epsilon_1 + \epsilon_2) = \epsilon_3 \quad 7-36$$

then

$$\frac{\epsilon_1'}{\epsilon_2'} = \frac{\epsilon_1 - \delta}{\epsilon_2 + \delta} \neq \lambda \quad (\text{in general}) \quad 7-37$$

Continued.....

and

$$\frac{\Delta \epsilon_1'}{\Delta \epsilon_2'} = \frac{\epsilon_1' - (\epsilon_1)_0}{\epsilon_2' - (\epsilon_2)_0} = \frac{\epsilon_1 - (\epsilon_1)_0 - \delta}{\epsilon_2 - (\epsilon_2)_0 + \delta}$$

$$= \frac{\Delta \epsilon_1 - \delta}{\Delta \epsilon_2 + \delta} \neq \lambda = \frac{\sigma_1'}{\sigma_2'}$$
7-38

Therefore it is proved that <sup>the</sup> Lévy-Mises equations are not valid for <sup>the</sup> non-coaxial case.

### 7.5 Stress-Strain Relationship

In simple tension, although it involves a three-dimensional deformation, only the load and the strain in <sup>the</sup> loading direction are interesting and <sup>can be</sup> plotted in Cartesian co-ordinates. The stress-strain relation is very simple, and the area under the curve represents the total work done.

In other deformations, the stressing condition is more complicated and can not be represented in <sup>such</sup> a simple way as that in the tension test. Therefore, the effective or equivalent stress and the effective strain are used to represent the stress-strain relation, where the effective or equivalent stress is as defined in Eq. 7-5 and <sup>the</sup> effective or equivalent strain is the integral of the incremental strain along the strain path, as follows.

$$\bar{\epsilon} = \int d\bar{\epsilon} = \int \left( \frac{2}{9} \{ (d\epsilon_1 - d\epsilon_2)^2 + (d\epsilon_2 - d\epsilon_3)^2 + (d\epsilon_3 - d\epsilon_1)^2 \} \right)^{1/2} \quad 7-39$$

Continued.....

If the incremental strain ratios are kept constant all the time in the strain path, in other words, if there is a linear strain path, or

$$d\epsilon_1 : d\epsilon_2 = d\epsilon_3 = 1 : \alpha : - (1+\alpha) \quad 7-40$$

where  $\alpha$  is a constant

then,

$$\begin{aligned} d\bar{\epsilon} &= \left( \frac{2}{3} (d\epsilon_1^2 + d\epsilon_2^2 + d\epsilon_3^2) \right)^{\frac{1}{2}} \\ &= \frac{2}{\sqrt{3}} (1+\alpha + \alpha^2)^{\frac{1}{2}} d\epsilon_1 \end{aligned} \quad 7-41$$

and

$$\begin{aligned} \bar{\epsilon} &= \int d\bar{\epsilon} = \frac{2}{\sqrt{3}} (1+\alpha + \alpha^2)^{\frac{1}{2}} \int d\epsilon_1 \\ &= \frac{2}{\sqrt{3}} (1+\alpha + \alpha^2)^{\frac{1}{2}} \epsilon_1 \\ &= \frac{\sqrt{2}}{\sqrt{3}} (\epsilon_1^2 + \epsilon_2^2 + \epsilon_3^2)^{\frac{1}{2}} \end{aligned} \quad 7-42$$

In the coaxial case, when the effective stress and effective strain are used to represent the stress-strain relation, the area under the curve,  $\int \bar{\sigma} d\bar{\epsilon}$ , is the total work done. In the non-coaxial case, if the non-coaxiality is neglected and only the stresses and <sup>the</sup> principal strains are measured, then the stress-strain relation represented by the effective stress and effective strain will be different from that in <sup>the</sup> coaxial case. The area under the curve will represent not the total work done but the total work done minus  $\sum_i^{n-1} \Delta w_i$  as shown in Eq. 7-19. Because  $\bar{\sigma}$  is a function

Continued.....

of total plastic work done only, therefore, for a certain amount of total plastic work done,  $\bar{\sigma}$  is determined. But the resultant strains in coaxial and non-coaxial cases for the same amount of total plastic work are different. This is the reason why the stress-strain relationship in coaxial and non-coaxial <sup>deformations</sup> are different.

Take, for example, the cases discussed in the last section. The stress ratios are the same but the directions of the principal axes of stress with respect to the material are different from each other, <sup>and</sup> the ratio of the resultant strains is

$$\frac{\epsilon_1 - \delta}{\epsilon_2 + \delta}$$

instead of  $\epsilon_1/\epsilon_2$  in <sup>the</sup> non-coaxial case. The stress-strain relations in the first stage are exactly the same, but in the second stage,

$$\frac{\Delta \epsilon_1}{\Delta \epsilon_2} = \lambda \tag{7-43}$$

and  $\frac{\Delta \epsilon_1'}{\Delta \epsilon_2'} = \frac{\Delta \epsilon_1 - \delta}{\Delta \epsilon_2 + \delta} = \lambda' \neq \lambda \tag{7-44}$

The effective strain increment in the second stage in the coaxial case is

$$(\Delta \bar{\epsilon})_c = \frac{\sqrt{2}}{\sqrt{3}} \left[ (\Delta \epsilon_1)^2 + (\Delta \epsilon_2)^2 + (\Delta \epsilon_3)^2 \right]^{\frac{1}{2}} \tag{7-45}$$

and in <sup>the</sup> non-coaxial case,

$$(\Delta \bar{\epsilon})_n = \frac{\sqrt{2}}{\sqrt{3}} \left[ (\Delta \epsilon_1')^2 + (\Delta \epsilon_2')^2 + (\Delta \epsilon_3')^2 \right]^{\frac{1}{2}} \tag{7-46}$$

Continued.....

Because  $\Delta \epsilon_3 = \Delta \epsilon_3'$  7-47

therefore,

$$\Delta \epsilon_1 + \Delta \epsilon_2 = \Delta \epsilon_1' + \Delta \epsilon_2'$$

and

$$(1+\lambda) \Delta \epsilon_2 = (1+\lambda') \Delta \epsilon_2' \tag{7-48}$$

From Eqs. 7-43 and 7-44

$$(\Delta \epsilon_1)^2 + (\Delta \epsilon_2)^2 = (1+\lambda^2) (\Delta \epsilon_2)^2 \tag{7-49}$$

and

$$(\Delta \epsilon_1')^2 + (\Delta \epsilon_2')^2 = (1+\lambda'^2) (\Delta \epsilon_2')^2 \tag{7-50}$$

$$= (1+\lambda'^2) \left[ \frac{(1+\lambda)^2}{(1+\lambda')^2} \right] (\Delta \epsilon_2)^2 \tag{7-51}$$

If we assume that  $(\Delta \bar{\epsilon})_c$  is equal to  $(\Delta \bar{\epsilon})_n$ , then,

$$(1+\lambda^2) (\Delta \epsilon_2)^2 = (1+\lambda'^2) \left[ \frac{(1+\lambda)^2}{(1+\lambda')^2} \right] (\Delta \epsilon_2)^2$$

$$(1+\lambda^2) (1+\lambda')^2 = (1+\lambda'^2) (1+\lambda)^2$$

$$(1+\lambda^2) [(1+\lambda'^2) + 2\lambda'] = (1+\lambda'^2) [(1+\lambda^2) + 2\lambda]$$

$$(1+\lambda^2) \cdot 2\lambda' = (1+\lambda'^2) \cdot 2\lambda$$

$$2\lambda' + 2\lambda^2\lambda' = 2\lambda + 2\lambda\lambda'^2$$

Continued.....

$$\lambda - \lambda' = \lambda \lambda' (\lambda - \lambda')$$

$$\therefore \lambda \lambda' = 1$$

$$\text{or } \lambda' = \frac{1}{\lambda}$$

7-52

Eq. 7-52 shows that only when  $\lambda' = \frac{1}{\lambda}$  then

$$(\Delta \bar{\epsilon})_c = (\Delta \bar{\epsilon})_n$$

otherwise they are not equal.

This is a clear proof that the stress-strain relations in coaxial and non-coaxial cases are different.

The whole theory of plasticity is hitherto built on the basis of Lévy-Mises and Prandtl-Reuss equations. Now it is proved that <sup>the</sup> Lévy-Mises and Prandtl-Reuss equations are valid only in <sup>the</sup> coaxial case. Therefore, the theory of plasticity or the stress-strain relationship in <sup>the</sup> non-coaxial case needs to be modified, depending on the non-coaxiality of the principal axes of stress and strain as discussed in this Chapter.

#### 7.6 The Effect of Non-coaxiality on Formability

In sheet metal forming, very often, the material fails due to excessive thinning, leading to fracture. But

Continued.....

excessive thinning is not the only reason which leads the material to fracture. For instance, low cycle fatigue could lead the material to fracture. In <sup>the</sup> non-coaxial case, part of the work done is consumed without producing measurable strain, therefore, it is very possible that the material fails not because of excessive thinning but because of too much work done on it. In other words, the material fails because of being too severely work-hardened so that the stress exceeds the strength of the material.

Because of the non-coaxiality of the principal axes of stress and strain, the strain path of a non-coaxial deformation deviates from that of a coaxial one. Because the formability is dependent on the strain path, the deviation of <sup>the</sup> strain path in <sup>a</sup> non-coaxial deformation will affect the formability of material. In addition, the non-coaxiality, because <sup>of</sup> the associated excess work consumed, may induce fracture without excessive thinning. This is the possibility that the forming limiting curve of sheet metal in which hitherto the forming limit is determined based on the material failure of excessive thinning leading to fracture can be extended to cover the forming limits which are due to fracture without excessive thinning. An example of material failure without excessive thinning will be shown in Chapter 10.

Continued.....

CHAPTER 8

THE DRAWABILITY OF SHEET METAL

### The Drawability of Sheet Metal

As briefly described in the Introduction of this thesis, the formability of sheet metal is investigated in two aspects, one is the forming limits of the material under metal forming conditions and the other, the performance of sheet metal in a forming process. The forming limit of a material is dependent on the strain path under which the material is deformed. This path dependence requires the investigation of non-coaxial deformation. In the last few Chapters, non-coaxial deformation and strain path are analysed in detail. In this Chapter the second aspect of the formability of sheet metal, namely, the performance of sheet metal in a forming process will be discussed.

A sheet metal test was originally proposed to test the material property. When the test result failed to predict the material behaviour in an actual forming process, another test was proposed. The large number of tests is a good indication that a sheet metal test is only one of an infinite number of forming processes and the test result is only the performance of the material in that forming process. Formability of sheet metal, as the performance in a forming process, is, therefore, dependent on the forming process.

"Stretchability" and "drawability" are used to present the performance of sheet metal in a forming process. But

Continued.....

because the failure of material in most of the forming processes is due to stretching, the forming limits of a material, in fact, has included the stretchability of the material. However, there are some other presentations such as the height of the punch travel in the Erichsen test and the height of the shell at the maximum pressure in the hydrostatic bulge test, which represent also the stretchability of the material in purely stretch — forming processes. Since stretching always occurs in a forming process, such cases as those in the Erichsen test and the hydrostatic bulge test will be tackled as the performance in a forming process without drawing. Therefore, this Chapter is mainly devoted to the drawability of sheet metal in a forming process.

The definition of drawability, hitherto, is based on and limited to the drawing of round cups as in the Swift's test, and the limiting drawing ratio is used to represent the drawability of sheet metal. But it is well known that the Swift's test can not predict the drawing properties of all materials in all drawing processes. Even in cylindrical cup drawing, the Swift's test can not predict accurately if the forming conditions deviate from those in the Swift's test. The more the forming conditions in the actual forming operations deviate from those in the test, the less reliable the test results are for predicting the behaviour of the material in non-cylindrical cup drawing. This is not because the Swift's test fails to

Continued.....

reveal the "true drawability", or that a drawability test has not, but can some day be found, by discovering perhaps the right combinations among the practically infinite sets of testing conditions, but because the drawability so defined is only for round cup drawing.

The Swift's test was proposed thirty five years ago (22) and at that time the understanding of the behaviour of sheet metal under forming was relatively limited. It can hardly be expected that the first proposal should be perfect. In fact, Professor Swift did notice that a more complex effect existed in non-axisymmetrical pressing. If Professor Swift were still alive, he might have done the extension and generalisation of the definition of drawability and the test, as is being done in this thesis. Two paragraphs of Professor Swift's words (22) are quoted here to show that he did point out the complexity in non-axisymmetrical forming but did not investigate it because the simple problem of axisymmetrical forming was still unsolved.

"A material which is best able to withstand its own drawing action and which at the same time is best able to endure the stretching action imposed by impressed conditions which combine drawing and stretching in uncertain or varying proportions. When two materials A and B are compared in which A is superior

Continued.....

under simple stretching and B superior under drawing, the preference for any particular press operation must depend on the relative severity of the impressed stretching and impressed drawing conditions."

"Those observations are made with some confidence so far as symmetrical pressings are concerned. When, however, the intensity of the drawing and blank-holding actions vary from one point to another, as, for example, in the case of a pressing of square plan with round corners, local distortions necessarily occur in the regions of transition and the possibility of another mode of failure arises which may bring into play another property of the material. But while the simple drawing and stretching problem is still unsolved little purpose would be served by pursuing this more complex effect."

In the first paragraph, he pointed out that the comparison of two materials in any particular press operation must depend on the relative severity of the impressed stretching and drawing. This emphasises the importance of the analysis of a forming process and the quantitative distinction between stretching and drawing in the forming process.

Continued.....

In the second paragraph, he mentioned that local distortions necessarily occur in the regions of transition in a pressing of square plan with round corners. This is true and can be easily observed as will be shown in Chapter 12.

In addition, he also mentioned that local distortions might give rise to another mode of failure. It is reasonable to assume that the other mode of failure is the failure under non-coaxial deformation. This mode of failure will be shown in Chapter 10 as fracture without excessive thinning.

In order to extend and generalise the definition of drawability and the test to cover non-circular cup drawings, it is necessary to re-examine the Swift test first.

#### 8.1 Arbitrary Elements in the Swift Test.

In the Swift test of which the forming operation is shown in fig.8-1, the extent of drawing is measured by the drawing ratio, namely, the ratio between the blank diameter and the punch diameter in the fully drawn cup. The drawability, defined as the largest extent of drawing without failure, is measured by the limiting drawing ratio which is the largest drawing ratio.

There are four arbitrary elements in the Swift test and it is significant and necessary to identify them before the definition of drawability based on them can be extended to include non-circular cup drawings.

Continued.....

A. Forming Conditions and Process Parameters.

The forming conditions and process parameters like punch profile radius, die profile radius, lubrication condition and holding pressure are chosen arbitrarily in the standard Swift test. It is known that those parameters have influence on the limiting drawing ratio or the drawability. Thus, strictly speaking, a Swift test result is reliable only for a drawing operation with the forming conditions and process parameters which are the same as those in standard Swift test.

B. The Assumed Boundary.

In the Swift test, <sup>the</sup> drawing ratio in a successfully drawn cup is used to represent the extent of drawing, and "successfully drawn" means the edge of the blank is drawn in, passing the die profile and becomes part of <sup>the</sup> vertical wall of the cup. In other words, the definition of the extent of drawing used in the Swift test, namely, the drawing ratio in a successfully drawn cup, implies a boundary for the cup, and the boundary is a circle between the vertical and the non-vertical parts of the die. The successfully drawn cup is a flangeless cup. There is no theoretical reason why such a boundary should be assumed. Indeed, in practice, a small flange is often required in the product for holding a cover or screw fastenings or further forming. The Swift test result applies, therefore, only to the drawing of flangeless cups, and the maximum

Continued.....

extent of drawing in a flanged cup can differ from that determined in the Swift test.

C. The Assumed Shape and Orientation of A Blank.

In the case of a round cup drawing, it is natural to assume that the blank should be circular and should be located symmetrically with respect to <sup>both the</sup> <sub>A</sub> punch and <sup>the</sup> <sub>A</sub> die. When non-circular cups are to be drawn, however, the largest possible extent of drawing depends on the shape of the blank as well as the orientation of the blank with respect to <sup>the</sup> <sub>A</sub> punch and die, hence the shape and the orientation of the blank are inevitably the arbitrary elements in the definition of drawability. In fact, even in the Swift test, the circular blank is not, theoretically speaking, the correct shape for the largest possible extent of drawing, if earring occurs, as it usually does.

Of the four above mentioned arbitrary elements in the definition of drawability implied in the Swift test, the first, in the forming conditions and process parameters, is readily recognised. The second, the third and the fourth, related to the boundary of the cup, the shape and the orientation of the blank, are less obvious, and are, in fact, unimportant within the limited scope of the Swift test.

It will be shown later in this thesis how these arbitrary elements are involved in the generalised definition of

Continued.....

drawability which is applicable to all shapes of cup drawing.

### 8.2 The Boundary and the Completion of A Drawing Operation.

As mentioned in <sup>the</sup> last section, although in the Swift's test, the boundary is not defined explicitly, it is implied in the definition of the extent of drawing. In the Swift test, "successfully drawn" means all the material is drawn in to form part of the cylindrical wall of the cup, and when the cup is "successfully drawn", it is the completion of the drawing operation. The circle around the cylindrical wall is supposed implicitly to be <sup>the</sup> boundary. If earring is neglected, at the moment of the completion of drawing, the blank edge everywhere reaches the implied boundary at the same time. In non-circular cup drawing, it is possible to set the boundary at the wall of the cup, but the large ears would make the setting impractical. In fact, the boundary should depend on the purpose of the product. Suppose the dotted line in fig.8-2 is the boundary of the product, which is also the closed curve where the drawn cup is to be cropped, the cup then must be reckoned to have been fully drawn when the edge of the blank anywhere first touches the boundary. If the drawing is finished without the blank edge touching the boundary at all, it is a waste of material and a smaller blank could be used for that drawing operation. If the drawing operation is stopped after the blank edge touches and goes into the boundary, then the drawn cup is not the product, but is

Continued.....

scrap. Therefore, the completion of the drawing operation should be when the blank edge anywhere first touches the boundary and to be "successfully drawn" means the drawing operation is completed without failure.

### 8.3 The Extent of Drawing.

The main idea of using <sup>the</sup> drawing ratio in the Swift test as the measure of the extent of drawing has a subtle strength which will be exploited in the following. If, following the term "deep drawing" one chose the depth of a successfully drawn cup as the measure of the extent of drawing, one would have included in that measure stretching of the material and the measure would be a mixture of stretching and drawing of unknown proportion. The drawing ratio, on the other hand, measures only the extent of drawing because it represents the amount of material being drawn in. To explain how the drawing ratio is a measure of draw-in, suppose we consider the diameter of the punch in the Swift test as a conventionalised way of expressing the mean diameter of the cup, and a circular ring with its diameter the same as the mean diameter of the cup, at the level of the point (as Q in fig. 8-1) where the work leaves the die profile is taken as the boundary. Draw-in then is the amount of material that has passed through the boundary and can be measured in various ways, such as an absolute value of so many in.<sup>2</sup> or in some non-dimensional ratio. It will be shown that the drawing ratio is one of the measures of the draw-in in the completed cup. By

Continued.....

definition,

$$\text{Drawing ratio} = \frac{D}{D_0} \quad 8-1$$

where D is the diameter of the blank and D<sub>0</sub> is, for the purpose of the present discussion, the mean diameter of the cup and, also the diameter of the boundary. Draw-in can be adequately measured by the following ratio R (60),

$$R = \frac{(\text{Area of undeformed material drawn in}) + (\text{Area of undeformed material originally inside the boundary})}{(\text{Area of undeformed material originally inside the boundary})} \quad 8-2$$

$$= \left( \frac{D}{D_0} \right)^2 \quad 8-3$$

The simple relation between the drawing ratio and R is obvious. In fact, the use of areas in measuring draw-in, as in Eq 8-2, serves a better purpose than the use of linear dimensions, as in the drawing ratio, because the latter gives a distorted scale of the areas. For instance, it is well known that a relatively small increase in the limiting drawing ratio corresponds to a large increase in the height of the cup. It is also more logical to use an area ratio than to use a length ratio to represent the amount of material being drawn because the amount of

Continued.....

material in sheet metal can be represented by the area in the blank in the undeformed state.

#### 8.4 Generalised Definition of Drawability.

When <sup>the</sup> limiting drawing ratio is used to represent the drawability of sheet metal, it is, in fact, simply a measure of draw-in in the flangeless cylindrical cup drawing, maximised through the right choice of blank size. It is now proposed to specify the generalised test for drawability to cover all shapes of cup drawing.

It is proposed to define draw-in as the natural logarithm of the ratio  $R$  in Eq. 8-2 in conformity with the natural strains used in studying plastic deformations in sheet metal. Thus,

$$\text{Draw-in, } \psi \equiv \ln R \qquad 8-4$$

and  $\psi$  is analogous to a surface strain, like that used in the analysis of stretching in sheet metal forming. The choice of this measure of draw-in in the generalised definition of drawability is necessitated by the fact that the drawing ratio is no longer a feasible quantity in non-circular cups and blanks. Now, the draw-in in any cup drawing can be expressed as  $\psi$  in Eq. 8-4. Take, for example, the square cup drawing operation shown in fig.8-3. At a certain stage of drawing, let the curve a in the blank

Continued.....

(fig. 8-3) be the locus of the particles which occupy the boundary at that stage of drawing, then the amount of draw-in (61) at that stage is

$$\psi_a = \ln \frac{A_{da}}{A_b} \quad 8-5$$

where  $A_{da}$  is the area inside the curve a in the blank and  $A_b$ , the area inside the boundary. If the cup is drawn further and becomes a completed drawn cup then at the completion of drawing, the curve c in the blank (fig. 8-3) is the locus of the particles which reach the boundary, and the amount of draw-in at the completion of drawing,

$$\psi_c = \ln \frac{A_c}{A_b} \quad 8-6$$

where  $A_c$  is the area inside the curve c. In the Swift test, if the boundary is to be modified as that in section 8.3, then,

$$\psi_c = 2 \ln (\text{Drawing Ratio}) \quad 8-7$$

It is generally believed that drawability represents how much a material can "withstand" drawing, or how "well" it draws. For a scientific definition of drawability, the ideas of "withstanding drawing" and "drawing well" have to be translated in more precise terms capable of quantitative expressions. The drawability, therefore, is defined as the

Continued.....

greatest achievable draw-in, or in other words, the maximum achievable  $\psi_c$ . The drawability so defined, need not only be applied to cylindrical cup drawing as shown in Eq. 8-7, but also be applied to any shape of cup drawing. It will be shown later in this thesis, that the drawability of sheet metal is not a purely material property, like ~~the~~ Poisson's ratio or <sup>the</sup> tensile yield stress but is the performance of the material under the composite influence of a set of forming conditions in a forming process. Therefore it is dependent on the forming conditions as well as the geometry of the forming process.

In the last section, the definition of drawability, based on the idea of the Swift test, is generalised to cover non-circular cup drawings, and it was said that stretching is always associated with drawing in a deep drawing process. However, ~~the~~ drawability has been defined so as to exclude the stretching in the drawing process. It is desirable and necessary to distinguish between drawing and stretching quantitatively because the performance of a material in a drawing process depends on the relative severity of drawing and stretching in that process.

In order to make the distinction between drawing and stretching, a square cup drawing as shown in fig. 8-3 is taken as an example. A flat blank is held between the die and the pressure plate and a punch pushes it through the die to form a cup. As the drawing operation progresses,

Continued.....

some material near the centre of the blank is stretched by the punch so that it becomes thinner. At the same time the material still held between the die and the pressure plate, called the flange, moves generally inwards and part of it becomes the vertical walls of the cup. As the flange moves inwards, the material in it is generally compressed in the circumferential direction and part of such material becomes thereby thicker than the blank.

To illustrate the difference between stretching and drawing, let the following somewhat hypothetical processes be assumed to take place. First, let it be assumed that the surfaces of both the die and the pressure plate are so rough, and the blank is held so firmly between them that no movement of the material occurs in the flange. In such a process the material is pushed through the die purely by stretching. The stretchability of sheet metal is usually measured by the strain at the thinnest section where fracture eventually occurs.

Now, suppose that there is a different process in which the material in the flange moves inwards, or is drawn in freely to form the walls of the cup, and that the relative amounts of stretching and draw-in in the cup are such that it has the same average thickness as the blank. In such a cup it can be said that there is no overall stretching and that the flat blank is formed into a cup purely by drawing. The drawability is measured as defined in <sup>the</sup> last

Continued.....

section. In actual drawing operations both drawing and stretching occur. The drawability is a measure of how much the material <sup>is</sup> being drawn in, but the practical engineer is usually interested in knowing how deep the cup can be drawn. In fact, the greatest achievable depth depends not only on the amount of drawing, but also on that of stretching. It is only correct, to avoid confusion, to define and measure the amounts of drawing and stretching separately because a material less drawable but more stretchable than another may well be capable of being formed into a deeper cup.

It is easy to see that the amount of stretching in the material varies from one point to another in the cup and is related to the local thickness, because the area of any vanishingly small part of the blank can be increased only at the expense of the thickness. The total amount of stretching (62) in the cup is therefore related to the average thickness taken over the whole cup. The amount of stretching is defined as follows:

$$\begin{aligned} \text{Amount of stretching, } \varphi_a &= \ln \frac{\text{Surface area of the cup inside the boundary}}{\text{Area of the blank inside curve } \underline{a}} \\ &= \ln \frac{A_{sa}}{A_{aa}} \end{aligned} \quad \begin{array}{l} \text{8-6} \\ \text{8-7} \end{array}$$

where  $A_{sa}$  is the surface area of the cup inside the boundary and  $A_{aa}$  is the area of blank inside curve a as described in <sup>the</sup> last section.

Continued.....

Obviously, the amount of stretching is also equal to the natural logarithm of the ratio between the average thickness of the cup and <sup>the</sup> thickness of the blank. At least theoretically, it is possible for the cup to have <sup>an</sup> average thickness larger than the blank thickness and for the amount of stretching to be negative. The area  $A_{sa}$  in Eq. 8-7 is, strictly speaking, that of a geometrical surface midway between the outer and inner surfaces of the cup but, for practical purposes, it is usually adequate to use the outer surface of the cup instead.

The amount of draw-in defined in Eq. 8-5 is rewritten here for the convenience of discussion,

$$\text{Amount of draw-in, } \psi_a = \ln \frac{A_{da}}{A_b} \quad 8-5$$

Then,

$$\begin{aligned} \psi_a + \varphi_a &= \ln \frac{A_{da}}{A_b} + \ln \frac{A_{sa}}{A_{da}} \\ &= \ln \frac{A_{sa}}{A_b} \quad 8-8 \end{aligned}$$

Eq. 8-8 represents the overall surface area increase inside the boundary. Before the drawing operation, the area inside the boundary is  $A_b$  and at certain stages of drawing, the surface area inside the boundary would be  $A_{sa}$ , and this increase is partly due to the draw-in  $\psi_a$  and partly due to the stretching, both of which produce increase in area inside the boundary. The amount of draw-in and

Continued.....

the amount of stretching in a drawing process can be represented quantitatively in percentage of the overall surface area increase as  $\left[ \psi / (\psi + \varphi) \right] \times 100\%$  and  $\left[ \varphi / (\psi + \varphi) \right] \times 100\%$ .

With the generalised definition of drawability, it is possible to compare the performance of a material in different forming processes and to investigate the "more complex effect" as in non-circular cup drawing. Because the failure of material in a deep drawing<sup>process</sup> normally occurs at the stretching region and the stretching and the drawing actions are interrelated, it is possible, with the quantitative distinction between stretching and drawing, to have a better understanding of the behaviour of the material in a forming process so as to improve the performance of the material.

Continued.....

CHAPTER 9

EXPERIMENTAL TECHNIQUE

9.1 Experimental Equipment (Experimental Technique)

A. Test Machines

(1) Denison Testing Machine

Capacity : 50 tons

Model : T42/B4

(2) Hounsfield Tensometer.

(3) Hille 20/40 ton Universal Sheet Metal Testing Machine.

The Hille 20/40 ton Universal Sheet Metal Testing Machine designed for sheet metal research workers, is a hydraulic press incorporated with an electronic X - Y recorder so that the punch load and punch penetration during a pressing operation can be recorded. The die, the pressure plate and the punch are all changeable, therefore, with a square die and punch, a square cup can be drawn in this machine.

Performance Data :

Maximum depth of draw 5in. (127.0 mm)

Maximum blank diameter 6.5 in. (165.1 mm)

Maximum drawing load 20/40 ton (199.28/398.56 KN)

Clamping load ranges :

Low pressure : 800 - 5000 lb (3.56 - 22.24 KN)

High pressure : 2000 - 25000 lb (8.89 - 111.20 KN)

Drawing speed : infinitely variable up to

approximately 15.7 in./min. (398.78 mm/min.)

Continued.....

- (4) Hordern, Mason & Edward O.P. 55, Geared Single Action, Open Front Inclinable Power Press.

This machine is used for the blanking of circular blanks.

B. Forming Tools.

- (1) Punches.

Circular punch :

diameter 1.968 in. (50 mm)

profile radius 0.394 in. (10 mm)

Square punch :

the dimension is shown in fig.9-1.

- (2) Dies.

Circular die :

die hole diameter 2.156 in. (54.76 mm)

die profile radius 0.788 in. (20 mm)

Square die :

as shown in fig.9-1.

C. Measuring Machines

Societe Genevoise Universal Measuring Machine, model MU 214B is used for measuring the deformed grids and for scribing linear lines. The smallest unit of measuring is 0.00001 inch and a cutter could be put on the machine so that very high accuracy of parallel<sup>scribed</sup> lines could be achieved on the specimen.

Continued.....

In addition to the Universal Measuring Machine, a travelling microscope and a planimeter are also used for measuring grids and areas.

## 9.2 Data on Work Material.

The material used in this project is the "Deep Drawing Quality" mild steel sheet (B.S.S. 1449, Part I, 1972, CR3) with its chemical composition as follows:

C	0.10% max.
Mn	0.50% max.
S	0.040% max.
P	0.040% max.

The thickness of the sheet is 0.048" (1.22 mm) and the R-value is 1.028.

## 9.3 Experimental Technique

### A. Preparation of Specimens

#### (1) Specimens for non-coaxial deformation test:

Specimens are cut to a coupon form of dimension  $3\frac{1}{4}$ " x  $\frac{3}{4}$ " (82.55 x 19.05 mm) first. The edges of the coupon are well filed. Then the coupons are milled to be as shown in fig.9-2 in different values of  $\xi$  and different width (d) between the cuts.

Continued.....

The area between the cuts, ( $P_1, P_2, Q_1, Q_2$  in fig.9-2) called the effective region, is covered with square grids scribed in the Universal Measuring Machine.

(2) Specimens for zigzag strain path test:

The preparation is divided into two steps. In the first one, the specimen is cut into coupon form with dimensions  $5" \times 2\frac{1}{2}"$  ( $127 \times 63.5\text{mm}$ ) as shown in fig.9-3. The edges of the coupon are well filed and square grids are scribed in the Universal Measuring Machine at the central position of the coupon. The second step is that, after the specimen is pulled in <sup>the</sup> Denison Testing Machine under a certain load, small coupon pieces as shown in fig 9-3 are milled out from the central portion of the deformed specimens at different angles  $\alpha$  (fig.9-3).

(3) Specimens for deep drawing:

Circular blanks are blanked out in the Hordern, Mason & Edward O.P.55, geared, single action, open front inclinable power press and then turned in a lathe to the required sizes of  $4\frac{3}{4}"$ ,  $4\frac{7}{8}"$ ,  $5"$ ,  $5\frac{1}{8}"$ ,  $5\frac{1}{4}"$ ,  $5\frac{3}{8}"$  and  $5\frac{1}{2}"$  ( $120.65\text{mm}$ ,  $123.82\text{mm}$ ,  $127.0\text{mm}$ ,  $130.17\text{mm}$ ,  $133.35\text{mm}$ ,  $136.52\text{mm}$  and  $139.70\text{mm}$ ) in diameter.

Square and octagonal shape of blanks are cut by a guillotine and the edges are well filed.

Continued.....

Orthogonal parallel lines are scribed over one-eighth or one quarter of the blank for later measurement.

B. Line Scribing

In order to scribe square grids with high accuracy, the Universal Measuring Machine is used to scribe the line. By putting a weight onto the cutter, a uniform line of 0.0012" (0.03 mm) in width can be scribed on the specimen. The specimen is clamped on the turning table in the Universal Measuring Machine and parallel lines with spacing 0.025" (0.635mm) are scribed. Then the table is turned through 90°, and an orthogonal set of parallel lines is obtained.

C. Reprinting of Deformed Grids

Grids are scribed on the surface of the specimens. In the experiments, the forming operation is stopped at several stages and the deformed grids are reprinted by a special technique (51). Colour pencils are used to scratch over the grids and then the surface is wiped clean so that the colour particles are left only in the scribed lines. A strip of clean transparent adhesive tape is used to cover the grids on the specimen so that the colour particles stick to the tape. Then the tape is taken from the specimen and put on a flat surface for measuring.

With some care, the stretching of the tape when the tape is taken from the specimen could be avoided. The stretch-

Continued.....

ing is so small that under a travelling microscope reading to 0.0001", no change could be observed. This reprinting technique makes it possible to record the deformation of a small piece of material in which the deformation is uniform. Also, by using this reprinting technique, the metal flow in a forming process can be traced.

#### 9.4 Experimental Procedure.

##### A. Non-coaxial Strain Path.

Specimens with different inclined angle of cuts and different distances between the cuts are tested in the preliminary test (will be discussed in next Chapter), to find the suitable inclination of the cut and the suitable distance between the cuts.

The specimen is clamped in the tensometer and pulled by the manual operation wheel so that the forming speed is low enough to observe the occurrence of necking. Because the stressing in the effective region is very complicated and is outside the scope of this project, the load to pull the specimen is taken only for reference but <sup>is</sup> not recorded on the drum.

The scribed grids are reprinted at several stages. The deformed grid at every stage of the point where necking,

Continued.....

and final, fracture occurs can be traced, measured and calculated. From this the three principal strains and the magnitude of non-coaxiality are obtained and <sup>the</sup> non-coaxial strain path can be plotted.

B. Non-coaxial Zigzag Strain Path

Square grids are scribed at the central part of the specimen ( $2\frac{1}{2}$ " x 5") which is shown in fig.9-3 with the grid lines aligned to the edges of the specimen. Then the specimen is pulled in <sup>the</sup> Denison testing machine to a certain strain under <sup>a</sup>certain load. Four other specimens were pulled by repeating the above procedure. The deformed grids are reprinted. The strain at the central part of the specimen is checked to ensure that the deformation at that part is uniform and the amount of strain at each specimen is exactly the same.

Then the specimens are cut and machined to the shape shown in fig.9-3 (small piece) with <sup>a</sup>different angle to the direction of loading in the first pulling.

The small specimen is pulled again in a tensometer and the grids are reprinted at several stages during the pulling. This procedure is repeated in the other small specimens. The strain path under which the material fails is obtained from the deformed grids.

Continued.....

C. Deep Drawing Tests

(1) Cylindrical cup drawing:

Different sizes of circular blanks on which two diameters along and perpendicular to the rolling direction are scribed, are drawn by a circular punch in the Hille Machine. The blank is centred by means of three centering fingers. A polyvinyl chloride (P.V.C) sheet of 0.004" (0.10mm) thick is used as lubricant between the blank and the die. The holding pressure is set at 2500 lb (11.12 KN) for all drawing operations. Punch load against punch penetration is recorded by the X-Y recorder.

The drawing operation is stopped at several stages and at each stage, the edge of the unfinished cup is traced with marks for the position of the two perpendicular diameters. By joining the marks and taking the average of these two current diameters, the movement of blank edge at each stage is obtained.

(2) Square cup drawing:

(a) Alignment of punch, holding plate and die,

Although the square punch, die and holding plate were made so that they would be allocated automatically at the central position in the Hille machine, the relative positions among the punch, die and holding plate still have to be aligned due to the <sup>lack of</sup> axisymmetry of a square.

Continued.....

- (a) two perpendicular lines passing <sup>through</sup> the centre of the punch cross-section and parallel to the sides of the cross section are drawn on the punch head.
  
- (b) two tiny copper wires perpendicular to each other, passing through the centre of the die and parallel with the sides of the die hole, are hung and stuck on the die face by covering a strip of adhesive tape. (fig.9-4a)
  
- (c) the same procedure as (b) is repeated on the holding plate (fig.9-4a).
  
- (d) the punch is screwed into the position in the Hille Machine. The orientation is decided by screwing down the punch to the limit so that the screws could not be further tightened and the punch is fixed in the machine.
  
- (e) holding plate and die are put in the Hille Machine. The alignment is done by aligning the strings on the holding plate, the die face and the lines on the punch head together.

Continued.....

(f) marks are put on the holding plate and the site of the holding plate in correspondence to each other and on the die and the die holder as well, so that the positions of the die and the holding plate can always be checked (fig.9-4b).

(g) the copper wires on the holding plate and the die face are removed and four tiny lines are scribed on the holding plate for blank location (fig.9-4b).

(3) Location of Blank:

Four equally spaced lines passing <sup>through</sup> the centre of the blank are scribed on the blank. By aligning these four lines with those on the holding plate, the blank is located centrally with respect to the die (fig.9-4b).

(4) Forming procedures:

(a) the grids on the blank are reprinted so that the material particles which reach the boundary in the drawing operation can be traced back to the stage zero of the drawing operation.

Continued.....

- (b) the blank is drawn in the Hille Machine by the square punch and die and the machine is stopped at <sup>a</sup>certain punch penetration as stage 1 of the drawing operation.
- (c) by mounting a ring (fig.9-5) which specifies the boundary on the work piece, the boundary is drawn on the surface of the workpiece, and then the grids near and outside the boundary are reprinted so that the particles which occupy the boundary at stage 1 of the drawing operation are recorded.
- (d) the drawing operation is continued and the procedures (b) and (c) are repeated for the stage 2, 3, ..... until the edge of the flange touches the boundary. This is the completion of the drawing operation.

(5) Measurement of draw-in:

From the reprinted grids at every stage of the drawing operation, the points which occupy the boundary can be traced back to the original positions at stage zero of the drawing operation. In other words, the points on the blank before the drawing operation, which would reach the boundary at different stages of the drawing operation

Continued.....

could be traced. As shown in fig.9-6, the curve marked by a number, say 2, is the locus of the points which will reach the boundary at stage 2 of the drawing operation.

The amount of draw-in at certain stages of the drawing operation is obtained by Eq. 8-5, namely,

$$\text{Draw-in, } \psi_i = \ln \frac{\text{the area inside the closed curve } i \text{ (fig.9-6)}}{\text{the area inside the boundary}}$$

The maximum draw-in of the drawing operation is obtained at the completion of the drawing operation, so

$$\text{Max. Draw-in, } \psi_c = \frac{\text{the area inside the curve 4 (fig.9-6)}}{\text{the area inside the boundary}}$$

#### D. Determination of the End Point.

Many sheet metal research scientists have experienced the difficulty of determining the end point of the forming process. This difficulty is due to the lack of a precise definition of plastic instability in sheet metal.

In this project the determination of the end point is not so difficult as in other investigations. There are two kinds of end point determination due to different types of forming. The first one is the determination of the end point in the non-coaxial and the non-coaxial zigzag strain path experiments. Because the experiments are similar to the tension test, the determination of <sup>the</sup> end point can be referred to that in the non-coaxial strain

Continued.....

path experiment, <sup>where</sup> the deformation concentrates in the effective region and is not so uniform as that in the tension test. However, because the progress of forming is recorded by the reprinted grids at that region in a very small forming interval, the grids just before the occurrence of fracture is taken as the end point of the forming process.

The second one is the determination of <sup>the</sup> end point in the cup drawing tests. Because the measurement in this experiment is the amount of draw-in or the movement of the flange, as soon as the onset of plastic instability occurs, draw-in or the movement of the flange stops. By the observation of necking in the punch profile region or the sudden drop of punch load in the X-Y recorder, the end point of the drawing operation can be judged well enough in an unsuccessful draw. For successful drawing, when the flange edge is near the boundary, the interval between stages of the drawing operation is set so small, ~~such that~~ that the completion of the drawing operation can be located.

Continued.....

CHAPTER 10

NON-COAXIAL AND NON-COAXIAL  
ZIGZAG STRAIN PATHS

Non-coaxial and Non-coaxial Zigzag Strain Paths.

As has been briefly mentioned before, most of the sheet metal tests in current use are axisymmetrical forming operations in which only coaxial strain paths are involved. It is easy to see <sup>that</sup> most of the sheet metal products are not axisymmetrical and sheet metal products are often not manufactured in one forming operation. Lack of axisymmetry of the product will obviously induce non-coaxial deformations. In multiple manufacturing operations, unless they are all axisymmetrical and well aligned in all forming operations, non-coaxial and non-coaxial zigzag strain paths are bound to be involved. Again, even in nominally axisymmetrical forming operations, the strains are non-coaxial owing to earing. Therefore, for the better understanding of material behaviour under forming, it is not only significant but also necessary to test sheet metal under non-coaxial conditions.

In the workshop it is difficult to avoid non-coaxial strains, but in the laboratory it is difficult to obtain the desired non-coaxial strain paths. The reason for the experimental difficulty is easy to see. The experimental strain paths must be such as to lead to necking and fracture. In one set of unsymmetrical die and punch, one such path may be obtainable at the critical section. For another non-coaxial strain path, either the punch or the die or both have to be changed. Even where a different strain path is obtained in this way, it is difficult to

Continued.....

control it, so that, for instance, a whole set of punch and die could be prepared only to find that the strain path at the critical section is nearly the same as that of the last set. Therefore, to obtain significant experimental results on the non-coaxial strain paths in actual forming operation, a very large investment in both expenses and experimental time is required, which lies outside the scope of this Ph.D, project. It is doubtful if such research expenses are justifiable unless they are directly related to large scale manufacture, like the car industry.

In this project, a more manageable and workable experimental technique is chosen, namely that of tension test specimens in coupon form, (as shown in fig.9-2 and fig. 9-3). In this technique, the variables can be controlled adequately, as will be shown later.

The experimental results obtained in this manner—the first results on non-coaxial strain paths in the field of sheet metal forming research—provide the theoretical and experimental techniques with which research and development work on specific problems can be tackled, as well as some significant results of general validity. The objection may, of course, be raised that these are not the non-coaxial strain paths in actual forming operations, but, as explained in the preceding paragraphs, the cost of the dies and punches alone makes such pursuit of realism impracticable.

Continued.....

### 10.1 Preliminary Tests.

In order to pursue non-coaxial strain paths, the specimens in coupon form with inclined cuts at the edges (fig.9-2) are tested. Preliminary tests are done for finding the suitable inclination of the cut and the width between the cuts. As shown in fig.9-2, the area between the cuts,  $(P_1, P_2, Q_1, Q_2)$  is called the effective region where the deformation occurs when the specimen is tested. The inclination of the cut is represented by an angle  $\xi$  (fig.9-2) which is the angle between the cut and the transverse direction of the coupon form. The width between the cuts is represented by  $d$  (fig.9-2).

The preliminary tests show that when  $\xi$  is very large, the deformation is localised at  $P_2$  and  $Q_2$  (fig.9-2), and then two necks or even tearing will occur. When  $\xi$  is very small, the non-coaxiality of principal axes of strain of the deformation in the specimen is too small to be detected within the accuracy of measurement, and the deformation in the effective region is localised at the line connecting the ends of the cuts so that the strain can not be accurately measured due to <sup>the</sup> insufficiently fine grid used. If <sup>a</sup> finer grid is used, the deformation inside the grid will be more uniform than that in the larger grid. But because the strain is obtained by measuring the deformed grid and the accuracy of the measuring machine which is a fixed absolute value, the finer the grid is, the larger the percentage of error due to <sup>the</sup> smaller gauge length. A finer grid is not

Continued.....

helpful unless a <sup>measuring machine of</sup> higher accuracy ~~measuring machine~~ is provided. When  $d$  is very small, the effective region ( $P_1, P_2, Q_1, Q_2$  in fig.9-2) is turned rigidly with bending along the sheet surface at the corners soon after the test is started. Necking and fracture take place <sup>afterwards</sup> as those in <sup>the</sup> coaxial case afterwards. Fig.10-1 shows the different regions.

Only those specimens are tested in which the inclination of cut and the width between the cuts are not too small to produce detectable non-coaxiality of principal axes of strain and not so large as to produce tearing.

The inclinations and widths between the cuts together with the labelling of the specimens to be tested are listed in the following table.

labelling	A1	A2	A3	A4	A5	B1	B2	B3	B4
$\xi$ (degree)	0	20	25	30	45	0	20	25	30
$d$ (in.)	0.125	0.125	0.125	0.125	0.125	0.150	0.150	0.150	0.150

10.2 Non-coaxial Strain Paths.

The strain paths of the material in the specimens being tested are plotted in a three-dimensional triangular co-ordinates in fig.10-2. The coloured curves, except the one covering the points  $B_2', B_3'$  and  $B_4'$ , are the strain paths of the material in the specimens B1, B2, B3 and B4. The

Continued.....

strain path  $OB_1$  is coaxial, because the specimen B1 has cuts perpendicular to the edge<sup>and</sup><sub>A</sub> therefore the material in the effective region is deformed under a coaxial strain path. It is coaxial, so it lies on the clock diagram in ~~the~~ triangular co-ordinates. The other three curves  $OB_2$ ,  $OB_3$  and  $OB_4$  are non-coaxial <sup>therefore</sup> and are<sub>A</sub> space curves in ~~the~~ 3-D triangular co-ordinates. The projection of the non-coaxial strain paths  $OB_2$ ,  $OB_3$  and  $OB_4$  on the clock diagram, called projected strain paths, are also shown as  $OB_2'$ ,  $OB_3'$  and  $OB_4'$  in fig.10-2. The vertical distance from the projected strain path to the spaced non-coaxial strain path represents the magnitude of non-coaxiality of <sup>the</sup><sub>A</sub> principal axes of strain with respect to the material.

The magnitude of non-coaxiality at a certain state of strain is defined as the angle between the fibres which lie along the direction parallel to the principal axis of the major strain at the beginning of the deformation, and the fibre which will lie along the direction parallel to the principal axis of the major strain at the <sup>current</sup><sub>A</sub> state of strain. The angle<sup>is</sup><sub>A</sub> measured ~~so~~ in the material in the undeformed state. But practically it is rather difficult to determine it accurately because it is difficult to find the exact fibre which lies along the direction parallel to the principal axis of the major strain at the beginning of the deformation. This difficulty is due to the inaccuracy of measurement at very small ~~amounts of~~

Continued.....

strains. If a higher accuracy or more powerful measuring machine and technique is provided, this difficulty could be overcome. In this project, the magnitude of the non-coaxiality is determined by using the state of strain when the major principal strain is around 0.2 as an equivalence of that at the beginning of the deformation. Therefore, the space curves of non-coaxial strain paths in fig.10-2 and fig.10-3 leave the clock diagram into the space at the state of strain when  $\epsilon_1$  is around 0.2.

In fig.10-3 the strain paths of the material in specimens A1, A2, A3, A4 and A5 are shown. The strain paths except the non-coaxial one OA<sub>5</sub> in fig.10-3 are similar to those in fig.10-2. The projected strain path of OA<sub>5</sub> is shown and the characteristic of the strain path is between 3 and 4 o'clock in the clock diagram. The strain path reaches its end point at<sup>a</sup> very small thickness strain (-0.17), which is rarely seen in sheet metal forming. But it is not difficult to visualise the failure of material in this case, say, a failure due to simple shear or twist at the cross-section of the sheet could happen even without any thickness strain. This type of failure may be reckoned as fracture without excessive thinning and it, in fact, is the case which Professor Swift pointed out thirty five years ago,

"local distortions necessarily occur in the

Continued.....

regions of transition and the possibility of another mode of failure arises which may bring into play another property of the material." (22)

The local distortion is a shearing or twisting as will be discussed in Chapter 12, and the material is obviously deformed under a non-coaxial strain path. Professor Swift might well have observed the type of failure due to this local distortion when he mentioned another "mode of failure".

This is the first time the non-coaxial strain path *has been* investigated and represented graphically. It is found that although the strain path ends at the region between 4 and 5 o'clock on the clock diagram, the early part of the strain path is mostly in the region between 3 and 4 o'clock. The downward shifting of the strain path is obviously due to local thinning. If the thickness strain at <sup>an</sup> early stage of the deformation is small (like A5 in fig.10-3), the material will fail without local thinning.

### 10.3 Forming Limit Curve.

In the coaxial case, the forming limiting curve such as Lee and Hsu's curve, is the forming limit of the material under coaxial deformation. In a non-axisymmetrical forming process, the material somewhere or even everywhere in the workpiece is bound to be deformed under non-coaxial strain paths. It is possible that fracture occurs at the

Continued.....

a place where the material is deformed under a non-coaxial strain path, especially in a cup of irregular shape and in forming processes with several stages of re-drawing. Then like the forming limits in <sup>the</sup> coaxial case, there should be forming limits for the material under non-coaxial deformation.

A curve passing the end points ( $B_2'$ ,  $B_3'$  and  $B_4'$ ) of the projected strain paths in fig.10-2 is drawn. This curve represents part of the forming limits of the material under non-coaxial strain paths and this is only to illustrate that <sup>a</sup> forming limiting curve of sheet metal under non-coaxial strain paths like that under coaxial strain paths can be pursued. The forming limiting curve of material under non-coaxial deformation can be pursued on several bases, for example, on the same degree of non-coaxiality, where a series of forming limiting curves of different degree of non-coaxiality including the one under coaxial deformation (zero degree of non-coaxiality) can be drawn on the clock diagram in a triangular co-ordinate. In fact, instead of the series of forming limiting curves on the clock diagram, a formability surface covering all the end points of strain paths including coaxial and non-coaxial ones in a 3-D triangular co-ordinates is the complete forming limit of a material.

#### 10.4 Non-coaxial Zigzag Strain Paths.

The zigzag strain path discussed in this thesis is a strain

Continued.....

path zigzagged due to non-coaxiality of the principal axes of stress with respect to the material instead of changing of the stress ratio in the deformation. The strain paths shown in fig.10-4 are those of material deformed under the stressing with the same stress ratio but different directions of principal axes of stress with respect to the material.

As described in <sup>the</sup> last Chapter, specimens of the same size  $2\frac{1}{2}$ " x 5" (as shown in fig.9-3) are deformed under the same load so that the material at the central part in every specimen is deformed to the same state of strain under the same strain path. The strain path is shown as OC on the clock diagram in 3-D triangular co-ordinates in fig.10-4 and it is coaxial. Then the deformed specimens are cut into the small specimens from the central part of the specimens with different angles  $\alpha$  (fig.9-3). The state of strain of the material in each small specimen is the same, ~~as one specimen~~, but the angle between the axis of the major strain with respect to the material and the axis the small specimen is going to be stressed, namely, the angle  $\alpha$ , is different, ~~from one specimen~~. After the small specimens are cut from the deformed specimens, the angle  $\alpha$  in each small specimen is measured and the small specimens are labelled as in the following table:

Specimen	C1	C2	C3	C4	C5
$\alpha$	$0^\circ$	$30.3^\circ$	$46.9^\circ$	$60.8^\circ$	$90^\circ$

Continued.....

Then the small specimens are tested again in a tensometer. Because the small specimens are of the same material at the same degree of work-hardening and of the same shape and size, if the material is assumed to be isotropic all the time through the deformation, the stress-strain relation under ~~the~~ testing in <sup>the</sup> tensometer would be the same in every small specimen. But the strain paths plotted in fig.10-4 turn out very differently from one another, not only in the degree of non-coaxiality of <sup>the</sup> principal axes of strain with respect to the material, but also in the strain ratio. Coloured curves in fig.10-4 except the red one are the strain paths, OC is the coaxial strain path representing the deformation in the large specimens and, OCo' and CoC<sub>1</sub>, CC<sub>2</sub>, CC<sub>3</sub>, CC<sub>4</sub> and CC<sub>5</sub> are those of the deformation in the small specimens C1, C2, C3, C4 and C5, respectively. The small specimen C1 is cut from the large deformed specimen in such a way that the axis of <sup>the</sup> major principal strain is perpendicular to the direction of loading in the small specimen. At the early stage of testing in the small specimen, the major principal strain is decreasing and the minor is increasing. But the principal axes of strain remain unchanged with respect to the material. Therefore the strain path is coaxial. When the strain path reaches Co' where the major and minor principal strains are equal, suddenly the axis of minor principal strain becomes that of major principal strain and the axis of major principal strain becomes that of minor principal strain. This is

Continued.....

explained as a sudden  $90^\circ$  rotation of the principal axes of strain with respect to the material. The strain path in this case is represented in 3-D triangular co-ordinates by discontinuous curves  $CC_0'$  and  $CC_1$ , with a  $90^\circ$  of non-coaxiality.

The curves  $CC_2$ ,  $CC_3$  and  $CC_4$  are strain paths with different amounts of non-coaxiality of principal strains with respect to the material, which is due to different amount of non-coaxiality of the axes of principal stress.  $CC_5$  is coaxial because the small specimen C5 is cut such that the axis of major principal strain is along the direction of loading in the small specimen.

A curve passing the end points of the projected strain paths on the clock diagram is drawn. It represents the formability of sheet metal under non-coaxial zigzag strain paths. Like that under coaxial zigzag strain paths, the formability curve depends on the amount of prestrain. Those non-coaxial zigzag strain paths shown in fig.10-4 are due to the same type of failure, namely, excessive thinning leading to fracture, therefore, the formability curve is nearly a curve of constant thickness strain.

It is clearly shown that the strain path may be zigzagged without changing the stress ratio. If the non-coaxiality of the principal axes of strain is neglected, a zigzag

Continued.....

strain path would lead to the wrong conclusion that the stress ratio changes in the forming operation. In non-axisymmetrical forming processes, especially forming processes involving irregular shapes and multiple-stage forming operations, it is very likely that the material at the critical section is deformed under a non-coaxial strain path or a non-coaxial zigzag strain path. As most of the sheet metal products are non-axisymmetrical, it is significant and necessary to examine the strain path under which the material at the critical section is deformed. Even in those axisymmetrical ones, earing will bring the involvement of non-coaxial deformation to the material in the workpiece. Therefore, for a strict investigation of material behaviour in a forming process, the coaxiality of the principal axes of strain should always be examined.

Continued.....

CHAPTER 11

DRAWABILITY - A GENERALISED DEFINITION

### Drawability - A Generalised Definition.

In Chapter 8, the Swift test *was* re-examined and the drawability, originally defined as the largest drawing ratio, was generalised to be the largest draw-in at the completion of the drawing operation. By the generalised definition of drawability, the amount of draw-in in a forming process is to be maximised. The factors which affect the drawability of sheet metal in a forming process will be investigated and illustrated with experimental results in this Chapter.

#### 11.1 Process Parameters and Forming Conditions.

In a cup drawing operation, the process parameters are partly dictated by the requirements of the finished product and partly chosen for the ease of the operation. Thus, the shape of the cup and the punch and <sup>the</sup> die profiles are usually dictated by the purpose to which the product is put. The forming conditions such as holding load and lubrication condition are chosen to avoid both excessive friction and the tendency to wrinkling. It is understood in any drawability test that, within the limits of the required shape of the product, the process parameters and forming conditions are roughly those conducive to the maximum extent of drawing. In other words, it is understood that in the drawability test the process parameters and forming conditions are nearly optimized. They are optimized because they should be nearly those used in manufacturing practice where the drawing operations are

Continued.....

made as easy as they can possibly be; and they are only nearly optimized because the optimum conditions vary from one work material to another. The Swift test fulfils these optimum conditions but is limited to circular cup drawing. It fails to measure the drawability or the performance of sheet metal in a non-circular cup drawing operation. Now the definition of drawability is generalised, therefore, it should be possible to measure the drawability in any shape of cup drawing. In a non-circular cup drawing operation, the process parameters and the forming conditions such as holding load and lubrication conditions shall be optimized as they are in the Swift test.

Apart from those factors mentioned above, there are some other factors which affect the drawability, such as the blank shape and the blank orientations with respect to the rolling direction and with respect to the punch and die. But before they are investigated, one significant factor, namely, the boundary of the product, should be discussed first.

#### 11.2 Boundary and Blank.

The cup drawn in the Swift test is confined to not only a circular one but a flangeless circular cup. The implied boundary of the product is the closed curve around the vertical cylindrical wall of the cup. As stated before, many cup drawing products are not flangeless, in other words, the boundary of the product is not set like that

Continued.....

in the Swift test. Therefore, for better service of the test result, the position of the boundary should be taken into account in the test, and, whether and how the position of the boundary affects the drawability should be investigated.

The importance of the position of the boundary in the definition of drawability can be illustrated by considering the variation of the drawing force in the Swift test. The drawing operation in that ~~Swift~~ test is shown in fig. 8-1. The drawing force is plotted against the current position of the edge of the flange in fig. 11-1. The strength of the cup is based on the maximum drawing force of curve b, because a larger diameter of blank can not be successfully drawn. In fact, the strength of the cup is dependent on the strength of the material near the punch profile (point P in fig. 8-1) and is nearly constant with respect to the blank size (29). When the maximum drawing force in the drawing operation is equal to or lower than the strength of the cup, the drawing operation can proceed till a flangeless cup is formed (curves a and b). If the drawing force reaches and then exceeds the strength of the cup, the material near the punch profile (point P in fig. 8-1) breaks and the drawing operation can not go further.

For every particular drawing operation, there is a critical size of blank (represented by the radius OB in fig. 11-1) for which the maximum drawing force is equal to ~~the~~

Continued.....

the strength of the cup. Such a blank is called <sup>the</sup>critical-sized blank; a blank which is larger than the critical-sized blank is called supercritical-sized blank and one that is smaller is called subcritical-sized blank.

If a boundary is set at the position which is reached by the critical-sized blank when the drawing force is at its maximum, then such a boundary (represented by the horizontal distance OK in fig.11-1) is called the critical-sized boundary. Similarly, a boundary which is larger than the critical-sized boundary is called supercritical-sized boundary and that which is smaller is called subcritical-sized boundary.

In order to find the drawability of the material in circular cup drawing, the amount of draw-in should be maximised. For choosing the optimum blank size, two different ranges of the product boundary must be considered, the supercritical-sized ones and the subcritical-sized ones. For a subcritical-sized boundary, say that represented by the point M in fig.11-1, the amount of draw-in at the completion of the drawing operation is maximised by using a critical-sized blank. Then the maximised draw-in can be represented by the horizontal distance between B and M in fig,11-1. If a subcritical-sized blank is used, say, blank A, the amount of draw-in at the completion of

Continued.....

the drawing is represented by the horizontal distance AM in fig.11-1, which is obviously smaller. Suppose a supercritical-sized blank is used, say, blank C. The movement of the blank edge is restricted to the horizontal distance between C and H. If the position of B is marked in blank C, it is easy to see that when C reaches H, the mark B can not reach M or even K, but reaches a point to the right of K. In other words, a point to the left of the mark B in blank C reaches the boundary M. Then the maximum draw-in by using a supercritical-sized blank for a subcritical-sized boundary is less than that obtainable by using a critical-sized blank. For a critical-sized boundary, the arguments are the same as those for the subcritical-sized boundary and the critical-sized blank is the optimum blank to use.

Now consider a supercritical-sized boundary, say, at H in fig.11-1. It is to be shown that the optimum blank is that whose edge touches the boundary when the drawing force just reaches the strength of the cup, as blank C in fig.11-1. In any blank smaller than blank C, the draw-in at the completion of the drawing, as explained before in the subcritical-sized boundary case, would be smaller than that in blank C. Suppose a blank D which is larger than blank C is used and the position of C is marked in the blank D. As blank C is used for a critical-sized or subcritical-sized boundary, a point to the left of C will

Continued.....

reach the boundary when the drawing force reaches the strength of the cup, therefore the amount of draw-in is smaller.

The amount of draw-in at the completion of the drawing operation is plotted against the blank size in fig.11-2 for different size of boundaries. Each curve in fig.11-2 represents a boundary, and a point on the curve represents a blank size and the amount of draw-in at the completion of the drawing operation associated with the boundary. The size of the boundary can be seen from the curve because it is the blank size when the draw-in at the completion of the drawing operation is zero. Curves A and B are for subcritical-sized boundaries, curve C for the critical-sized boundary and curve D is for a supercritical-sized boundary. The point K represents the size of the critical-sized boundary (4.22", 107.19mm diameter). From the curves in fig.11-2, the arguments in the last few paragraphs are clearly shown. For the drawing operations with subcritical-sized or critical-sized boundary, the blank which achieves the largest draw-in at the completion of the drawing operation is 5" (127.0mm) diameter as shown in the curves A, B and C, and it is the critical-sized blank. When a larger blank is used, the draw-in drops as shown in the dotted line. For the drawing operation associated with a supercritical-sized boundary, as shown in the curve D, the blank which achieves the largest draw-in at the completion of the drawing operation is not the critical-sized

Continued.....

blank (5" or 127.0mm diameter) but is a supercritical-sized one ( $5\frac{1}{8}$ " or 130.17mm diameter). When too large a supercritical-size blank (greater than  $5\frac{1}{8}$ " diameter) is used, the draw-in at the completion of the drawing operation drops. The supercritical-sized blank should be that in which the edge touches the boundary when the drawing force is equal to the strength of the cup.

Now a conclusion can be drawn, namely, to achieve the largest draw-in in a drawing process, the critical-sized blank should be used for a boundary smaller than or equal to the critical-sized boundary, and the blank, ~~that~~ the edge of which touches the boundary when the drawing force is equal to the strength of the cup, should be used if the boundary is supercritical-sized.

In fact, the blank having the limiting drawing ratio in the Swift test is the critical-sized blank, and the boundary implied is the smallest possible, yielding the maximum amount of draw-in at the completion of the drawing operation. It can be easily observed in fig.11-2, ~~for~~ a certain size of blank which is critical-sized or subcritical-sized, the smaller the boundary, ~~the~~ the larger the amount of draw-in at the completion of the drawing operation. For instance, in the critical-sized blank (5" or 127.0mm diameter), when the boundary is 3.5" (88.9mm) diameter, the draw-in is 0.713 (curve A) and it is 0.446 when the boundary is 4" (101.6mm)

Continued.....

diameter (curve B), and is only 0.339 when the boundary is set at the critical position (4.22" or 107.19mm diameter, curve C). The Swift test can not measure the drawability or the performance of sheet metal in a non-circular cup drawing. It can not even measure the drawability in a circular cup drawing if the boundary is a supercritical-sized one.

The above arguments apply equally to non-circular cup drawing operation. Fig.11-3 shows the drawing force plotted against the current position of the edge of the flange in a square cup of which the punch and die is shown in fig.9-1. The current position of the edge of the flange refers to the edge on the line OX (the inset of fig.11-3) chosen for convenience because it is on this line that the edge of the flange touches the boundary first. The three solid line curves are taken from the actual pen records of the drawings represented in fig.11-3 by the line TT. The strength of the cup is determined from the maximum drawing force in blank C (fig.11-3). Thus a curve (dotted line) can be extrapolated in which the maximum drawing force just reaches the strength of the cup. The reason that it is extrapolated instead of being taken from the experimental data is that scattering occurs near the critical size for a successful drawing.

Figure 11-3 is labelled in the same way as that in fig.11-1 as far as possible, so that the arguments in the last few

Continued.....

paragraphs can be applied easily to the drawing operation in which a square cup is drawn from a square blank. As for the curves in fig.11-1, in fig.11-3 the point K represents the critical size of the boundary and the point B represents the critical size of square blank. If the boundary is subcritical (to the left of K), the critical-sized blank or a square blank with its side equal to twice OB should be used for achieving the largest draw-in at the completion of the drawing operation. A supercritical-sized blank will bring about premature failure in the cup and a subcritical-sized blank will produce a smaller draw-in than that in the critical-sized blank. If the boundary is supercritical-sized (to the right of K), then the blank should be such that the edge of the flange touches the boundary when the drawing force is just reaching the strength of the cup. These arguments in the cup drawing process are valid in ~~the~~ square cup drawing as much as in ~~the~~ circular cup drawing. A line which is normal to the boundary at the point where the edge of the flange touches the boundary first, can always be found. This line is taken to be the reference for the movement of the edge of the flange. The movement of the point at the edge of the flange which touches the boundary first is not necessarily on the line of reference but can always be projected to it. Therefore, for cup drawing of any shape, a figure like fig.11-1 or fig.11-3 can always be plotted and the arguments about the boundary and the drawability can be

Continued.....

applied to it.

The definition of drawability is generalised to be the largest draw-in at the completion of the drawing operation. For both "draw-in" and "completion of the drawing", a boundary should be defined first. The necessity of defining the boundary is strengthened by the above arguments, especially because when the boundary is super-critical-sized the drawability is different from that when it is subcritical or critical sized. Following the discussion about the effect of the boundary on drawability, the other factors are discussed below.

In circular cup drawing, because the punch and die are circular, it is natural to choose a round blank for the cup drawing because a circle is non-directional. Although the sheet metal is anisotropic there is only one way to cut the round blank, and because the blank, the punch and die are all circular, it is easy to locate the blank with respect to the punch and die. But all this simplicity does not exist in a non-axisymmetrical forming process. If the punch and die are not circular, a round blank is usually not the most suitable blank to use. Then the blank cutting with respect to the rolling direction of the sheet is not simple and the location of the blank with respect to the punch and die is not simple either. It will be clearly shown later that these factors in a forming process, in fact, are interrelated. In order to investigate the effect of an individual factor in the drawing process, it is

Continued.....

necessary to fix the other factors and vary only that one which is being investigated.

### 11.3 The Orientation of the Blank with Respect to the Rolling Direction.

In the circular cup drawing, the anisotropy of sheet metal produces earring and apart from changing the blank shape, there is nothing more to be done about the earring. In a non-circular cup drawing process, usually a non-circular blank is used for the best performance of the material in the process and the geometry of the blank is no longer non-directional. Then, the anisotropy of the material which in a circular cup drawing process can not be optimized may become an advantage with careful blank cutting. In order to investigate the effect of the anisotropy of the material on drawability, the other factors like blank shape and the location of the blank with respect to the punch and die should be fixed.

Blanks of the same size (5" x 5" or 127.0mm x 127.0mm), same shape (square) and same orientation of the blank with respect to the punch and die (as shown in the inset of fig.11-4) but of different orientation with respect to the rolling direction, were drawn in a square cup drawing process with the same size of boundary (subcritical-sized). The angle  $\phi$  as shown in the inset of fig.11-4, which is the angle between the blank edge and the rolling direction of the sheet, is used to represent the orient-

Continued.....

ation of the blank with respect to the rolling direction of the sheet. In a square cup drawing, the angle  $\phi$  varies from  $0^\circ$  to  $45^\circ$ . The amount of draw-in against the punch penetration is plotted in fig.11-4. It is seen from fig. 11-4 that the current values of the draw-in, and the draw-in at the completion of the drawing operation are almost the same for all the blanks with different values of  $\phi$ . However, it would be unwarranted to judge in fig.11-4 that the rolling direction or the anisotropy of the material has no effect on the drawability in the square cup drawing process. In this square cup drawing process, the boundary is set to be a subcritical one (6.24" in size or 158.50mm), therefore, the largest draw-in, defined as drawability, should be achieved by the critical-sized blank. So, apart from those shown in fig.11-4, it is necessary to check whether the blank is a critical-sized one or not. This checking is done by comparing the maximum drawing force in the drawing process for each blank. The maximum drawing forces for the blanks with different value of  $\phi$  are shown together with the strength of the cup (line TT as that in fig.11-3) in fig.11-5. It is understood that an increase in the blank size will result in a larger drawing force. Because the maximum drawing forces for those blanks of the same size are all below the strength of the cup, their sizes can be increased to reach the strength of the cup by increasing the blank size. Because the blanks are all of the same size, the one for which the maximum drawing force

Continued.....

is the lowest will have the largest increase in size to become a critical-size blank. Such a blank is that which is cut in such a way that the rolling direction of the sheet is  $45^{\circ}$  degree to the edge of the square blank. The larger the critical-sized blank is, for the same boundary, (subcritical-sized), the larger the draw-in at the completion of the drawing operation. Therefore, when the shape and the orientation of the blank with respect to the punch and die are fixed in a square cup drawing process, the drawability is the highest if the square blank is cut in such a way that the edge of the square blank is  $45^{\circ}$  degree to the rolling direction of the sheet.

#### 11.4 The Orientation of the Blank with Respect to the Punch and Die.

In the last section the orientation of the blank with respect to the rolling direction is shown to have an effect on the drawability of sheet metal in the forming process. In this section, the effect of the orientation of the blank with respect to the punch and die is investigated and for clarity, the other factors such as the orientation of the blank with respect to the rolling direction and the blank shape, are fixed.

Square blanks, sized 5" x 5" (127.0mm x 127.0mm), cut with the blank edges along and perpendicular to the rolling direction of the sheet but located in different orientations

Continued.....

with respect to the punch and die, were drawn in a square cup drawing process. The orientation of the blank with respect to the punch and die is represented by an angle which is the angle between the blank edge and the flat edge of the square punch cross-section. The angle  $\zeta$  varies from  $0^\circ$  to  $45^\circ$  for a square blank in a square cup drawing process. The amount of draw-in is plotted against the punch penetration in fig.11-6 when a subcritical-sized boundary is taken. At a certain punch penetration the amount of draw-in of the blank orientated at small  $\zeta$  is larger than that of the blank at large values of  $\zeta$ . This is because (say for the blank at  $\zeta = 0$ , curve A), the material that will be drawn in at the flat part of the punch has less resistance due to <sup>the</sup> small flange in that part, therefore the draw-in is large, and the drawing force is small. When  $\zeta$  increases, the flange at the flat part of the punch is relatively increased, so that the resistance to the drawing action becomes larger. The draw-in is then lessened but the drawing force increases. Until the drawing force reaches the strength of the cup, the angle  $\zeta$  for successful drawing reaches its critical value. From the maximum drawing force in the drawing process as shown in curve A in fig.11-7, it can easily be seen that the critical value of  $\zeta$  for a square blank sized 5" x 5" (127.0mm x 127.0mm) for successful drawing in this square cup drawing process is around  $32.5^\circ$ . If the 5" x 5" square blank is located at an orientation of  $\zeta$  over  $32.5^\circ$ , fracture will occur in the cup. A set of blanks

Continued.....

sized  $4\frac{1}{8}$ " x  $4\frac{1}{8}$ " (123.82mm x 123.82mm) were drawn in the same drawing process and the maximum drawing forces of the blanks at different values of  $\zeta$  are shown in curve B. The critical value of  $\zeta$  for successful drawing in curve B is around  $42^\circ$ . This immediately leads to a guess that a smaller square blank can be found which is capable of being drawn successfully at any orientation. This guess is, in fact, true, because a  $4\frac{3}{4}$ " x  $4\frac{3}{4}$ " (120.65mm x 120.65mm) square blank is drawn successfully at any value of  $\zeta$ . From these maximum drawing forces, the strength of the cup can be found and is nearly constant with respect to the blank size or orientation of blank location.

It is well known that in a square cup drawing, the material moves faster at the flat side than at the corner of the punch cross-section. When  $\zeta$  increases, it provides a larger amount of material at the flange corresponding to the flat side of the punch cross-section. It increases the resistance to drawing due to the larger amount of material to be drawn but it delays the completion of the drawing operation and increases the draw-in at the completion of the drawing operation. Therefore, the orientation of a square blank of fixed size in a square cup drawing process, for the largest draw-in at the completion of the drawing operation, is that which provides as much material as possible at the flange corresponding to the flat side of the punch cross-section where the material movement is fast, while the maximum drawing force does not exceed the strength of the

Continued.....

cup. Such an orientation may be called the critical orientation of the blank of fixed shape and size in a forming process. If the blank shape is fixed to be square, for any orientation of blank location with respect to the punch and die there should be a critical size of blank so that the maximum drawing force in the drawing operation is equal to the strength of the cup. Similarly, for a certain size of square blank, there is a critical orientation for it. The relation between the critical size of the square blank and the critical orientation of blank location in a square cup drawing process (dimensions of the punch and die are shown in fig.9-1) is shown in fig. 11-8. Any square blank which is equal to or smaller than the  $4\frac{3}{4}$ " x  $4\frac{3}{4}$ " (120.65mm x 120.65mm) square can be drawn successfully at any orientation of blank location with respect to the punch and die. The curve in fig.11-8 separates the successful and unsuccessful regions.

So far the blank shape has been assumed to be square. But it is easy to see from the insets of fig.11-7, that the position of the flange edge at the completion of the drawing operation is not everywhere on the boundary. In other words, for that boundary, the square blank is not the most suitable blank for that square cup drawing. Therefore it is necessary to explore what shape is the best for a drawing process. The blank shape and size for the best performance in a drawing process is discussed in the next section.

Continued.....

11.5 Blank Shape and Size.

For a circular cup, it is natural to choose a round blank for the cup drawing. For non-circular cups, the choice of the shape for the blank is always less obvious than that for the round one. The drawing operation is considered to be completed when the edge of the flange touches the boundary. In a non-circular cup drawing, the edge of the flange does not normally touch the boundary everywhere at the completion of the drawing operation (fig. 11-9). The material between the boundary and the edge of the flange at the completion of the drawing operation is called the residual flange. In practice, the residual flange is cropped off and its area represents roughly the amount of wasted material. ~~Thus~~ Ideally it is desirable to eliminate the waste and have the right shape of blank so that there is no residual flange at the completion of the drawing operation. Practically, a better shape or a blank of smaller area is not always accompanied by any saving in the material because of the stacking consideration and the expenses of the additional stamping tool. However, in some drawing operations, material saving can be achieved without the need of expensive stamping tools, and apart from material economy, there is a better reason to choose a good blank shape, namely, for a better performance in the drawing process.

From the discussions in the previous sections, a clear

Continued.....

guide line for the shape and size of the blank emerges. To achieve the largest draw-in in a drawing process a blank must be such that the maximum drawing force in the drawing operation is equal to the strength of the cup to ensure a successful drawing, and the edge of the flange everywhere must reach the boundary simultaneously at the completion of the drawing operation. A blank so shaped that the edge of the flange everywhere reaches the boundary simultaneously at the completion of the drawing operation is called the zero-residual-flange blank. An abbreviation Z.R.F. will be used for "zero-residual-flange" in the following discussions. It is possible to have a series of Z.R.F. blanks for a drawing process. The blank capable of achieving the largest draw-in in the drawing process is not only a Z.R.F. blank but also one in which the maximum drawing force is equal to the strength of the cup. This later requirement, in fact, is the limiting size of the Z.R.F. blank. In other words, the blank capable of achieving the largest draw-in in a drawing process is the largest Z.R.F. blank.

It has been said that a Z.R.F. blank is the best shaped blank for a drawing process. Why can a non-Z.R.F. blank not achieve the largest draw-in at the completion of the drawing operation? The reason can be explained by the energy consideration in the drawing operation. Consider a vanishingly short step of the drawing operation just before the drawing force reaches the maximum, when a non-

Continued.....

Z.R.F. blank is drawn in the drawing operation. In this small step the energy of deformation goes partly into the flange which includes the residual flange at the completion of the drawing operation, and partly into the cup inside the boundary. The total energy is supplied by the drawing force in the punch which moves through a small distance into the cup. If the residual flange were cut off before the drawing operation, the drawing force in this small step in the trimmed workpiece would be smaller than that in the untrimmed one. Take an example, curve b in fig.11-3 when it reaches the maximum point which is also the strength of the cup at L. If the residual flange were cut off before the drawing operation, the maximum drawing force would be below the strength of the cup. Therefore a larger trimmed blank could be drawn successfully, thereby increasing the draw-in at the completion of the drawing operation. The increase in the draw-in at the completion of the drawing operation is shown in fig.11-10. The amount of draw-in is plotted against the current position of the flange edge on the line OX (inset of fig.11-10). Curve B is that of the square blank B (fig.11-3) with size 5" x 5", and curve A is that of the blank shown in fig.11-11, which is trimmed from a  $5\frac{1}{4}$ " x  $5\frac{1}{4}$ " square blank and near to a Z.R.F. blank. The draw-in at the completion of the drawing operation in curve A (1.16) is larger than that in curve B (1.04) due to the longer distance and the more material to be drawn along the line OX.

Continued.....

Although it has been shown that a Z.R.F. blank is the best shaped blank for a drawing process, it is both difficult and unnecessary to find the exact shape of the Z.R.F. blank. It is difficult because the problem does not lend itself readily to any theoretical solution and cut-and-trial treatment is tedious. It is unnecessary because small variation in the mechanical properties of the material from one blank to another and small variations in the forming conditions may change the exact shape of Z.R.F. blank, and the change would make it difficult even to define the exact shape of the Z.R.F. blank. Even if the exact shape of the Z.R.F. blank could be found easily, it is still impractical and expensive to cut it.

However difficult it is to find the exact shape of the Z.R.F. blank it is relatively easy to find the approximate shape of the Z.R.F. blank, and in an approximate Z.R.F. blank the performance of the material in the drawing process can be considerably improved. Therefore it is worthwhile to pursue the approximate Z.R.F. blank for a drawing process. Some approximate Z.R.F. blanks for a square cup drawing process have been tried and found in this project.

A square with round corners is symmetrical with respect to four planes passing through the centre and perpendicular to the cross-section. It is justifiable to assume that the exact or an approximate shape of the Z.R.F. blank would have

Continued.....

also these four planes of symmetry and therefore rather like an octagon. A series of octagonal blanks of equal sides were drawn in the square cup drawing process and the largest one successfully drawn was found. Although it is not the exact shape and size of the Z.R.F. blank, it is near to the Z.R.F. blank. The largest regular octagonal blank was cut from a  $5\frac{1}{4}$ " x  $5\frac{1}{4}$ " (133.35mm x 133.35mm) square blank so that its side is  $2\frac{5}{8}$ " (66.67mm) long. It was observed that the movement of the material in the flange corresponding to the flat side of the punch cross-section was faster than that at the corner. Thus simple advantageous modifications of the shape can be made by increasing the amount of material around the line OX (fig.11-12) where the edge of the flange touches the boundary first and decreasing the amount of material around the line OY (fig.11-12) where the residual flange is found at the completion of the drawing operation. This "increasing and decreasing modification" was done in steps of  $\frac{1}{8}$ " in the directions of OX and OY (fig. 11-12). Therefore a series of approximate Z.R.F. blanks was cut and drawn in the square cup drawing process. The dimensions and area of these blanks and the size of the boundary and the draw-in at the completion of the drawing operation are listed in the following table.

Continued.....

Table 11-1.

Blank	A	B	C	D
the size of square blank the blank is cut from	$5\frac{1}{4}" \times 5\frac{1}{4}"$	$5\frac{1}{8}" \times 5\frac{1}{8}"$	$5" \times 5"$	$4\frac{7}{8}" \times 4\frac{7}{8}"$
distance in OX direction (fig.11-12)	$2\frac{5}{8}"$	$2\frac{11}{16}"$	$2\frac{5}{8}"$	$2\frac{9}{16}"$
distance in OY direction (fig.11-12)	$2\frac{5}{8}"$	$2\frac{7}{16}"$	$2\frac{3}{8}"$	$2\frac{5}{16}"$
Blank area ( $ln^2$ )	22.83	22.76	22.53	22.15
size of the boundary	6.24	6.24	6.24	6.24
Draw-in at the completion of the drawing operation.	1.120	1.120	1.169	1.144

Those blanks are shown in different colours in fig.11-12 and the amount of draw-in against the current position of the edge of the flange on the line OX is shown in fig.11-13.

It is seen in fig.11-13 that the curve for blank D does not touch the vertical line in the co-ordinate which represents the boundary, as the others do. This is because in blank D, the distance on the line OX between the boundary and the blank edge is too long so that at the completion of the drawing operation the point at the edge of the flange on the line OX does not reach the boundary

Continued.....

because some other points reach it first (as F in fig.11-14).  
The Blank D together with the position of the flange at the completion of the drawing operation is shown in fig.11-14. There is a hint here that further "increasing and decreasing modifications" will not help. When the dimensions of the blanks A,B,C and D are increased in <sup>the</sup>OX direction without decreasing in <sup>the</sup>OY direction, the blanks are, in fact, greatly enlarged in area and are all found to be incapable of being drawn successfully. This is the proof that the size of the blanks A,B,C and D are near to the critical size. In fig.11-12, apart from the corners, the blanks are very near to the Z.R.F. blank. Therefore, the blanks A,B,C and D are, in fact, very near to the largest Z.R.F. blank.

As shown in the table 11-1, blank C achieves the largest draw-in at the completion of the drawing operation. But if ~~the~~ material economy is taken into account, one may sacrifice a little draw-in and prefer using blank D rather than blank C. Blank C is cut from a 5" x 5" (127mm x 127 mm) square blank and blank D is cut from a  $4\frac{7}{8}$ " x  $4\frac{7}{8}$ " (123.83mm x 123.83mm) square one. If blank D is used, the material saving is  $(5 \times 5 - 4\frac{7}{8} \times 4\frac{7}{8}) / (5 \times 5) = 5\%$ .

Now an overall conclusion about the blank used in a drawing process can be drawn. There is a unique combination of the shape, the size and the orientation of the blank with respect to the punch and die, which yields the best performance in a drawing process. This combination is

Continued.....

represented by the largest Z.R.F. blank. When the anisotropy of the material is taken into account in a square cup drawing process, the largest Z.R.F. blank should be cut in such a way that the rolling direction of the sheet is along the direction OY (fig.11-12). In the Swift test, any round blank is a Z.R.F. blank and the blank with the size of the limiting drawing ratio is the largest Z.R.F. blank (unless Z.R.F. blanks are considered, for the elimination of the ears).

#### 11.6 The Stretching and the Drawing Actions.

In a drawing process, a piece of sheet material is clamped between a holding plate and a die, and a punch pushes it through the die hole. The energy supplied by the punch is transferred into stress in the material around the punch profile and transmitted as drawing force to draw the material in the flange into the die hole. When the resistance to drawing of the material in the flange is large, the stress in the material around the punch profile should be large so that the drawing force is large enough to draw the material in the flange into the die hole. If the stress induced is so large that it exceeds the yield stress of the material, stretching takes place. If the material around the punch profile is strong enough to sustain the stress which transmits the drawing force to the flange being drawn, the drawing operation will be successful, otherwise, fracture will occur in the cup. Therefore the success of a drawing operation depends on the balance

Continued.....

between the strength of the material around the punch profile and the resistance to drawing of the material in the flange. The strength of the material is related to the forming limit curve and the resistance to drawing of the material in the flange is rather a complicated problem which will be investigated by considering the shape of the cup in the next Chapter. In this section, only the quantitative distinction between the stretching and the drawing actions in a drawing process is discussed.

As defined in Chapter 8, draw-in at a certain stage, say, stage a, of the drawing operation is the logarithm of the ratio of the amount of material inside the boundary at stage a to that before the drawing operation, namely,

$$\text{Draw-in, } \psi_a = \ln \frac{\text{the amount of material inside the boundary at stage a}}{\text{the amount of material inside the boundary before the drawing operation.}}$$

It can be written in terms of the area in the blank because the amount of material is just the product of the area and the thickness of the blank. Thus:

$$\begin{aligned} \text{Draw-in, } \psi_a &= \ln \frac{(\text{the area in the blank}) + (\text{the area in the blank inside the boundary})}{\text{the area in the blank inside the boundary}} \\ &= \ln \frac{A_{da}}{A_b} \end{aligned} \quad 11-1$$

Continued.....

where  $A_a$  is the area enclosed by a closed curve in the blank and the closed curve is the locus of the material particles occupying the boundary at stage  $a$  of the drawing operation; and  $A_b$  is the area in the blank inside the boundary.

The depth of the cup is not used as the measure of the drawability of sheet metal because in the cup drawing process it involves not only drawing but also <sup>a</sup>stretching action. A deep cup may be drawn with little draw-in and a shallow one may have a large draw-in. This is the reason why the depth of the cup is not used to represent the drawability. However, the practical engineer may well be interested in how deep a cup can be drawn from sheet metal, and indeed, the depth of the cup still has some meaning and can be used to represent the performance of sheet metal in a drawing process. It is important to explain clearly what the depth of the cup means in relation to drawability. The depth of the cup, in fact, represents the surface area in the cup. Suppose the surface area inside the boundary is considered. The surface area inside the boundary before the drawing operation is  $A_b$  and that at certain stage of the drawing operation is  $A_s$ . Then a gross surface strain  $\eta$  may be defined as follows:

$$\eta = \ln \frac{\text{surface area of the cup inside the boundary}}{\text{surface area inside the boundary before the drawing operation.}}$$

Continued.....

$$= \ln \frac{A_s}{A_b} \quad 11-2$$

It is "gross" because the material in the cup inside the boundary at a certain stage of the drawing operation is not the material in the blank inside the boundary before the drawing operation, but includes that which is outside the boundary before the drawing operation drawn into the boundary in the drawing operation. A net or average surface strain in the cup inside the boundary then can be defined as follows:

$$\begin{aligned} \phi &= \ln \frac{\text{surface area of the cup inside the boundary}}{\text{(amount of material in the cup inside the boundary)} \\ &\quad \text{the thickness of the blank}} \\ &= \ln \frac{\text{surface area of the cup inside the boundary}}{\text{surface area in the blank enclosed by a closed curve which is the locus of the material particles occupying the boundary in the drawing operation.}} \\ &= \ln \frac{A_s}{A_d} \quad 11-3 \end{aligned}$$

where  $\phi$  is the average surface strain in the cup inside the boundary. It can also be considered as the surface strain due to stretching in the drawing operation, in other words, the amount of stretching in the drawing operation.

From Eqs. 11-1, 11-2, and 11-3.

$$\eta_a = \ln \frac{A_{sa}}{A_b} = \ln \frac{A_{da}}{A_b} + \ln \frac{A_{sa}}{A_{da}} \quad 11-4$$

Continued.....

$$= \psi_a + \varphi_a \quad 11-5$$

where "a" means at stage a of the drawing operation.

In general, Eq. 11-5 can be written as :

$$\eta = \psi + \varphi \quad 11-6$$

Eq. 11-6 means that inside the boundary the change in the surface area in the drawing operation is due partly to the stretching action and partly to the drawing action.

According to the definitions stated above, the drawing action consists of compression in one direction and an equal amount of tension in the perpendicular direction so that no change in surface area occurs. If the surface area of the cup inside the boundary  $A_s$  is equal to  $A_d$ , there is no average surface strain, and the deformation may be said to be a pure drawing operation. If the blank is clamped firmly so that no material in the flange is drawn into the boundary,  $A_d$  is equal to  $A_b$ , then the gross surface strain is equal to the average surface strain and it is a pure stretching operation.

The relation and quantitative distinction between the amount of stretching and drawing actions in the square cup drawing process in which the blank C (fig.11-12) is drawn, are shown in fig.11-15. At stage a (punch penetration 1.75"), for example,  $PoP_i$  (0.78) represents the amount of

Continued.....

draw-in  $\psi_a$  and  $P_1 P_2$  (0.17) represents the amount of stretching and,  $\frac{\psi_a}{\eta_a} \times 100\% = 82.1\%$  and  $\frac{\phi_a}{\eta_a} \times 100\% = 17.9\%$ . The percentage of the drawing action increases with the progression of the drawing operation. The amount of stretching is increasing at the early stage of the drawing operation and becomes nearly constant after the maximum drawing force is reached (at 1.5" punch penetration). There is a little decrease at a later stage because near the completion of the drawing operation the material around the point which is going to touch the boundary first is compressed severely and drawn across the boundary. This peculiar phenomenon decreases the average surface strain and if the drawing operation continues, ironing may occur.

Continued.....

CHAPTER 12

CHARACTERISTICS OF THE FORMING PROCESS

### Characteristics of the Forming Process.

In the previous Chapters it has been explained and demonstrated that there is an aspect of drawability which depends as much on the characteristics of the forming process as on the material properties. By recognising that drawability is inseparable from the characteristics of the forming process, it has been possible to define drawability in such a general way as to make it applicable to all shapes of cups. It is therefore natural to ask what characteristics it is in the forming processes that determines their relative drawabilities. The object of this Chapter is to provide the answer to this question.

#### 12.1 Convergence of Metal Flow.

A hint of this answer lies in the well known fact that, other things being equal, the drawability is largest in a round cup. The characteristic of the forming process which determines its drawability must, therefore, be unique in the axisymmetrical process and, if this characteristic is expressed quantitatively, it is likely to reach an extremum value in the axisymmetrical process. One may justifiably guess at this stage that it has to do with some definition of roundness.

As it turns out, this characteristic, although not having been noticed hitherto by those investigating sheet metal forming, is a simple geometrical property of the process,

Continued.....

and lies in a fundamental aspect of the drawing action. It has been pointed out previously in this thesis that cup drawing or deep drawing consists essentially of movement and deformation of the flange to form the walls of the cup. It is now proposed to take a particular view of the kinematics of this drawing action, namely, the velocities of the material particles in the plane of the flange as in fig.12-1. In the plan views shown in fig.12-1 the velocities are schematically represented by the relative lengths of the arrowheads, and it is understood that, where the actual velocities are not in the plane of the flange, the velocities represented here are the projections in that plane. In other words, it is proposed to examine the two-dimensional vector field in the plane of the flange.

Obviously, in a cup drawing process, the velocities must be generally directed inwards whatever the shape of the cup. The velocities leave the plane of the flange when the material is drawn into the die profile region, and their projections in the plane of the flange are zero when the material leaves the die surface and becomes the vertical wall of the cup. The only external force exerting on the material is from the punch and is transmitted to the cross-section of the vertical walls of the cup. To identify and to describe quantitatively the drawing operation of non-circular cups, it is necessary to analyse in detail the kinematics of the metal flow involved in it. In the following, the square cup with rounded corners is chosen

Continued.....

to represent non-circular cups in general and it can be readily seen that the analysis applies equally to all other cups of non-circular shapes.

As shown in fig.12-2, the wall of the cup is the portion above the line abcd, the flange is represented by the region lehn, and between the two regions, namely, the part marked adhe, lies the part of the workpiece in contact with the die profile. In the wall above the line abcd the material mostly moves bodily upwards with no or very little deformation, and the velocities of the material particles is constant in both magnitude and direction. Consider now the material particles just below the line abcd. The principal tensile stress is everywhere vertical and perpendicular to abcd and the velocity of the material just above it is also perpendicular to it. The constraints are such, therefore, that the velocities just below abcd must be perpendicular to abcd.

We now examine a quantity, called convergence, defined as the product of the velocity and the curvature of a line drawn perpendicular to it, namely,

$$v \cdot \frac{d\phi}{ds}$$

In the region bcgf, assuming that all the velocities lie in the planes passing through the axis of the cup, the

Continued.....

convergence is

$$V \cdot \frac{\sin \beta}{r_0}$$

where  $r_0$  is the radius of the circular arc in the section normal to the axis of the cup and angle  $\beta$  is the angle of inclination of the velocity with respect to the vertical line, as shown in the inset (fig.12-2). As can be seen in the expression  $V \frac{\sin \beta}{r_0}$  the convergence is zero at line bc and equal to  $\frac{V}{r_0}$  at the line fg; where both  $V$  and  $r_0$

refer, of course, to the local conditions.

At this point it is desirable to make a clear distinction between actual empirical conditions and the idealized flow. In actual square cups the flow across line efgh is in general not perpendicular to it and the deviations, and the reasons for them, will be discussed in the last part of this Chapter. Here, however, we are not concerned with the analysis of the actual flow patterns, but rather with the characteristics of a non-circular cup drawing process. The essential characteristic of such a process is the deviation of the shape of the cup from the circular shape, and the essential feature of the drawing process is the effect of such a deviation on the flow of the material in the workpiece.

Any closed curve can be chosen as the boundary of the

Continued.....

product. But there is one which is significantly related to the shape of the cup and the characteristic of the drawing process. That is the line efgh which is the line where the material leaves the die face. In order to study the characteristic of the drawing process, such a boundary is chosen as the reference line and an assumption is made that all the velocities passing this reference line are perpendicular to it. Then it can be readily seen that the characteristic of the forming process we seek concerns the convergence of the velocity across such a boundary as the line efgh. One may tentatively surmise that the reason for the maximum drawability in the round cup is the unique kinematic characteristic of uniform convergence of the flow in that shape. Since the convergence is defined as the product of the velocity and the curvature of a line drawn perpendicular to it, and since the velocities are assumed to be perpendicular to the reference line or boundary, the convergence in a forming process is the product of the velocity and the curvature of the reference line (or boundary) chosen in this section. It is now important to explore these two factors, the velocity and the curvature of the boundary, which determine the convergence of the flow.

## 12.2 The Index of Nonsymmetry.

The velocities across the boundary are determined not only by the material property and the shape of the cup but also by the forming conditions of the drawing operation such as

Continued.....

lubrication condition, blank size and shape. The velocity field is complex and will be discussed later. Now, in order to know how the shape of the cup or the boundary affects the convergence of the flow, the velocities across the boundary are assumed to be equal everywhere at the boundary. A very short length  $\Delta S_0$  on the boundary is considered (fig. 12-3).

$$\Delta S_0 = \rho_0 \Delta \phi_0 \quad 12-2$$

where  $\rho_0$  is the radius of curvature of the boundary at  $\Delta S_0$  and  $\Delta \phi_0$  is the angle the direction of the curve  $\Delta S_0$  changes through. Because the instantaneous speed of the flow crossing the boundary is assumed to be the same everywhere at the boundary, the particles at  $\Delta S_0$  will reach  $\Delta S$  after  $\Delta t$ , and

$$\Delta S = \rho \Delta \phi_0 \quad 12-3$$

Then the circumferential strain along the boundary is

$$\epsilon = \ln \frac{\Delta S}{\Delta S_0} = \ln \frac{\rho}{\rho_0} \quad 12-4$$

and

$$\frac{d\epsilon}{d\rho} = \frac{1}{\rho} \quad 12-5$$

Because  $\rho_0 - \rho = V \cdot \Delta t$

therefore  $\dot{\rho} = V \quad 12-6$

and  $\dot{\epsilon} = \frac{\dot{\rho}}{\rho} = \frac{V}{\rho} \quad 12-7$

Continued.....

$$\frac{d\phi}{ds} = \frac{1}{\rho} = \frac{\dot{\epsilon}}{V} \quad (V = \text{constant}) \quad 12-8$$

Curvature of the reference line is thus seen to be the circumferential strain rate per unit particle velocity in the drawing process. In a non-circular cup this specific circumferential strain rate varies from one point to another along the reference line, hence the less favourable drawing conditions than in the circular cup. These consequences of the deviation from axial symmetry in the geometry of the cup are characterised in the preceding discussion by assuming that the velocities are perpendicular to the reference line efgh (fig.12-2), for the sake of elucidating the relationships between the cup geometry and the drawability, and for the sake of expressing these relationships in quantitative terms. That the sharp inequalities of convergence, strain rate and so on assumed in the ideal cases are ameliorated in the actual cups by the continuity of stress and strains in the material in no way invalidates the characterisation of the non-circular drawing process presented here.

In so far as drawability is concerned, the significant characteristic is not, of course, the absolute value of the convergence, but rather the uniformity of the convergence, or the uniformity of the curvature of the boundary. Therefore, an index of nonsymmetry is defined as follows:

$$\xi = \frac{1}{2\pi} \int_0^{2\pi} \left| \frac{\frac{1}{\rho}}{\left(\frac{1}{\rho}\right)_{av.}} - 1 \right| d\theta \quad 12-9$$

Continued.....

where  $\theta$  (fig.12-4) is the polar co-ordinate of a point on the boundary when the centroid of the shape of the boundary is chosen as the origin of the co-ordinate system, and

$$\left(\frac{1}{\rho}\right)_{av.} = \frac{1}{2\pi} \int_0^{2\pi} \frac{1}{\rho} d\theta \quad 12-10$$

Eq. 12-9 defines the quantitative deviation of a shape from a round one. When  $\xi$  is zero, the shape is a circle. The larger the value of  $\xi$  is, the more uneven the convergence along the boundary will be, and the worse the characteristic of the forming process is.

The indices of nonsymmetry of a square and a rectangular shape with round corners and an elliptical shape are formulated as follows.

- (1) A square shape of  $2a \times 2a$  with round corners of radius  $r$ , (fig.12-4)

$$\tan \theta_1 = \frac{a-r}{a}$$

$$\left(\frac{1}{\rho}\right)_{av.} = \frac{\frac{1}{r} \left(\frac{\pi}{4} - \theta_1\right)}{\frac{\pi}{4}}$$

$$\begin{aligned} \xi &= \frac{8}{2\pi} \int_0^{\frac{\pi}{4}} \left| \frac{1}{\rho} - \left(\frac{1}{\rho}\right)_{av.} \right| d\theta \\ &= \frac{8}{2\pi} (2\theta_1) \end{aligned}$$

Continued.....

- (2) A rectangular shape of  $2a \times 2b$  with round corners of radius  $r$ , (fig.12-5)

$$\tan \theta_1 = \frac{b - r}{a}$$

$$\tan \theta_2 = \frac{b}{a - r}$$

$$\left(\frac{1}{\rho}\right)_{av.} = \frac{\frac{1}{r} (\theta_2 - \theta_1)}{\frac{\pi}{2}}$$

$$\begin{aligned} \Xi &= \frac{4}{2\pi} \int_0^{\frac{\pi}{2}} \left| \frac{\frac{1}{\rho}}{\left(\frac{1}{\rho}\right)_{av.}} - 1 \right| d\theta \\ &= \frac{4}{2\pi} \times 2 \times \left(\frac{\pi}{2} - (\theta_2 - \theta_1)\right) \end{aligned}$$

- (3) An elliptical shape (fig.12-6)

$$\frac{X^2}{a^2} + \frac{Y^2}{b^2} = 1$$

$$\frac{1}{\rho} = \frac{\dot{X}\ddot{Y} - \dot{Y}\ddot{X}}{(\dot{X}^2 + \dot{Y}^2)^{3/2}} = \frac{-a^4b^4}{(a^4Y^2 + b^4X^2)^{3/2}}$$

$$\left(\frac{1}{\rho}\right)_{av.} = \frac{\int_0^{\frac{\pi}{2}} \frac{1}{\rho} d\theta}{\frac{\pi}{2}}$$

$$\Xi = \frac{4}{2\pi} \int_0^{\frac{\pi}{2}} \left| \frac{\frac{1}{\rho}}{\left(\frac{1}{\rho}\right)_{av.}} - 1 \right| d\theta$$

Continued.....

$$\frac{4}{2\pi} \int_0^{\frac{\pi}{2}} \left| \frac{\frac{-a^4 b^4}{(a^4 Y^2 + b^4 X^2)^{\frac{3}{2}}} - 1}{\frac{2}{\pi} \int_0^{\frac{\pi}{2}} \frac{-a^4 b^4}{(a^4 Y^2 + b^4 X^2)^{\frac{3}{2}}} d\theta} \right| d\theta$$

### 12.3 Stresses in a Non-circular Cup Drawing Process

The deviation of a shape from a circle is defined by the index of nonsymmetry. It is not only a geometrical property of the forming process, but also represents the uniformity of the distribution of the incremental circumferential strain at the boundary. It is known that when the shape of the cup deviates from a circle, the velocities crossing the boundary will not be the same everywhere at the boundary. Even in a round cup drawing operation, if the blank is not a round one or if there is anisotropy of the material, the velocities crossing the boundary will be different too. The unequalness of the velocities across the boundary is due partly to the uneven curvature of the boundary which is determined by the shape of the cup, and partly to the resistance to drawing of the material in the flange which is determined by the forming conditions such as the lubrication condition, the blank shape and size and so on. The larger the curvature of the boundary is, the smaller the velocity across the boundary will be. The resistance to drawing of the material in the flange is investigated by the consideration of the energy of deformation in the flange as will be discussed in the following.

Continued.....

Now consider the cross-sectional surface of the workpiece at the exit of the die throat where the material leaves the die, surface to become the vertical wall of the cup (fig.12-7). The energy for the drawing action is supplied by the force transmitted across this cross-sectional area and the movement of the material at this curve,

Thus,

Energy input per unit length of the boundary

$$= (\sigma t) U$$

Energy of deformation = (Area) x  $t_{av.}$  x (Strain rate) $_{av.}$   
x(average yield stress)

where  $\sigma$  is the stress and  $t$  is the thickness at the cross-section, and  $U$  is the velocity of the material particle at that cross-section; (Area) is here idealised as the area in the flange between the lines normal to the ends of a unit length at the cross-section (as station 1 or 2 in fig.12-7) and  $t_{av.}$  the average thickness in the flange. To compare the stresses at two stations in the wall of a square cup, one at the corner (station 1 in fig.12-7) and one at the flat side (station 2 in fig.12-7), we have

$$\frac{\sigma_1 t_1 U_1}{\sigma_2 t_2 U_2} = \frac{(Area)_1}{(Area)_2} \times \frac{(t_{av.})_1}{(t_{av.})_2} \times \frac{(strain\ rate)_{av.1}}{(strain\ rate)_{av.2}} \times \frac{(\sigma_Y)_1}{(\sigma_Y)_2}$$

or

$$\frac{\sigma_1}{\sigma_2} = \frac{t_2}{t_1} \times \frac{U_2}{U_1} \times \frac{(Area)_1}{(Area)_2} \times \frac{(t_{av.})_1}{(t_{av.})_2} \times \frac{(strain\ rate)_{av.1}}{(strain\ rate)_{av.2}} \times \frac{(\sigma_Y)_1}{(\sigma_Y)_2}$$

Of the ratios in the right hand side of Eq. 12-11, the thickness ratios  $t_2/t_1$  and  $(t_{av.})_1/(t_{av.})_2$  are nearly unity because the thickness in the wall and in the flange are nearly the same at the corner and at the flat side, the speed ratio  $U_2/U_1$  is nearly unity because the velocities of material particles in the wall of the cup are nearly equal around the cup, and the  $\sigma_Y$ -ratio is <sup>nearly</sup> unity too. The area ratio and the ratio of the strain rates in the square cup drawing as shown in fig.12-7 are much larger than unity. Hence, the stress at the corner where the convergence is high is very much higher than that at the flat side of the cup. If the stress per unit length of the cup periphery is plotted with respect to the length of the cup periphery, a curve can be obtained, (conjectured results are shown in fig.12-8). The blank of which the stress distribution curve (curve A in fig.12-8) reaches the strength of the material is the critical sized blank in that drawing process. The area under the curve (curve A) represents the force the cup can sustain or the maximum drawing force transmitted to draw the flange into the boundary.

In a round cup drawing process, if a round blank is used and the anisotropy of the material is neglected, the stress distribution along the cylindrical wall of the cup is everywhere uniform, and if plotted as that in fig.12-8, is a horizontal line. The blank size can be increased until the stress in the wall of the cup reaches the strength of the material. The maximum drawing force transmitted to

Continued.....

draw the flange into the boundary in a round cup drawing operation is then represented by the area under the horizontal line B which also represents the strength of the material. It is obvious that the maximum drawing force transmitted to draw the flange into the cup in a non-circular cup drawing process is smaller than that in a circular cup drawing process. This is the reason why the drawability drops in a non-circular cup drawing process. By considering the drawing force in the forming processes, an equivalent round blank represented by curve C in fig. 12-8, can be found that the area under curve C is equal to that under curve A. In other words, the maximum drawing force transmitted to draw the flange into the cup in a non-circular cup drawing process when a critical-sized blank (of certain shape) is drawn, is equal to that in a circular cup drawing process when the equivalent blank is drawn. The larger the force<sup>that</sup> can be transmitted to draw the flange into the cup is, the larger the draw-in will be. The size of the equivalent blank is dependent on the variation of curve A. The smaller the difference between the peak and the valley of the curve is, the larger the equivalent blank is. The variation of the stress distribution curve will be discussed in the following.

Equation 12-11 may be written as:

$$\frac{\sigma_1}{\sigma_2} = \frac{(\text{Area})_1}{(\text{Area})_2} \times \frac{(\text{strain rate})_{\text{av. 1}}}{(\text{strain rate})_{\text{av. 2}}} \quad 12-12$$

Continued.....

after the cancellations of the velocity ratio, the thickness ratio and the yield stress ratio. In order to equalize the stresses, it is found from Eq. 12-12 that it concerns the product of the area ratio and the average strain ratio. The  $(Area)_A^{term}$  in Eq. 12-12 is determined by the curvature of the boundary and the distance between the boundary and the edge of the blank. If the distance between the boundary and the edge of the blank is constant, the larger the curvature of the boundary is, the larger the  $(Area)_A^{term}$  corresponding to the unit length of the boundary is (as station 1 in fig. 12-7). The curvature of the boundary as well as the shape of the cup is determined by the punch and die. Thus the  $(Area)_A^{term}$  depends on the distance between the boundary and the edge of the blank. For a constant area, the blank should be such that the distance between the boundary and the edge of the blank is nearly inversely proportional to the curvature of the corresponding boundary. The average strain ratio is a bit more complicated than the area ratio as will be explained as follows. In a square cup drawing process, if a square blank is drawn (as that in fig.12-7), it is possible to draw the line SS (fig.12-7) which separates the flat side region and the corner region. If all the particles moved in the directions normal to the boundary, then there would be no circumferential stress and strain in the flat side region and a sudden jump of circumferential stress and strain on the line SS. In practice it is impossible to have such a jump of stress and strain because the two regions are in the same piece of material. If the line SS were a rigid wall, then when the corner region

Continued.....

moved in, there would be a large circumferential stress near the boundary and the material <sup>would</sup> exert a compressive force into the imagined wall SS. The imagined wall would exert, as a reaction, a compressive force onto the material in the corner region to produce strain in that region. The average strain rate is therefore dependent on the inward velocities of the particles in that region, and the area of that region which depends on the curvature of the boundary, as well as the distance between the boundary and the edge of the blank. But, in fact, the line SS is not a rigid wall. When there is a compressive force acting on the line SS, the force is transmitted through it to the adjacent region and balanced by stresses in the material in the two regions. That stress should be greater than the yield stress of the material and produce circumferential strain somewhere or everywhere so that the material can move in. In the case shown in fig.12-7, at the first moment of the drawing operation, every particle in the corner region, for example the point P, tries to move in a direction  $\overline{PN}$  (fig.12-7) so that it is moving without being deformed. But in a drawing process it is impossible for every particle to do so, and, in fact, every particle should go in the direction  $\overline{PM}$  which is normal to the boundary. Therefore the direction of the movement of the particle is determined by the balancing of the stresses in that region and the adjacent region. If the particles in the corner region are moving in the directions normal to the boundary, then the average strain in that region is

Continued.....

the largest and if they are moving in the directions parallel to TT (fig.12-7) so that it is a rigid body translation, the average strain is the smallest. Therefore, the average strain rate depends on the velocity of the feeding-in of the material, and the swinging of the lines, which are the border of that region, from the directions normal to the boundary. The larger swinging of the border to the adjacent regions, the more the decrease in average strain rate is in that region. Of course, the swinging of the border to the adjacent regions will increase the average strain rate in the adjacent regions. For a constant average strain rate in different regions, the region corresponding to a large curvature of boundary should invade the region corresponding to a small curvature boundary.

#### 12.4 The Optimization of the Blank Shape and Size.

In order to approach the equalisation of the stresses at the wall of the cup, the blank corners (fig.12-7) are cut off to decrease the area corresponding to the boundary with large curvature at the corner. This cut-off decreases the area ratio (in Eq. 12-12). But the portions being cut off are normally less strained, <sup>and</sup> the cut-off will increase the average strain rate in that region. The decrease in area in the corner region also decreases the swinging of the border thus increasing the average strain rate. The variation of the stress ratio is therefore dependent on the variations of the area ratio and the average strain rate ratio. Because of the cut-off, the energy of deform-

Continued.....

ation needed at the corner region will decrease and so will the stress at the wall of the cup at the corner. A square blank of critical size is drawn in the square cup drawing process (fig. 12-7),<sup>and</sup> the guessed distribution curve of the stress at the wall of the cup is shown at curve A in fig. 12-8. When the corners of the blank are cut off, the distribution curve of stress will lower ~~down~~ due to the decrease in the energy of deformation needed. Because of the variations of the area ratio and the average strain rate ratio, the stress ratio has three possible variations. It may increase or decrease or keep constant. The stress ratio, in fact, represents the uniformity of the stress at different stations. The smaller the stress ratio ~~is~~, the more uniform<sup>is</sup> the stress distribution in the wall of the cup ~~is~~. Therefore, the favourable way of cutting is that leading to a decrease in the stress ratio. Then the distribution curve of stress at the wall of the cup lowers ~~down~~ (fig 12-9) and the difference between the peak and the valley of the curve is thereby decreased. Because the highest stress at the wall of the cup in the cut blank is lower than the strength of the material, a larger blank of the same shape can be drawn without failure and the distribution curve of stress in the wall of the cup will be that as shown in fig. 12-9. The difference between the peak and the valley is smaller in the larger blank with a cut than that in the square blank of the critical size; in other words, the uniformity of the stress distribution at the wall of the cup is improved by the cutting. If the

Continued.....

cutting off is done on "the larger blank with cut", the distribution curve of stress at the wall of the cup could be smoothed further and further, and finally a nearly horizontal line is obtained. This in fact, is another approach to getting the largest Z.R.F. blank.

12.5 The Involvement of Non-coaxial Deformation in Non-circular Cup Drawing Processes.

The velocities ( $U$  in fig.12-7) of the particles in the vertical wall of the cup are nearly equal everywhere along the cup. But the velocities of the material particles across the boundary are certainly not equal unless the forming process is axisymmetrical. This difference in speed, as said before, is mainly due to the variation of the curvature of the boundary and partly due to the resistance of the material in the flange to being drawn in. Because the shape of the cup is not circular, the curvature of the boundary is not equal everywhere. The boundary in a drawing process is like a bottle-neck. The larger the curvature of the boundary, the narrower the neck will be, and the slower the velocity of moving-in will be. When the curvature changes, the velocity of moving-in will change as well. The differential velocities of particles crossing the boundary will result in shear deformation which is positively a non-coaxial deformation (as described in Chapter 5). And this difference in velocity across the boundary will induce the rotation of the material in the flange so that the direction of moving of the material

Continued.....

particle in the flange is changing all the time before it reaches the boundary. This changing of moving direction, obviously, will produce non-coaxial deformation somewhere in the material. It is understood that the deformation of the material in the flange varies from one point to another. It is very complex, but it is a fact that the material is under non-coaxial deformation in <sup>the</sup> non-circular cup drawing process.

Material particles moving across the boundary with different velocities produce shear deformation. There is a great possibility that material failure occurs due to large shearing, especially at the transitional region where the changing rate of the boundary curvature is large. The severity of shearing is proportional to the velocity gradient along the boundary. The larger the velocity gradient along the boundary, the more severe the material is sheared. Let  $\vec{V}$  be the velocity vector of the material particle across the boundary and  $s$  be the boundary, then the velocity gradient along the boundary is

$$\frac{d}{ds} (\vec{V} \cdot \vec{n})$$

where  $\vec{n}$  is the unit normal to the boundary  $s$ . Because the velocities across the boundary are, or are almost normal to the boundary, the velocity along the boundary is zero, or

$$\vec{V} \cdot d\vec{s} = 0$$

Continued.....

Therefore,

$$\begin{aligned}\nabla \times \vec{V} &= \left( \frac{d}{ds} (\vec{V} \cdot \vec{n}) - \frac{d}{dn} \left( \frac{\vec{V} : d\vec{s}}{|d\vec{s}|} \right) \right) \\ &= \frac{d}{ds} (\vec{V} : \vec{n})\end{aligned}$$

In other words, the severity of the shearing can be represented by the curl of the velocity across the boundary. The larger the curl of the velocity is, the larger the possibility of material failure due to shearing at that region.

This Chapter provides the basic analysis of a non-circular cup drawing process. Without the quantitative measurement of a shape different from a circle, it is difficult to start the investigation. Although only a square cup drawing process is discussed and illustrated, the arguments are well applicable to any shape of cup drawing.

Continued.....

CHAPTER 13

CONCLUSIONS

## Conclusions

"Formability" is not a new term in sheet metal forming and there has been a large number of research papers about the formability of sheet metal. But hitherto there has not been a clear, precise and generally agreed definition for the formability of sheet metal. Because of the ambiguity of the meaning of "formability", it is sometimes difficult to communicate between the research worker and the engineer in industry, or even among sheet metal forming research workers themselves. In this thesis, in order to give a clear definition of the formability of sheet metal, the forming process is to mean a blank held between a blank holder and a die, and a punch pushes it through the hole in the die; and only ~~the~~ excessive thinning and fracture of the material are considered as material failure. The formability of sheet metal is then defined ~~as~~ the forming limits of the material and the performance of the material in a forming process. The forming limit of the material is the limiting strain the material under forming can withstand. It is dependent on the strain path under which the material is deformed. Therefore, the formability which means the forming limits of the material is not a single <sup>property</sup>, but is a spectrum of material properties. It can not be represented by a single index but can only be represented by a curve, such as the forming limit ~~the~~ curve. On the other hand, the performance of the material in a forming process, because the forming process is defined as a drawing process, is represented by the drawability

Continued.....

in a forming process. Because drawability is the performance of sheet metal in a forming process, it is obviously dependent on the forming process. Therefore, the drawability of sheet metal, like the forming limits of the material is a spectrum of material properties depending on the forming process.

The strain or a state of strain used to be represented by the three principal strains only. The directions of the principal axes of strain with respect to the material were neglected all the time. In sheet metal forming, in fact, there are many cases in which the material is deformed with the principal axes of strain rotating with respect to the material. For example, any forming process other than cylindrical cup drawing, involves a deformation in which the principal axes of strain rotate with respect to the material, namely, a non-coaxial deformation. Even the cylindrical cup drawing process, if the anisotropy of the material is taken into account, involves non-coaxial deformation as well. The strain path of the material in the redrawing of a circular cup is normally a zigzag path, but the principal axes of strain are fixed with respect to the material. In other words, it is zigzag but coaxial. But in the redrawing of a non-circular cup, due to the nonalignment of the principal axes of strain and stress in the different stages of forming, the strain path is not only zigzag but also non-

Continued.....

coaxial. As many sheet metal forming products are not axisymmetrical, for the better understanding of the material behaviour in the forming process, it is necessary and significant to investigate what the non-coaxial deformation is and how to find the formability when non-coaxial deformation is involved.

The lack of development and investigation in non-coaxial deformation is obviously due to the incomplete representation of a state of strain by using a circular grid system for strain measurement. The state of strain as measured by a circular grid system is represented by the three principal strains only. A complete representation of a state of strain should involve not only the three principal strains but also the directions of the principal axes of strain with respect to the material. In this thesis, a state of strain is therefore fully represented by not only the three principal strains but also a factor specifying the directions of the principal axes of strain with respect to the material. The coaxiality of the principal axes of strain with respect to the material can therefore be easily detected. The non-coaxial strain analysis by using a square grid system, which was firstly developed by Professor Hsü<sup>(48)</sup>, is further developed. A three-dimensional triangular co-ordinate system in which not only the three principal strains but also the directions of the principal axes of strain with respect to the material are represented explicitly, is proposed, so that

Continued.....

the non-coaxial strain path can be actually plotted.

The significant difference between a coaxial and a non-coaxial deformation lies on the fundamental basis of strain measurement. The theory of plasticity hitherto proposed is built up on the basis that the principal axes of stress and strain are coincident to each other in the deformation, in other words, the coaxial case is assumed. Based on this fundamental assumption, the work-hardening hypothesis and the stress-strain relationship are developed. In this thesis, this fundamental assumption is removed and the work-hardening and the stress-strain relationship in <sup>the</sup> non-coaxial case are discussed by considering the work consumption in the deformation. It is shown that <sup>the</sup> Lévy-Mises and Prandtl-Reuss equations, if they are true in <sup>the</sup> coaxial case, are not true in <sup>the</sup> non-coaxial case.

There is another significant difference between a coaxial and a non-coaxial deformation. The strain path can be shifted or zigzagged without changing the stress ratio, in a non-coaxial deformation. This is just due to the non-coaxiality of the principal axes of stress and strain with respect to the material. In other words, under the same stresses, the strain paths are different in coaxial and ~~in~~ non-coaxial deformations. There is a danger that if the non-coaxiality of the principal axes of strain with respect to the material is neglected in ~~the~~ non-coaxial deformation, the shift or the zigzagging of the

Continued.....

strain path may mislead research workers to consider it as a change of stress ratios. For any forming process which may involve non-coaxial deformation it is important to consider the coaxiality or otherwise of the principal axes of strain with respect to the material.

The energy consumption for producing a certain strain in a non-coaxial deformation is more than that in a coaxial one. Owing to this effect, it is possible that the material is severely work-hardened with small strains (without unloading and reloading). Because of the severity of work-hardening, the material, if it fails, will fracture without excessive thinning. This is another type of material failure which does not normally happen in the coaxial case. The forming limits of the material are dependent on the strain path. Therefore the material should have forming limits under non-coaxial strain paths. Apart from the type of material failure, in <sup>the</sup> non-coaxial case, the strain path is shifted or zigzagged due to the non-coaxiality of the principal axes of stress and strain. When the strain paths are different, the forming limits are bound to be affected.

The definition of drawability, hitherto, is based on and limited to the drawing of circular cups as in the Swift's test. As said before, the drawability is the performance of sheet metal in a forming process and is dependent on the forming process, and the drawability of sheet metal

Continued.....

should be a spectrum of performance depending on <sup>the</sup> forming processes. Therefore, it is necessary to extend the investigation of the drawability of sheet metal to some other forming processes. In fact, the need for extending the investigation to the drawing of non-circular shape was stated thirty-five years ago by Professor Swift. After thirty five years, it is certainly opportune to do it. In ~~the~~ circular cup drawing process, the material everywhere is deformed under a coaxial strain path and the material at the critical section is deformed under a coaxial strain path too. But in a non-circular cup drawing process, the material in the blank is in general deformed under a non-coaxial strain path. The material at the critical section may be deformed under a non-coaxial strain path and the type of material failure may not be the same as that in a circular cup drawing process. This non-coaxial deformation ~~is~~ makes the material behaviour in a non-circular cup drawing process deviate from that in the Swift test so that the test results in the Swift test are not applicable to non-circular cup drawing. In the Swift test, the drawability is defined by the limiting drawing ratio which is the ratio of the diameter of the largest blank capable of being drawn successfully, to the punch diameter. In <sup>the</sup> non-circular cup drawing process, although round blanks can still be used so that there is a blank diameter, there is no longer a punch diameter. Therefore, in order to extend ~~the~~ the investigation to the cup drawing of non-circular shapes,

Continued.....

the definition of drawability should be generalised first.

The Swift's test is re-examined and the implication of the limiting drawing ratio in the Swift's test is explored. In the Swift's test, the blank shape, the boundary of the product and the location of the blank are concealed. The blank shape is circular. In fact, it is the best shape for a circular cup drawing. But it does not mean that a square blank is the best one for a square cup drawing. The circular cup drawn in the Swift's test is a flangeless cup. The boundary of the product is therefore set implicitly at the vertical wall of the cup and when the cup is drawn completely, the edge of the flange everywhere just reaches the boundary of the product. But there is no theoretical reason why the cup should be flangeless. The position of the boundary of the product can be set in a position depending on the purpose of the product and the completion of the drawing operation should be such that the edge of the flange anywhere first touches the boundary. In the Swift test, it is easy to locate the blank with respect to the punch and die because of the axial symmetry of both the blank and the punch and die. But in a non-circular cup drawing process, <sup>because</sup> there is no longer axial symmetry, the blank location should be taken into account. After exploring these concealments, the drawing ratio was found to be the square root of the ratio of the area of the blank to the area inside the boundary (which is roughly the area of the punch cross-section). Based on

Continued.....

this idea, the definition of drawability was generalised to be the largest draw-in at the completion of the drawing operation. With the generalised definition of drawability the performance of sheet metal in any forming process and the distinction between the drawing and the stretching actions in a forming process can be quantitatively represented.

The factors affecting the drawability such as the boundary of the product, the blank shape and size, the orientations of blank with respect to the rolling direction and to the punch and die were discussed independently first. Finally, all the factors are considered together and the conclusion is obtained that the blank for the best performance in a forming process is the largest Z.R.F. blank. Although there is no equation proposed for the shape of the Z.R.F. blank, an approximate Z.R.F. blank for a reasonable shape of cup drawing can be obtained by a few steps of cut-and-trial method.

A square cup drawing is illustrated as an example following the arguments. The arguments are well applicable to any shape of cup drawing process. Because the characteristics of a forming process are so much dependent on the shape of the cup, an index of nonsymmetry is proposed for a systematic investigation in non-circular cup drawing. The differential draw-in near the die profile region where large shearing

Continued.....

occurs is shown to be the curl of the velocity. Further investigation requires a lot of experimental work which will be discussed in the next Chapter.

The aim of this project <sup>been</sup> has <sub>A</sub> to investigate ~~the~~ sheet metal forming processes at the fundamental level. The need for such an investigation is conspicuous in the very narrow range of topics hitherto dealt with in the research papers in this area; for example, the confinement of measurements of drawability to round cups, the neglect of non-coaxial strains, the theoretical and practical consequences of non-coaxiality and the exclusion of forming conditions from concepts and the measurement of formability. In such an investigation it is inevitable that the principles unearthed cover a large theoretical area and point to many possible specific experimental studies, too wide and too many to be undertaken here. The experimental results shown in this thesis are therefore for illustrating the theory and elucidating the principles rather than for data-logging in preparation for practical applications.

Continued.....

CHAPTER 14

SUGGESTIONS FOR FUTURE WORK

Suggestions for Future Work.

Following the theoretical analysis and development in non-coaxial deformations <sup>in particular the</sup> and non-circular cup drawing process in this thesis, some suggestions for future work emerge clearly. There are two lines, one in experimental study and the other in theoretical development. In fact, they can be considered as only one line because after <sup>a</sup>certain depth of investigation in theoretical development, it is necessary to have some experimental results to support and verify the theory and the experimental results will provide hints on further investigations in the theoretical development. Some suggestions for future work are listed as follows.

(1) Non-coaxial Strain Paths.

In this thesis, non-coaxial and non-coaxial zigzag strain paths are obtained from ~~the~~ specimens of coupon form due to <sup>the</sup> huge expense of searching for non-coaxial strain paths in actual forming processes as has been explained in Chapter 10. In non-axisymmetrical forming, non-coaxial deformation is bound to be involved. In the redrawing or multiple-stage forming of non-circular shapes, the strain path of the material in the workpiece is non-coaxial and zigzag. With the strain measurement <sup>by</sup> using the square grid system, non-coaxial <sup>simple</sup> and non-coaxial zigzag strain paths in actual forming processes can be found. It is suggested that when the material in actual forming processes is found to be deformed under non-coaxial <sup>simple</sup> or non-coaxial

Continued.....

zigzag strain paths, by similarity, a simulate forming process can be made for investigation and improvement.

(2) Forming Limits of Sheet Metal.

The forming limit is the limiting strain the material can sustain under a strain path, in other words, it is the end point of the strain path under which the material is deformed. When a set of strain paths, coaxial or non-coaxial, is obtained, the precision of the forming limit curve of the material depends on the precise determination of the end points of the strain paths. As the determination of the end point of the strain path is a crucial matter in the formability of sheet metal, the material failure or the development of excessive thinning (or necking) may be further investigated so that a more precise criterion of the end point of a strain path can be established.

The comparison of forming limits among different materials requires not only a precise ~~of the~~ end point determination but also a control of the strain paths. When the forming limits of two materials are compared, they should be compared on the same basis, namely, under the same strain path. Therefore, a more reliable control of the strain path at the critical section of the workpiece in a forming process is needed.

(3) Stress-Strain Relationship and Theory of Plasticity

It has been shown theoretically in this thesis that the

Continued.....

stress-strain relationship in the non-coaxial case is different from that in the coaxial case. It is desirable to find the actual stress-strain relationship in a non-coaxial case so that a comparison between coaxial and non-coaxial cases can be made.

It may be difficult to find the stress in an unsymmetrical forming product. But with a special device, for example, rotating the punch when it is proceeding in a drawing process (fig. 14-1) with the central part of the blank fixed to the punch head, so that twisting occurs in the workpiece in the forming process, the stress in the workpiece may be obtainable after some calculations. As shown in fig. 14-1,

$$P = 2 \pi r \sin \phi \sigma_s t \quad 14-1$$

$$T = 2 \pi r \cdot r t \cdot \tau \quad 14-2$$

where  $P$  is the punch load;  $r$ , the current radius of a point in the workpiece;  $\phi$ , the slope of the profile;  $\sigma_s$ , the tensile stress in the meridional direction;  $T$ , the torque applied to rotate the punch;  $t$ , the current thickness of the workpiece and  $\tau$ , the shear stress along the circumferential tangential direction. From Eqs. 14-1 and 14-2,

$$\frac{\sigma_s}{\tau} = \frac{P}{T} \frac{r t}{\sin \phi} \quad 14-3$$

Continued.....

If  $\tau = 0$  or  $T = 0$ , the directions of the principal axes of stress and strain are in the meridional and the circumferential tangential directions respectively. If  $\tau \neq 0$ , then because of the shear stress, the principal axes of stress will shift from the meridional and the circumferential tangential directions. Therefore, the deformation in the workpiece is non-coaxial. By using Eq. 14-3 and the equation for membrane stresses, the stresses and the directions of the principal axes of stress with respect to the material can be found. The strain, by using the square grid system for strain measurement, can also be obtained. The relation between the stresses and the strains ~~would therefore be~~ obtained. By changing the punch penetration and the punch rotating speed in the forming operation, another ratio of the stress  $\sigma_s$  to the shear stress  $\tau$  in Eq. 14-3 can be obtained. Therefore, a set of stress — strain relations in the non-coaxial case ~~would be~~ found.

With these experimental results, the theory of plasticity including the strain-hardening, the deviation of the stress-strain relation from that in <sup>the</sup> Lévy-Mises equations in the non-coaxial case can be greatly extended.

#### (4) Drawability of Sheet Metal.

The drawability of a sheet metal used to mean the performance of the material in a circular cup drawing process as the limiting drawing ratio in the Swift test. With the

Continued.....

generalised definition of drawability, namely, the largest draw-in, it is possible to represent the drawability of the material in any forming process including the circular cup drawing process.

It is useful to have the limiting drawing ratio shown in a handbook for sheet metal properties. If the drawabilities of sheet metal in other shapes of cup drawing processes can be provided in a handbook as well, it would be more useful for applications because the limiting drawing ratio provides very little information on the performance of the material in a non-circular cup drawing process. Therefore, in the future work, the drawability of sheet metal if not in all possible shapes of sheet metal forming products, at least, in some popular shapes like squares, rectangles and elliptical shapes of cup drawing processes could be pursued and shown in a handbook.

The index of nonsymmetry is proposed to specify the characteristic of a forming process. Of course, there may be some other representations for this index. For example, the length of the periphery of the shape could be used instead of the position angle  $\theta$  (Chapter 12) so that the index of nonsymmetry is represented as follows:

$$\xi' = \frac{1}{S} \int_0^S \left| \frac{\frac{1}{\bar{r}}}{\left(\frac{1}{\bar{r}}\right)_{av.}} - 1 \right| dS \quad 14-4$$

Continued.....

where  $S$  is the length of the periphery.

The index of nonsymmetry defined in Eq. 14-4 is related to that defined in Eq. 12-9. It is rather more complicated but is more powerful when the shape is irregular and without any plane of symmetry.

With the experimental results, the relation between the drawability of sheet metal and the index of nonsymmetry can be found. This would be extremely useful for practical applications as well as for the sheet metal forming designer.

ACKNOWLEDGEMENTS

&

BIBLIOGRAPHY

ACKNOWLEDGEMENTS

The author gratefully acknowledges all who have offered their assistance towards the project, especially to his Supervisor, Professor T.C. Hsü, for the valuable guidance and advice received. The author is also grateful to Professor A.J. Ede, Head of the Department of Mechanical Engineering, and Professor R.H. Thornley, Head of the Department of Production Engineering, for permitting the use of all <sup>the</sup> equipment in the Departments as well as the assistance of all <sup>the</sup> technicians within the two Departments.

The author is greatly indebted to Miss S. Bird for the typing of the manuscript.

BIBLIOGRAPHY

1. S.P. Keeler, Determination of Forming Limits in Automotive Stampings, Sheet Metal Industries, 42, 1965, 683-691.
  
2. S.P. Keeler & W.A. Backofen, Plastic Instability and Fracture in Sheets Stretched Over Rigid Punches, Trans, A.S.M., 56, 1963, 25-48.
  
3. S. P. Keeler, Understanding Sheet-metal Formability, Part IV, Sheet Metal Industries, 48 1971, 589-618.
  
4. G. M. Goodwin, Application of Strain Analysis to Sheet Metal Forming Problems in the Press Shop, la metallurgia italiana, I.D.D.R.G. 5th biennial congress on sheet metal forming and testing, 60(8), 1968, 767-774.
  
5. P. K. Lee & T. C. Hsü, Four Aspects of Sheet Metal Formability and Their Assessment, J. of Testing and Evaluation, JTEVA, 1, No. 3, 1973, 244-249.

Continued.....

6. American Deep Drawing Research Group, Analysis of Sheet Metal Formability, I.D.D.R.G., 1972, Amsterdam.
7. C. Chr. Veerman, Hoogovens-IJmuiden BV, The Determination and Application of the FLC-Onset of Localised Necking, I.D.D.R.G., 1972, Amsterdam.
8. T. Kobayashi, H. Ishigaki & T. Abe, Effect of Strain Ratios on the Deforming Limit of Steel Sheet and its Application to Actual Press Forming, I.D.D.R.G., 1972, Amsterdam.
9. P. Brozzo & B. De Luca, On the Interpretation of the Formability Limits of Metal Sheets and Their Evaluation by Means of Elementary Tests, Proceedings ICSTIS, Suppl. Trans. ISIJ, 11, 1971, 966-968.
10. T. Matsuoka & C. Sudo, The Effect of Strain Path on the Fracture Strain of Steel Sheets, The Sumitomo Search, No. 1, 1969, 71-80.

Continued.....

11. H. Kubotera & Y. Ueno, Influence of Strain History on Formability of Steel Sheet, Nippon Kokan Technical Report - Overseas, 1975, 19-25.
12. T. Kobayashi, H. Iida & S. Sato, Deformation Analysis in Press Forming of Autobody Parts, Proceedings ICSTIS, Suppl. Trans. ISIJ, 11, 1971, 837-841.
13. G.S.A. Shawki, Assessing Deep-Drawing Qualities of Sheet, Sheet Metal Industries, 42, 1965, 363-368; 417-424; 524-532.
14. A.M. Erichsen, Ein neues Prüfverfahren für Feinblech, Stahl und Eisen, 34, 1914, 879-882.
15. B. Kaftanoglu & J. M. Alexander, An Investigation of the Erichsen Test, J. of the Institute of Metals, 90, 1961-62, 457-470.
16. W.F. Brown Jr. & G. Sachs, Strength and failure characteristics of thin circular membranes, Trans. ASME, 70, 1948, 241-249.

Continued.....

17. P.B. Mellor, Stretch forming under fluid pressure, J. Mech. Phys. Solids, 5 (1), 1956, 41-56.
18. J. Chakrabarty & J.M. Alexander, Hydrostatic Bulging of Circular Diaphragms, J. of Strain Analysis, 5, No. 3, 1970, 155-161.
19. R. Hill, A Theory of the Plastic Bulging of a Metal Diaphragm by lateral pressure, Phil. Mag. 41. (Ser.7) 1950, 1133-1142.
20. B. Storakers, Finite Plastic Deformation of a Circular Membrane Under Hydrostatic Pressure, International J. of Mechanical Sciences, 8, 1966, 619-628.
21. T.C. Hsü, H.M. Shang, T.C. Lee & S.Y. Lee, Flow Stresses in Sheet Material Formed Into Nearly Spherical Shapes, ASME Winter Annual Meeting 1974, Paper No. 74-WA/Mat.-1.
22. H.W. Swift, Drawing Test for Sheet Metal, Proceedings, The Institution of Automobile Engineers, 34, 1939-40, 361-432.

Continued.....

23. S.Y. Chung & H. W. Swift, Cup-drawing from a flat blank, Proceedings, I. Mech. E., 165, 1951, 199-228.
24. H.W. Swift, The Mechanism of a Simple Deep-drawing Operation, Sheet Metal Industries, 31, 1954, 817-828.
25. I. Blume, Ermittlung der ziefahigkeit von tiefstanzblechen, Metallborse, 12, 1922, 1945-1946.
26. G.R. Fischer, A.E.G. tiefziehprufverfahren, A.E.G. Mitterlungen, 1, 1929, 483-486.
27. M. Schmidt, Die prufung von tiefziehblech, Arch. Eissenhutzenwesen, 3, 1929, 213-222.
28. I.D.D.R.G. WG III- Recommended procedure for carrying out the Swift - I.D.D. R.G. cup forming test - I.D.D. R.G./WG, III (14A), 67.
29. D.V. Wilson, B.J. Sunter & D.F. Martin, A Single-blank Test for Draw-ability, Sheet Metal Industries, 43, 1966, 465-476.

Continued.....

30. J.C. Wright, The phenomenon of Earing in Deep Drawing, Sheet Metal Industries, 42, 1965, 814-831.
31. M. Atkinson & I.M. Maclean, Normal Plastic Anisotropy in Sheet Steel, Sheet Metal Industries, 42, 1965, 290-298.
32. L. Lilet & M. Wybo, The Effect of Plastic Anisotropy and Rate of Work-hardening in Deep Drawing, Sheet Metal Industries, 41, 1964, 783-815.
33. K.M. Frommann & W.F. Barclay, A Theoretical Analysis of the Influence of Normal Anisotropy  $r$ , and Strain Hardening Exponent  $n$ , on the Drawability of Sheet Metal, Proceedings ICSTIS, Suppl. Trans. ISIJ, 11, 1971, 897-902.
34. T. Kobayashi, Deformation Analysis in Press Forming of Autobody Parts, Proceedings ICSTIS, Suppl. Trans. ISIJ, 11, 1971, 837-841.
35. Y. Hayashi, C. Sudo & M. Kozima, The Study on Press Formability in Forming of Automotive Panel, I.D.D.R.G. 1972, Amsterdam.

Continued.....

36. S.D. Brootzkooos, How to calculate Blanks for Seamless Rectangular Shells, American Machinist, 93, 1949, 67-72.
37. S. Fukui, Studies on the Deep-Drawing of Rectangular Shells, Rept. Inst. Sci. Tech., University of Tokyo, 5, 1951, 121-133, (In Japanese).  
H. Takeyama &  
K. Yoshida,
38. S. Fukui, Studies on the Deep-Drawing of Square Shells, Rept. Inst. Sci. Tech., University of Tokyo, 8, 1954, 13-22. (In Japanese).  
H. Takeyama,  
K. Yoshida &  
H. Okawa,
39. K. Miyauchi & Hydroforming and Rigid-Die Forming in Deep-Drawing of Square Shells, Rept, I.P.C.R., 41 (2), 1965, 91-112. (In Japanese).  
S. Fukui,
40. M. Masuda & On the Plastic Deformation of Rectangular Drawing, Trans. Jap. Soc. Mech. Eng., 18, 1952, 94-97. (In Japanese).  
O. Mishiro,

Continued.....

41. L. Lilet, Suitability of Sheets for Pressing, Sheet Metal Industries, 43, 1966, 949-957.
42. D.V. Wilson, Controlled directionality of mechanical properties in sheet metals, Metallurgical Reviews, (Metals and Materials), 14, 1969, 175-188.
43. K. Miyauchi, Non-axisymmetric Combined Punch-  
K. Yoshida & Stretching Characteristics and  
C. Sudo, Combined Punch-stretchability of Sheet Metals, Rept. I.P.C.R., 45 (3), 1969, 55-71, (In Japanese).
44. K. Yoshida, Classification and Systematization of Sheet Metal Press-Forming Process, Sci. Pap. I.P.C.R., 53, 1959, 125-187.
45. K. Yoshida, Peculiarity of Deep Drawing of  
H. Ueno, Elliptic<sup>Shells</sup> with Respect to Material  
U. Furukawa, Flow, Rept. I.P.C.R., 47 (6),  
T. Mori, & 1971, 230-241. (In Japanese).  
T. Nakagawa,

Continued.....

46. K. Yoshida, Fracture Behaviour, Forming  
K. Yoshii, Severity and Metal Flow in Deep  
H. Komorida & Drawing of Irregular-shaped  
K. Miyauchi, Shells, I.D.D.R. G. 1972,  
Amsterdam.
47. T.C. Hsü, Some Implications of Non-  
coaxiality in Finite Deform-  
ations, Transactions, A.S.M.E.,  
Series H, 95, 1973, 87-93.
48. T.C. Hsü, A Study of Large Deformations  
by Matrix Algebra, J. of Strain  
Analysis, 1 (4), 1966, 313-321.
49. T.C. Hsü, The Effect of the Rotation of  
the Stress Axes on the Yield  
Criterion of Prestrained  
Materials, A.S.M.E., Paper No.  
65-WA/Met.-4, 1965.
50. T.C. Hsü, The Characteristics of Coaxial  
and Non-coaxial Strain Paths,  
J. of Strain Analysis, 1 (3),  
1966, 216-222.

Continued.....

51. T.C. Hsü, Strain Histories and Strain  
W.R. Dowle, Distributions in a Cup Drawing  
C.Y. Choi & Operation, A.S.M.E., Paper No.  
P.K. Lee, 70-WA/Prod-6.
52. R. Hill, The Mathematical Theory of  
Plasticity. Chapter II, Oxford  
Clarendon Press, 1950.
53. W. Johnson & P.B. Plasticity For Mechanical  
Mellor, Engineers, Chapter 5. Van Nostrand,  
1962.
54. Hugh Ford & Advanced Mechanics of Materials,  
J.M. Alexander Chapter 26, Longmans.
55. B. de Saint-Venant, Comptes Rendus Acad, Sci, Paris,  
70, 1870, 473.
56. M. Levy, Journ. Math. pures et app. 16,  
1871, 369.
- 57 R. von Mises, Gottingen Nachrichten, math-phys.,  
Klasse, 1913, 582.
58. L. Prandtl, Proc. 1st Int. Cong. App. Mech.,  
Delft, 1924, 43.

Continued.....

59. A. Reuss, Zeits. ang. Math. Mech. 10,  
1930, 266.
60. T.C. Hsü & On the Measurement of Deep  
S. Y. Lee, Drawability of Sheet Metal in  
Non-circular Cups. (In Press).
61. T.C. Hsü & On the Drawability of Sheet  
S. Y. Lee, Metal in Non-circular Cups.  
(In Press).
62. T.C. Hsü, Present scope and future trend  
of sheet metal forming research,  
Int. J. Prod. Res., 12 (1),  
1974, 99-115.

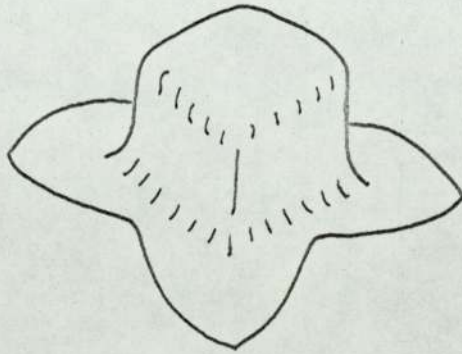
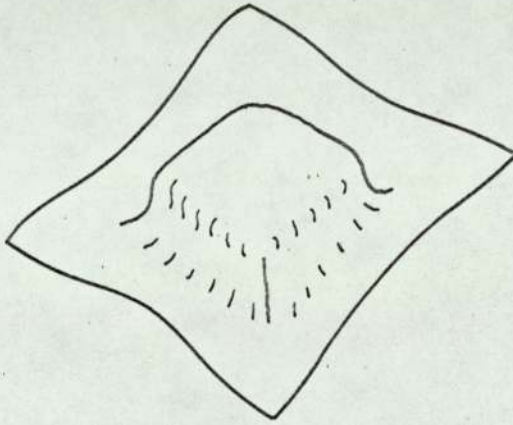
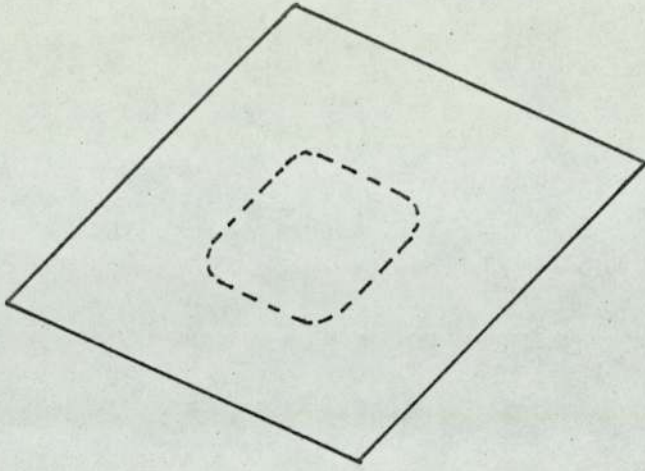
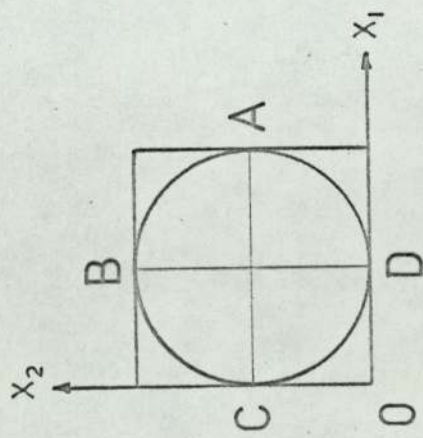
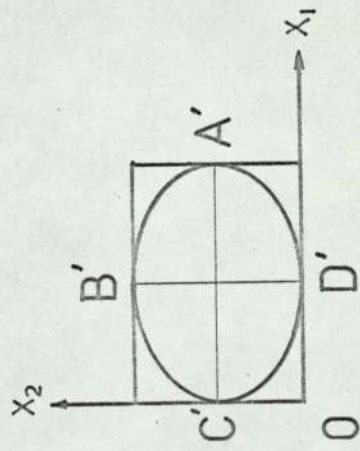


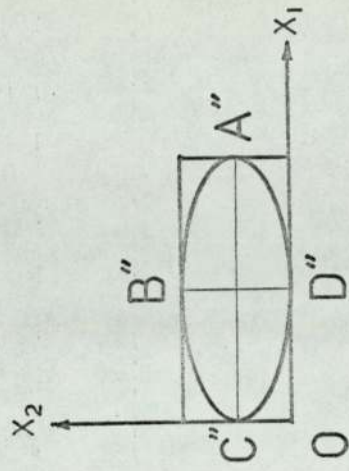
Fig. 1 - 1



(a)

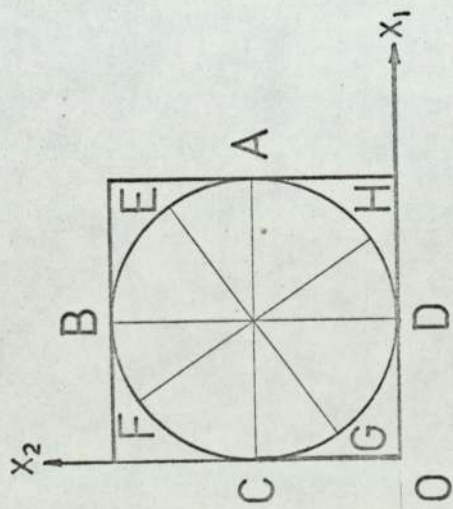


(b)

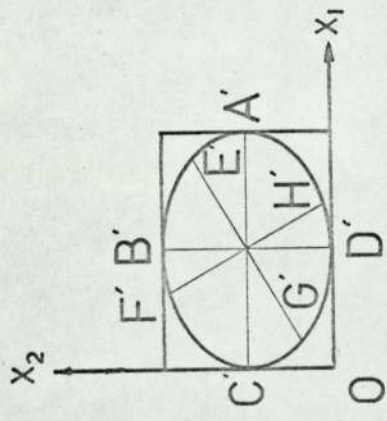


(c)

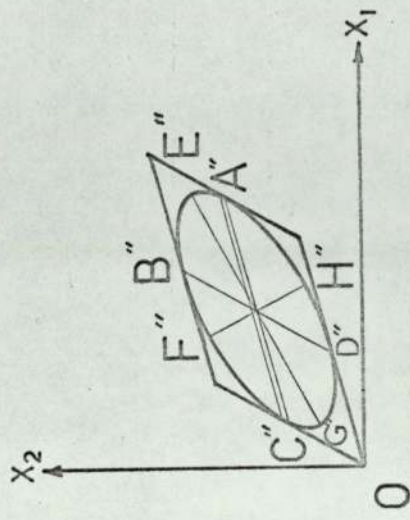
Fig. 1 - 2



(a)

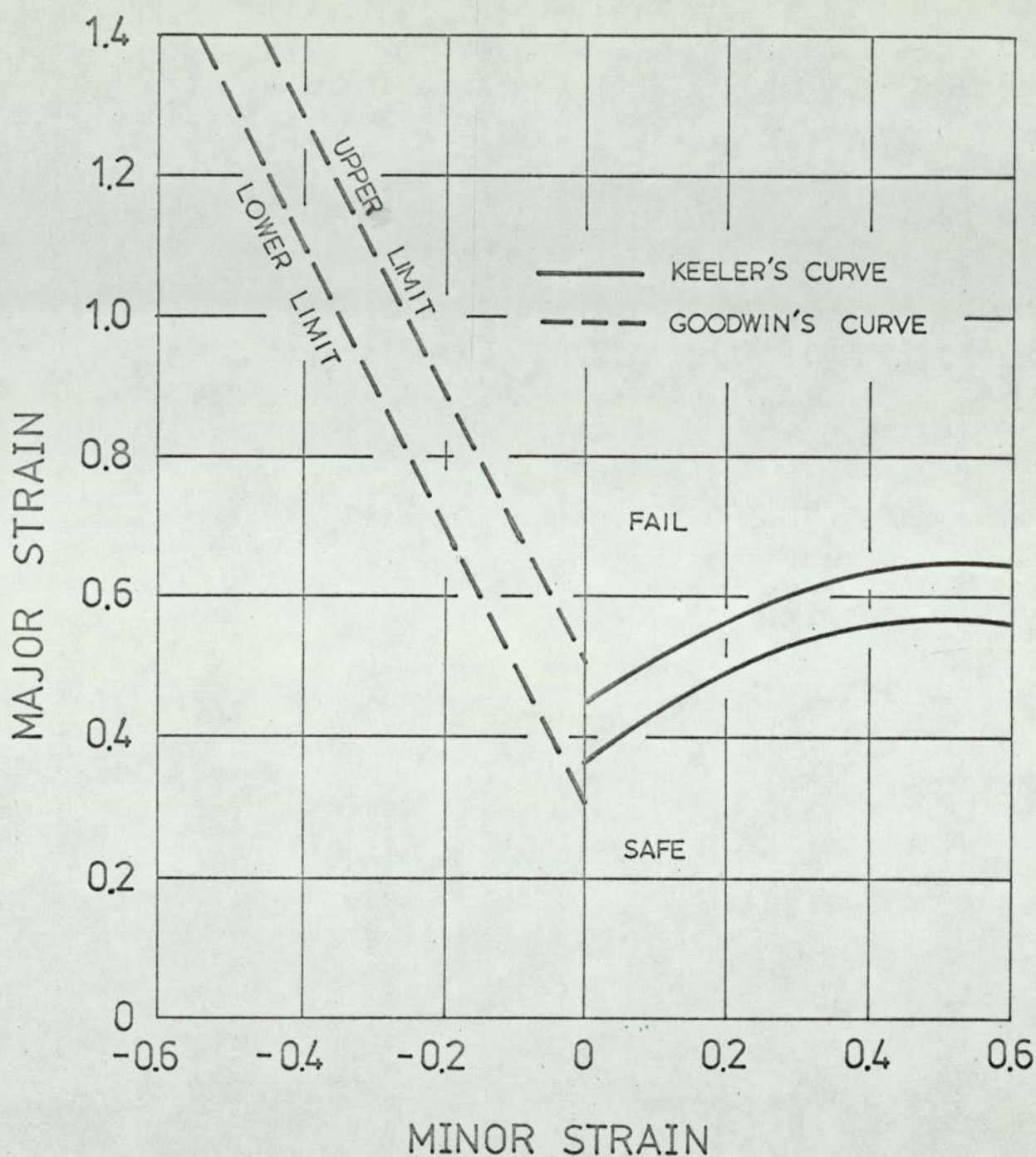


(b)



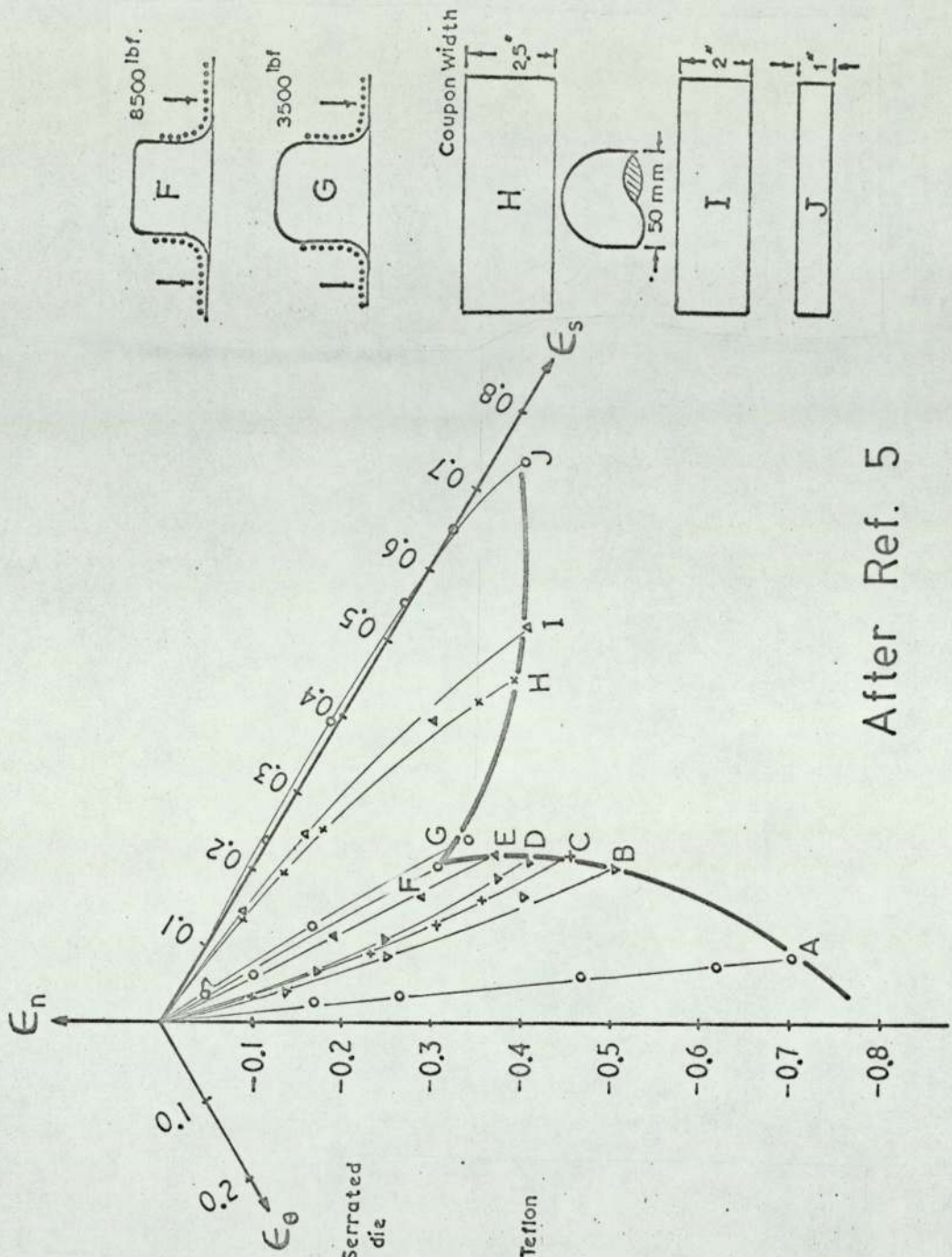
(c)

Fig. 1 - 3



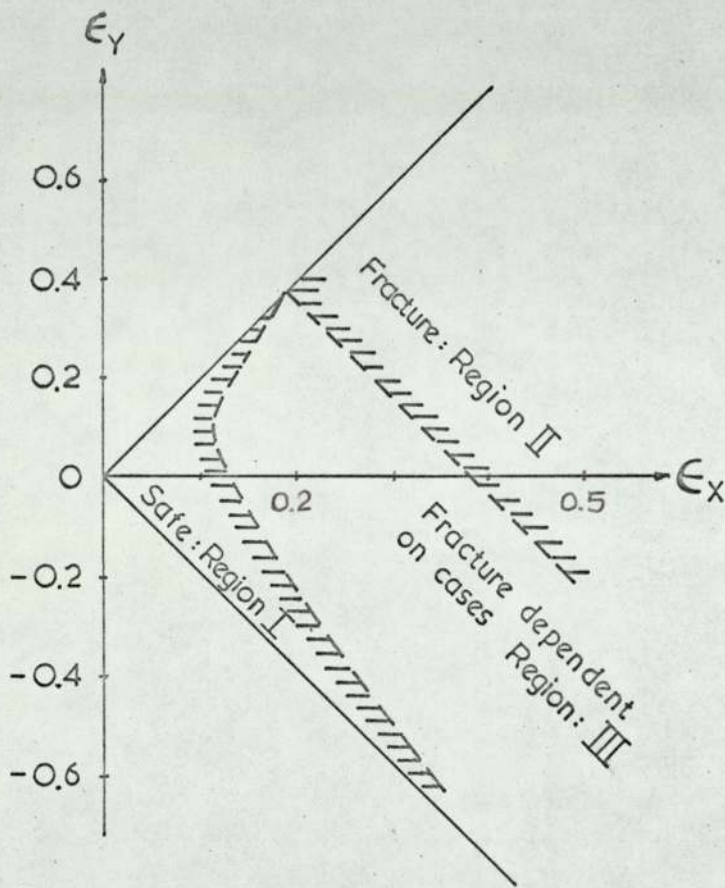
After Ref. 4

Fig. 3 - 1



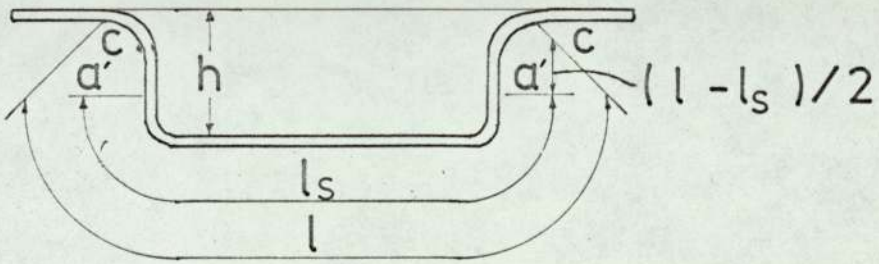
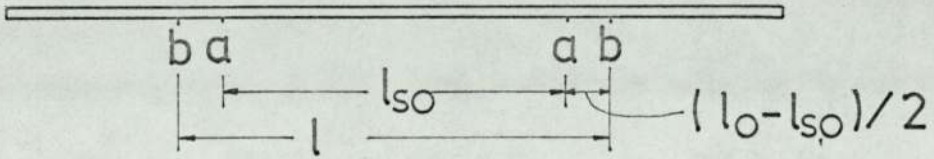
After Ref. 5

Fig. 3 - 2



After Ref. 10

Fig. 3 - 3



After Ref. 43

Fig. 3 - 4

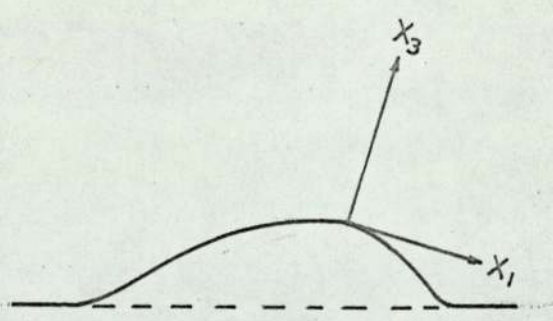
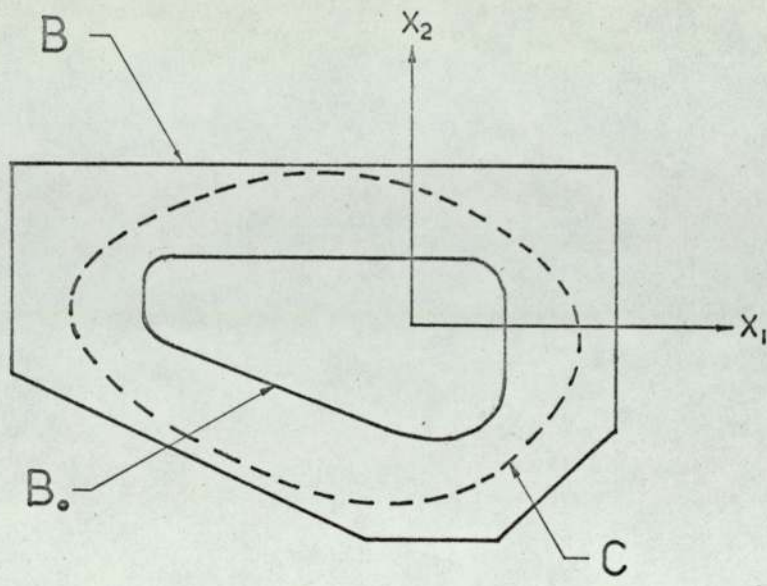


Fig. 4 - 1

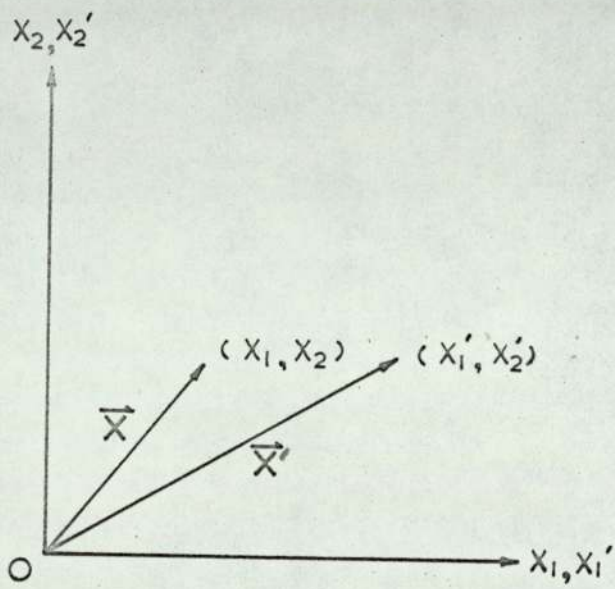


Fig. 4 - 2

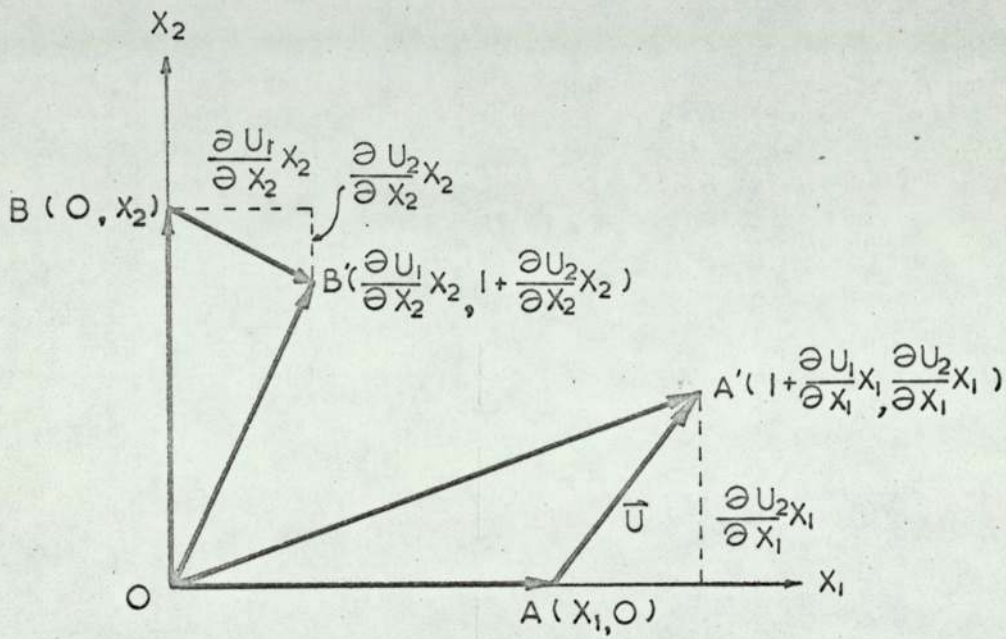


Fig. 4 - 3

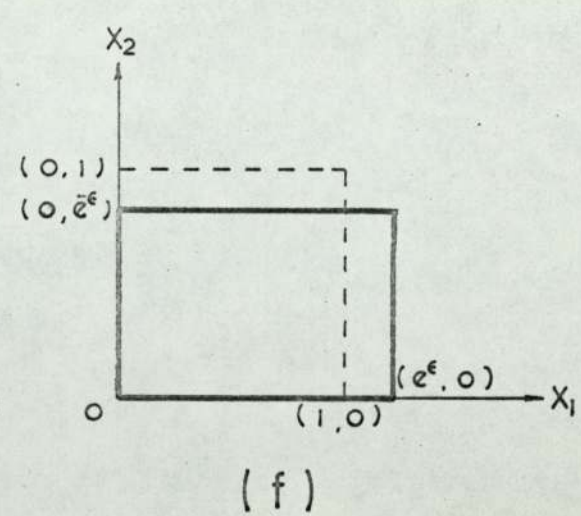
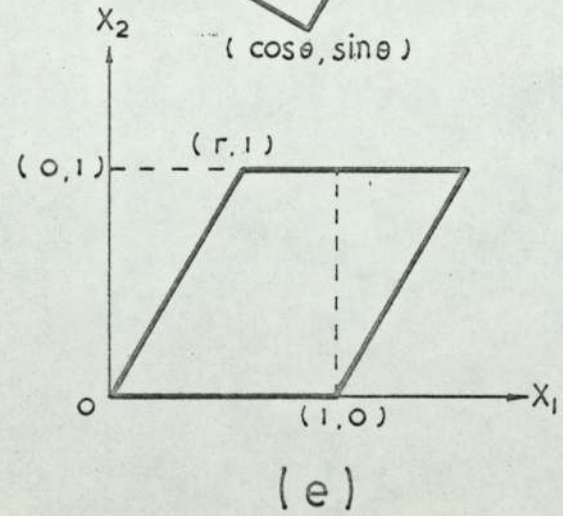
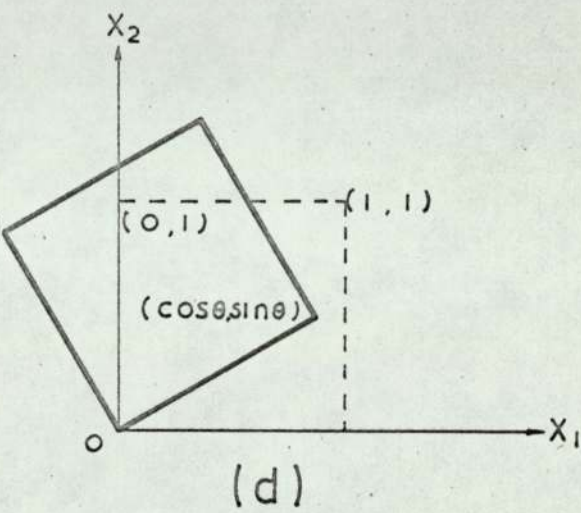
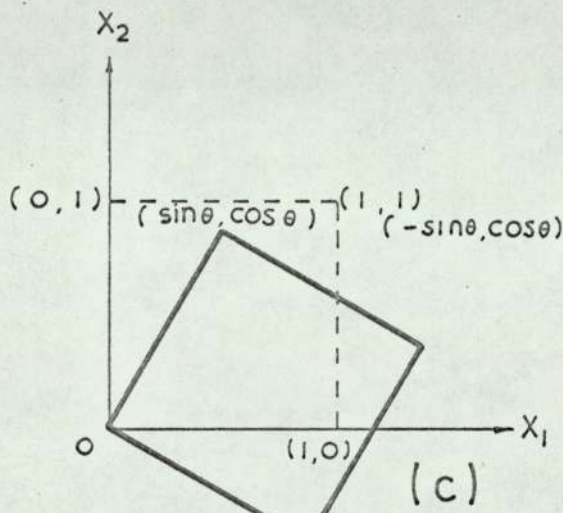
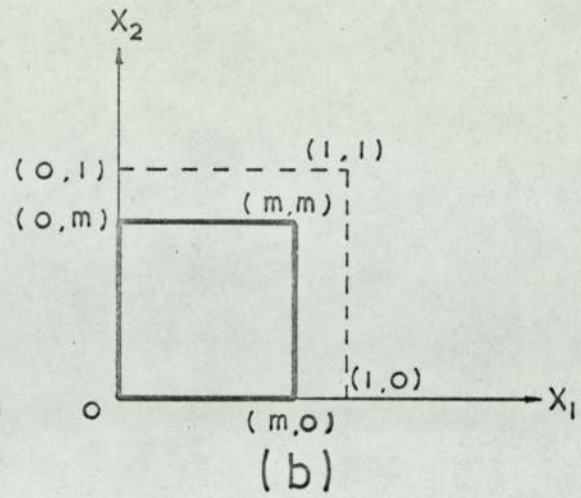
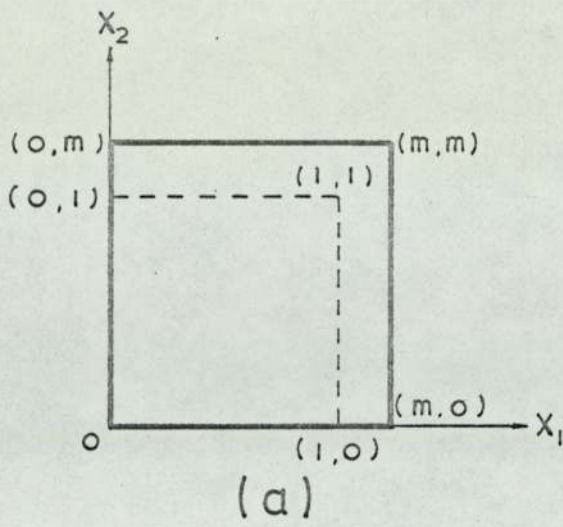


Fig. 4 - 4

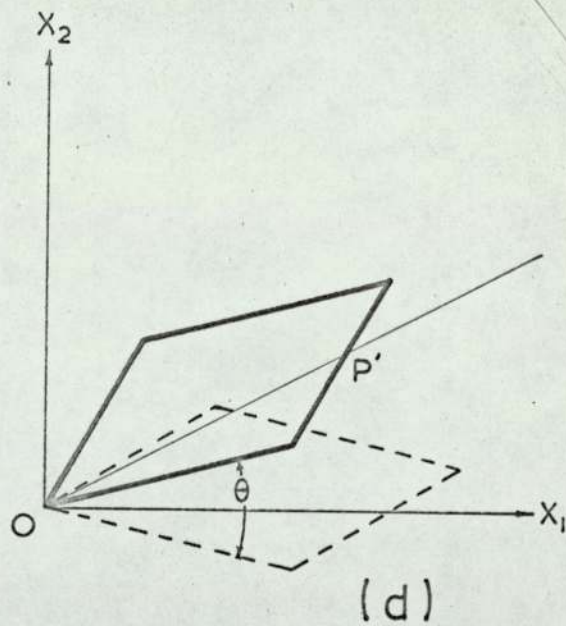
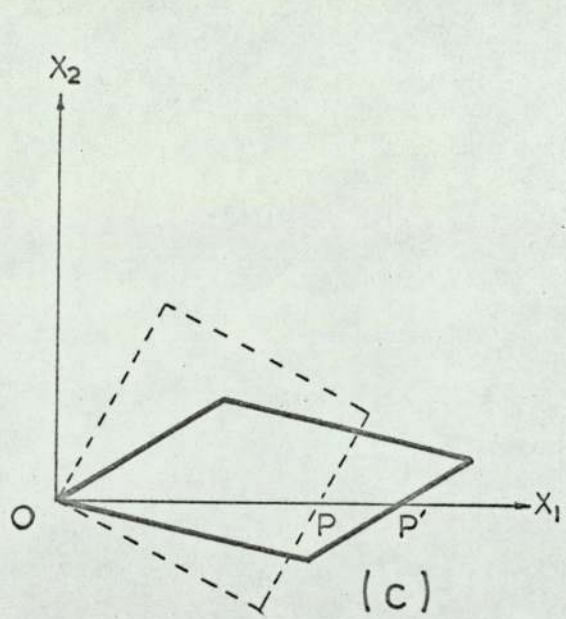
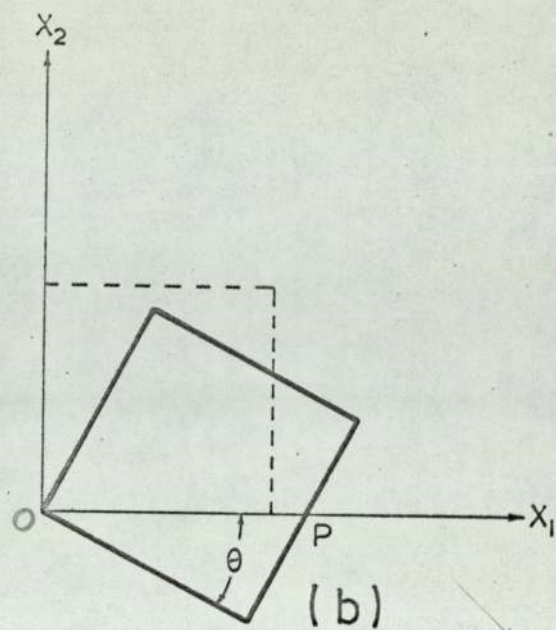
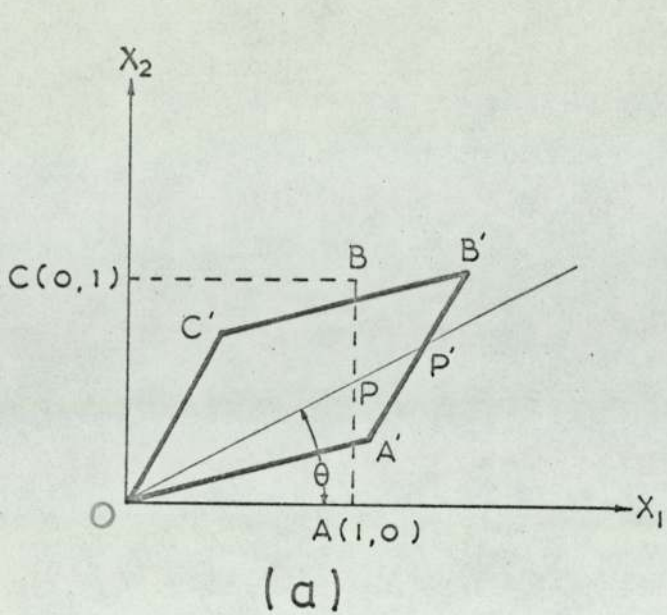


Fig. 4 - 5

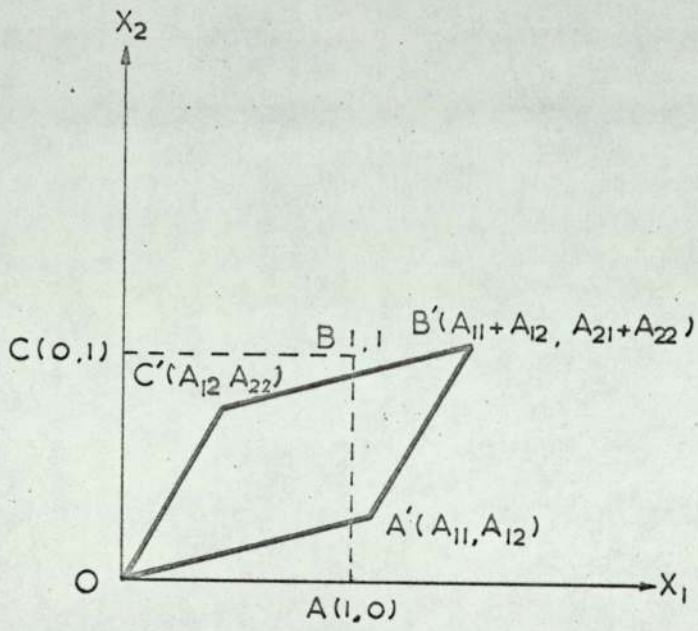


Fig. 4 - 6

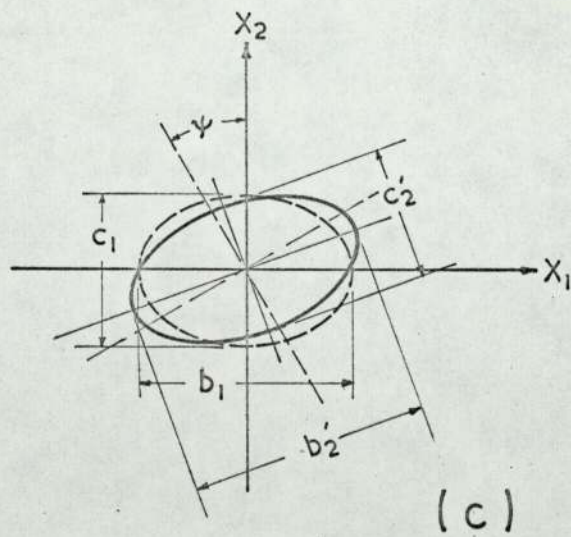
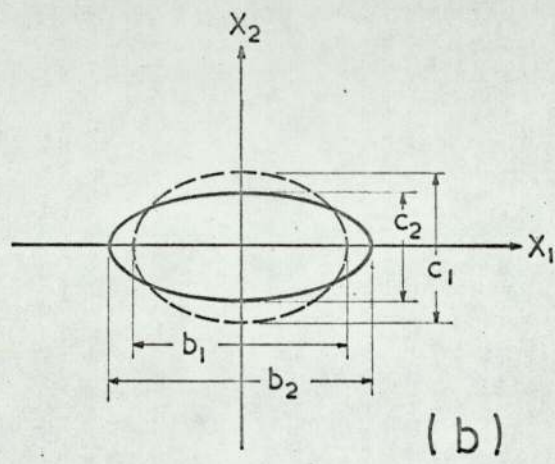
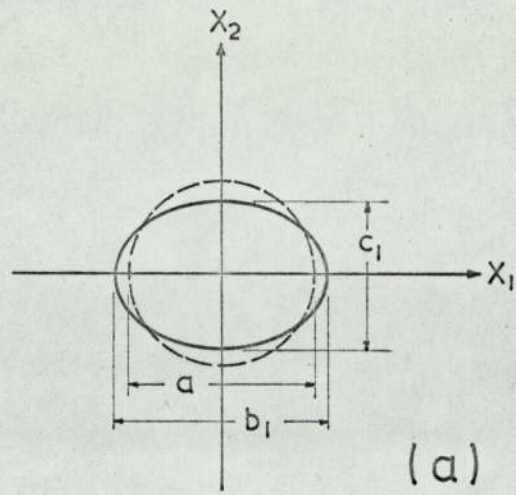
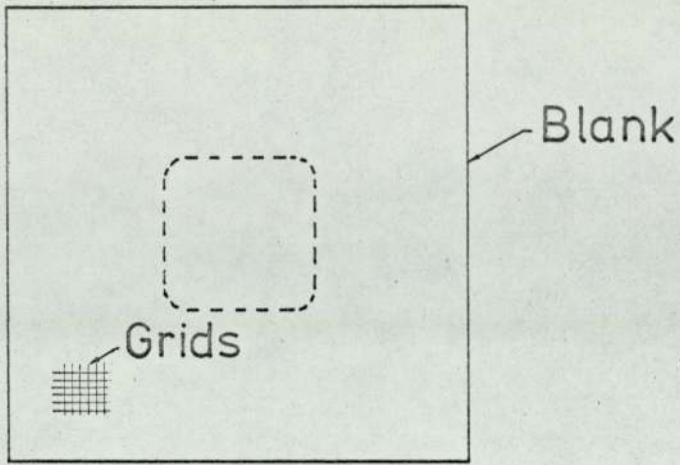
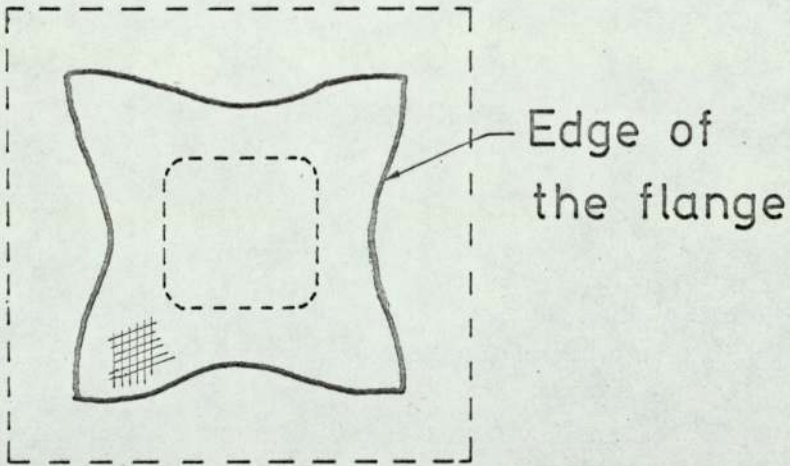


Fig. 4 - 7



(a)



(b)

Fig. 4 - 8

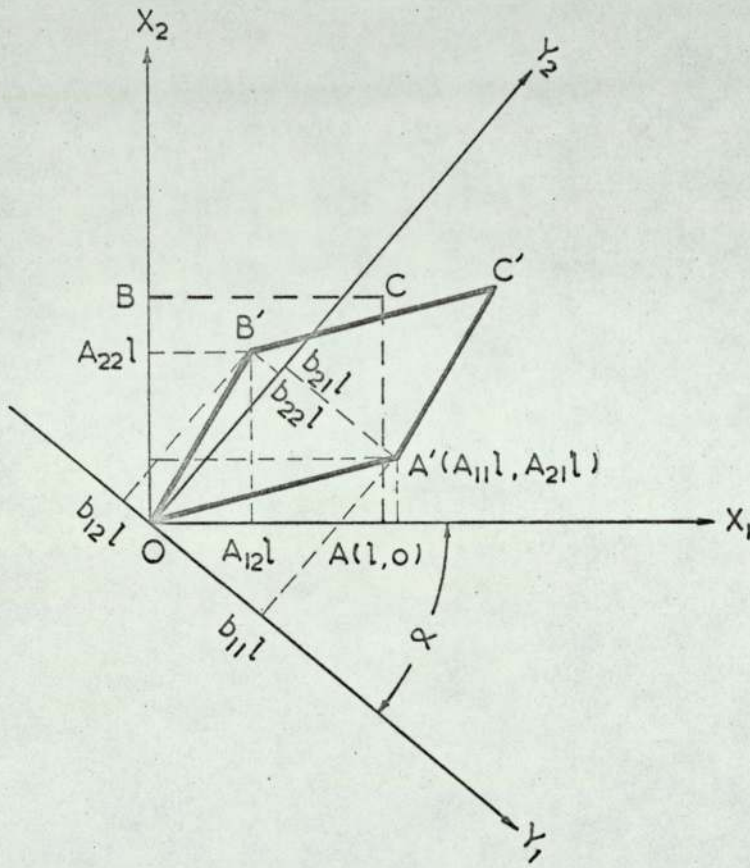


Fig. 4 - 9

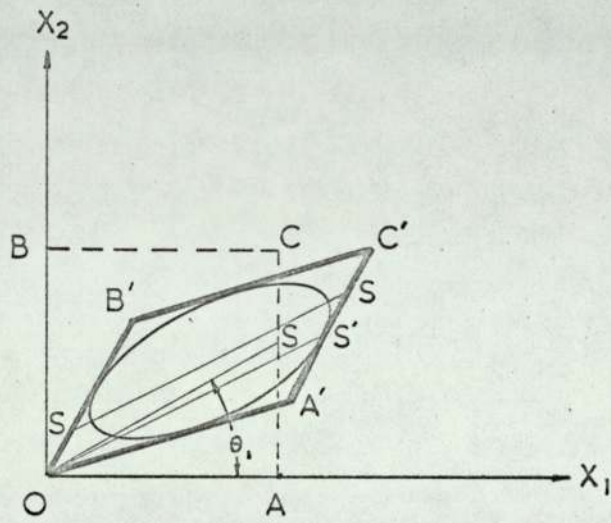


Fig. 4 - 10

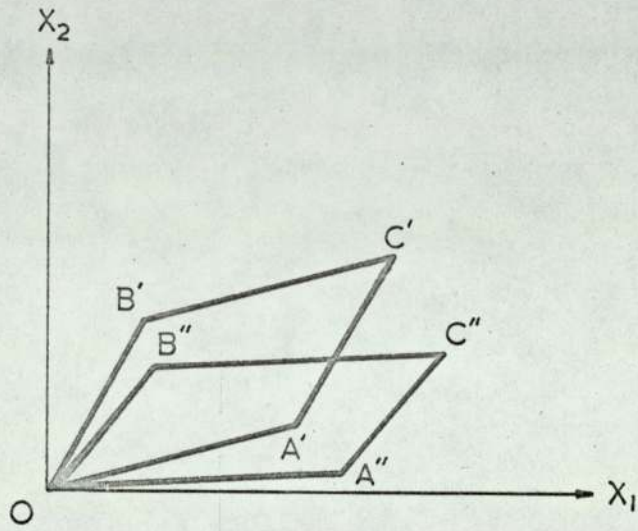


Fig. 4 - 11

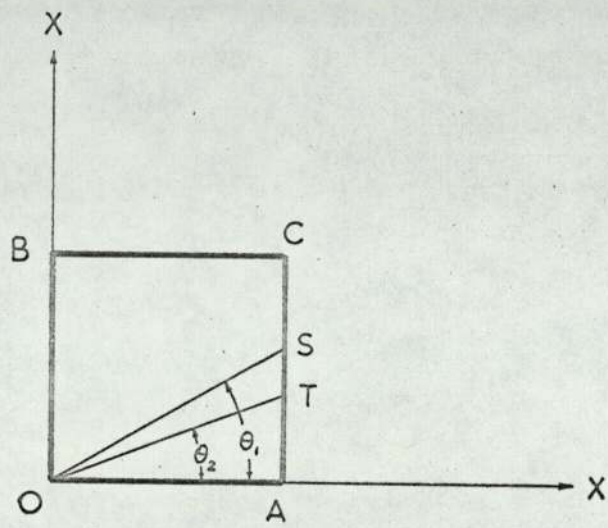


Fig. 4 - 12

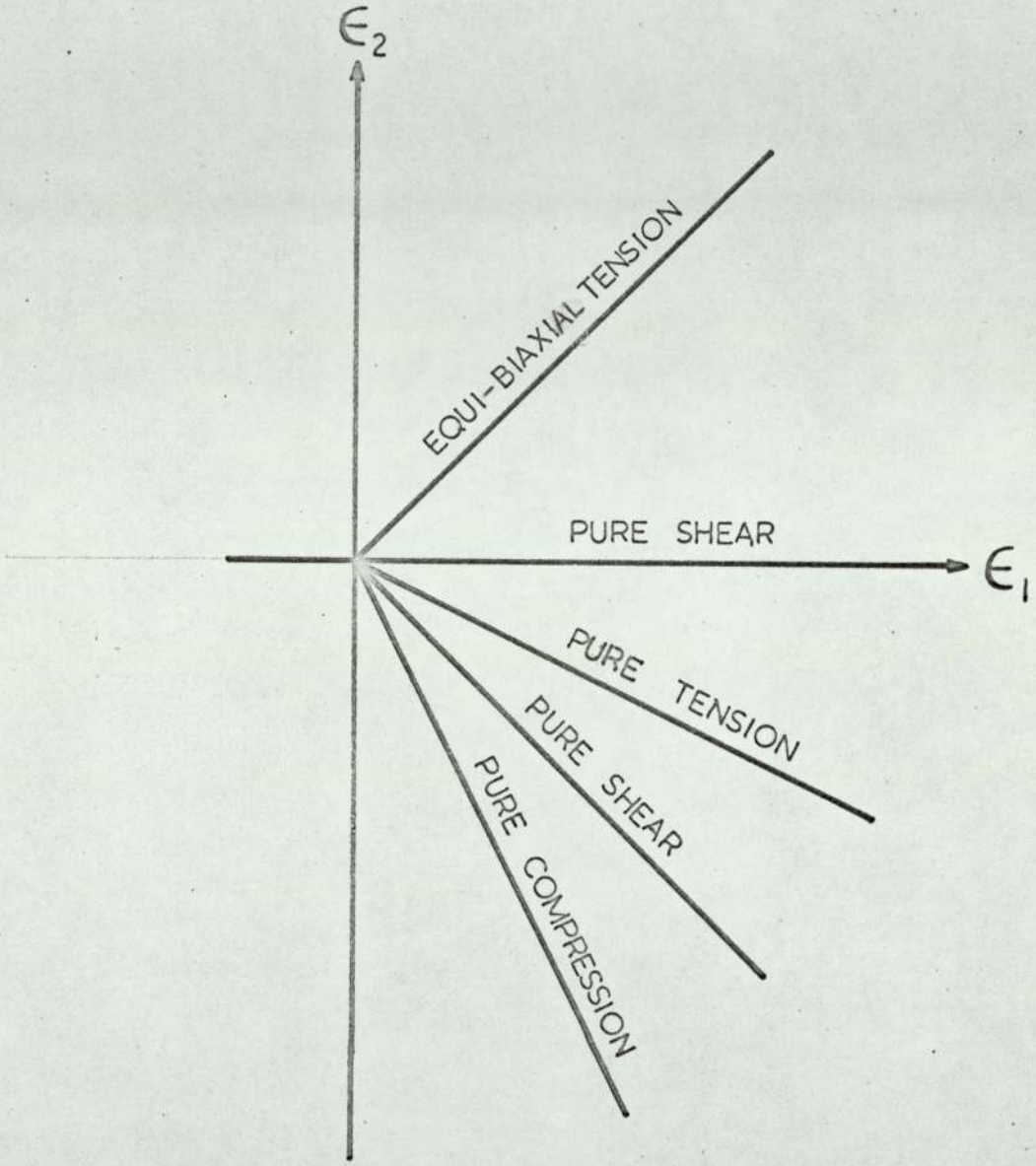


Fig. 5 - 1

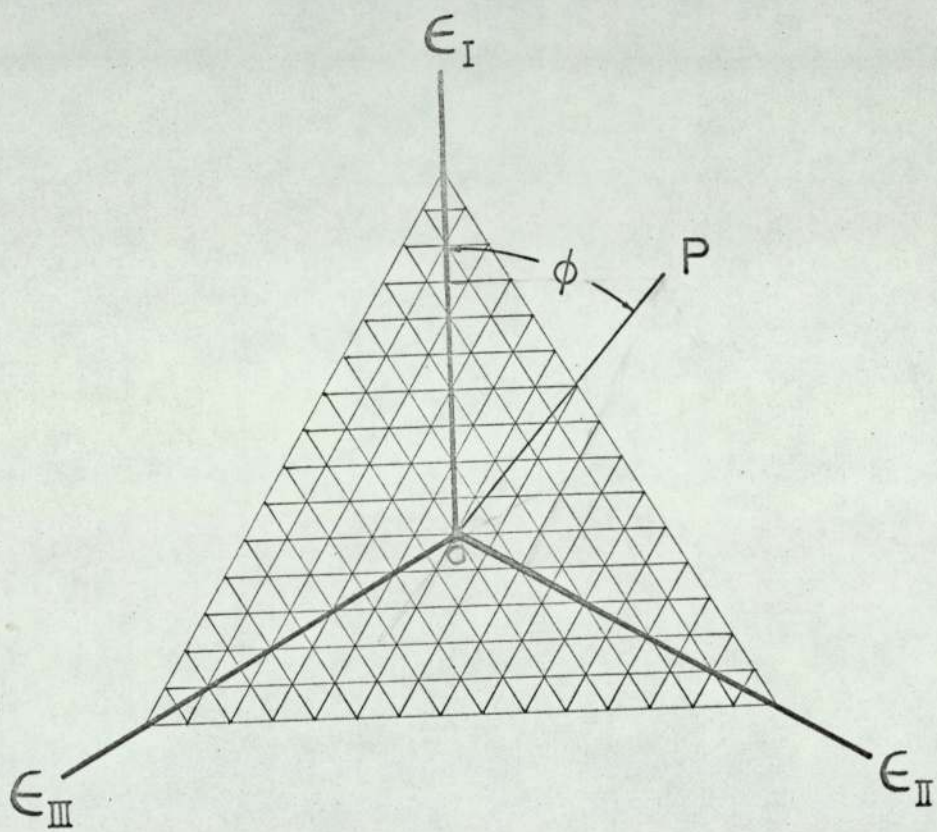


Fig. 5 - 2

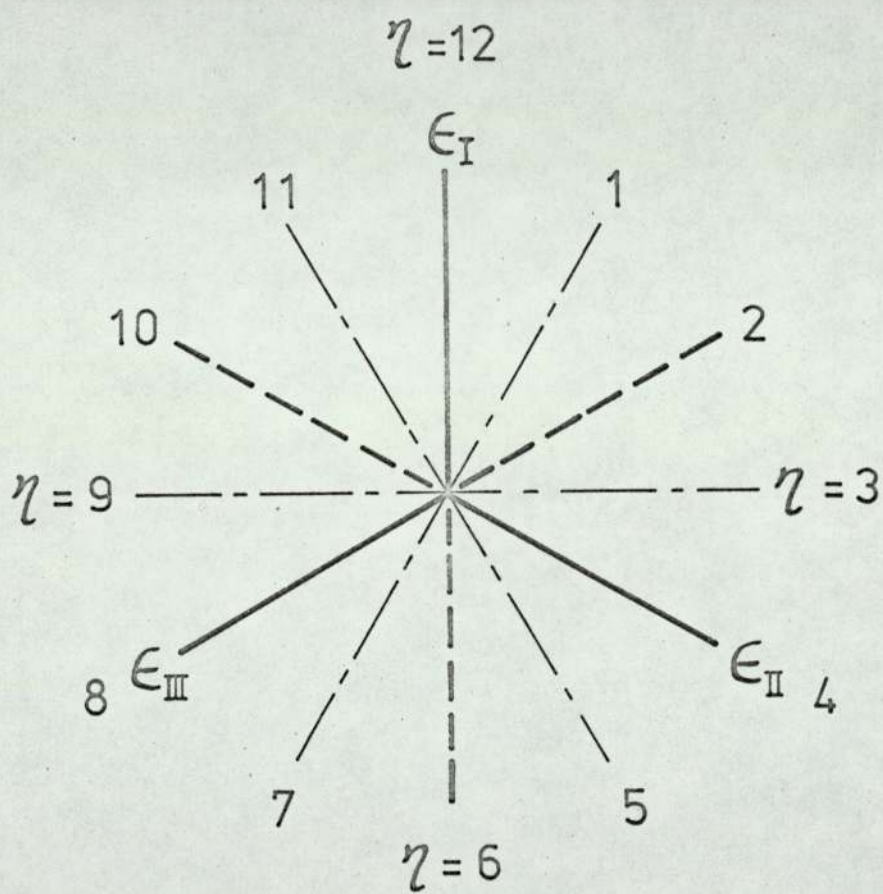


Fig. 5 - 3

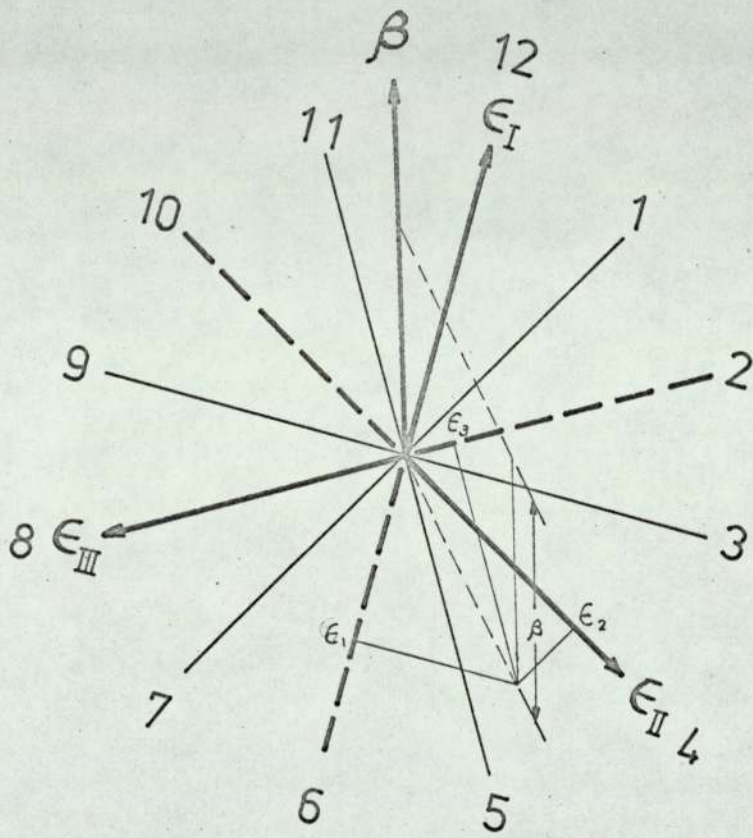


Fig. 5 - 4

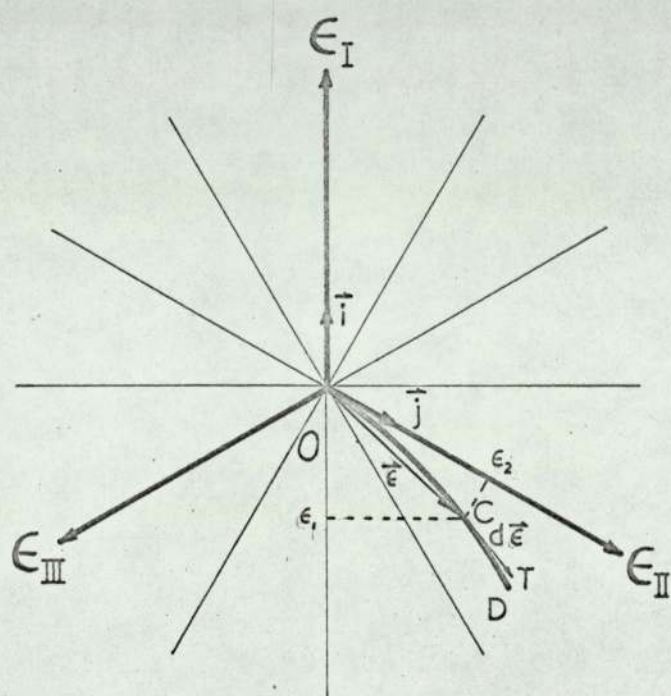


Fig. 5 - 5

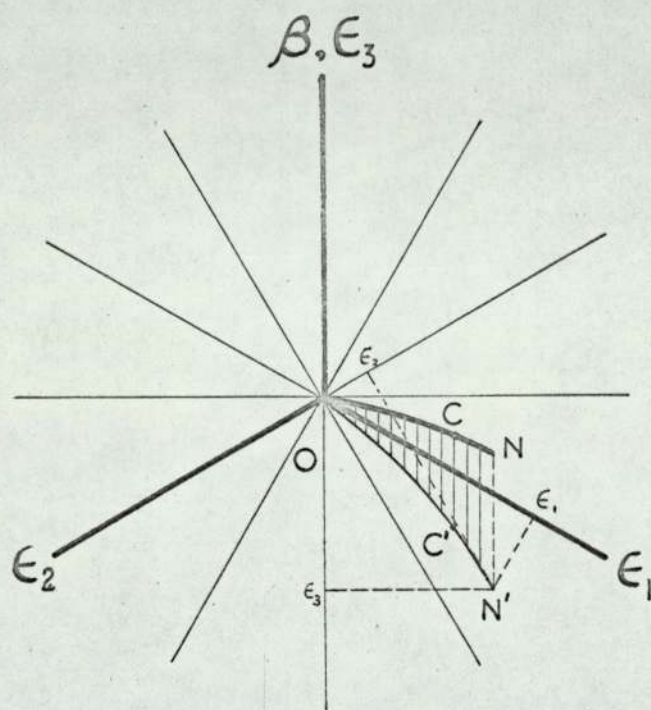


Fig. 5 - 6

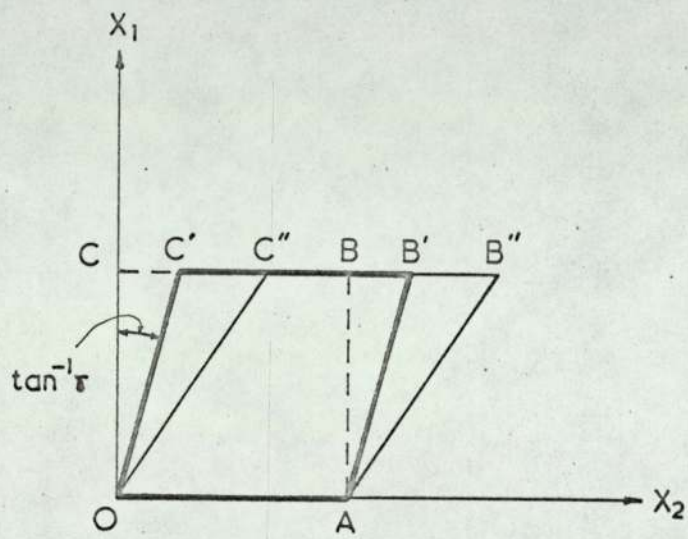


Fig. 5 - 7

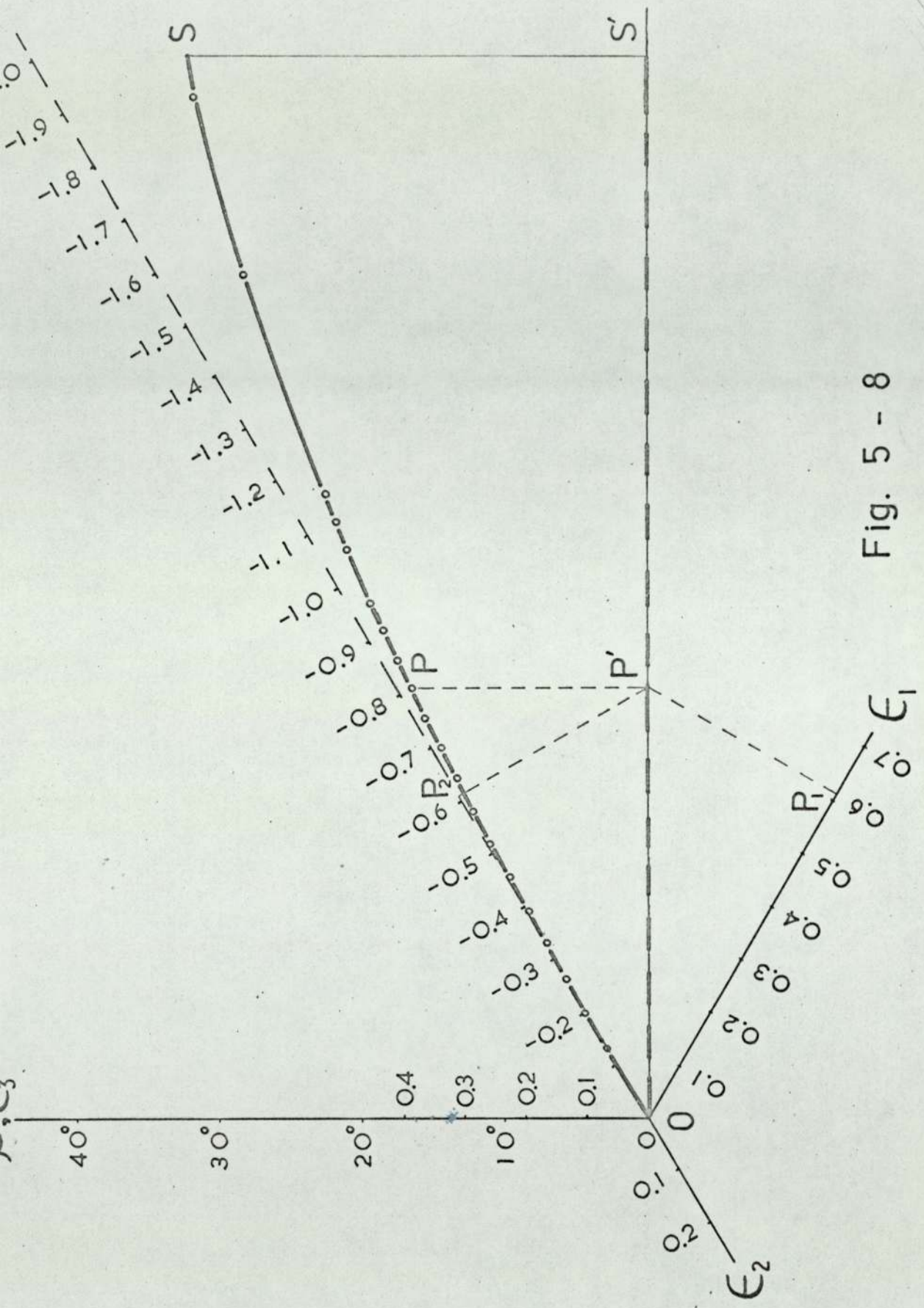


Fig. 5 - 8

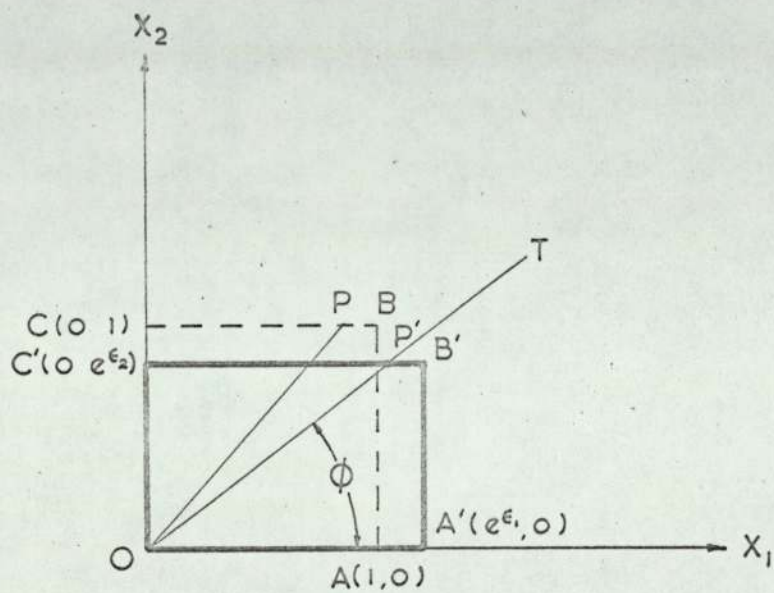


Fig. 6 - 1

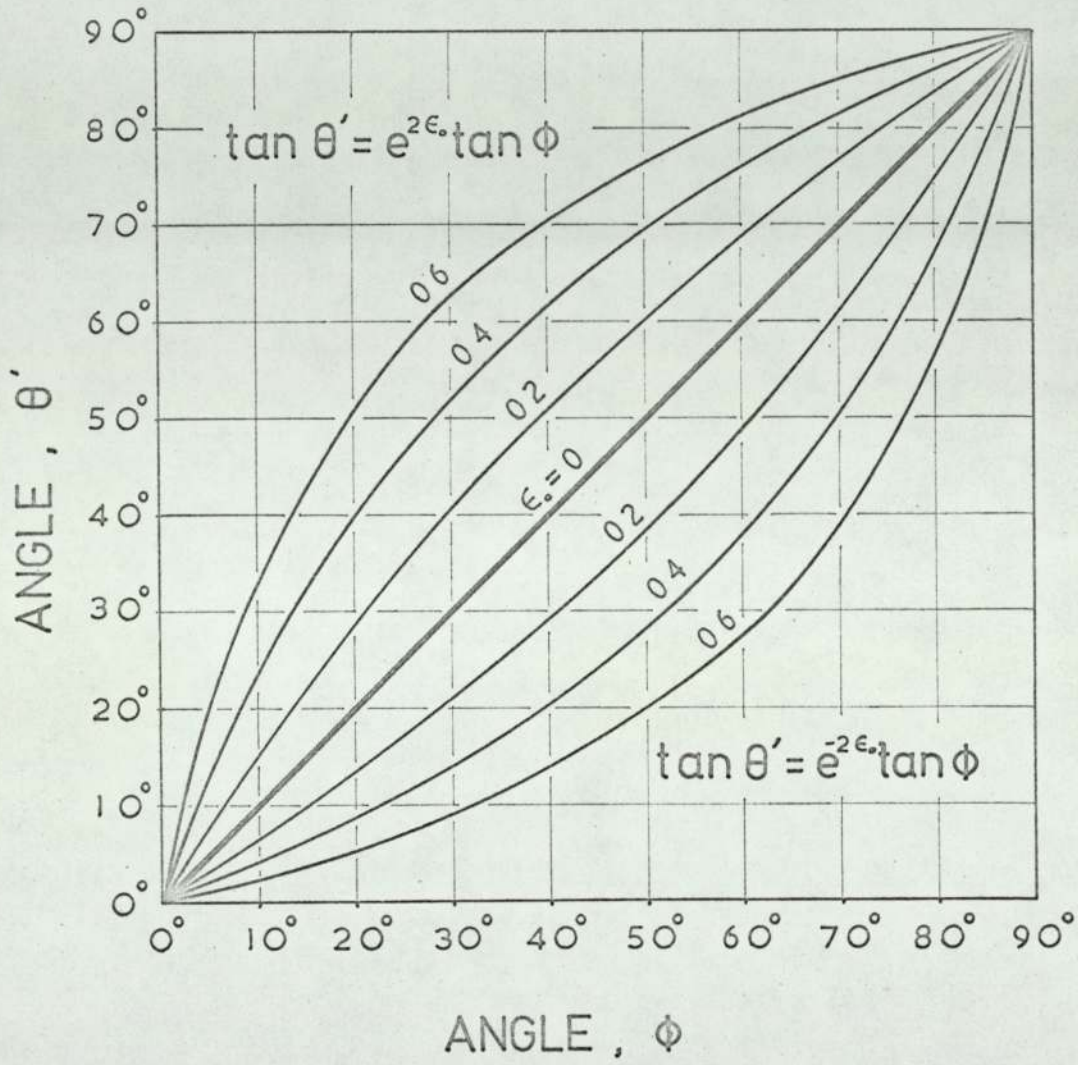


Fig. 6 - 2

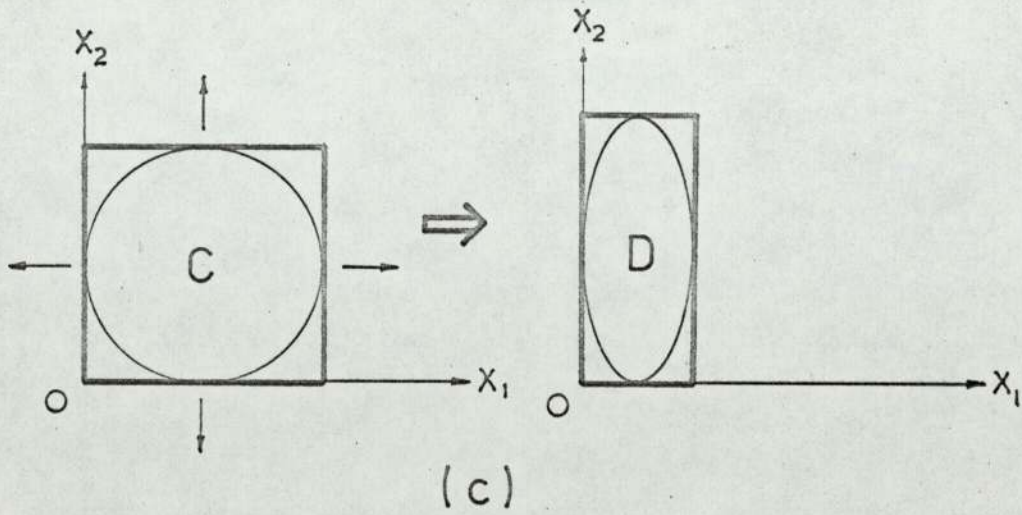
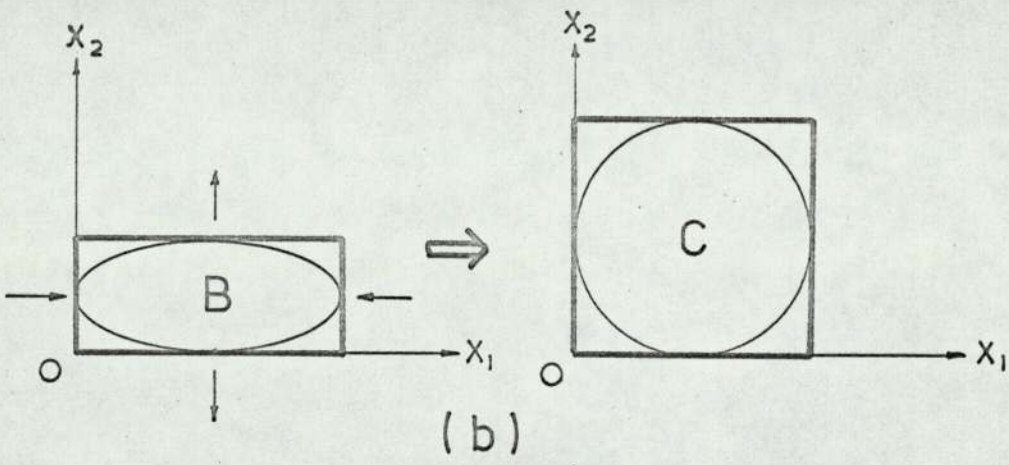
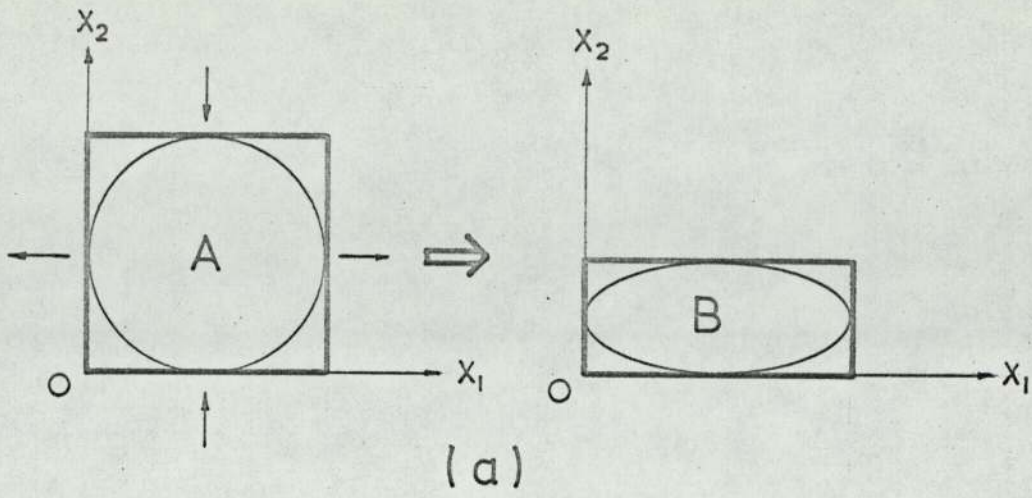


Fig. 6 - 3

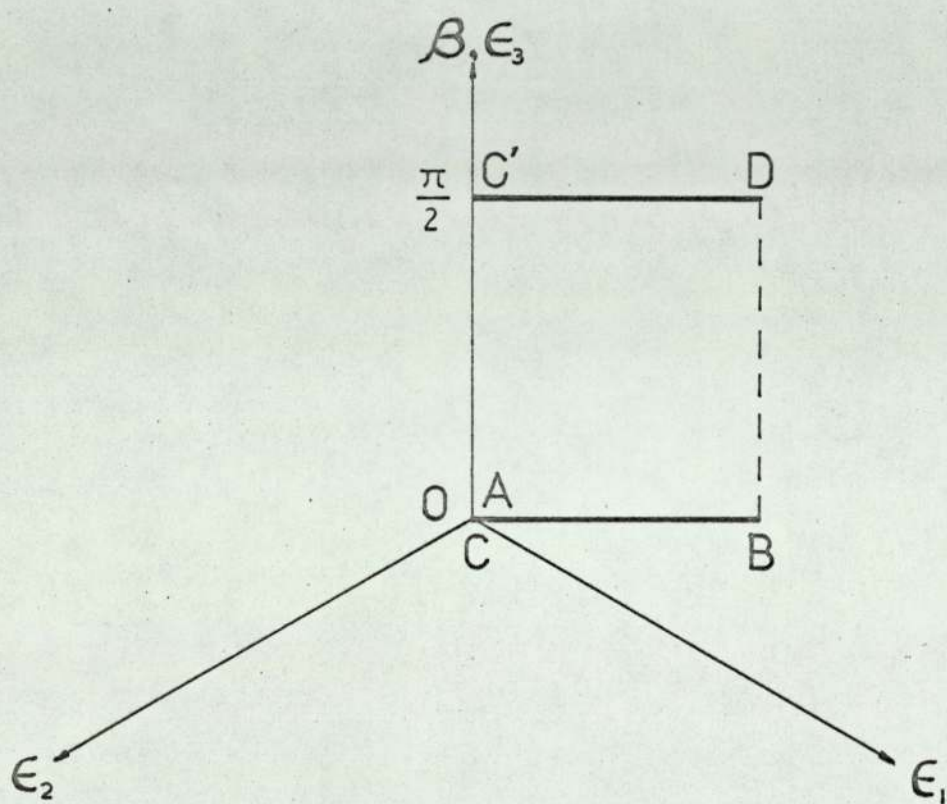
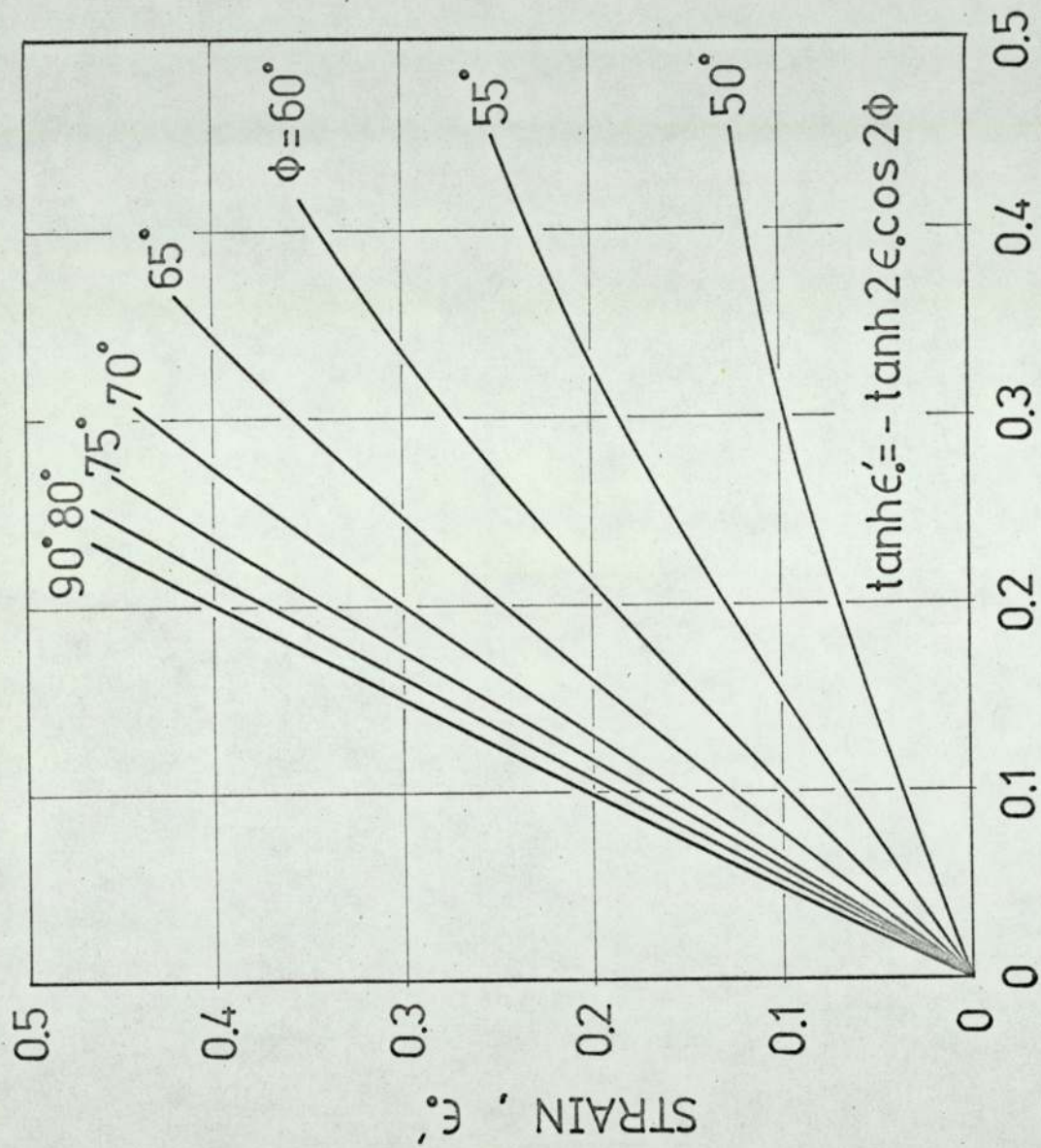


Fig. 6 - 4



STRAIN ,  $\epsilon$ .

Fig. 6 - 5

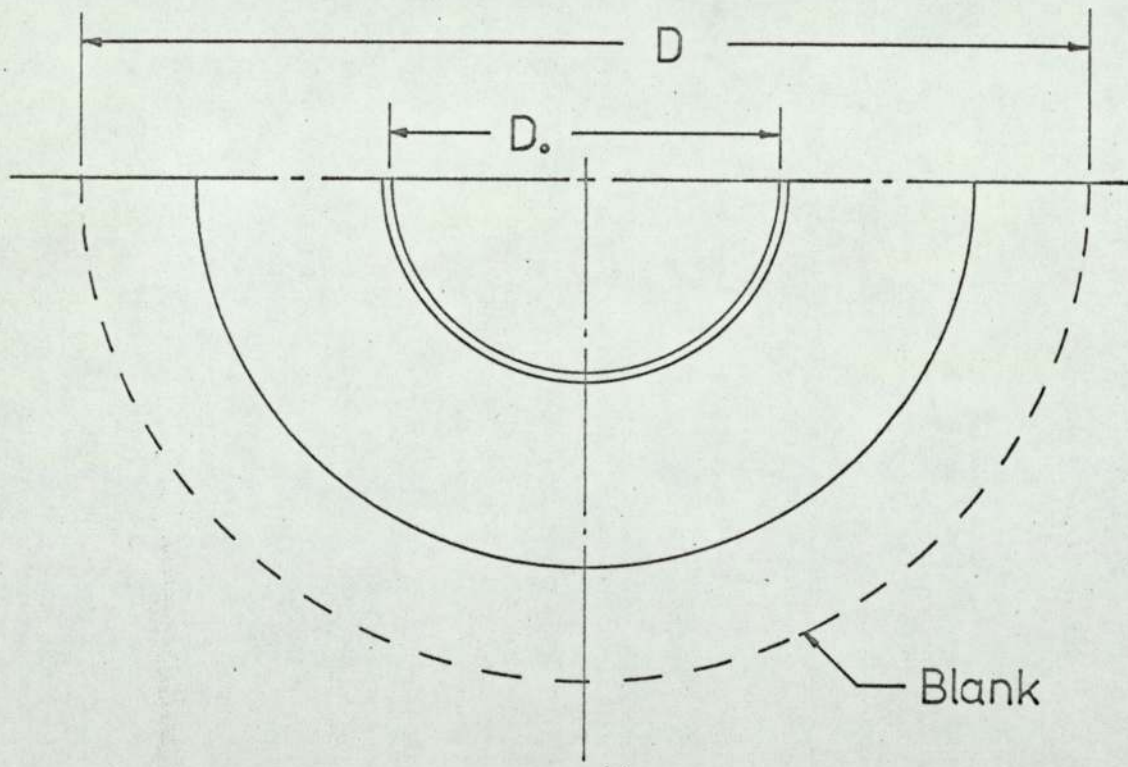
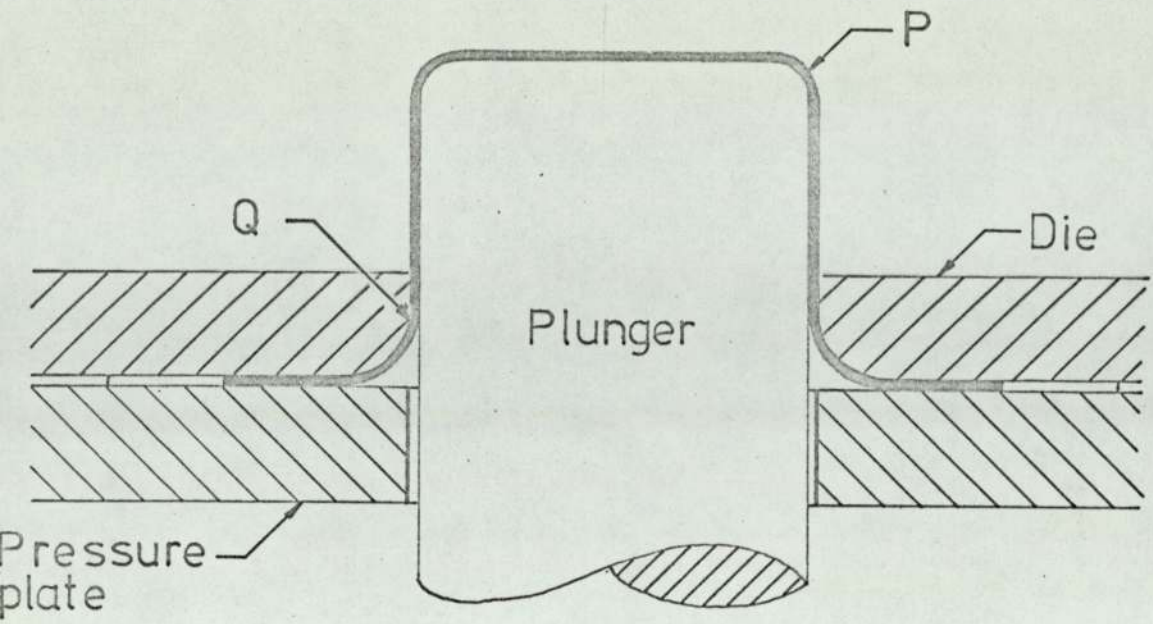


Fig. 8 - 1

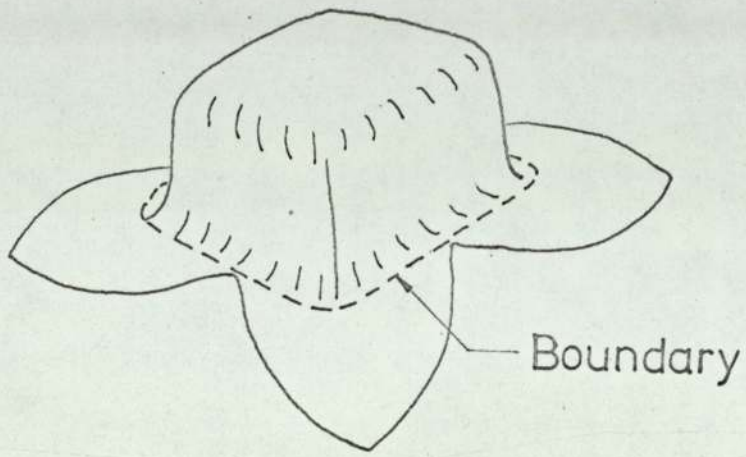


Fig. 8 - 2

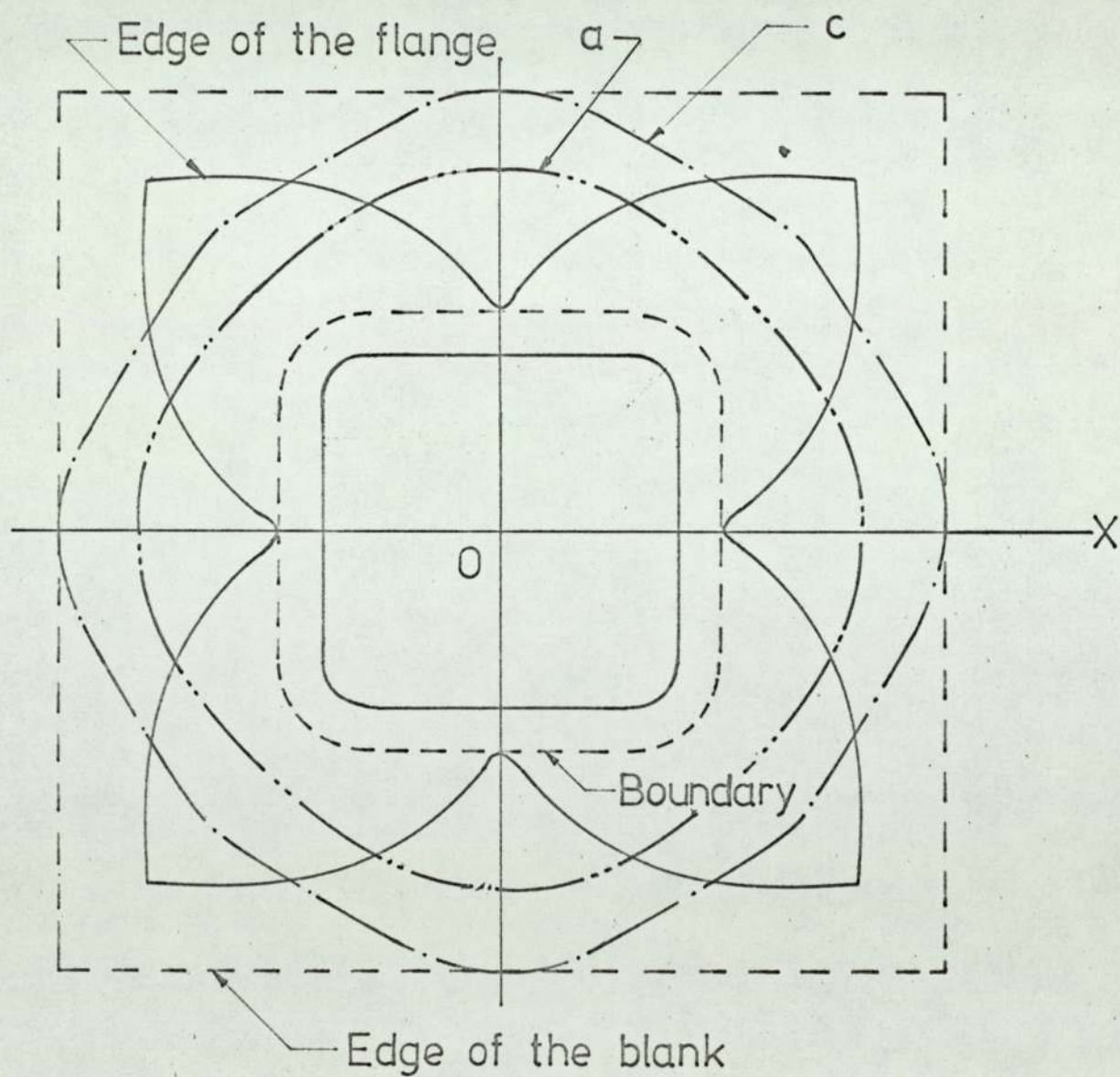
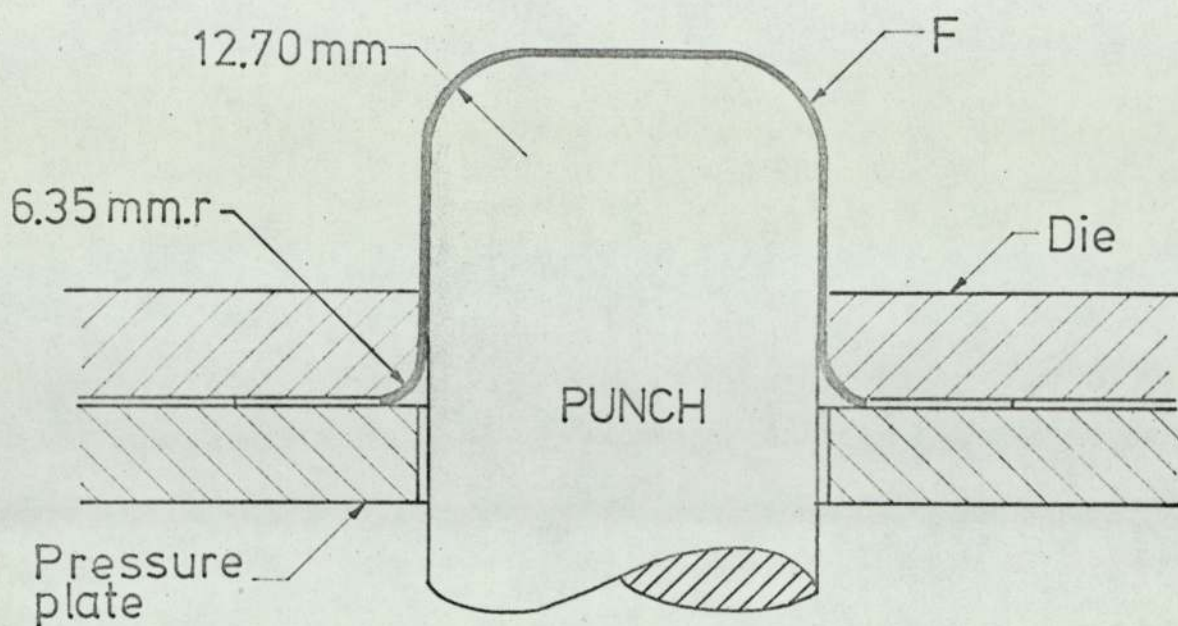


Fig. 8 - 3

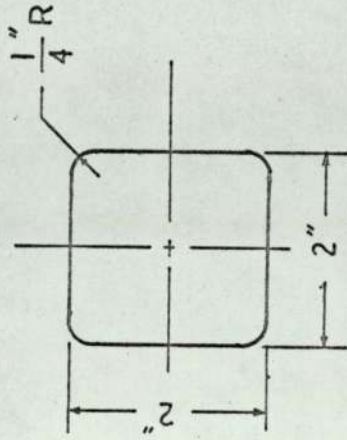
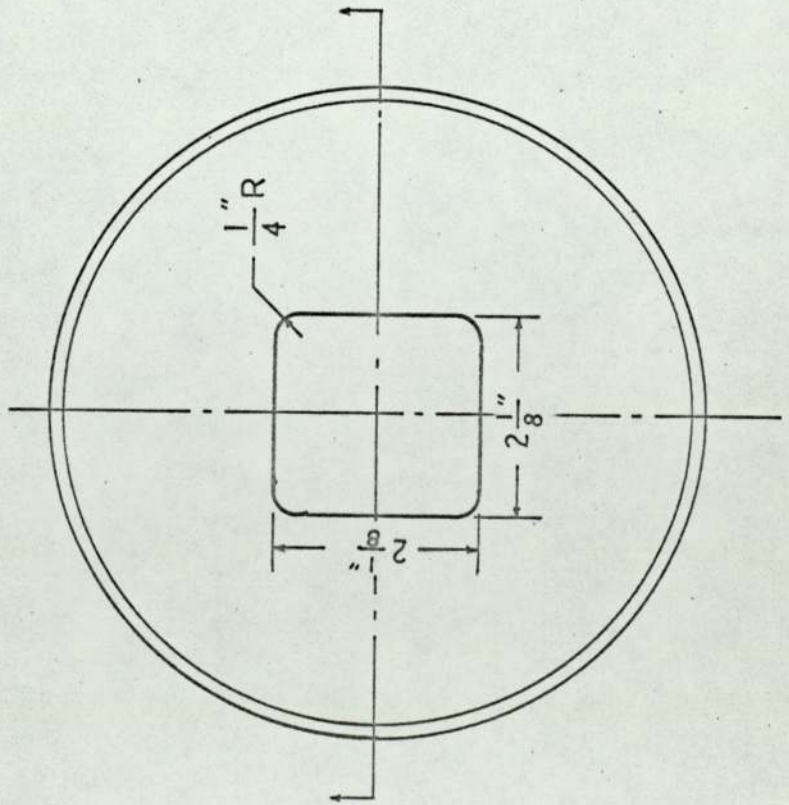
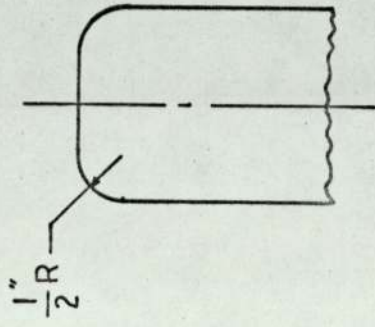
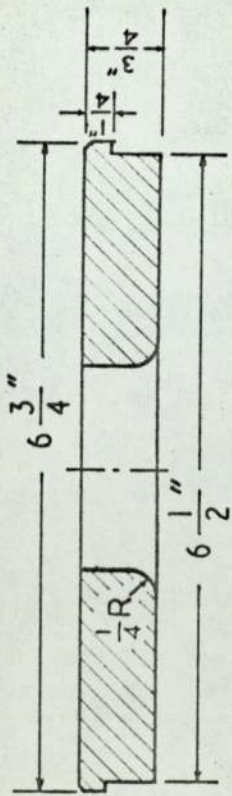


Fig. 9 - 1

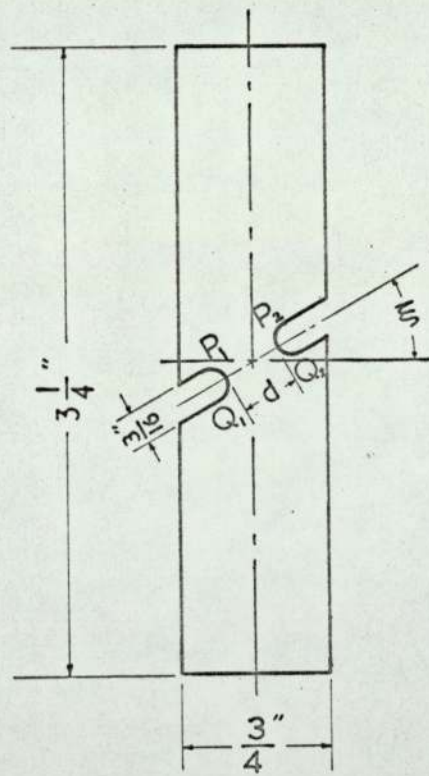


Fig. 9 - 2

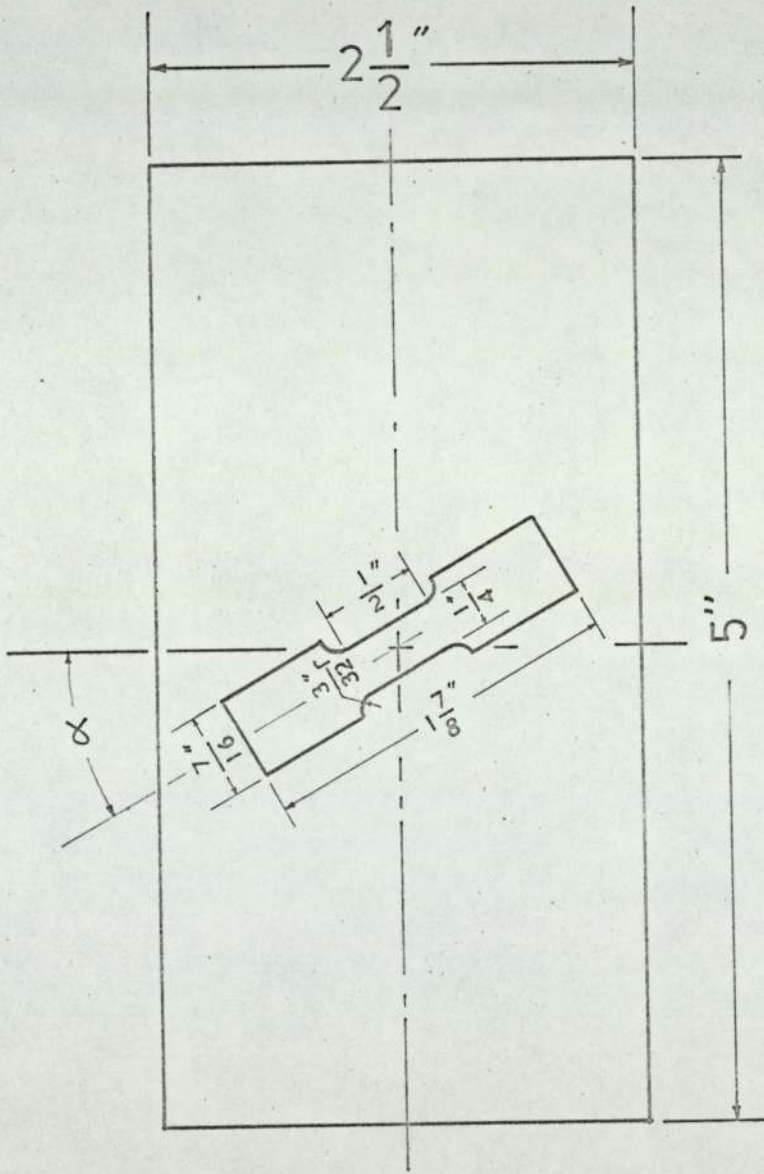


Fig. 9 - 3

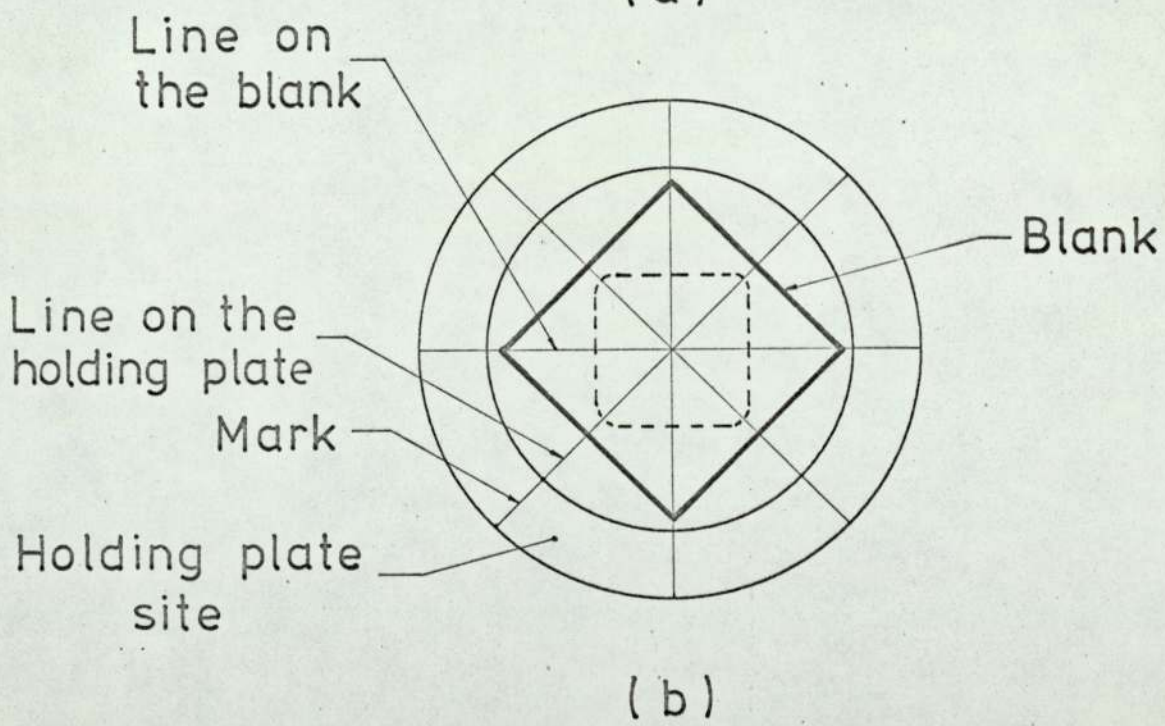
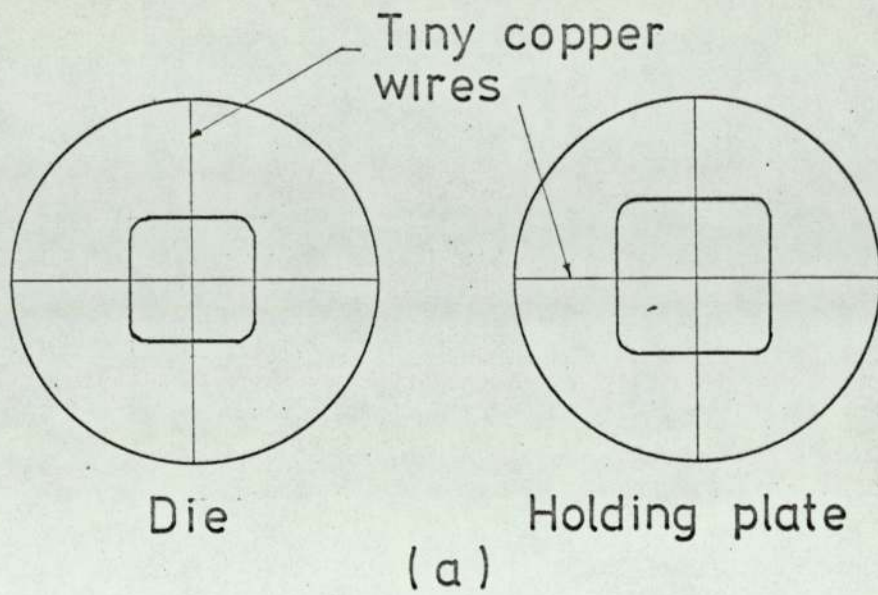


Fig. 9 - 4

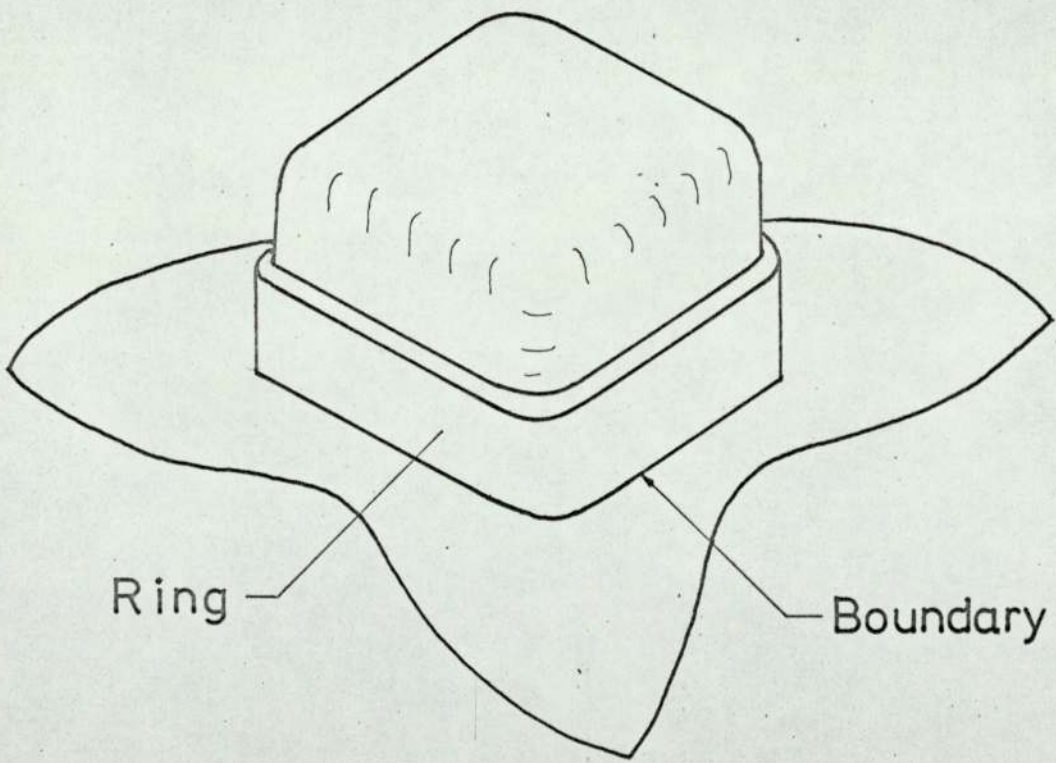
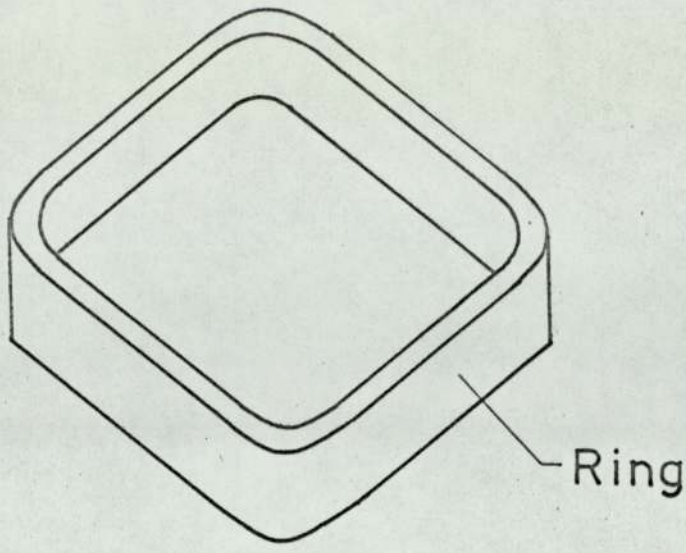
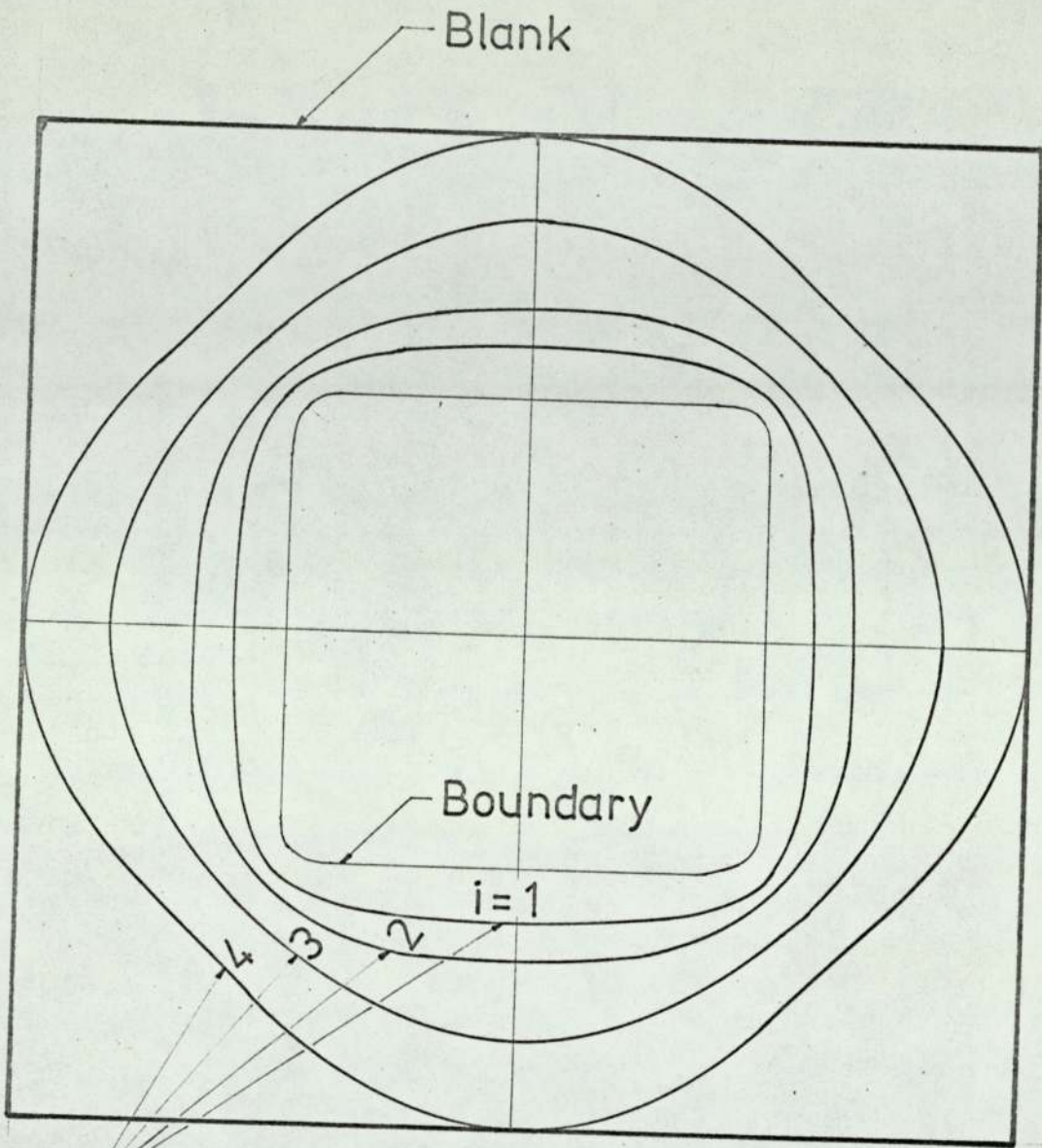


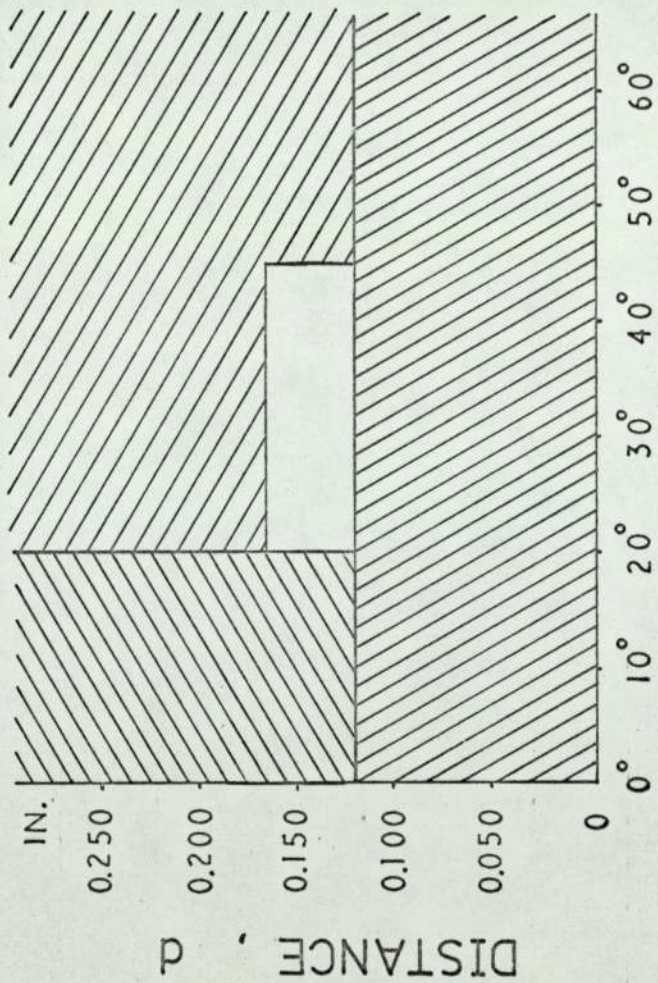
Fig. 9 - 5



The locus of the points which will reach the boundary at stage  $i$  of the drawing operation

Fig. 9 - 6

 two necks or tearing  
 non-coaxiality undetectable  
 necking as in coaxial case



INCLINATION ANGLE,  $\xi$

Fig. 10 - 1

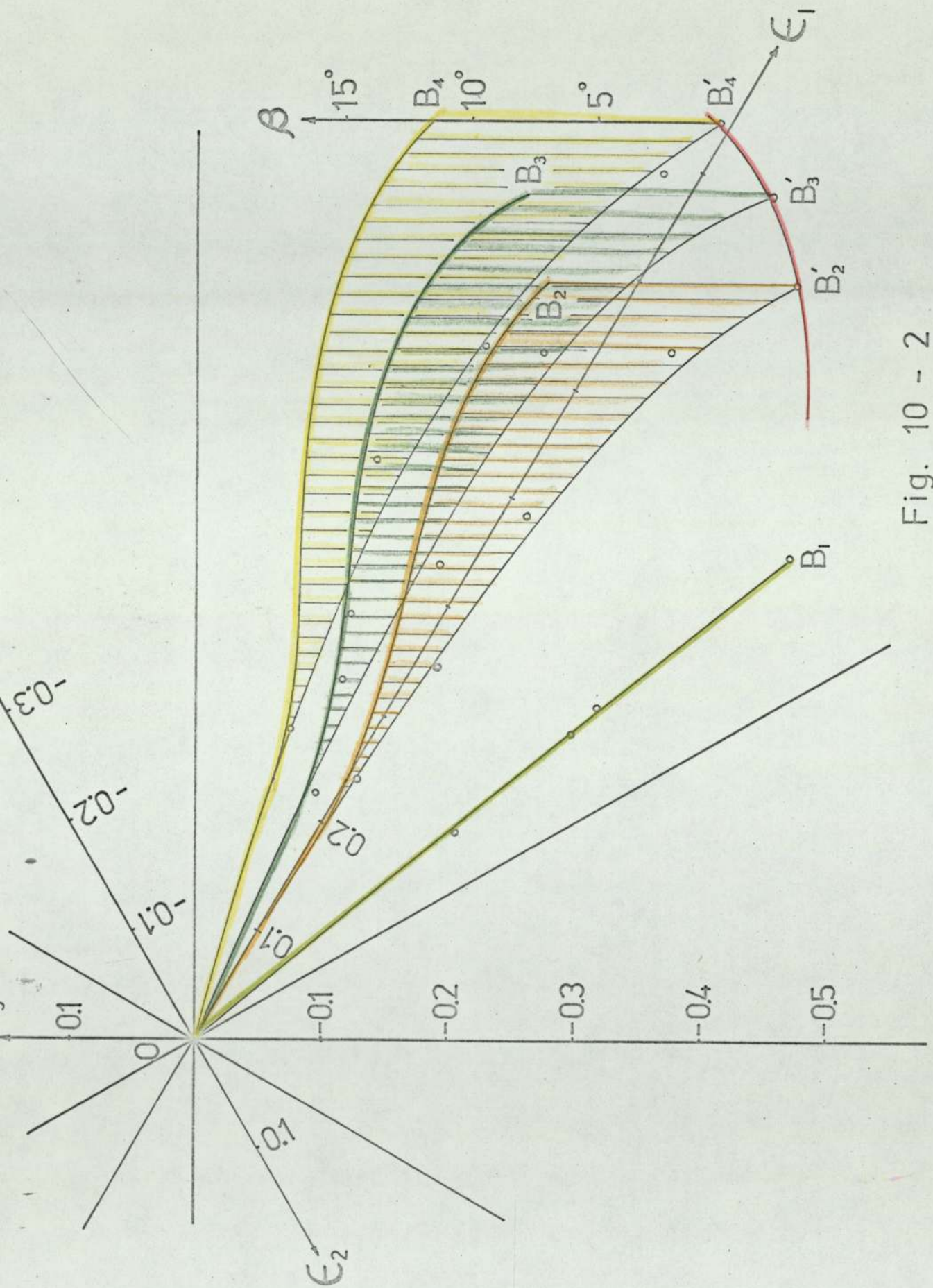


Fig. 10 - 2

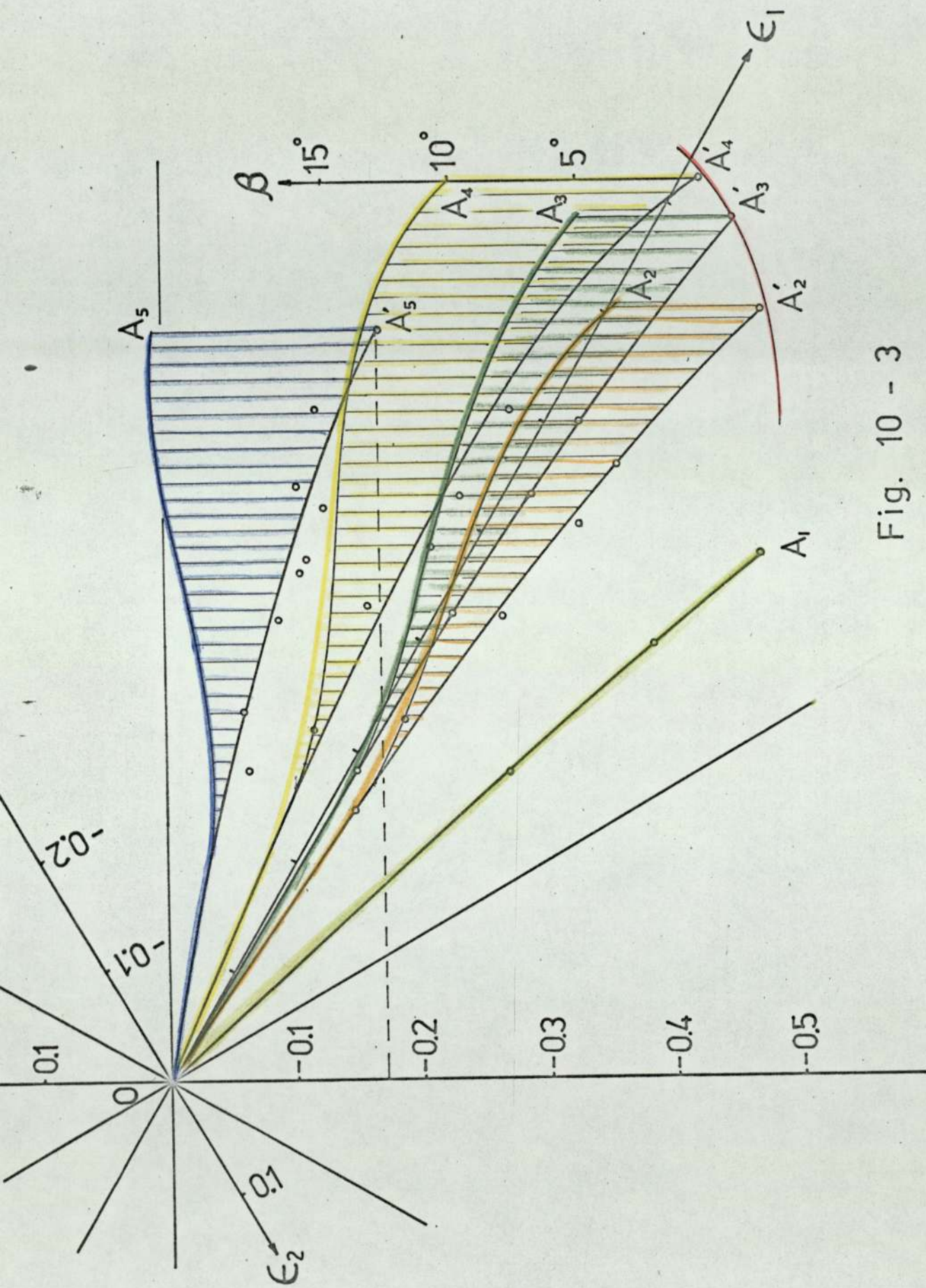
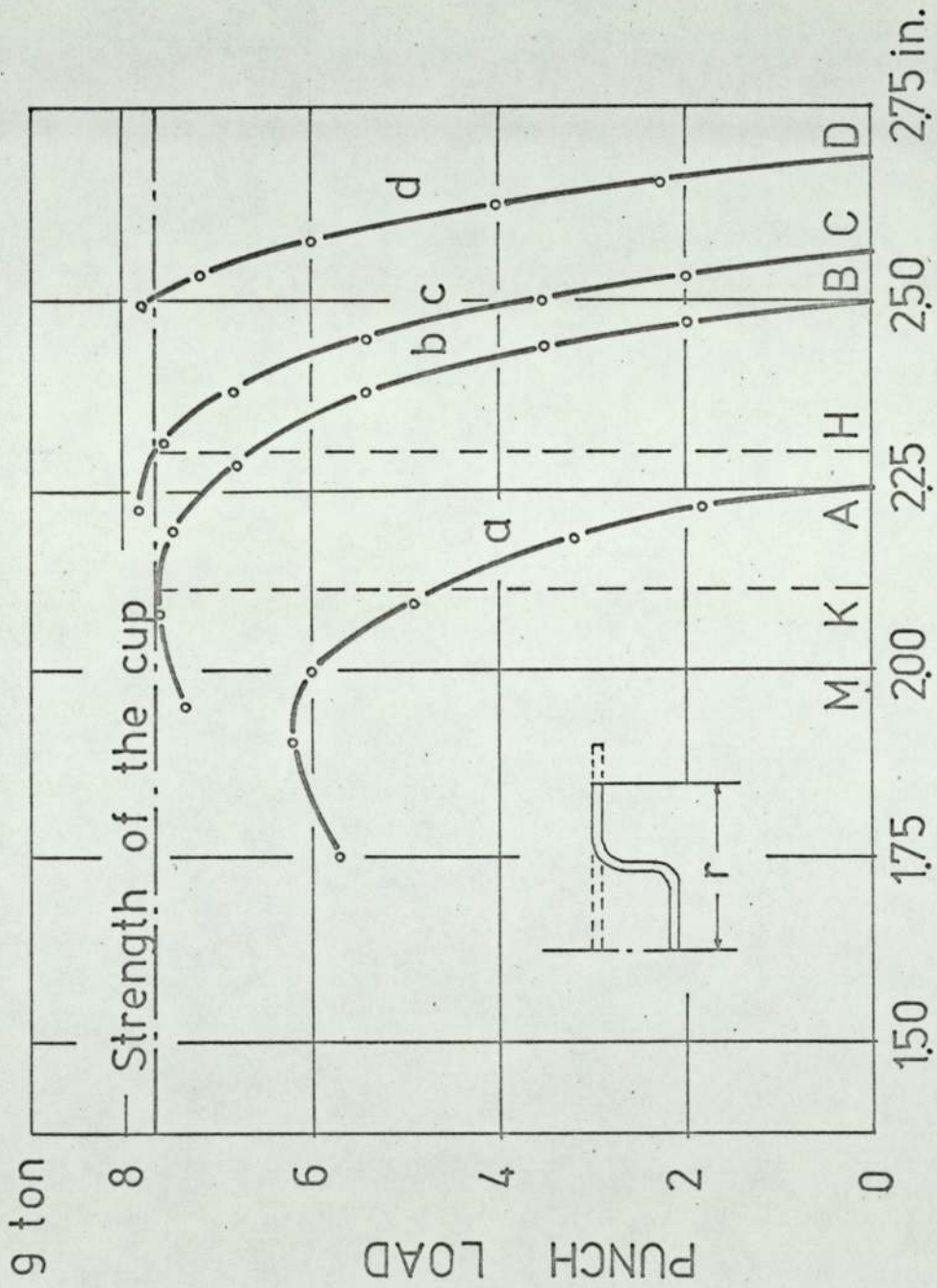


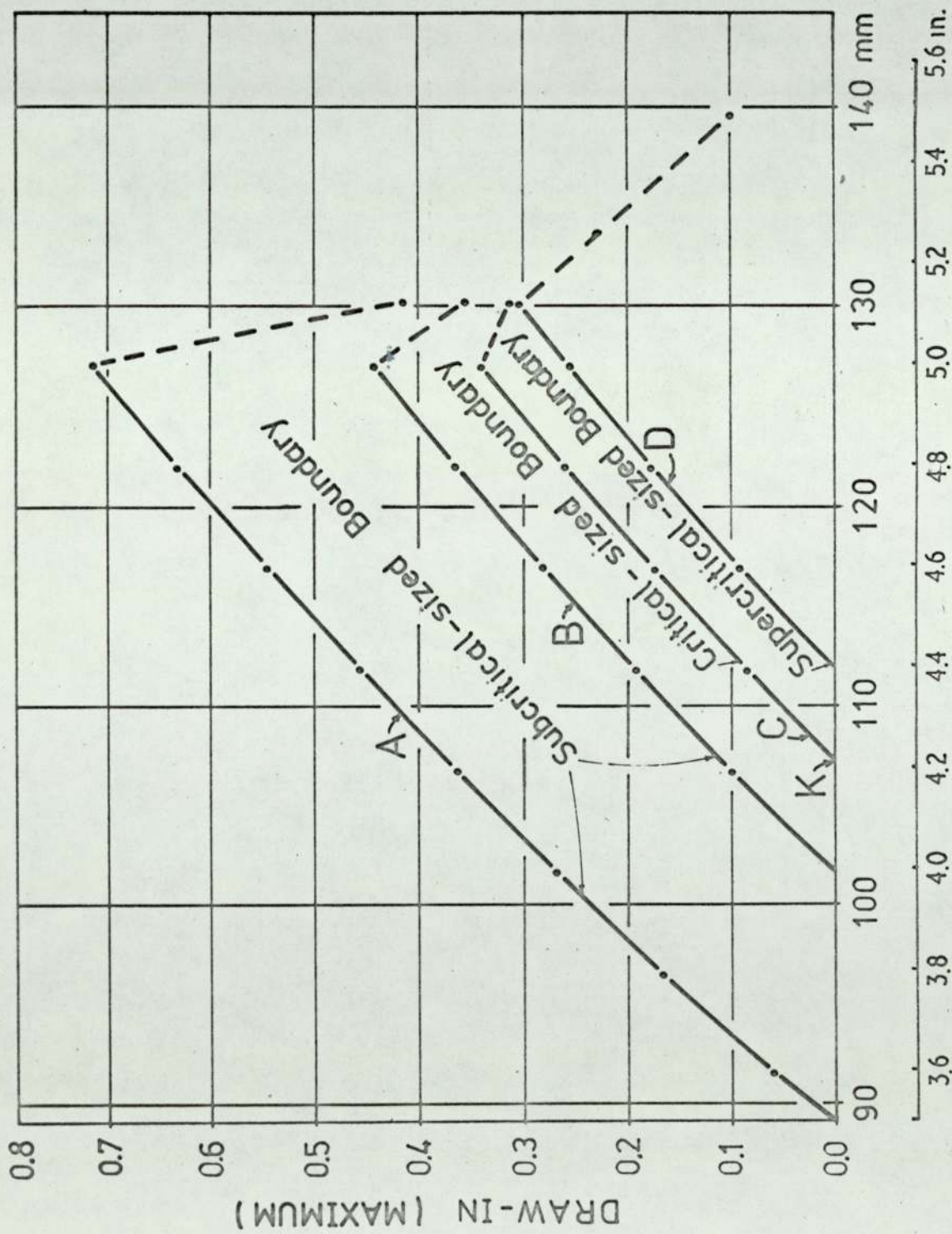
Fig. 10 - 3





CURRENT RADIUS , r

Fig. 11 - 1



BLANK DIAMETER

Fig. 11 - 2

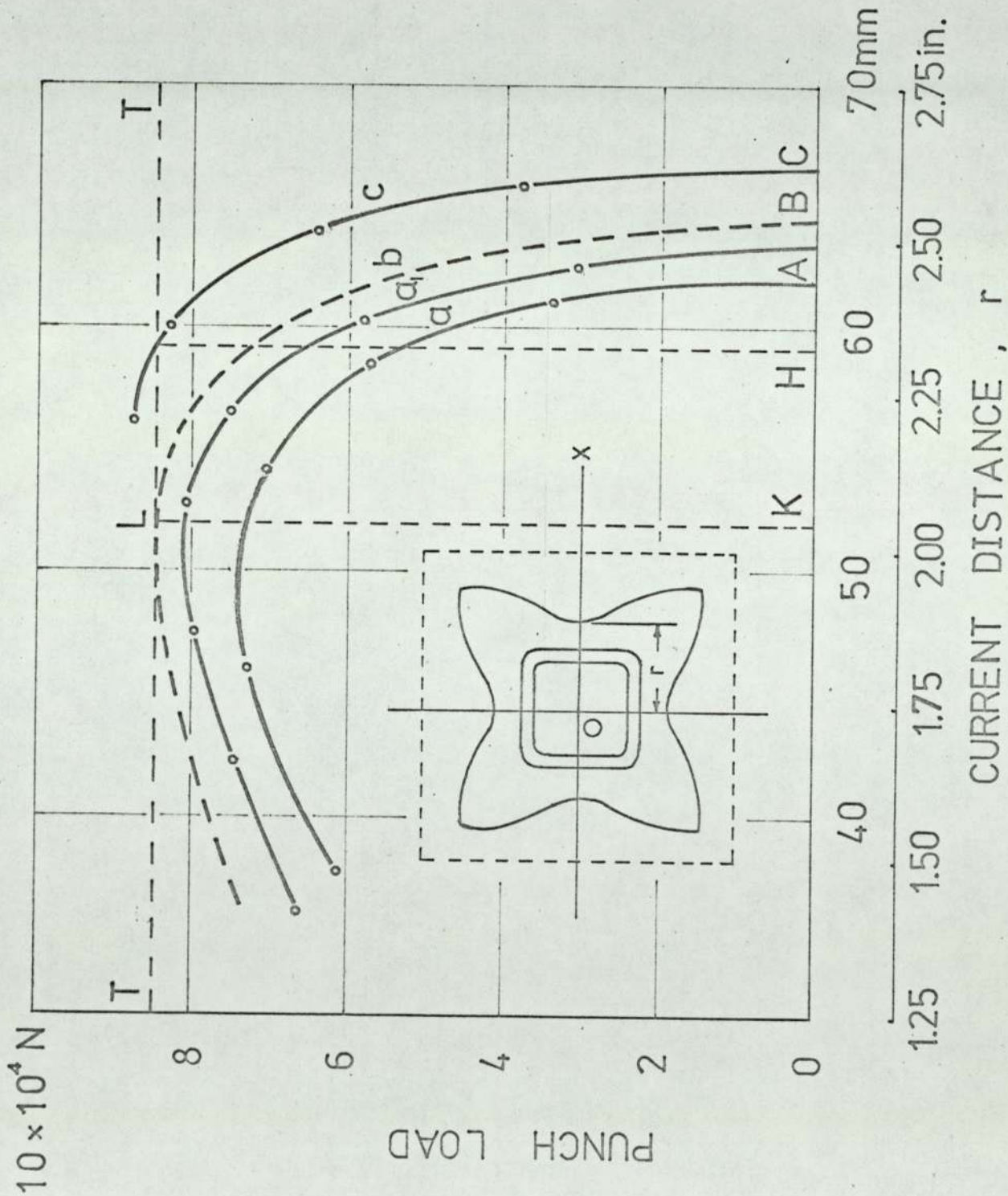
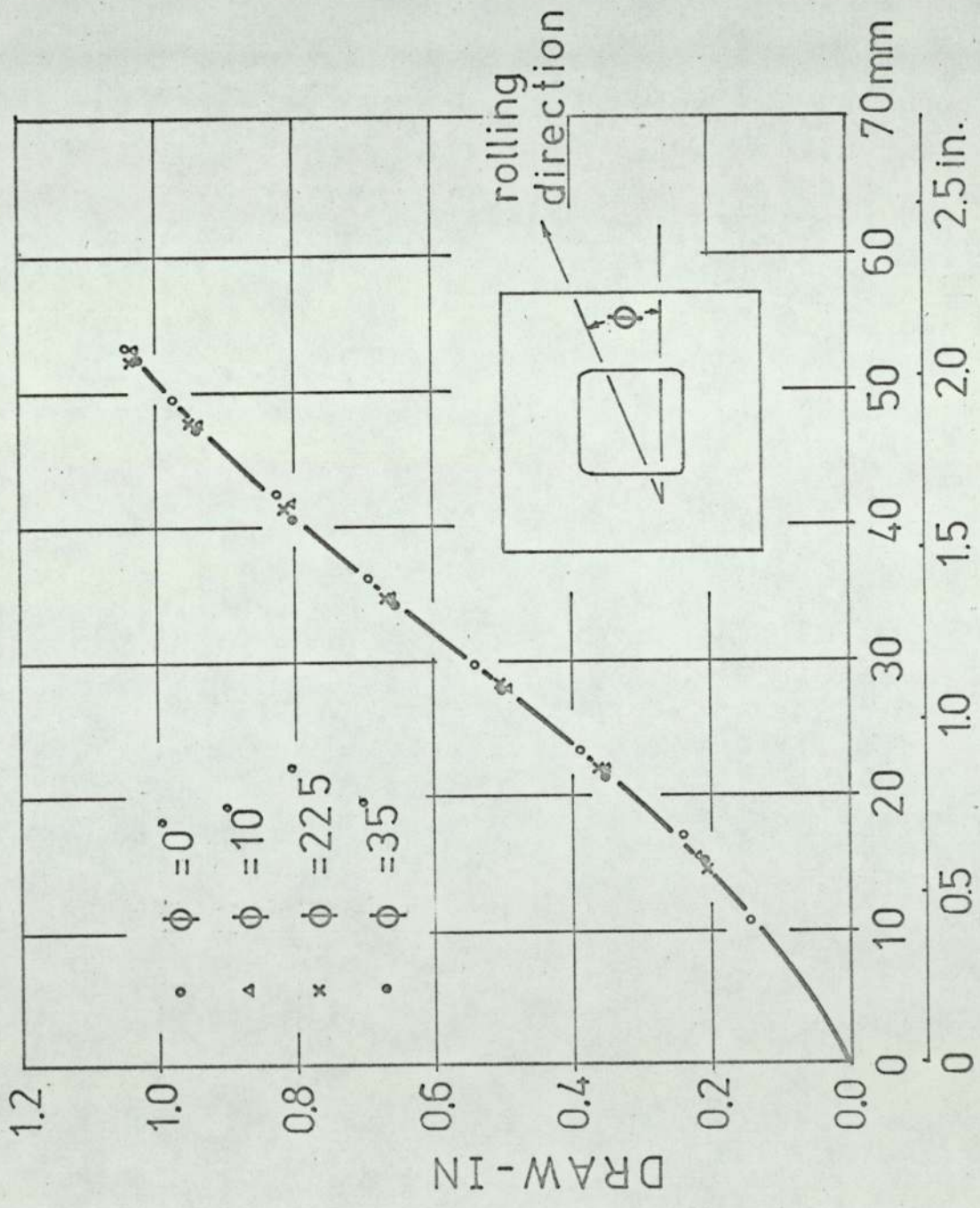
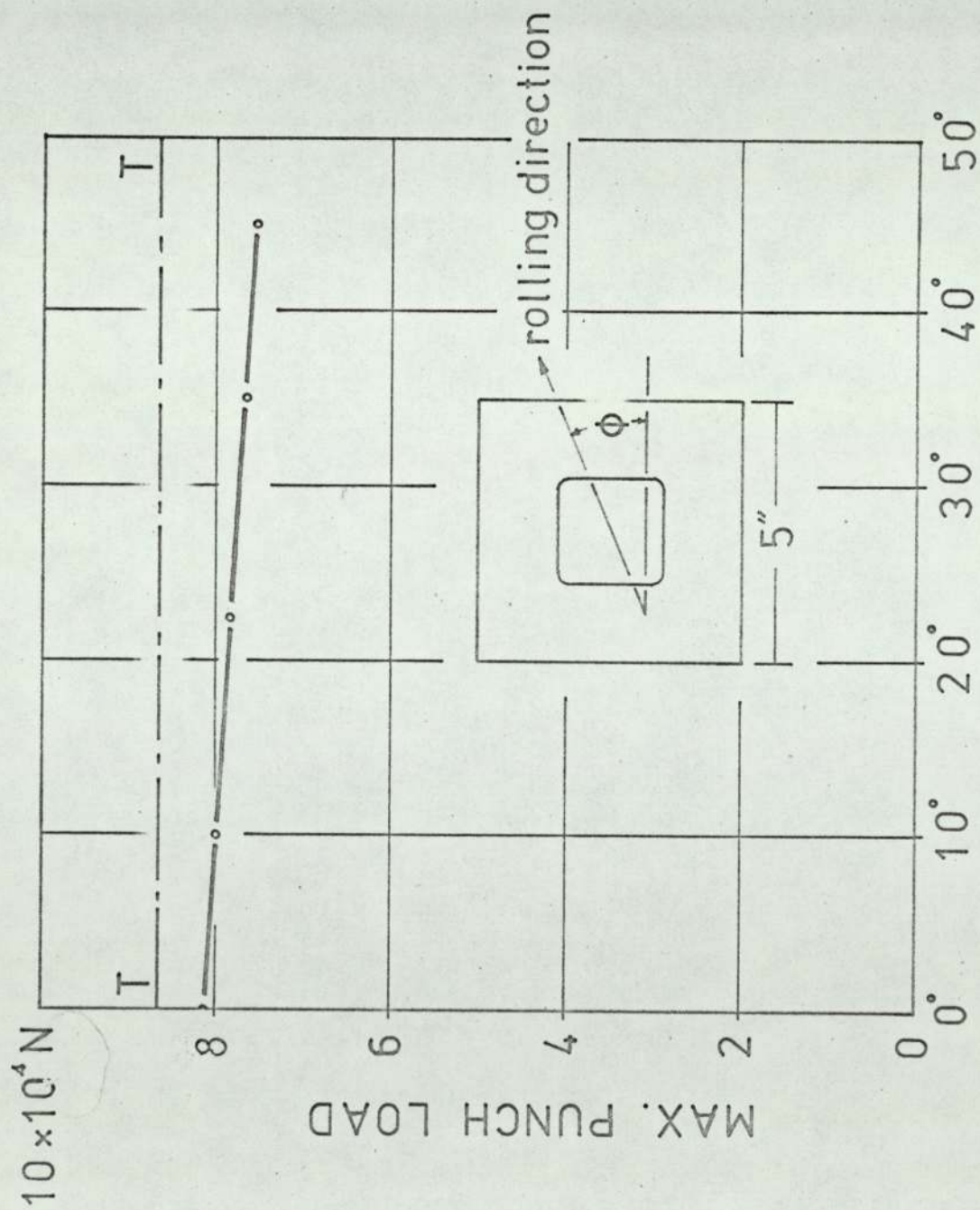


Fig. 11 - 3



PUNCH PENETRATION

Fig. 11 - 4



ORIENTATION,  $\phi$

Fig. 11 - 5

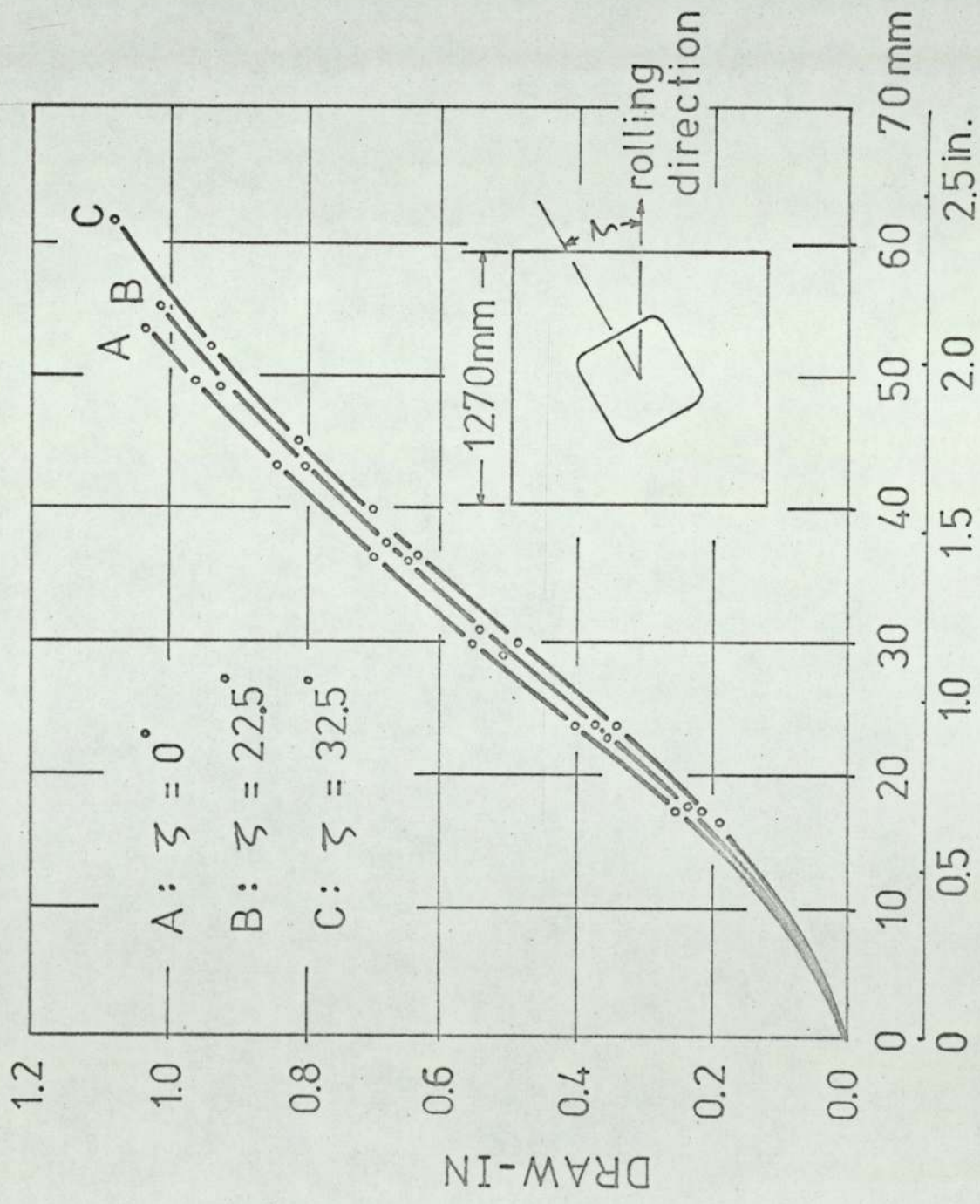
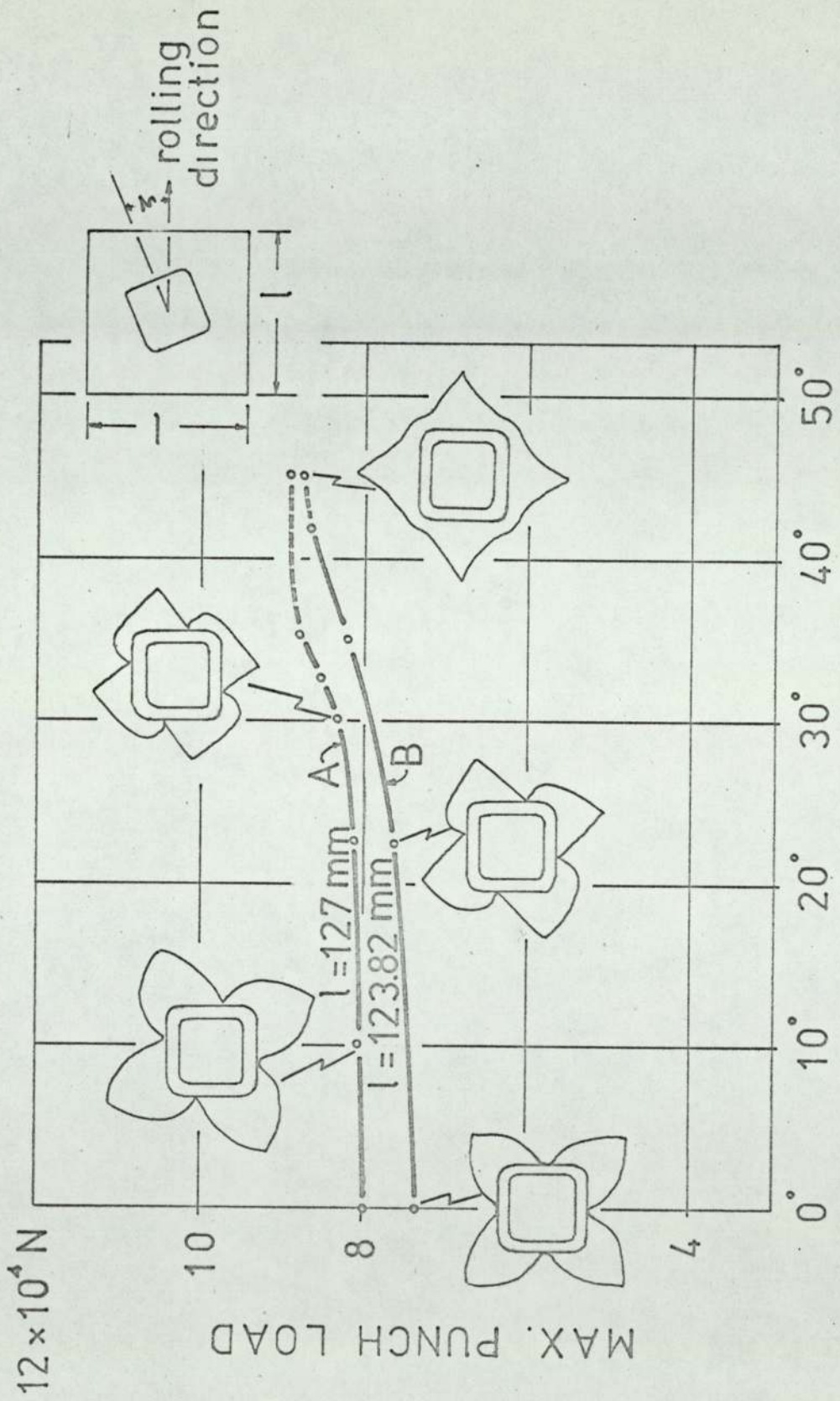
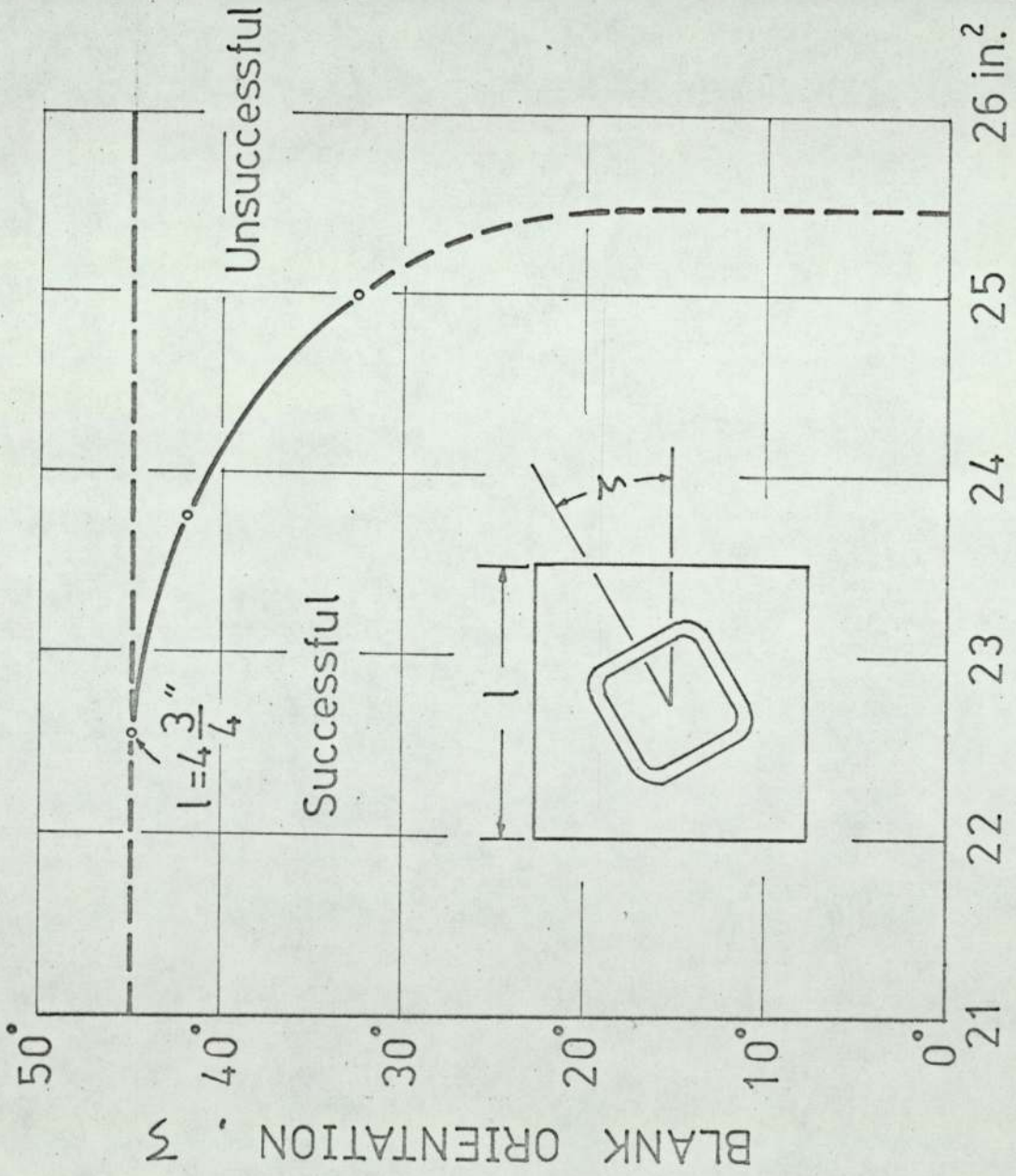


Fig. 11 - 6



ORIENTATION,  $\zeta$

Fig. 11 - 7



BLANK SIZE,  $l \times l$

Fig. 11 - 8

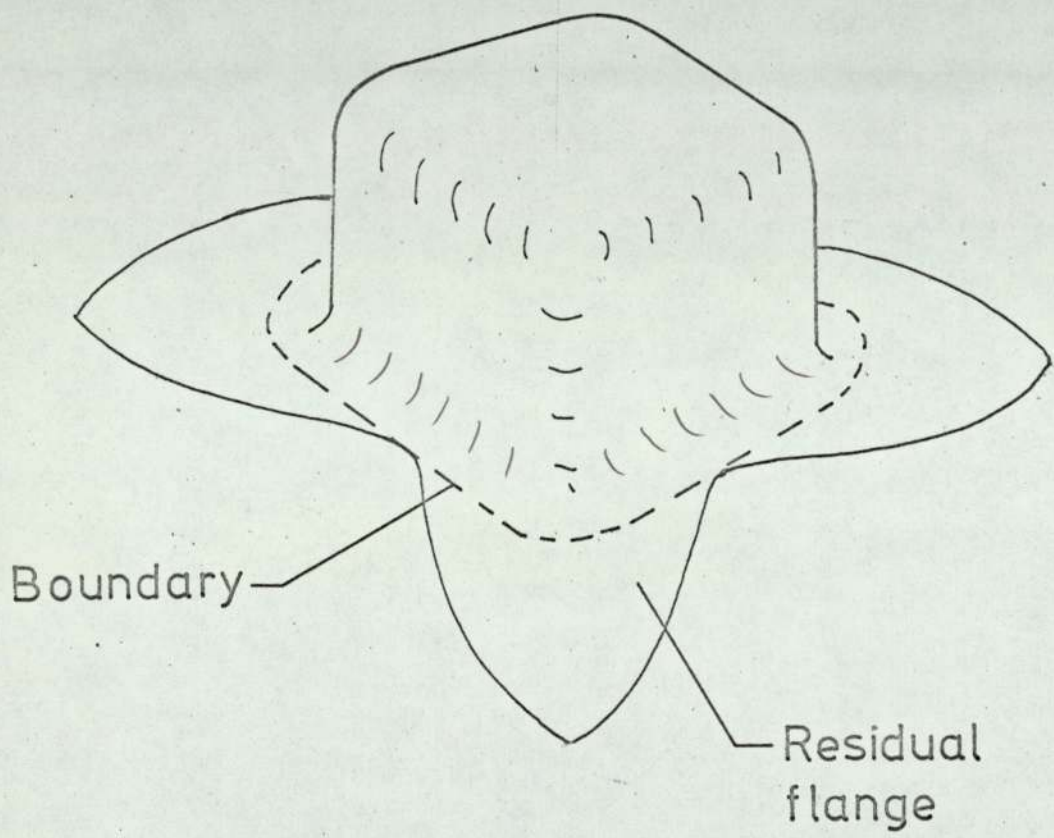


Fig. 11 - 9

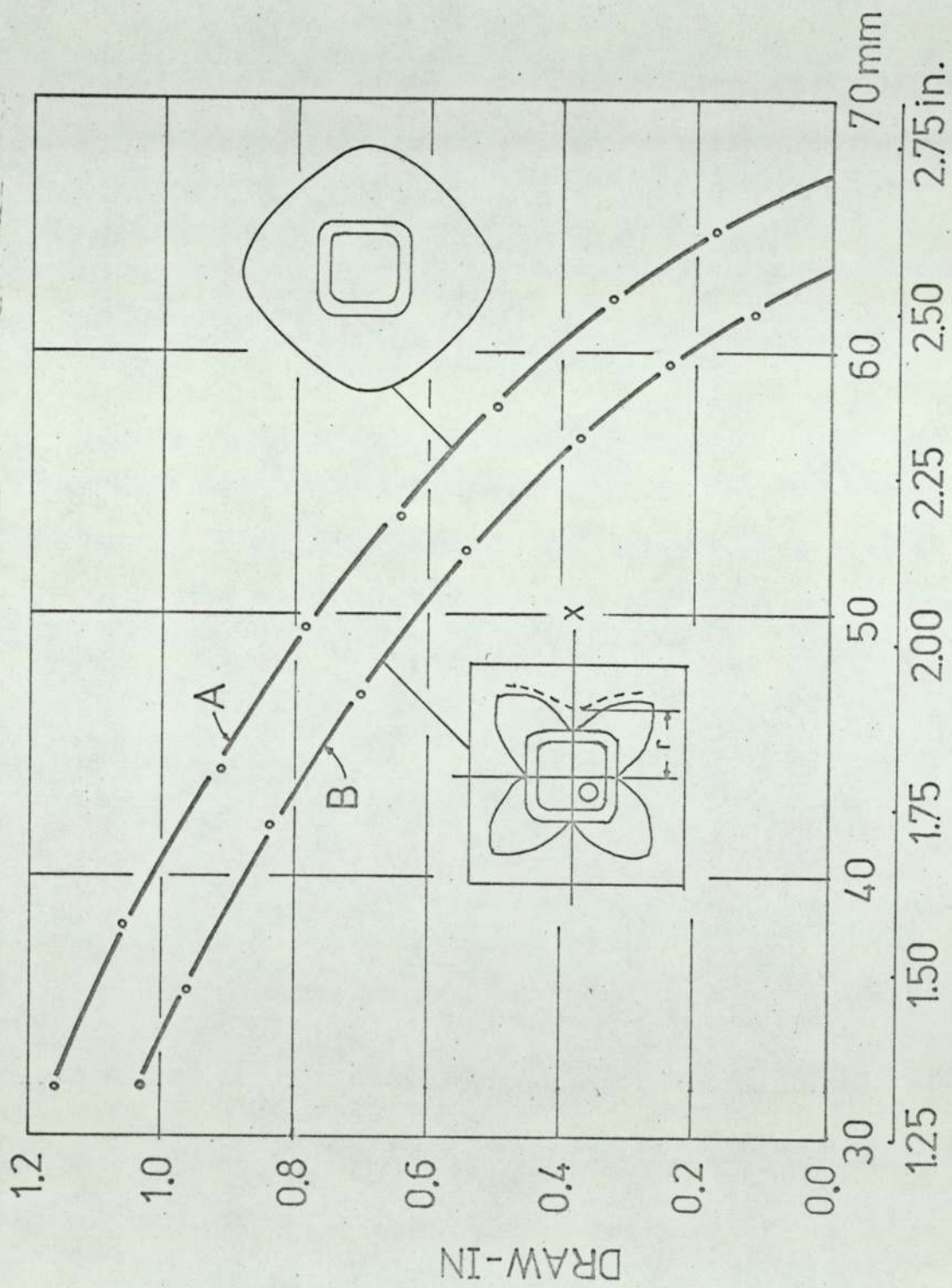


Fig. 11 - 10

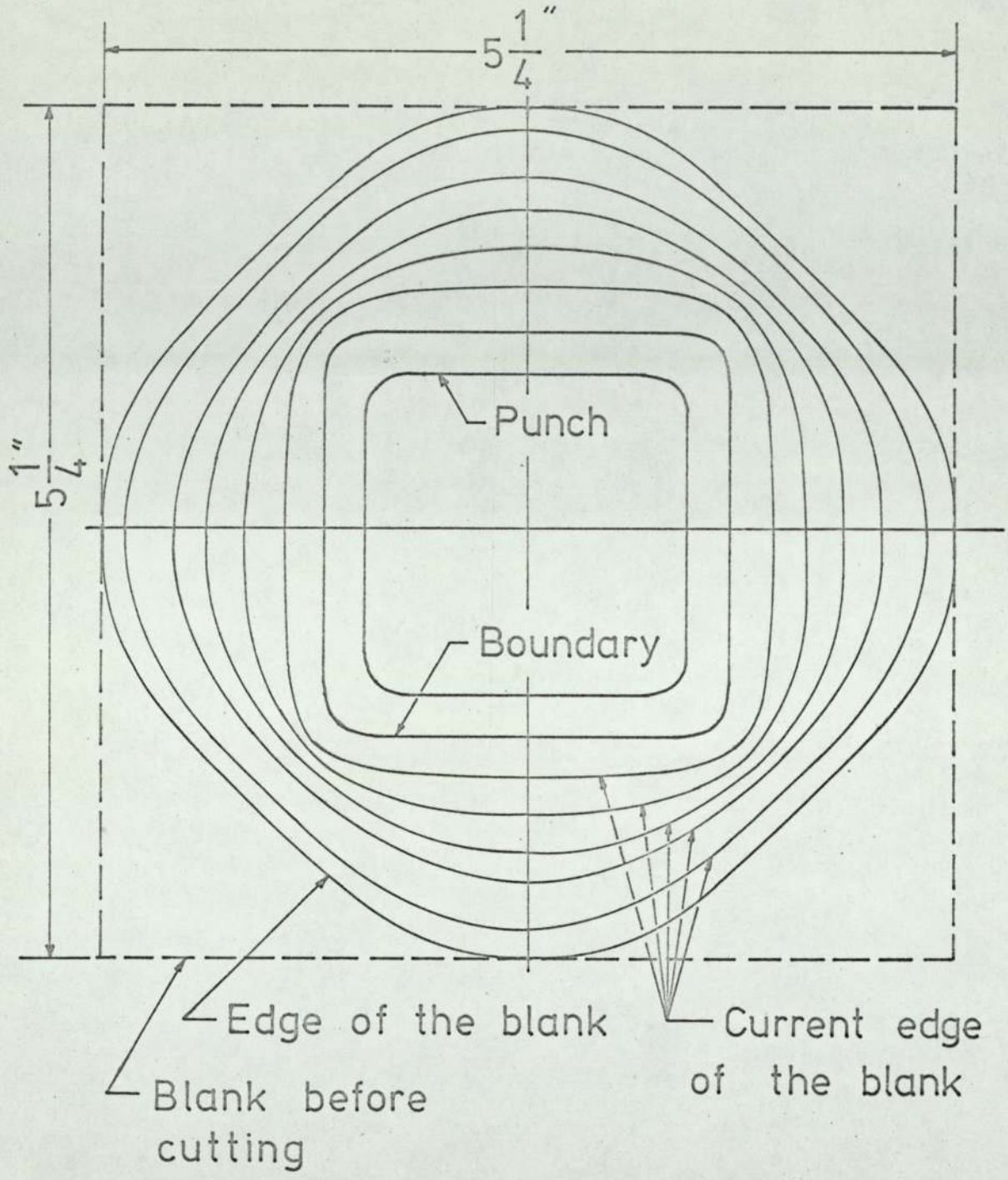


Fig. 11 - 11

- A ———
- B ———
- C ———
- D ———
- Z.R.F. ———

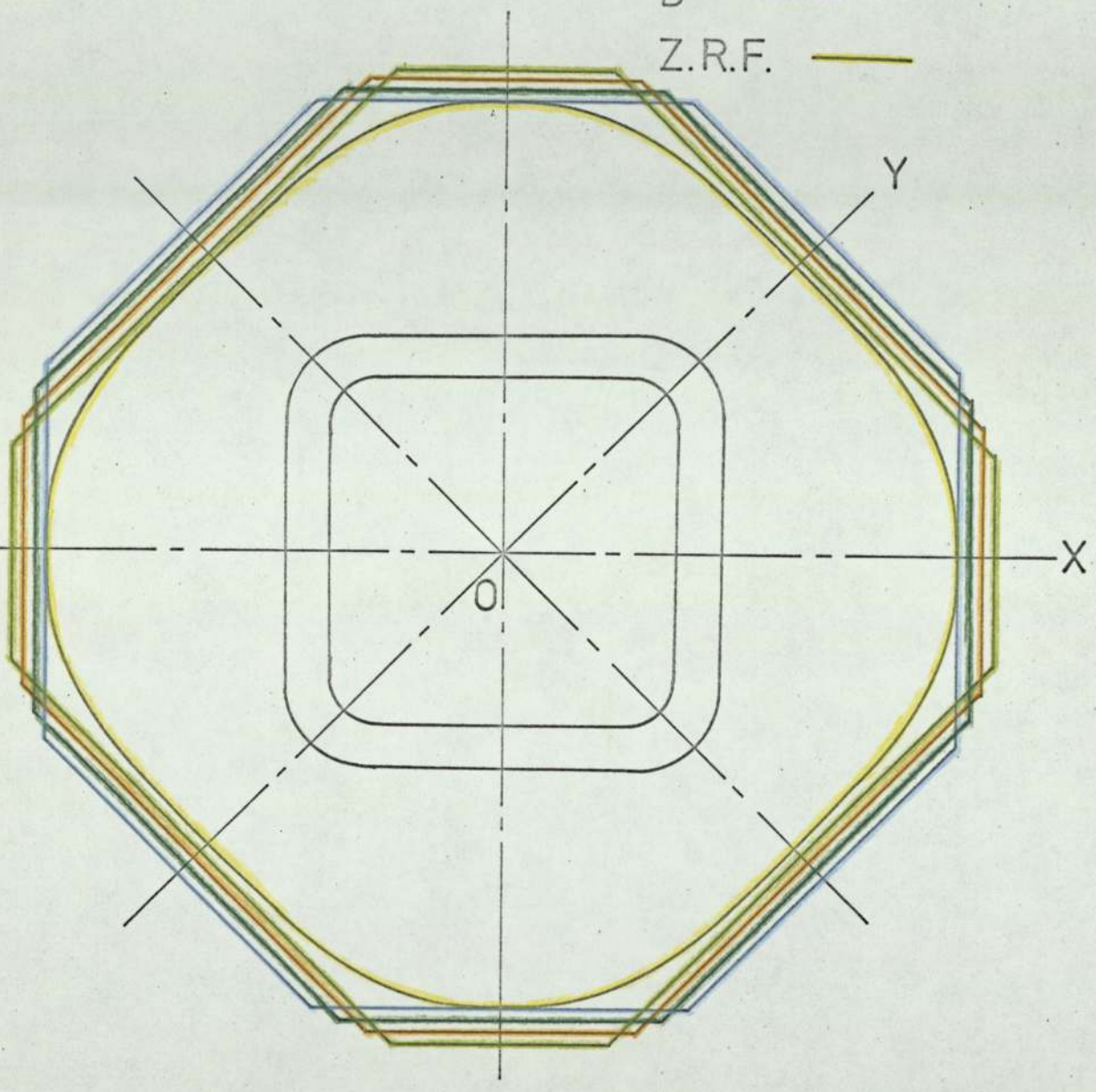
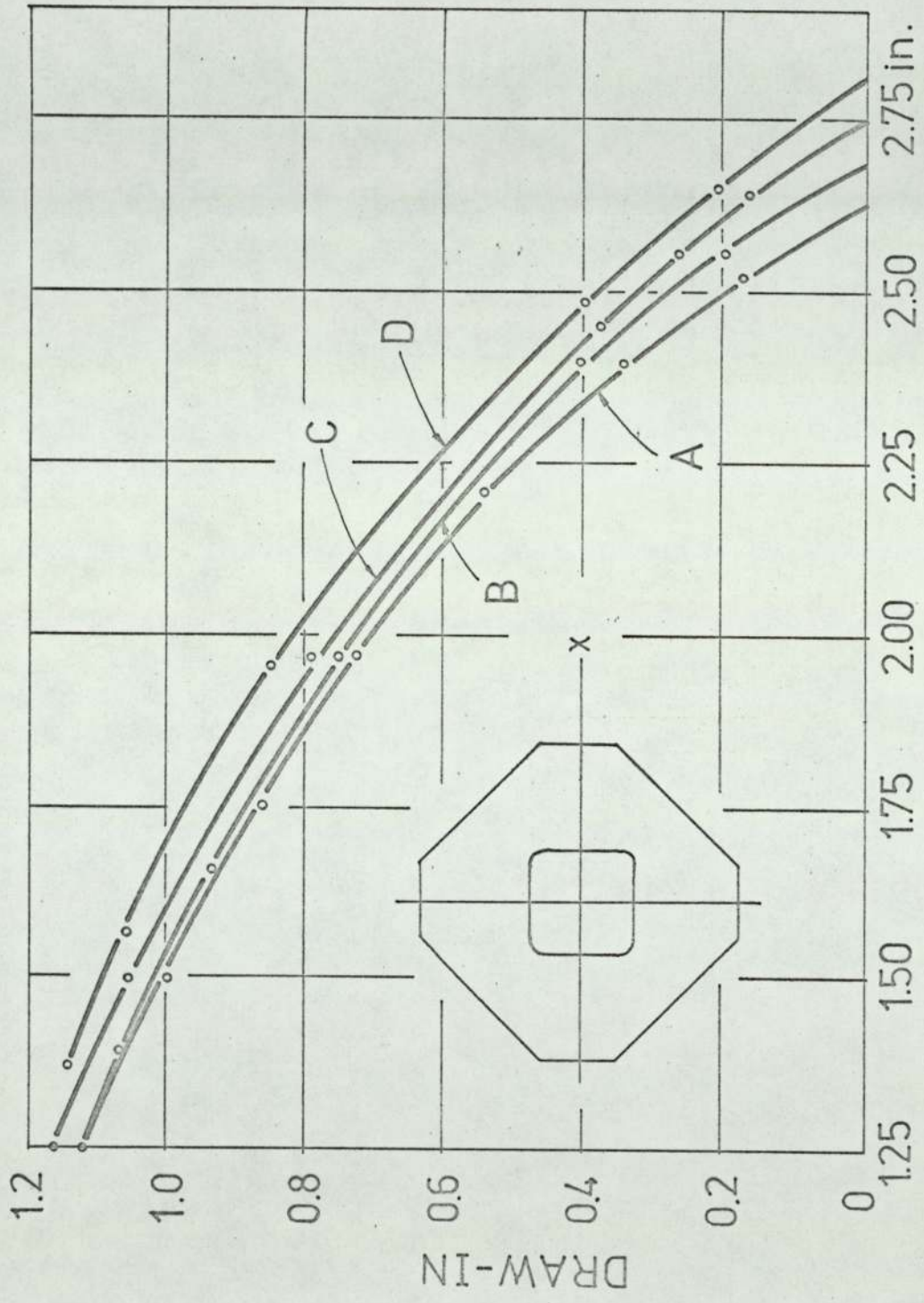


Fig. 11 - 12



CURRENT POSITION OF THE BLANK EDGE

Fig. 11 - 13

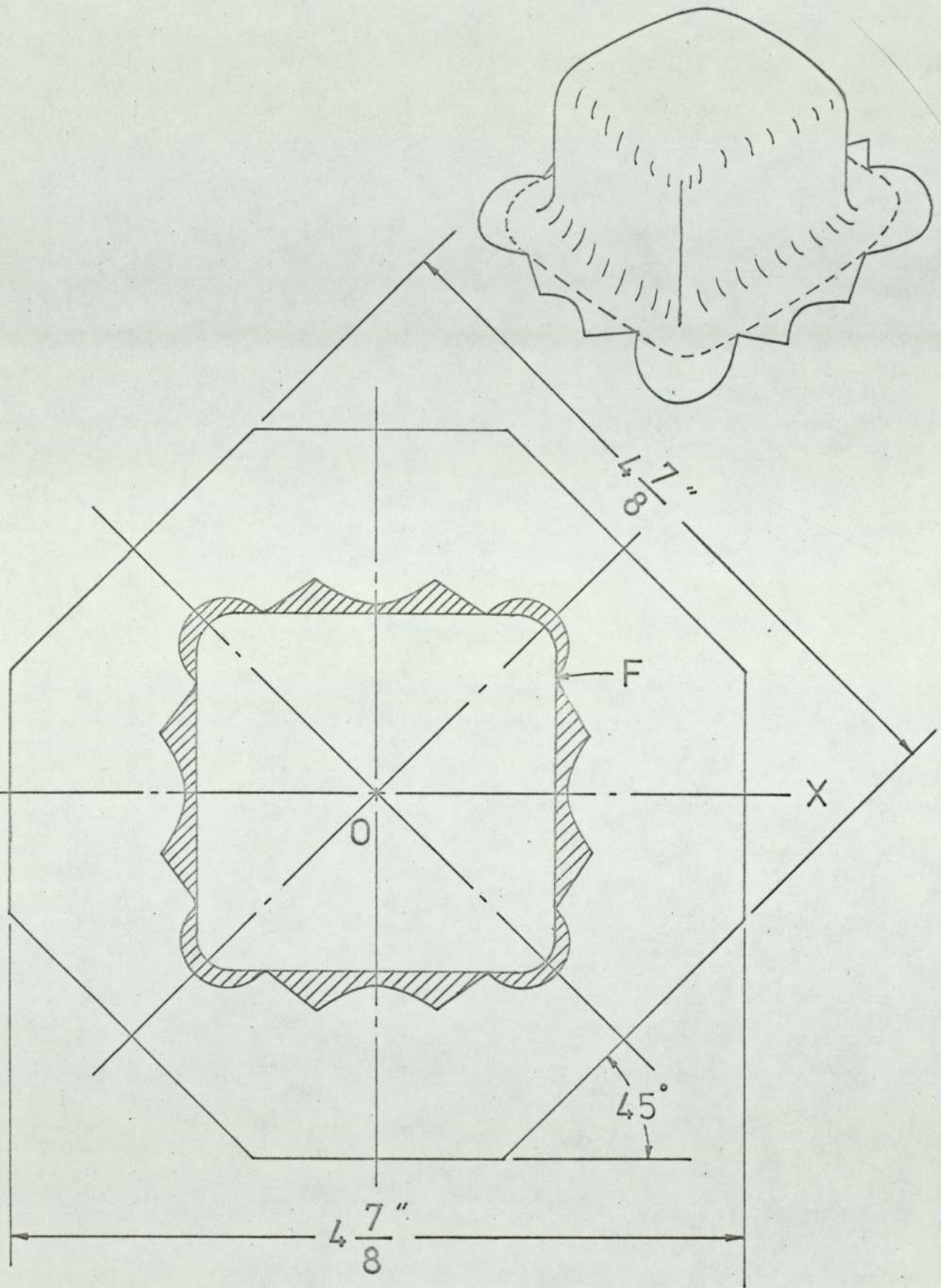
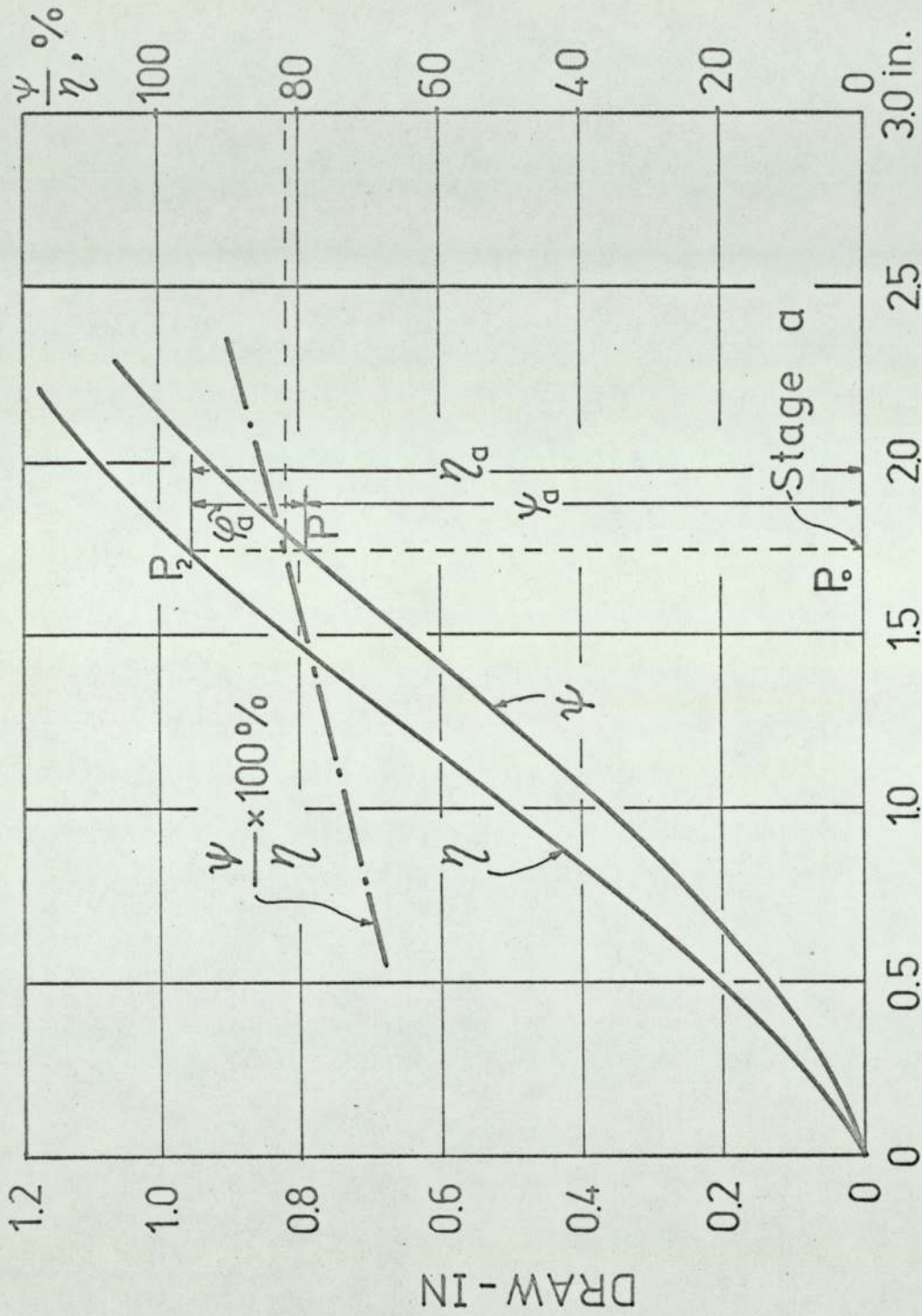


Fig. 11 - 14



PUNCH PENETRATION

Fig. 11 - 15

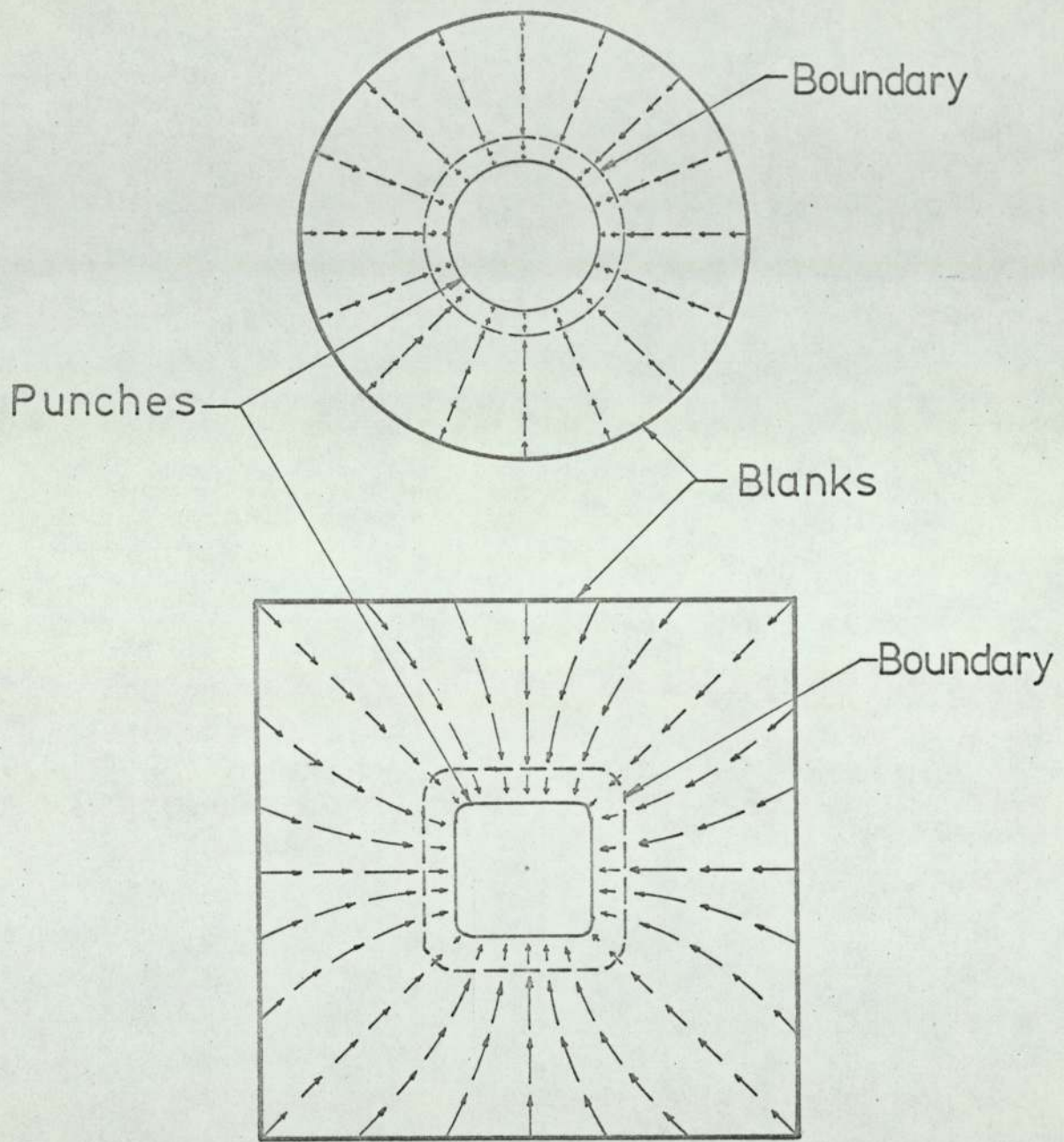


Fig. 12 - 1

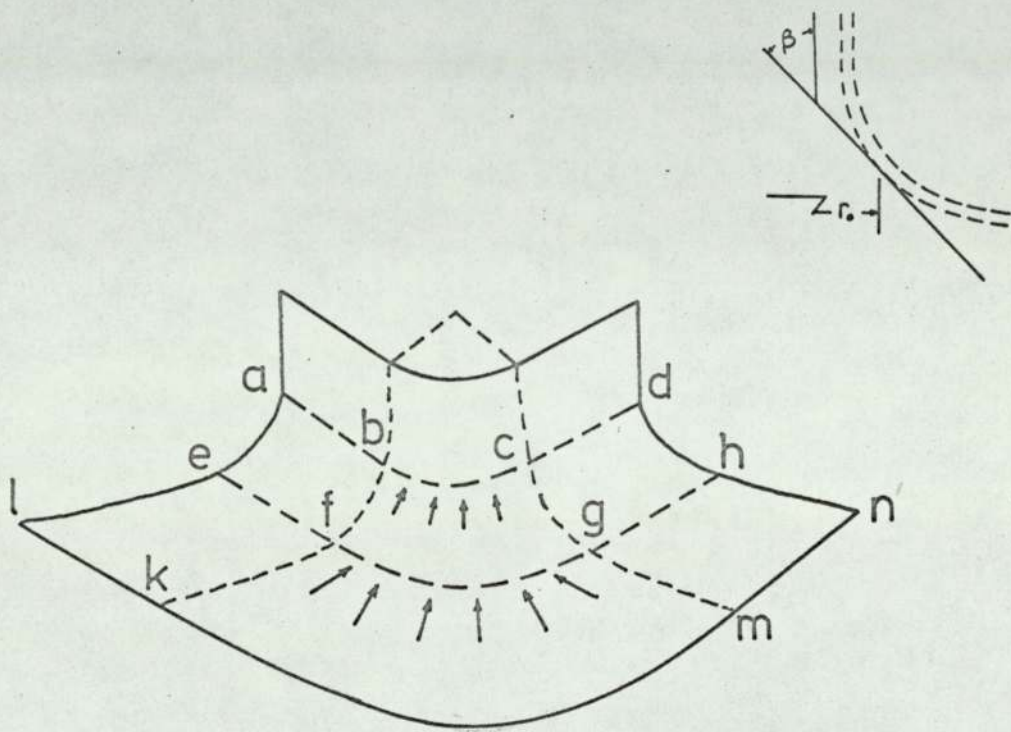


Fig. 12 - 2

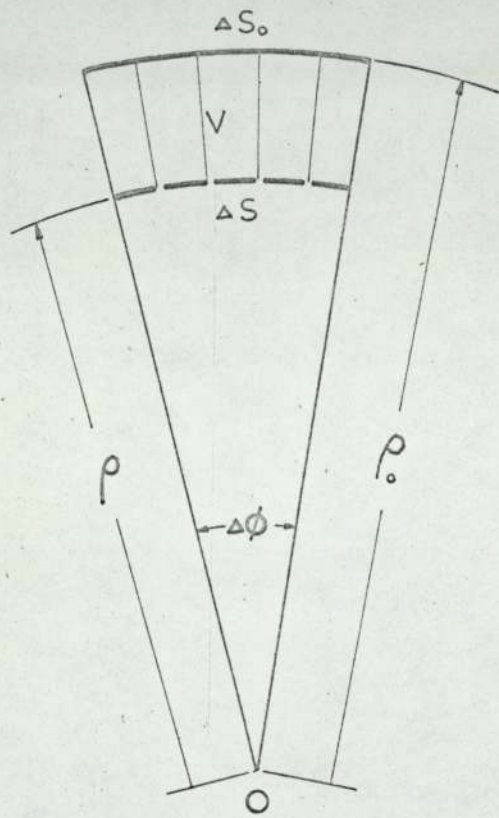


Fig. 12 - 3

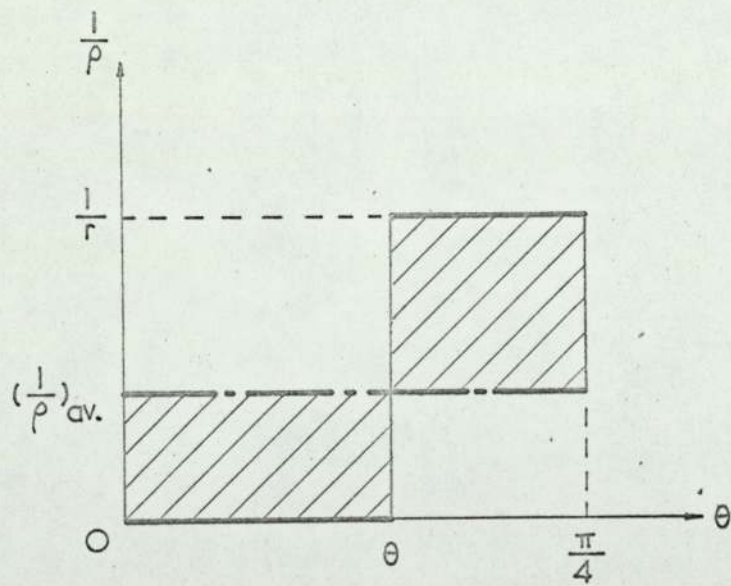
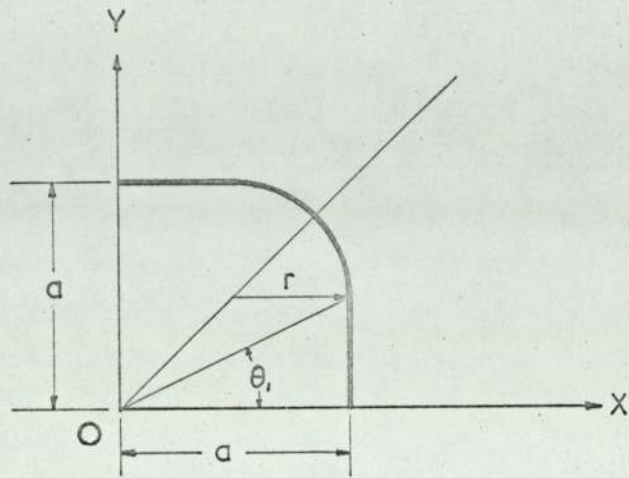


Fig. 12 - 4

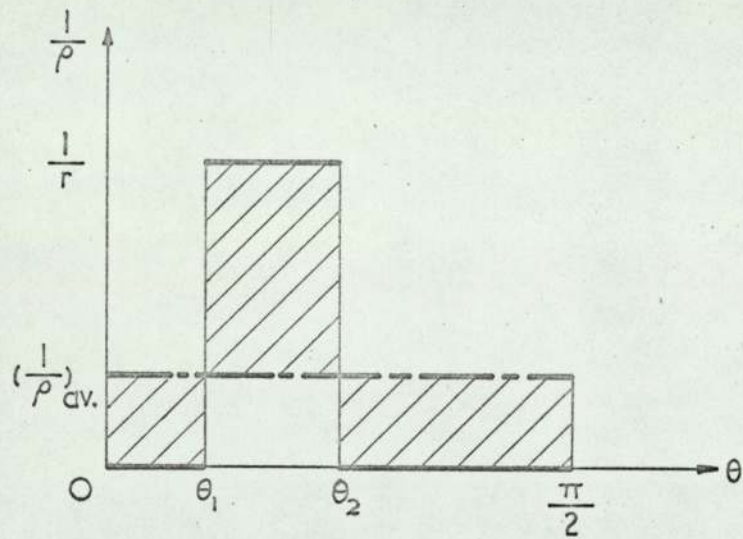
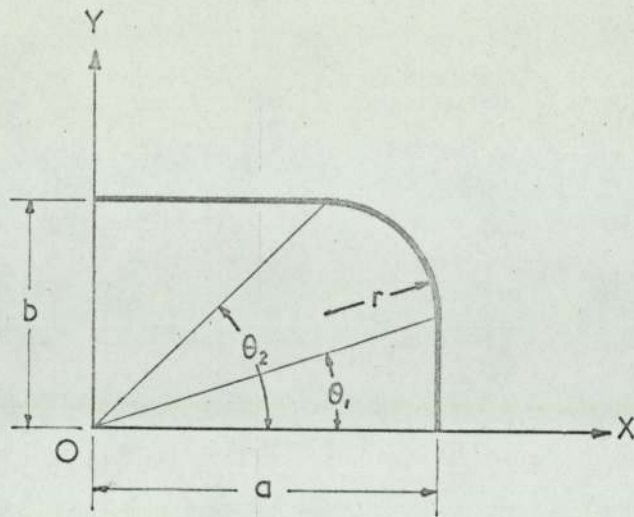


Fig. 12 - 5

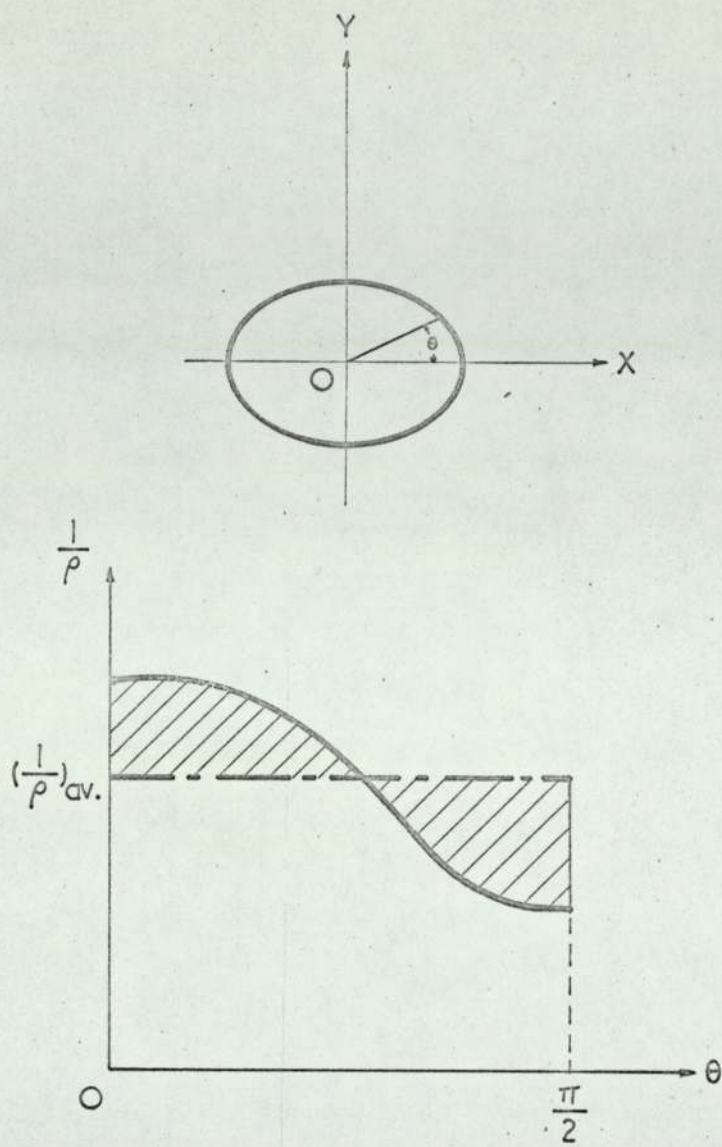


Fig. 12 - 6

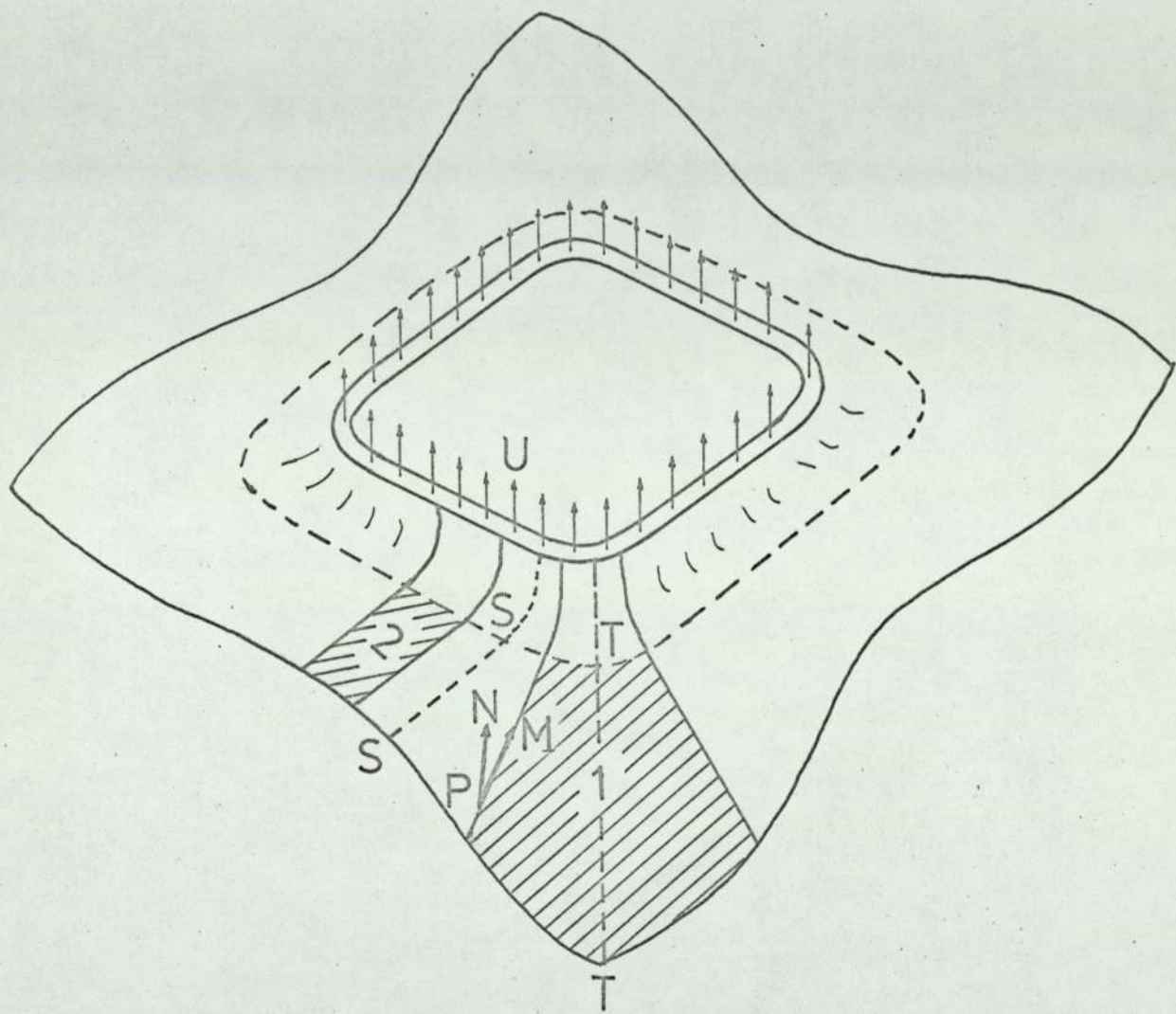


Fig. 12 - 7

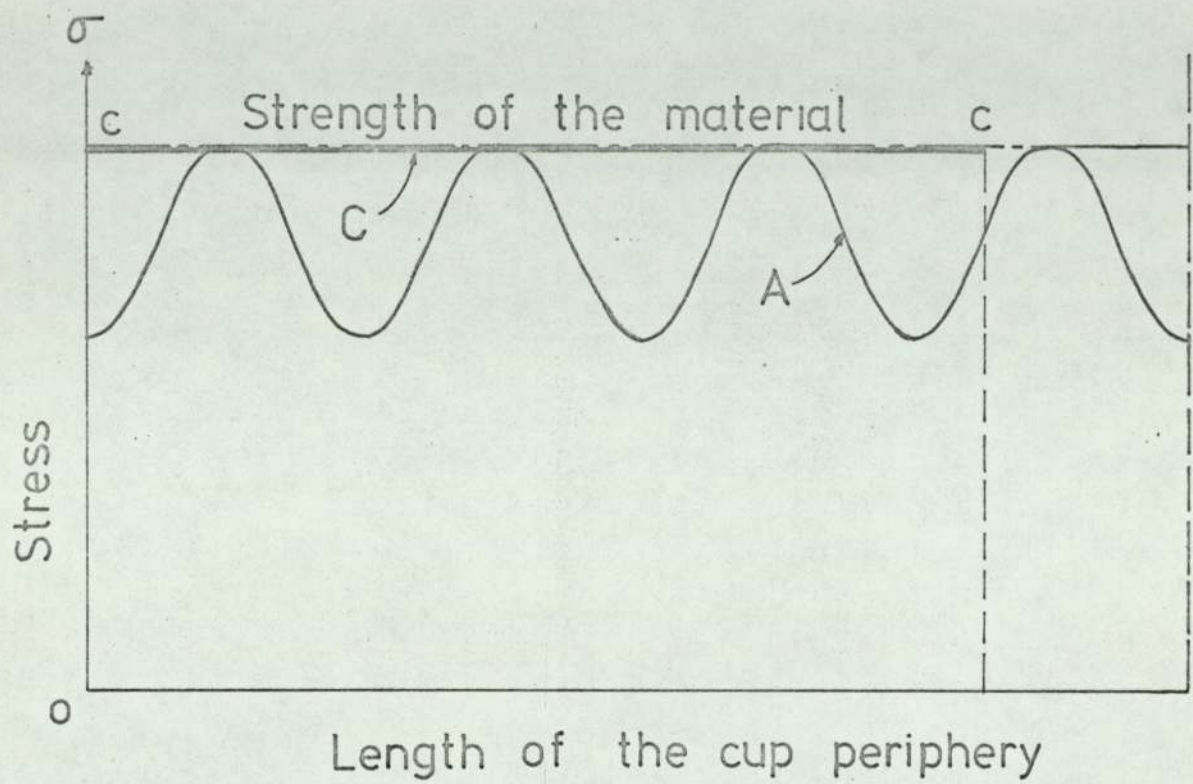


Fig. 12 - 8

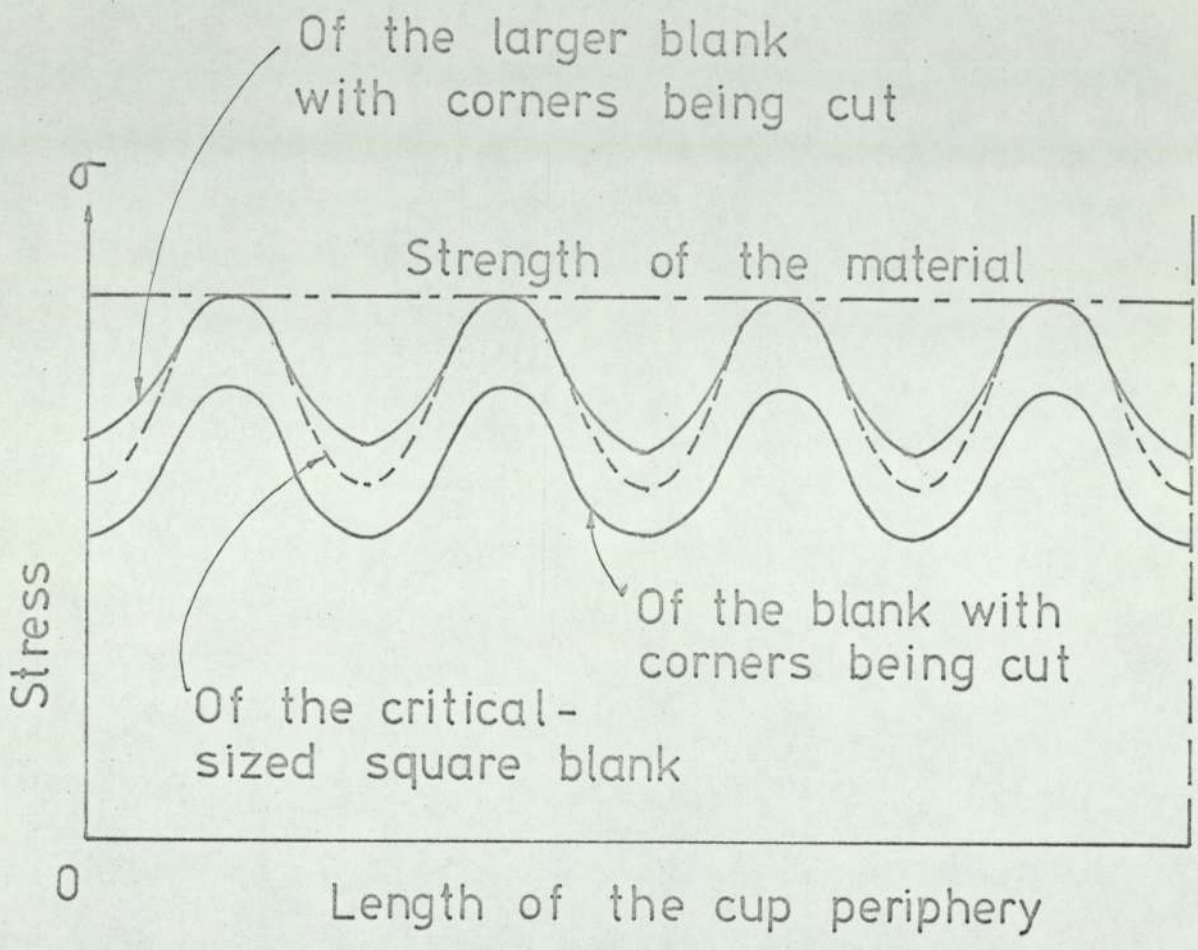


Fig. 12 - 9

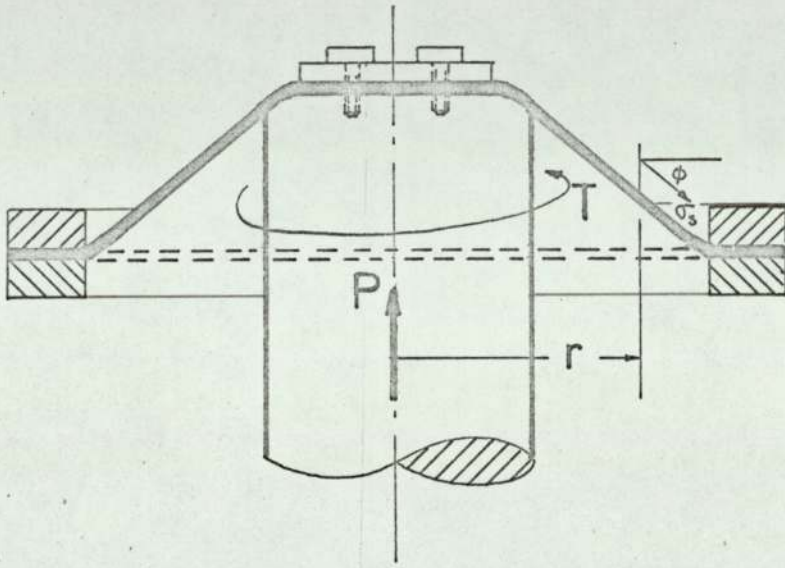


Fig. 14 - 1